SMALL AND LARGE-SCALE GENE REGULATION IN KAPOSI'S SARCOMA-ASSOCIATED HERPESVIRUS

Isaac Blair Hilton

A dissertation submitted to the faculty of the University of North Carolina at Chapel Hill in partial fulfillment of the requirements for the degree of Doctor of Philosophy in the Curriculum in Genetics and Molecular Biology

Chapel Hill
2013

Approved by:

Dirk P. Dittmer, PhD

Albert S. Baldwin, PhD

Blossom A. Damania, PhD

Ian J. Davis, MD, PhD

Jason D. Lieb, PhD

ABSTRACT

ISAAC BLAIR HILTON: Small and Large-Scale Gene Regulation in Kaposi's Sarcoma-associated Herpesvirus
(Under the direction of Dirk P. Dittmer, PhD)

Viruses depend upon host cells for genome replication and propagation. Viral genomes must be labile in order to exist inertly within infectious extracellular virions and also dynamically as self-replicating entities within infected host cells. Herpesviruses are large double-stranded DNA viruses which can establish persistent lifelong infections in vertebrates. Kaposi's Sarcoma-associated Herpesvirus (KSHV) is the most recently discovered human herpesvirus. KSHV infects endothelial and B cells which can lead to three human cancers: Kaposi's Sarcoma, Multicentric Castleman's Disease, and Primary Effusion Lymphoma. KSHV alternates between a latent replication phase, during which viral gene expression is restricted and no progeny virions are produced; and a lytic replication phase, which entails robust viral transcription and genome replication as well as host cell lysis and the release of new infectious daughter virions. Both replication patterns are implicated in KSHV pathology, however nearly all infected cells, including those within tumors, display latent infection.

The balance between lytic and latent KSHV infection is sensitive and complex. Viral latency is characterized by the expression of a multifunctional viral protein called the KSHV Latency-Associated Nuclear Antigen (LANA). LANA maintains the viral genome and modulates gene expression to ensure persistent latent infection. KSHV latency can be reversed upon appropriate stimuli in a process called reactivation. Reactivation of KSHV is coordinated through a virally-encoded transcription factor called RTA. In this dissertation I have characterized a novel small-scale regulatory mechanism by which RTA acts to selectively synthesize either latent (i.e. LANA) or lytic

transcripts from within the major KSHV latency locus. This selective bidirectional gene expression results in competitive RTA-mediated transactivation, the potency of which varies in proportion to RTA concentration. The resulting transcriptional circuit may have a role in the early establishment of KSHV latency, in attenuating and fine-tuning viral transcription, or both. In a second study presented here I have investigated how nucleosome depletion, or "open chromatin" is dispersed in latent KSHV genomes. This effort integrates our own work with that of others in the KSHV community, and collectively the data indicate that open chromatin in KSHV may be programmed for latency; with select latent regions accessible and most others insulated by CTCF and Cohesin. CTCF-free and CTCF-enriched subsets of latent open chromatin occur proximal to mapped H3-ac/H3K4-me3 modifications on the KSHV genome. Many of these regions also contain identified RTA Recognition Elements (RRE's) and RNA polymerase II occupancy, including the viral lytic replication origins. This pattern of nucleosome depletion is mostly shared among latent episomes in both B and endothelial cells, implying a common latent open chromatin landscape in the viral genome. These studies of small-scale bidirectional gene induction and of large-scale latent nucleosome depletion in KSHV are connected. This work extends our understanding of KSHV biology and could reveal novel targets of therapeutic intervention.

For My Loving Family
Whom I Have Missed

ACKNOWLEDGEMENTS

I would like foremost to thank my graduate mentor Dr. Dirk Dittmer for his guidance and for the excellent training opportunities I received in his laboratory and under his auspices. I am grateful for his support, understanding, and generosity throughout our time working with one another. I am thankful for his assistance with my first manuscript adapted herein as Chapter II and for his revisions of the manuscript currently in preparation and included as Chapter III. He has taught me the skills needed to effectively perform sophisticated scientific research and to communicate my results. He has allowed me to independently explore my research, while adeptly providing an environment rich with resources, advice, and ideas; and I am deeply grateful. I would also like to thank the members my dissertation committee. Dr. Blossom Damania always proffers remarkable insight, and I am consistently impressed by her scientific acumen in joint lab meetings, at committee meetings, and in passing. Her input has been instrumental in my scientific development and she has been an encouraging figure throughout my graduate career. I am very thankful for her wisdom, guidance, and support.

Dr. Ian Davis always has a profoundly informed perspective on chromatin biology as well as an inspiring passion for scientific research from bench to patient. He has a way of offering honest and constructive advice that I truly admire. His input in committee meetings and regarding the FAIRE-Seq manuscript in preparation were encouraging, extremely useful, and very much appreciated. Dr. Al Baldwin is an outstanding instructor and taught one of the best courses I have ever had. His enthusiasm and breadth of scientific knowledge are incredible and I am still motivated by the infectious zeal for lambda phage he displayed during my first year coursework. His guidance during committee meetings was helpful in refining experimental design and in my growth as a scientist. Dr. Jason Lieb produces fascinating research and his drive and success are extraordinary. His input in committee meetings and elsewhere has always been helpful. His expertise and leadership skills are qualities I sincerely respect. I have been truly fortunate to have had such a talented cadre of

gifted scientists to guide my graduate career; all of whom I could respect and from whom I could gain meaningful perspective for which I am thankful.

Dr. Bob Duronio was an excellent director of the Curriculum in Genetics and Molecular Biology; somehow he was able to understand every single student's projects and needs. He also has a thoughtful question at every student seminar – it's amazing. Dr. Jeff Sekelsky, who has recently taken the reigns as Curriculum director, is a superb genetics instructor and mentor. His sincere and meaningful advice has been encouraging and motivational. Somehow Bob and Jeff always make time for advising, and the students in the UNC-GMB, including myself, owe a debt of gratitude to these men for their tireless efforts to enable our success. I am also very thankful for Sausyty Hermreck and Cara Marlow. I don't know how I would have been able to afford groceries or get any administrative tasks performed outside of lab without their assistance. I am proud and grateful to have had the opportunity to interact with the many exceptional members of the Curriculum in Genetics and Molecular Biology, the Microbiology Department, and the Virology community here at UNC-Chapel Hill.

It has been an honor to work with all of the past and present members of the Dittmer lab, especially Dr. Dirk Dittmer, Dr. Polly Chugh, Dr. Wuguo Chen, and Dr. Debasmita Roy. Mindy Feng was also an exceptionally bright undergraduate I mentored in the lab. Mindy's help in setting up the robotic hardware for high-throughput transfections was a valuable component of the work performed in Chapter II. Zhigang Zhang, a talented research associate in Dr. Blossom Damania's lab, facilitated potential extensions of the work in Chapter II through the generation of KSHV BAC's, and I thank him and Dr. Damania for this assistance. The kinetic modeling in Chapter II was a foreign technique to the lab, and I am also thankful for Dr. Tim Elston, who met with me repeatedly to discuss modeling the transcriptional circuit I was studying. His advice was critical in moving the project forward. I also received help from Dr. Uri Alon at the Weizmann Institute of Science through email. I was pretty astonished that he was so helpful and quick to respond to my questions about Hill coefficients over email. It gave me a lot of hope at the time. Dr. Nat Moorman has been a fantastic

person to get to know. His enthusiasm for science may be unparalleled, and he has been a continual resource for fruitful scientific discussion, motivation, and experimental design, for which I am thankful.

Jeremy Simon was very helpful with the FAIRE-Seq project in Chapter III. His help with the computational aspects of the project were integral to connecting the bench-work to KSHV biology, as was his assistance with troubleshooting sonication and library preparation. I thank him for all of his earnest efforts and also for his friendship. I would like to sincerely thank all of the friends I have made in Chapel Hill over the last six years. Specifically Dr. Kyle Gaulton and Dr. Colin Lickwar, who have been sources of intellectual stimulation and comic relief. Dr. Sara Hanna is a wonderful and exceptionally kind person who I am privileged to know. To list how meaningful all of the friends I have made in graduate school are to me would take a second dissertation. Regardless of where we all end up, many of these relationships will enrich our lives for decades to come. I am happy and lucky to know you all and I am indebted for your friendship.

In addition to intangible contributions such as rich relationships and intellectual guidance, many people including colleagues in the field and the taxpaying populous enabled my efforts. For the work in Chapter II, generous donations of reagents were provided by George Miller, Diane Hayward, and Jae Jung. This work was also supported by Public Health Service grant CA109232 to Dirk P. Dittmer, and I was supported by the virology training grant T32AI007419. For the work in Chapter III, we thank the UNC High-Throughput Sequencing Facility and also funding sources, which include NIH grants CA109232 to Dirk P. Dittmer, CA019014 to Blossom Damania, CA166447 to Ian J. Davis, T32GM067553 to Jeremy M. Simon, and T32AI007419 to me; Isaac B. Hilton.

As a first-generation college student I am constantly mindful of my parent's appreciation of the opportunities which education can provide. Their hard work every single day and their unwavering support of my desire to be a scientist and to help others through research is something I will never take for granted. My parents Dwight and Kathy Hilton inspire me to do my best, they inspire me to be compassionate, and they inspire me to do the right thing daily. While I am troubled

to have missed so much of their lives over these years, I am thankful for the brightness that their endless love and care continually brings into mine. My extended family has also always been a reservoir of admiration and strength; especially my cousin Brent Baker and my aunt Barbara Bilyeu, who have taught me so much about honor, generosity, and respect.

TABLE OF CONTENTS

LIST OF TABLES xiii

LIST OF FIGURES xiv

LIST OF ABBREVIATIONS xvii

I. INTRODUCTION 1

1.1 Kaposi's Sarcoma-associated Herpesvirus 2

1.2 KSHV-Associated Malignancies 3

Kaposi's Sarcoma 3

Primary Effusion Lymphoma 5

Multicentric Castleman's Disease 5

1.3 Latency and Reactivation of KSHV 6

KSHV Latent Gene Expression 6

Transcripts from the KSHV Latency Locus 7

Latent Transcription Outside of the Latency Locus 8

KSHV Latent Genome Maintenance and Replication 9

KSHV Reactivation and Lytic Gene Expression 10

RTA Promoter Specification 11

The RTA:RBPjκ Interaction 12

1.4 Selected KSHV-Encoded Oncogenic Factors 13

Latently Expressed Oncogenic Factors 14

Variably Expressed Oncogenic Factors 18

1.5 Epigenetic Regulation of the KSHV Genome 21

Epigenetically Programming the KSHV Episome for Latency 22

Reactivation from Latency in the Epigenetic Context 24

1.6 Figures 26

II. QUANTITATIVE ANALYSIS OF THE BIDIRECTIONAL VIRAL G-PROTEIN-COUPLED RECEPTOR AND LYTIC LATENCY-ASSOCIATED NUCLEAR ANTIGEN PROMOTER OF KAPOSI'S SARCOMA-ASSOCIATED HERPESVIRUS 32

2.1 Overview 32

2.2 Introduction 33

2.3 Materials and Methods 37
Plasmids 37
Tissue Culture and Transfection 38
Luciferase Data Acquisition 39
Data Fitting and Analysis 39
Immunoblotting 40

2.4 Results 41
LANApi and K14p Form a Bidirectional Promoter 41
Bidirectional Promoter is Dominated by K14p 42
LANApi TATA Element Limits K14p Activity 43
Direct DNA Binding by RTA Augments Promoter Efficiency 45
Sequence Architecture between TBP Elements Provided Directionality for RBPjκ Transactivation 48
RBPjκ binding sites are RTA specific and insensitive to Notch 48

2.5 Discussion 49

2.6 Figures 52

III. THE OPEN CHROMATIN LANDSCAPE OF KAPOSI'S-SARCOMA ASSOCIATED HERPESVIRUS 64

3.1 Overview 64

3.2 Introduction 65

3.3 Materials and Methods 67
Cell Culture 67
FAIRE-Seq 67
Sequence Analysis 68

3.4 Results 68
Open Chromatin Map of the KSHV Episome 68
Latent Episomal Open Chromatin is Adjacent to Activating Histone Markings 71
Open Chromatin Regions Overlap with CTCF Binding Sites at Lytic, but not Latent Promoters 72
Open Chromatin Regions Overlap with RNA PolII Deposition at Active and Poised Promoters 74

3.5 Discussion 75

3.6 Figures and Tables 79

IV. CONCLUSIONS AND PERSPECTIVES 88

4.1 The Nature of Bidirectional Transactivation via RTA:Paired RPBjκ 89
Potential Functions of the LANApi/K14p Bidirectional Promoter 89
A Conserved Transcriptional Brake in KSHV 92
Mechanistic Nuances of the LANApi/K14p Bidirectional Locus 93

4.2 Applications and Extensions of the LANApi/K14p Bidirectional Promoter 95
in vivo Mechanistic Consequences 95
Manipulation of the Bidirectional RTA:RBPjκ Mechanism: Implications for Therapy 96
(Re) Engineering the LANApi/K14p Transcriptional Circuit: Implications for Industry 96

4.3 Toward a Functional KSHV Epigenetic Atlas 97
KSHV Genome-Wide Epigenetic Regulation 97
Local Epigenetic Modifications and DNA Methylation in the KSHV Genome 102
Addressing the Missing Links in a Functional KSHV Epigenetic Atlas 105

4.4 Connecting the Dots; Open Chromatin:CTCF:Cohesin:RTA:LANA 107
Programmed Nucleosome Depletion and an Open Chromatin Code in the KSHV Genome 107
Interpreting the Code: KSHV Transcription 110
Transcriptional Utility of CTCF-Free Open Chromatin 110
Transcriptional Utility of CTCF-Enriched Open Chromatin 112
Interpreting the Code: KSHV Genome Conformation and Replication 113
Ghost(s) in the Machine: Potential Variance Associated with Cell Type, Cell Division, and Heterogeneic KSHV Genomes 117
The KSHV Episome Comes Full-Circle 121
Potential Targeting of Latent KSHV Open Chromatin 124
Potential Engineering of Gammaherpesviral Genomes; Substrates for Programmable Genetic Networks 126

4.5 Figures **127**

REFERENCES **142**

LIST OF TABLES

3.1 Summary of KSHV FAIRE-Sequencing Data 79

3.2 Correlation between FAIRE Peaks in BC1 and Other Notable Chromatin Marks..... 82

3.3 Nucleotide Resolution of KSHV FAIRE Regions in Infected Cells 84

LIST OF FIGURES

1.1 Human Herpesvirus Phylogeny 26

1.2 The KSHV Episome 27

1.3 KSHV-Associated Malignancies 28

14 The KSHV Life Cycle 29

1.5 Transcripts from the KSHV Latency Locus 30

1.6 The KSHV Lytic Switch Protein: RTA 52

2.1 KSHV Genomic Organization of the LANApi and K14p TSS's 53

2.2 WT LANApi and K14p Adhere to First-Order Hill Kinetics 54

2.3 LANApi and K14p are a Bidirectional Promoter Activated by RTA 55

2.4 The Relative Advantage in Efficiency of WT K14p over WT LANApi is Static 56

2.5 RTA Transactivation Based on Fit to Noncooperative Response Model (n = 1) 57

2.6 The LANApi-Proximal TATA Box Binding Protein (LANApi TATA) Element Limits K14p Output 58

2.7 Both RBPjκ Elements are Essential 59

2.8 Enhanced DNA Binding by RTA Augments Promoter Activity 60

2.9 At Saturating Levels, RTA DNA Binding Becomes Dispensable 61

2.10 Directionality of RTA-RBPjκ Transactivation 62

2.11 LANApi/K14p Response to Intracellular Notch (ICN) 63

2.12 Summary and Putative Model of LANApi/K14p Activation by RTA 64

3.1 FAIRE-Seq Analysis of PEL (BCBL1) 80

3.2 Regions of Latent Open Chromatin across the KSHV Genome (BC1) 81

3.3 Regions of Open Chromatin are Conserved in Latent KSHV Infected Endothelial and B cells 83

3.4 Regions of Latent KSHV Open Chromatin Occur Near Activated Histone Modifications 85

3.5 Regions of KSHV Open Chromatin Coincide with CTCF Binding Sites 86

3.6 RNA PolII Designates KSHV Latent Promoters 87

4.1 Potential Functions of the LANApi/K14p 127

4.2 A Conserved Transcriptional Brake in KSHV 128

4.3 RTA DNA Binding Increases Efficiency via TSS-Proximal Regulatory Elements 129

4.4 Promoter Reprogramming Creates a Refractory Period and Limits k_{cat} *in trans* 130

4.5 Applications and Extensions of the LANApi/K14p Bidirectional Promoter 131

4.6 Overview of KSHV Epigenetic Regulation 132

4.7 Roadmap to a Functional KSHV Epigenetic Atlas 133

4.8 An Open Chromatin Code for Latent KSHV Transcription 134

4.9 Overview of CTCF and Cohesin-Mediated Looping in the KSHV Episome 135

4.10 An Open Chromatin Code for Latent KSHV Conformation 136

4.11 Transcriptional Profile of “Latent” KSHV in BC1 PEL Cells 137

4.12 The KSHV Episome Comes Full-Circle 138

4.13 The Zipper Model of Latent Infection 139

4.14 Regions of Conserved Latent Viral Open Chromatin Contain CTCF binding sites and AT-rich Regions 140

4.15 Extensions to Profiling Latent Episomal Open Chromatin 141

ABBREVIATIONS

AIDS	Acquired immune deficiency syndrome
bp	base pair
CTCF	CCCTC binding factor
DNA	Deoxyribonucleic acid
EBV	Epstein-Barr virus
H3K9/K14-ac	Histone H3 lysine 9/14 acetylation
H3-ac	Histone H3 acetylation
H3K4-me3	Histone H3 lysine 4 trimethylation
H3K9-me3	Histone H3 lysine 9 trimethylation
H3K27-me3	Histone H3 lysine 27 trimethylation
HIV	Human immunodeficiency virus
“K” prefix	ORF unique to the KSHV genome
K12p	Kaposin promoter
K14p	K14/vGPCR promoter
LANA	Latency-associated nuclear antigen
LANApc	Constitutive LANA promoter
LANApi	Inducible LANA promoter
MCD	Multicentric Castleman’s Disease
miRNA	Micro-ribonucleic acid
NELF	Negative elongation factor
ORF	Open reading frame
OriLyt	KSHV lytic replication origin
PEL	Primary effusion lymphoma
PolII	RNA polymerase II

PAN	Polyadenylated Nuclear RNA
RNA	Ribonucleic acid
RTA	KSHV Replication and Transcription Activator
KS	Kaposi's sarcoma
KSHV	Kaposi's sarcoma-associated herpesvirus
TR	Terminal repeat
TSS	Transcription Start Site
"v" prefix	KSHV ORF encoding a cellular homologue

CHAPTER I

INTRODUCTION

Life expectancy in humans continues to rise as does the rate of human population growth (Burger et al., 2012). Along with other factors these realities translate into increasing rates and prevalence of oncogenesis in humans. This issue represents a philosophical, humanitarian, and economic burden; our mechanistic understanding of which is linked to our understanding of our biological origin and evolution as a species. The biomedical scientist is charged with the privilege and responsibility of furthering the collective understanding of our world on basic biological levels and in relation to human health and quality of life.

The mechanisms of oncogenesis in humans are varied and are incompletely understood. However, direct links exist between biological agents and many human cancers (Bouvard et al., 2009; Parkin, 2006). Moreover, a significant fraction of human cancers are mediated specifically by human viruses (reviewed in (Butt and Miggin, 2012; Martin and Gutkind, 2008)). The identification of the oncogenic mechanisms utilized by these viruses can enable the development of novel therapeutics and treatments aimed at limiting viral propagation and thus decreasing global cancer rates. Understanding how these viruses persist in human cells and how they hijack cellular regulatory mechanisms to cause malignancy can also provide insights into more general fields of human disease including non-viral associated cancers. In this dissertation it has been my goal to advance human understanding of the regulation of a persistent human oncogenic herpesvirus: Kaposi's sarcoma-associated herpesvirus (KSHV).

1.1 Kaposi's Sarcoma-associated Herpesvirus

At present, several oncogenic human viruses have been identified (reviewed in (2012; Butt and Miggin, 2012; Moore and Chang, 2010)). While many other human viral pathogens exhibit tumorigenic properties, their links to human cancers have yet to be verified. Truly oncogenic human viruses can be identified across the spectrum of virology; from retroviruses to persistent DNA viruses. The herpesviridae are a family of large, double-stranded DNA viruses which can persist within infected host cell nuclei for life (Davison, 2007). All herpesviruses are enveloped, double-stranded DNA viruses with relatively complex genomes. The herpesvirus lineage is biologically prevalent and is capable of infecting a wide range of vertebrate hosts.

To date eight human herpesviruses have been identified (Zamora, 2011). KSHV (also called Human herpesvirus 8; HHV-8) is the most recently discovered human herpesvirus and was identified in 1994 from skin lesions in an HIV-infected patient (Chang et al., 1994). The virus is a member of the gammaherpesvirus subfamily (Moore et al., 1996b) (Figure 1.1). Two known human gammaherpesviruses exist; Epstein-Barr virus (EBV) and KSHV; and both are etiologically linked with malignancy in infected human hosts.

The unique region of the KSHV genome is approximately 140,000bp in size (Russo et al., 1996) and is flanked by ~800bp terminal repeats (TR's) which vary in repeat number depending on viral isolate (Lagunoff and Ganem, 1997; Renne et al., 1996a). Russo et al. initially annotated 87 open reading frames (ORF's) and since then 12 pre-miRNA's have been discovered (reviewed in (Gottwein, 2012; Mesri et al., 2010)) as well as larger noncoding RNA's and antisense transcripts (Chandriani et al., 2010; Dresang et al., 2011; Lin et al., 2010; Sun et al., 1996; Xu and Ganem, 2010). Subsequent to infection the virion-associated linear viral genome is rapidly circularized as a multi-copy minichromosome called an episome (Figure 1.2) (Dezube et al., 2002; Renne et al., 1996a). Though largely conserved the KSHV genome can be sub-classified into four major subtypes based on DNA sequence variation, which correlate with ethnic and global distributions: A, B, C, and

D (Hayward, 1999). The variance observed among KSHV subtypes (~0.4%) is principally due to differences within the coding regions of two viral membrane signaling proteins near the genomic termini called K1 (30% variability) and K15 (predominant; P, and minor; M, alleles) (Poole et al., 1999).

1.2 KSHV-associated Malignancies

The principle target of KSHV *in vivo* is the B cell, however the virus is also found in endothelial cells and cells surrounding associated skin lesions (Ambroziak et al., 1995; Dupin et al., 1999; Parravicini et al., 2000). KSHV is the etiologic agent in three human malignancies (Figure 1.3). KSHV-mediated oncogenesis manifests in endothelial cells as Kaposi's sarcoma (KS) (Chang et al., 1994; Neipel and Fleckenstein, 1999). The virus also infects B cells to generate two lymphoproliferative malignancies; Primary Effusion Lymphoma (PEL) (Cesarman et al., 1995a) and Multicentric Castleman's Disease (MCD) (Soulier et al., 1995) described below.

Kaposi's Sarcoma

Kaposi's sarcoma (KS) is a tumor of endothelial cell origin and is caused by KSHV. KS was first described by Dr. Moritz Kaposi, a Hungarian dermatologist in the late 19th century (Kaposi, 1872). Dr. Kaposi described the skin as cutaneous lesions, which were evident in older men of Mediterranean origin. KS is histologically complex and at present, four forms of the disease exist (Dittmer et al., 2012; Ganem, 2006); the original form described by Dr. Kaposi is termed "Classical KS". Three other types of KS are now recognized: endemic KS, transplant-associated KS, and AIDS-associated KS.

Endemic KS largely occurs in sub-Saharan Africa and incidents of this sub-class of KS have been observed since long before the AIDS-epidemic (Maclean, 1963). This form of KS is commonly identified in African children and it has been characterized as aggressive (Slavin et al., 1970). In

certain parts of Africa the overwhelming prevalence of KSHV has made endemic KS the leading cancer in the male population. Treatment options are often limited, underscoring the need for a more thorough understanding of pathogenesis.

Transplant-associated KS is restricted to patients undergoing organ transplants and receiving immunosuppressant therapy as a preventative measure against transplant rejection. The onset is predicated upon KSHV seroprevalence in either the transplant donor or recipient and as such this disease sub-classification is closely correlated with KSHV infection rates. Hence, in locations where KSHV infection rates are high and transplantations are medically feasible such as Italy, Saudi Arabia, and Turkey, the incidence of transplant-associated KS is concordantly relatively high (Barozzi et al., 2003; Dittmer et al., 2012).

The last sub-classification of KS is AIDS-associated KS, or AIDS-KS. While classical KS is not generally life-threatening (Safai, 1984), KS in the context of HIV infection is often much more aggressive and can affect large areas of the body surface and viscera (Dezube, 1996; Ganem, 2010). Complications from AIDS-KS can give rise to disfiguring lesions and life-threatening issues; such as respiratory failure and gastrointestinal bleeding. Multifocal lesions are often observed in AIDS-KS, suggestive of independent multicentric occurrence rather than single lesion origin. In fact KSHV genomes from different lesions, but from the same AIDS-KS patient, are often from distinct viral subpopulations based on analysis of the viral genomic termini (Duprez et al., 2007).

With the onset of the AIDS epidemic in the 1980's a dramatic increase of KS was observed, so much so that AIDS-KS was initially termed "epidemic KS". The co-occurrence of KS in AIDS patients initially suggested that HIV might in fact be the causative agent, however the lack of proviral HIV and inequalities in KS risk among HIV-infected populations refuted this possibility (Ganem, 2010). With the discovery of KSHV in KS lesions by Chang and Moore in 1994 (Chang et al., 1994), the evidence was clear that KSHV was the cause of AIDS-KS. KS has now become the most common malignancy in AIDS patients, and is a *bona-fide* AIDS-defining cancer, the treatment and management of which demand a more complete understanding.

Primary Effusion Lymphoma

Subsequent to the identification of KSHV as the driving factor in KS in 1994, the virus was identified within AIDS-related B cell lymphomas (Cesarman et al., 1995a). One variant of these KSHV-associated lymphomas exhibit an accumulation of fluid in the serous cavities of the body, such as within the pleural and peritoneal cavities, and are known as primary effusion lymphomas; or PEL. PEL is a rare form of AIDS-related non-Hodgkin's lymphoma and the disease has a very poor prognosis (Cesarman, 2011; Komanduri et al., 1996; Nador et al., 1996; Wen and Damania, 2010). Most PEL presents within serous cavities in the absence of a solid mass, however there are instances of extra-cavity exceptions (Chadburn et al., 2004; Grubb et al., 2006).

Unlike in KS, PEL presents as a clonally expanded neoplastic entity of B cell origin. However despite bearing a B cell genotype, PEL often lack B cell-associated antigens (Cesarman, 2011; Nador et al., 1996). Similar to KS, KSHV is a necessary cofactor for the genesis of PEL. Within infected PEL cell nuclei there are estimated to be 50-100 copies of the double-stranded KSHV episome (Renne et al., 1996a), and in addition to harboring the KSHV genome, the majority of infected PEL cells are also co-infected with multiple copies EBV episomes; complicating both the understanding and treatment of this virally induced malignancy.

Multicentric Castleman's Disease

A second malignant entity of B cell origin has been confirmed as linked to KSHV infection: a plasmablastic variant of Multicentric Castleman's Disease, or MCD (Dupin et al., 2000; Hillier et al., 2004; Soulier et al., 1995). KSHV-associated MCD lymphomas are not co-infected with EBV, and are thought to arise from more naïve B cell precursor (Cesarman, 2011; Du et al., 2001). Moreover MCD exhibits a polyclonal origin, unlike PEL (Dupin et al., 1999) and MCD progression may be linked to alterations in key cytokines such as IL-6 (Parravicini et al., 1997). While it is clear that KSHV is linked to MCD, this disease is the least understood of the KSHV-associated malignancies at present (Uldrick et al., 2012).

1.3 Latency and Reactivation of KSHV

All viruses have obligatorily parasitic lifestyles which require host cell infrastructure for persistence and propagation. Outside of cells, human herpesvirus genomes are enclosed within proteinaceous viral capsids, which are further surrounded by a layer of tegument and finally by a lipid bilayer containing distinct viral glycoproteins, called the envelope (Chakraborty et al., 2012; Trus et al., 2001). The first stages of viral infections involve binding and entry into naïve cell targets, after which viral genomes are rapidly trafficked and accessed to modify host cells for infection and exploitation. A hallmark of herpesvirus infection is the ability to establish a persistent lifelong infection within host cells called latency. KSHV is no exception and after primary infection the virus can persist in latency, a semi-quiescent state, which can be reversibly interrupted by viral reactivation and subsequent reinfection (Figure 1.4). During KSHV latency the Latency-associated Nuclear Antigen (LANA) is expressed and ensures episome persistence (Ballestas et al., 1999). Latent infection is disrupted upon expression of the KSHV lytic-switch protein; the Replication and Transcription Activator (RTA) (Sun et al., 1998). Both replication phases are involved in KSHV-mediated oncogenesis; the autocrine/paracrine signaling and viral spread associated with lytic infection, and the modulation of host cells and maintained viral reservoirs characteristic of viral latency.

KSHV Latent Gene Expression

Like all known herpesviruses, KSHV displays two phases of replication; latency and lytic infection. Subsequent to primary infection KSHV adopts a latent infection program in the vast majority of infected cells and in almost all tumor cells (Krishnan et al., 2004; Renne et al., 1996b; Staskus et al., 1997; Zhong et al., 1996). During latency the KSHV genome exists as a non-integrated chromatin-associated circular episome and is thought to attach to host chromatin. Only a small subset of the viral genome is transcribed during latency and certain cell surface markers are down-regulated

such that the potential for viral recognition by host immune surveillance is minimized (Coscoy and Ganem, 2000, 2001; Ishido et al., 2000). Viral transcripts that are expressed during latency play important roles in modifying the host cell and the virus to ensure the persistence of stable latent infection.

Transcripts from the KSHV Latency Locus

The linearized incoming viral genome is circularized as an episome in the infected host cell nucleus and expression is limited during latency (Dezube et al., 2002; Fakhari and Dittmer, 2002; Jenner et al., 2001; Renne et al., 1996a). The most well characterized transcripts originate from a cluster known as the major KSHV latency locus (Figure 1.5). This locus encodes the viral genes LANA, vCyclin, vFLIP, all 3 isoforms of Kaposin (A-C), as well as 12 stem loops from which the KSHV miRNA's are derived (Cai et al., 2005; Dittmer et al., 1998; Pfeffer et al., 2005; Samols et al., 2005). LANA, vCyclin, and vFLIP are generated from the major latent promoter (the constitutive LANA promoter; LANApc) via the alternative splicing of co-terminal RNA's (Bieleski and Talbot, 2001; Dittmer et al., 1998; Jeong et al., 2004; Sarid et al., 1999; Talbot et al., 1999). Splicing events also allow derivation of the viral miRNA's and Kaposin isoforms from the LANApc (Cai and Cullen, 2006). Although the results are controversial, a second latently active downstream promoter called the LANAds is thought to generate all forms of Kaposin through alternative splicing and to also direct the expression of vCyclin and vFLIP and viral miRNA's, (Cai and Cullen, 2006; Li et al., 2002; Pearce et al., 2005).

Transcription from the latency locus is complex and in addition to constitutively active promoters, other transcription start sites (TSS's) can be induced during lytic infection. KSHV miR-K10, miR-K12, and all Kaposin isoforms can be transcribed from an inducible TSS upstream of Kaposin (Cai and Cullen, 2006; Sadler et al., 1999). A second lytic-phase promoter called LANApi directs the expression of LANA, vCyclin, and vFLIP (Lan et al., 2005b; Matsumura et al., 2005; Staudt and Dittmer, 2006). This promoter region acts bidirectionally to synthesize either a transcript

encoding LANA/vCyclin/vFLIP or a bicistronic message encoding a viral immunomodulatory glycoprotein (K14/vOX2) and a viral G-protein coupled receptor (vGPCR) (Hilton and Dittmer, 2012; Kirshner et al., 1999). Furthermore a lytically induced antisense transcript of unknown function called "antisense to latency transcripts" (ALT) originates upstream of miR-K7 from the ALTp, and is antisense to several viral miRNA's, vFLIP, vCyclin, and LANA (Chandriani et al., 2010).

Latent Transcription Outside of the Latency Locus

All of the products derived from true latent promoters at the latency locus are present in latently infected PEL and KS cells (Dittmer, 2003; Fakhari and Dittmer, 2002; Marshall et al., 2007). Certain viral transcripts also originate outside of the latency locus expressed during latent infection, albeit with more variable patterns. For instance vIRF-3 (also called LANA-2) is latently expressed in PEL but not KS, and thus latent expression of this viral ORF is restricted to B cells (Rivas et al., 2001). Latent expression of other viral ORF's is more controversial. vIRF-1 has classically been considered a lytic phase gene product (Jenner et al., 2001; Sarid et al., 1998), however others have observed latent expression, including within KS tumor cells (Chen et al., 2000; Cunningham et al., 2003; Dittmer, 2003). vIRF-1 may also use two distinct promoter elements, suggesting the possibility of cell type-specific gene expression. Evidence has also surfaced highlighting the fact that vIL-6, often considered to be a lytic gene, exhibits consistently high levels of expression during KSHV latency, but only in certain conditions, particularly MCD (Chandriani and Ganem, 2010; Nicholas et al., 1997).

In addition two membrane-bound signaling molecules at the left and right ends of the viral genome respectively; K1 and K15, have exhibited latent expression, further demonstrating that the latent KSHV episome may be transcriptionally active at loci outside of the latency cluster (Bowser et al., 2002; Chandriani and Ganem, 2010; Wong and Damania, 2006). This raises the possibility that KSHV latency may be more dynamic than previously thought. Recent evidence suggests large scale

production of previously underappreciated mRNA from the both strands of the latent KSHV episome, including antisense transcription at critical latent loci (Chandriani and Ganem, 2010; Dresang et al., 2011; Xu and Ganem, 2010). In the closely related EBV there are three distinct latency programs and given the phylogenetic and biological similarities between KSHV and EBV the prospect of adaptable patterns of latent KSHV infection has precedent and rationale. The situation is further complicated by the fact that in any given population of KSHV-infected cells (at least *in vitro*), a small percentage of cells undergo spontaneous lytic reactivation (Renne et al., 1996b), and vIRF-3, vIL-6, K1, and K15 are all induced early during lytic reactivation.

KSHV Latent Genome Maintenance and Replication

During latent infection the KSHV LANA protein tethers the viral genome to host chromatin through interactions between the episomal TR's and host chromatin (Ballestas et al., 1999; Cotter and Robertson, 1999; Grundhoff and Ganem, 2003). Both the amino (N) and carboxy (C) termini of LANA interact with chromatin (Barbera et al., 2004; Kelley-Clarke et al., 2007). The N-terminus of LANA binds to an acidic pocket between histones H2A and H2B (Barbera et al., 2006; Chodaparambil et al., 2007) and the LANA C-terminus binds the viral TR's (reviewed in (Ballestas and Kaye, 2011)). This interaction physically links the viral and host genomes during latency. LANA binds to host chromatin in the presence and absence of the viral genome, however in the presence of KSHV distinct punctate foci are formed at the sites of KSHV episomes, whereas without the viral genome LANA binding is diffuse on host chromatin (Ballestas et al., 1999).

LANA also directs the replication of the episome during latent infection. The carboxy terminus of LANA binds specific sequences of TR DNA and this interaction is essential for latent replication and persistence (Ballestas and Kaye, 2001; Garber et al., 2002; Komatsu et al., 2004; Srinivasan et al., 2004). LANA self-associates to cooperatively bind a minimal replicator element within the TR, which consists of two LANA Binding Sites (LBS's) and a 32bp GC rich element (Hu and Renne, 2005; Verma et al., 2007a). Data indicates that the LANA-mediated replication of the

latent episome requires the replication of host cell machinery (Hu et al., 2009; Purushothaman et al., 2012; Stedman et al., 2004), however the field remains bereft of a full understanding of how latent episomal replication occurs.

KSHV Reactivation and Lytic Gene Expression

While viral latency is relatively stable and is the default replicative phase for KSHV, it is not indefinite. The physiologic stimuli which interrupt KSHV latency are varied and are still being elucidated. Activation of toll-like receptors, cellular cytokines and transcription factors, and treatment with chemicals which activate the protein kinase C pathway or which inhibit histone deacetylase (HDAC) activity; such as 12-O-tetradecanoyl-phorbol-13-acetate (TPA) or sodium butyrate respectively, can interrupt latency and reactivate KSHV (Chang et al., 2000; Gregory et al., 2009; Lan et al., 2006; Mercader et al., 2000; Renne et al., 1996b; Yu et al., 2007; Yu et al., 1999). While these inputs are diverse, all reactivation stimuli are ultimately coordinated through a single viral gene encoded by KSHV ORF50 called the Replication and Transcription Activator; RTA (Sun et al., 1998).

RTA expression from the KSHV genome (or ectopic expression) initiates an ordered cascade of viral gene expression and genome replication. This ultimately results in host cell lysis and the production of new infectious virions. During reactivation nearly the entire KSHV genome is robustly transcribed in a stage-specific manner, with transcripts temporally designated as: (i) immediate-early (IE) – based upon their expression occurring in the absence of *de novo* protein synthesis. (ii) delayed-early (DE) – by default based upon expression which occurs after the IE class, but before the late (L) class of lytic viral transcripts. (iii) Late transcripts (L) – viral transcripts which are sensitive to DNA replication inhibitors, and hence require viral genome replication for synthesis (Lu et al., 2004; Nakamura et al., 2003; Paulose-Murphy et al., 2001; Zhu et al., 1999). Most viral transcripts encoding structural proteins (such as capsid proteins) are expressed after those encoding viral DNA replication proteins (Jenner et al., 2001; Paulose-Murphy et al., 2001). However, this temporal

pattern may be more complex, with large portions of both strands of the KSHV genome abundantly transcribed in both latency and reactivation (Chandriani and Ganem, 2010; Dresang et al., 2011; Xu and Ganem, 2010). Moreover RTA-independent mechanisms of KSHV lytic gene induction have been characterized (Chang et al., 2005a; Toth et al., 2012) and variance in viral gene expression across host cell cycle may also occur (Kang and Lieberman, 2009). Emerging data challenge the idea of such a clear transcriptional demarcation between two static viral lifestyles, and instead seem to suggest a more variable (and likely more adaptable), expression pattern.

RTA Promoter Specification

The RTA protein contains 691 amino acids (aa), two nuclear localization signals (NLS), an N-terminal DNA binding and dimerization domain, and a C-terminal transactivation domain, as shown in Figure 1.6a (Lukac et al., 1998). RTA is a DNA binding protein and physically interacts with a number of cellular and viral proteins (including itself) to activate transcription of cellular and viral genes; including activation of its own promoter (Bu et al., 2007; Carroll et al., 2006; Carroll et al., 2007; Chang et al., 2008; Deng et al., 2000; Gould et al., 2009; Gwack et al., 2002; Gwack et al., 2003b; He et al., 2010; Izumiya et al., 2003; Liang et al., 2002; Lukac et al., 2001; Lukac et al., 1999; Palmeri et al., 2007; Sakakibara et al., 2001; Song et al., 2002; Wang et al., 2003; Yada et al., 2006; Yang et al., 2008; Yu et al., 2005). Purified RTA rapidly forms multimers of decamers and tetramers by size-exclusion chromatography, however the transcriptionally active state of RTA appears to occur only in a tetrameric form (Bu et al., 2007).

RTA induces widespread transcription at multiple viral ORF's and is recruited to RTA-response elements (RRE's) by either by direct DNA binding or interaction with transcriptional cofactors (Figure 1.6b) (Chen et al., 2009; Ellison et al., 2009; Song et al., 2001; Song et al., 2003; Wang et al., 2004b; Wang et al., 2004d), though the mechanisms are not mutually exclusive (Chang et al., 2005b; Hilton and Dittmer, 2012; Song et al., 2003). Direct RTA-DNA binding is observed at the Polyadenylated Nuclear RNA (PAN) promoter and at the Kaposin promoter using a homologous

RTA-response element (RRE) (Chang et al., 2002). A similar RRE is bound by RTA at lytic replication origins (OriLyt's) (AuCoin et al., 2004; Wang et al., 2004d). Although RTA recognizes RRE's at many loci, a conserved consensus sequence for binding has not yet been established (Chang et al., 2002; Chen et al., 2009; Liao et al., 2003; Palmeri et al., 2011; Song et al., 2001; Ziegelbauer et al., 2006). Recent data suggests that RTA may recognize a 14bp consensus sequence containing the core nucleotides of Cytosine-Adenine-N-Thymine (where N is any base); termed "CANT" repeats (Palmeri et al., 2011). CANT repeat elements may co-occur with other *cis* recognition elements at RTA-responsive promoters, however only one instance of CANT repeat utility has been demonstrated (Guito and Lukac, 2012; Palmeri et al., 2011).

The RTA:RBPjκ Interaction

While RTA interacts with several proteins to activate transcription; the interaction with RBPjκ (also called CSL) is perhaps the most well established and ubiquitous (Liang et al., 2002). RBPjκ is the downstream effector on the Notch signaling pathway (reviewed in (Kovall and Blacklow, 2010)). The RBPjκ molecule canonically acts as a transcriptional repressor and binds to the sequence motif 5'-GTGGGAA-3 (Tun et al., 1994); although there is a significant degree of motif redundancy, including within the KSHV genome (Persson and Wilson, 2010). Moreover the surrounding sequence context also plays an important role in directing RBPjκ activation (Ong et al., 2006). Within the KSHV genome, over 260 RBPjκ binding motifs exist (variable depending on P or M allelic genomes), though it is unlikely that all are bound by RBPjκ (Persson and Wilson, 2010). RTA physically interacts with RBPjκ to activate a growing list of KSHV promoters (Chang et al., 2005a; Chang et al., 2005b; Hilton and Dittmer, 2012; Liang et al., 2002; Liang and Ganem, 2004; Liu et al., 2008; Lu et al., 2012b; Matsumura et al., 2005; Persson and Wilson, 2010; Wang and Yuan, 2007; Xu and Ganem, 2010; Ziegelbauer et al., 2006). The importance of this interaction is underscored by the fact that in the absence of RBPjκ latent KSHV is unable to be effectively reactivated (Liang and Ganem, 2003).

The RTA:RBPjκ interaction is transcriptionally robust; even artificial promoters containing RBPjκ recognition sites can be transcriptionally activated by RTA (Liang et al., 2002). RBPjκ binding to DNA is likely more dynamic than initially characterized, and it is thought that the RTA tetramer is able to "stabilize" RBPjκ binding to initiate a transactivation response at RTA-responsive promoters (Carroll et al., 2006). The mechanisms underlying this stabilization are not fully known, but recent evidence suggests that the presence of CANT repeats or AT repeats could coordinate this interaction (Liao et al., 2003; Palmeri et al., 2011). Both gammaherpesviruses rely on RBPjκ for the effective coordination of gene expression (Hayward, 2004). Given the widespread decoration of the KSHV genome with RBPjκ binding sites, it is not surprising that intracellular Notch, (the canonical activator of RBPjκ) is able to transactivate some RBPjκ-dependent viral genes, and has even been shown to reactivate latent KSHV (Lan et al., 2006). However many RPBjκ-dependent KSHV genes do not respond to Notch signals, indicating that at the majority of responsive loci, the RTA:RBPjκ interaction is exclusively required (Chang et al., 2005a; Hilton and Dittmer, 2012). The RTA:RBPjκ interaction is further complicated by the fact that LANA has also been shown to interact with RBPjκ with functional consequences (Jin et al., 2012; Lan et al., 2005a; Lan et al., 2005b). The interactions between RBPjκ and the major viral latent (LANA) and lytic (RTA) transcriptional regulators imply that RBPjκ is a central player in mediating the balance between latency and lytic reactivation.

1.4 Selected KSHV-Encoded Oncogenic Factors

KSHV-associated oncogenesis occurs in both endothelial cells and B cells, which manifests as KS and PEL or MCD respectively. This process is not completely understood, but at present we know that several factors encoded by KSHV contribute to cellular transformation and the progression of KSHV-associated malignancy. Gene expression from the KSHV genome is variable depending upon the viral replication cycle, which alternates between a restricted state of latency and a robust transcriptional/replication program called the lytic phase (see Section 1.3). Both phases of KSHV

replication are involved in the malignant pathology of the virus and outlined below are selected products generated by the virus which have characterized roles in viral oncogenesis.

Latently Expressed Oncogenic Factors

LANA

The KSHV Latency-associated nuclear antigen (LANA) is a virally encoded protein with a multitude of diverse functions in infected cells (reviewed in (Ballestas and Kaye, 2011)). LANA is constitutively expressed from the major latency locus of the viral genome in all infected cells (Dittmer et al., 1998; Gao et al., 1996; Kedes et al., 1997; Rainbow et al., 1997). The LANA protein is responsible for maintaining the KSHV genome and for systemic coordination of latency within infected cells.

LANA is critical for persistence of the KSHV genome though infected cellular divisions (Ballestas et al., 1999). LANA mediates this feat by tethering the KSHV episome to host chromosomes through a bridging interaction between the viral TR's and host nucleosomes (Ballestas and Kaye, 2001; Barbera et al., 2006; Cotter and Robertson, 1999; Grundhoff and Ganem, 2003; Skalsky et al., 2007a). This arrangement ensures that the viral genome is maintained during cellular mitotic division(s). In addition LANA directs episomal DNA replication at the latent viral replication origin during latency by binding to specific sequence elements within the viral TR's (Ballestas and Kaye, 2001; Hu et al., 2002; Stedman et al., 2004; Verma et al., 2006). LANA also has transcriptional and protein:protein interactions which modulate infected host cells to ensure continued cellular proliferation and growth and the stable preservation of viral latency.

LANA binds to several sites within the host and viral genome and has been shown to repress and activate transcription of both viral and cellular promoters, including its own (An et al., 2005; Jeong et al., 2004; Lan et al., 2004; Lu et al., 2012a; Ottinger et al., 2006; Renne et al., 2001; Roupelieva et al., 2010; Shamay et al., 2006; Tang et al., 2003; Verma et al., 2004). The LANA

protein also interacts with DNA methyltransferases, chromatin remodelers, and cellular transcription factors which contribute to its transcriptional modulatory functions (An et al., 2004; Bubman et al., 2007; Cai et al., 2006; Chen et al., 2012b; Kusano and Eizuru, 2010; Lan et al., 2005a; Lim et al., 2001; Lim et al., 2000; Liu et al., 2007; Roupelieva et al., 2010; Sakakibara et al., 2004; Shamay et al., 2006; Stuber et al., 2007; Verma et al., 2004). Furthermore, LANA interferes with cellular tumor suppressors functions, such as p53 and retinoblastoma protein, and several other pathways important to cell proliferation and oncogenesis (Ballestas and Kaye, 2011; Chen et al., 2010; Fakhari et al., 2006; Friborg et al., 1999; Fujimuro and Hayward, 2003; Fujimuro et al., 2003; Katano et al., 2001; Radkov et al., 2000). The transcriptional capacity and the interactions with other important proteins in infected cells make the KSHV LANA protein a nexus of viral genome persistence and cellular proliferation and oncogenesis.

vCyclin

vCyclin is a virally encoded homologue of cellular cyclin. In KSHV pirated homologues of cellular genes are denoted by a preceding "v" (see Figure 1.2). The protein is constitutively expressed from the viral latency locus along with LANA (Bieleski and Talbot, 2001; Dittmer et al., 1998; Pearce et al., 2005; Talbot et al., 1999). vCyclin is a functional cyclin that can stimulate retinoblastoma protein (Rb) to overcome cell-cycle arrest (Godden-Kent et al., 1997). Unlike cellular cyclin D, vCyclin is capable of degrading the cyclin-dependent kinase (CDK) p27Kip when complexed with CDK6, thus promoting cell cycle progression and proliferation in infected cells (Ellis et al., 1999). Moreover, transgenic mice with vCyclin develop lymphomas, albeit only in the absence of p53 (Verschuren et al., 2002) suggesting that in addition to cell cycle dysregulation, vCyclin may also have a role in the induction of genomic instability.

vFLIP

Viral FADD-like interleukin-1-β-converting enzyme (FLICE) inhibitory protein (called vFLIP) is the KSHV homologue of cellular FLIP (cFLIP). vFLIP is also latently expressed co-terminally with LANA and/or vCyclin (Bieleski et al., 2004; Bieleski and Talbot, 2001; Dittmer et al., 1998; Grundhoff and Ganem, 2001; Pearce et al., 2005; Talbot et al., 1999). vFLIP inhibits apoptosis induced by cellular death receptors which may provide a growth advantage to infected cells (Djerbi et al., 1999; Low et al., 2001; Thome et al., 1997). vFLIP can also induce the expression of anti-apoptotic genes via activation of NF-κB; a mechanism which protects cells against Fas-induced death (Chaudhary et al., 1999; Field et al., 2003; Guasparri et al., 2006; Matta and Chaudhary, 2004). vFLIP is essential for tumor cell survival in *in vitro* systems and can also prevent autophagy in B cells (Guasparri et al., 2004; Lee et al., 2009b). Additionally, transgenic mice bearing the vFLIP ORF develop B cell malignancies (Ballon et al., 2011; Chugh et al., 2005).

KSHV miRNA's

KSHV also constitutively expresses several miRNA's derived from 12 stem loops within the latency locus, some of which are also induced during lytic phase replication (Cai and Cullen, 2006; Cai et al., 2005; Gottwein, 2012; Pearce et al., 2005). At present the complete functionality of the KSHV miRNA's is unknown and our understanding thereof is continually expanding. Emerging evidence demonstrates that KSHV miRNA's are important in the context of oncogenesis and that they can modulate apoptosis, cell growth, cell cycle, and transcription in infected cells (Gottwein, 2012; Ramalingam et al., 2012). The KSHV miRNA's show some capacity to reprogram infected cells both transcriptionally and even epigenetically (Gottwein et al., 2011; Haecker et al., 2012; Hansen et al., 2010; Lu et al., 2010), and miRNA expression levels may even correlate with KSHV-associated disease progression (O'Hara et al., 2009; O'Hara et al., 2008).

KSHV encoded miRNA's can also target specific apoptotic factors such as Bcl2-associated factor (BCLAF1) and caspase 3, among others (Suffert et al., 2011; Ziegelbauer et al., 2009) to

overcome apoptosis in infected cells. KSHV miRNA expression also enhances angiogenic and proliferative phenotypes (Boss et al., 2011; Gottwein et al., 2007; Liu et al., 2012; Samols et al., 2007; Skalsky et al., 2007b). Although we do not fully understand the breadth of the KSHV miRNA repertoire, the known functions of these virally encoded factors suggest involvement in KSHV-associated malignancy.

Kaposin

The robust transcriptional program for the Kaposin ORF undergoes a complex splicing program to generate 3 different isoforms Kaposin A, B and C (Cai and Cullen, 2006; Li et al., 2002; Pearce et al., 2005; Sadler et al., 1999). Kaposin is abundantly expressed from the constitutive LANApc, and possibly also the LANAds, during latency (Cai and Cullen, 2006; Sarid et al., 1998; Sun et al., 1999), and low levels of latent expression have also been detected from the inducible Kaposin promoter (K12p) immediately upstream of the K12 ORF. Transcription from K12p is weak during latency but is potently induced during reactivation (Cai and Cullen, 2006). When transfected into Rat-3 cells Kaposin A generated focal transformation, and these cells subsequently generated highly vascular sarcomas after subcutaneous injection into athymic nu/nu mice (Muralidhar et al., 1998) and these phenotypic changes are thought to be driven by an interaction with cytohesin-1(Kliche et al., 2001). The Kaposin B isoform is capable of activating the p38 pathway and the stabilization of cytokine mRNAs which likely enhance the protein's transforming potential (McCormick and Ganem, 2005). Of note one of the KSHV miRNAs, miRNA- K12-10, is nested within the kaposin ORF and may contribute to the observed transforming potential of the Kaposin gene. While the levels of individual Kaposin isoforms can vary based upon cell line examined (Li et al., 2002; Sadler et al., 1999), expression from the Kaposin ORF is linked to the oncogenic capacity of KSHV.

Variably Expressed Oncogenic Factors

K1

Genes which are not found in other organisms but are instead unique to the KSHV genome are designated by the prefix "K". The K1 protein of KSHV is a transmembrane signaling protein encoded by the first ("leftmost") ORF of the viral genome. The K1 ORF is one of the most polymorphic viral ORF's (Hayward, 1999; Lagunoff and Ganem, 1997; Poole et al., 1999). K1 expression is induced during the viral lytic cycle, however low levels of latent expression have been observed (Chandriani and Ganem, 2010; Lagunoff and Ganem, 1997; Wang et al., 2006a). K1 has transforming potential and can immortalize endothelial cells in culture and can enhance angiogenesis and tumor vasculature *in vivo* (Lee et al., 1998b; Wang et al., 2006a). Cell signaling pathways relating to oncogenesis, angiogenesis, and proliferation are also perturbed via the K1 protein (Lagunoff et al., 1999; Lee et al., 1998a; Tomlinson and Damania, 2004; Wang et al., 2004a). Furthermore in transgenic mice the K1 protein can produce sarcoma-like tumors and lymphomas (Prakash et al., 2002).

K15

The K15 ORF of KSHV initiates near the distal ("rightmost") terminus of the viral genome and encodes a transmembrane protein with multiple spliced isoforms (Choi et al., 2000; Glenn et al., 1999; Wong and Damania, 2006). K15 is induced during the lytic cycle however some reports have identified expression in uninduced cultures (Choi et al., 2000; Jenner et al., 2001; Paulose-Murphy et al., 2001; Wong and Damania, 2006). Two different alleles of K15 are observed and are the basis for allelic differences in viral isolates; P and M (Poole et al., 1999). The K15 protein has been shown to have anti-apoptotic functions and is also capable of the activating NF-κB and mitogen-activated protein kinase pathways (Brinkmann et al., 2003; Sharp et al., 2002). The protein may also be able to generate pro-angiogenic signals and manipulate B cell activation in infected cells (Bala et al., 2012;

Pietrek et al., 2010).

vIRF-1

KSHV encodes 4 genes with homology to cellular interferon regulatory factors (IRF's) known as vIRF's. These proteins have roles in modulating host interferon system and innate immunity (reviewed in (Lee et al., 2009a)). In addition to innate immune perturbation, vIRF-1 and vIRF-3 have reproducibly demonstrated oncogenic properties (reviewed in (Jacobs and Damania, 2011)). vIRF-1 is considered a lytic gene, although latent expression has been detected in culture and in primary KS lesions (Dittmer, 2003; Jenner et al., 2001; Moore et al., 1996a; Sarid et al., 1998). Moreover, the vIRF-1 ORF is thought to contain two different start sites which could be under differential temporal regulation (Chen et al., 2000; Cunningham et al., 2003). vIRF-1 is capable of interfering with the tumor suppressor p53 and blocking p53-mediated apoptotic and transcriptional activities (Nakamura et al., 2001; Seo et al., 2001). vIRF-1 has also exhibited transforming potential *in vivo* (Gao et al., 1997), at least in part mediated through interactions with c-Myc (Jayachandra et al., 1999).

vIRF-3

Like vIRF-1, vIRF-3 (also called LANA2) also modulates the host immune system and is capable of suppressing p53 function (Jacobs and Damania, 2011; Lee et al., 2009a; Rivas et al., 2001). Unlike vIRF-1, vIRF-3 exhibits latent expression which is restricted to B cells and may or may not be induced during reactivation (Cunningham et al., 2003; Fakhari and Dittmer, 2002; Jenner et al., 2001; Lubyova and Pitha, 2000; Rivas et al., 2001; Wies et al., 2008). vIRF-3 is thought to inhibit apoptosis and NF-κB activity (Esteban et al., 2003; Seo et al., 2004) and stabilize hypoxia-inducible factor 1α (Shin et al., 2008). vIRF-3 may be required for the survival of KSHV-infected cells (Wies et al., 2008) and similarly to vIRF-1, vIRF-3 can also interact with c-Myc to promote lymphomagenesis (Baresova et al., 2012).

vIL-6

Human interleukin-6 (hIL-6) is an important cytokine involved in a wide array of cellular activities including cell grown and differentiation (reviewed in (Kishimoto, 2010)). KSHV encodes a homologue of hIL-6, called vIL-6 (reviewed in (Sakakibara and Tosato, 2011)). vIL-6 is expressed at low levels during viral latency and is up-regulated during lytic replication (Chandriani and Ganem, 2010; Moore et al., 1996a; Nicholas et al., 1997). The vIL-6 transcript can initiate at two different start sites and is responsive to RTA (Deng et al., 2002). RBPjκ binding is thought to mediate the RTA response and unlike most other viral genes also allows vIL-6 to respond to intracellular Notch (Chang et al., 2005a). Although vIL-6 expression has been differentially detected in KS, PEL, and MCD tumors; the role of vIL-6 in KSHV-associated malignancy has been established through various experimental means (Parravicini et al., 2000; Staskus et al., 1999).

T-cell immunodeficient mice injected with NIH3T3 cells transduced with vIL-6 demonstrated the potency of vIL-6 in augmenting angiogenesis, tumor growth, and plasmocytosis (Aoki et al., 1999). vIL-6 activates pathways such as MAPK, JAK/STAT, etc. similarly to hIL-6 (Molden et al., 1997; Osborne et al., 1999), which in addition to other effects can lead to increased VEGF expression and signaling effects (Liu et al., 2001). vIL-6 is not limited by the physiologic checkpoints that regulate endogenous hIL-6 activity, and hence this viral mimic has enhanced hIL-6-reponsive signaling capacity relative to hIL-6 (Molden et al., 1997).

vGPCR

KSHV also encodes a G-protein coupled receptor with homology to the cellular IL-8 receptor, and which contains seven transmembrane domains that are found in all cellular G-protein coupled receptors (Arvanitakis et al., 1997; Cesarman et al., 1996; Guo et al., 1997). vGPCR is considered one of the most potently induced lytic genes (Damania et al., 2004) and has constitutively active signaling capacity which can potently activate a multitude of cellular pathways important for

angiogenesis and proliferation including VEGF, p38, MAPK, Akt, mTOR, PI3 kinase, and small GTPases (Bais et al., 2003; Martin et al., 2011; Montaner, 2007; Montaner et al., 2001; Rosenkilde et al., 1999; Shepard et al., 2001; Sodhi et al., 2000). vGPCR can also upregulate transcription factors including NF-κB, HIF-α, CREB, and AP-1 which subsequently induce cytokines and proliferative/angiogenic factors (Cannon et al., 2003; Cannon and Cesarman, 2004).

Further, vGPCR is capable of direct immortalization and transformation of certain cell lines and can also generate tumors reminiscent of KS lesions in nude mice (Bais et al., 1998; Bais et al., 2003; Yang et al., 2000). vGPCR is expressed early in lytic infection as part of a bicistronic transcript which also encodes K14 (vOX2) (Kirshner et al., 1999), however expression may occur outside of viral reactivation during cell cycling (Kang and Lieberman, 2009) or in a subset of infected cells in culture or in tumors (Cesarman et al., 1995a) . Both vGPCR and vOX messages are expressed from the K14 promoter (K14p). The K14p is unusual as it is a member of the RTA-responsive bidirectional LANApi/K14p promoter which can also synthesize latent messages (Hilton and Dittmer, 2012; Matsumura et al., 2005). Notably, vGPCR expression can lead to both autocrine and paracrine signaling effects (Martin et al., 2011; Montaner et al., 2004), and hence vGPCR expression can affect infected cells and nearby cells which may or may not be infected.

1.5 Epigenetic Regulation of the KSHV Genome

The epigenetic regulation of eukaryotic genomes is a synthesis of chromatin structure and nucleosome positioning which serves to modulate transcription, differentiation, and the maintenance and replication of DNA (reviewed in (Luger et al., 2012)). Developments in the field have shed light on proteins that manipulate nucleosome structure, placement, modification, and ultimately the access to genomic DNA. The recent advances in epigenetic regulation extend beyond eukaryotic cells and into the realm of viral genomes (reviewed in (Knipe et al., 2013)). The study of epigenetic regulation in viral systems is tractable, and discoveries associated with viral epigenetics are

intrinsically interwoven with the understanding of chromatin biology in general. Moreover, such endeavors may prove invaluable in the pursuit of antiviral strategies.

Chromatin modifications during viral infections often occur in both the host and invading viral genomes. Large DNA viruses, especially those which establish long-live persistent infections are not excluded from epigenetic regulation. This is exemplified in KSHV, and the virus has evolved intricate tactics to utilize host epigenetic machinery to navigate existence within human cell nuclei, which are outlined below and are **discussed in greater detail in Chapter IV**.

Epigenetically Programming the KSHV Episome for Latency

In the incoming virion the linear KSHV genome is devoid of DNA methylation and nucleosomes (Bechtel et al., 2005; Gunther and Grundhoff, 2010). Shortly after *de novo* infection, the viral genome circularizes by joining of the TR's. Early in the stages of infection, before latency is effectively established, little is known about how the viral genome is epigenetically programmed for latency. Despite the relatively high GC content across the KSHV genome, DNA methylation of the viral genome is not an early event, but in culture models takes several days. The most noticeable effects of DNA methylation upon the viral life cycle are observed at the RTA promoter region, with a notably paucity of methylated viral DNA at the latency locus (Chen et al., 2001; Gunther and Grundhoff, 2010). DNA methylation occurs in KSHV during latency, but it is not required for the establishment of latency, and has only extensively (and inconsistently) been observed, at late time points in viral infection (Chen et al., 2001; Gunther and Grundhoff, 2010).

As viral latency ensues nucleosomes are incorporated through an unknown mechanism. However by five days post-infection, activating and repressive histone modifications are already present upon latent KSHV episomes, and these modifications persist after stable latent establishment (Gunther and Grundhoff, 2010; Stedman et al., 2004; Toth et al., 2010). Activating modifications on histone tails such as acetylated H3K9/K14 (H3K9/K14-ac; H3-ac) and trimethylated H3K4 (H3K4-me3) are found at the latency locus and other latent loci (i.e. the vIRF-3 promoter) in B cells.

Activating marks are also present at many immediate-early (IE) and delayed-early (DE) lytic cycle genes. IE/DE genes also contain so-called "bivalent" chromatin structures (Gunther and Grundhoff, 2010; Toth et al., 2010); histone tails modified with H3-ac or H3K4-me3 in addition trimethylated H3K27 (H3K27-me3). ORF's of the viral genome encoding late-lytic phase (L) products are generally marked by the sole presence of heterochromatic H3K27-me3 or trimethylation H3K9 (H3K9-me3). These observations have led the field to theorize that the modification of histone tails during latency generates poising at key lytic IE/DE genes and repression at L genes.

Histone-modifying enzymes are also bound to the viral genome including; (i) a Polycomb group repressive complex 2 (PRC2) member called EZH2, and (ii) a histone H3K9-me3 demethylase called JMJD2A (Chang et al., 2011; Toth et al., 2010). The EZH2 methyltransferase is co-localized with H3K27-me3 on the KSHV genome is thought to maintain the bivalency or repression at lytic loci. JMJD2A binding to the viral genome is anti-correlated with H3K9-me3 and instead binds at activated histone modifications where it serves to prevent H3K9 methylation. Other reports suggest wide scale genomic binding of the heterochromatic organizing protein Kruppel-associated box domain-associated protein-1 (KAP-1) (Chang et al., 2009).

Some lytic IE and DE genes adopt euchromatic structures in the latent episome yet remain transcriptionally inactive. Near the left lytic KSHV replication origin (called OriLyt-L) lie RTA-responsive promoters involved in immune-modulation and lytic viral genome replication: OriLyt-L, K5, K6, K7, and KSHV Polyadenylated Nuclear RNA (PAN) (Karki et al., 2011; Nakano et al., 2003; Wang et al., 2002; Wang et al., 2004d). Although RNA polymerase II (PolII) localization occurs at these lytic promoters during latency, productive transcriptional elongation is repressed by cellular components such as Negative Elongation Factor (NELF) (Toth et al., 2012). This phenomenon allows for rapid induction at this locus during lytic infection as well gene expression outside of the context of *bona fide* lytic induction. Productive PolII association which is not subject to repression occurs at latent episomal loci, such as the major LANA promoter; LANApc. Other reports indicate that the CCCTC binding factor (CTCF) and associated Cohesins can program PolII at the latency

locus, manipulate KSHV lytic transcription, control episomal maintenance, and coordinate long range inter-episomal linkages (Chen et al., 2012a; Kang et al., 2013; Kang et al., 2011; Stedman et al., 2008).

CTCF is emerging as a master regulator of stable latency in both human gammaherpesviruses (Kang et al., 2011; Knipe et al., 2013; Tempera et al., 2011). CTCF is a zinc finger DNA binding protein that can insulate chromatin, mediate interactions between distal regulatory elements, structurally configure DNA into looped structures, and regulate transcription (Donohoe et al., 2009; Merkenschlager, 2010; Phillips and Corces, 2009; Rubio et al., 2008; Wendt et al., 2008). In addition CTCF affects nucleosome positioning and the modification of histone tails (Barski et al., 2007; Fu et al., 2008). CTCF binding is widespread in the latent KSHV episome and a major peak exists within the KSHV latency locus. Here CTCF/Cohesins are thought to regulate a balance between latent and lytic transcription through local PolII programming and physical connections to other episomal (Chen et al., 2012a; Kang et al., 2013; Kang and Lieberman, 2009; Kang et al., 2011; Stedman et al., 2008). CTCF/Cohesin may be involved in silencing lytic viral gene expression and in coordinating long-range interactions between the viral genome during latency. Several questions still remain to be addressed regarding CTCF/Cohesin-mediated epigenetic regulation of KSHV latency, including how long-range interactions are specified and how CTCF programming unfolds at specific loci.

Reactivation from Latency in the Epigenetic Context

At present a full understanding of the epigenetic regulation of both the latent and lytic viral replication programs is lacking, moreover it is possible that latency and lytic infection are not as clearly demarcated as once suspected. Recent evidence indicates that even within a single cell, different viral genomes exhibit distinctly different epigenetic accessibility (Darst et al., 2013). It is clear however, that indirect as well as direct epigenetic mechanisms control reactivation. Canonical reactivation from latent infection is ultimately dependent upon relieving repressive chromatin at the RTA promoter (Lu et al., 2003). During latent infection the RTA promoter is covered in so-called

"bivalent" chromatin but is repressed by PRC2 and histone deacetylases (Toth et al., 2010). Upon reactivation the KSHV lytic gene PAN chaperones H3K27-me3 histone demethylases and H3K4-me3 methyltransferases to the RTA promoter (Rossetto and Pari, 2012). RTA then recruits histone acetyltransferases and chromatin remodelers to lytic promoters; including its own (Gwack et al., 2003a).

RTA expression is autoregulated at its own promoter to generate a positive transcriptional feedback loop with the aid of cellular transcriptional cofactors (Deng et al., 2000; Harrison and Whitehouse, 2008; Sakakibara et al., 2001; Wang et al., 2004b; Wang et al., 2003). Indirect epigenetic mechanisms prevent RTA activity to fine tune the dynamic balance between latency and reactivation (He et al., 2010; Jin et al., 2012; Lan et al., 2004; Lu et al., 2010; Yada et al., 2006). The extent to which LANA epigenetically organizes the viral genome outside of the TR's and how RTA overcomes CTCF/Cohesin-mediated repression at lytic loci is unknown. Understanding these biophysical phenomena would have broad applicability within and beyond our understanding of KSHV.

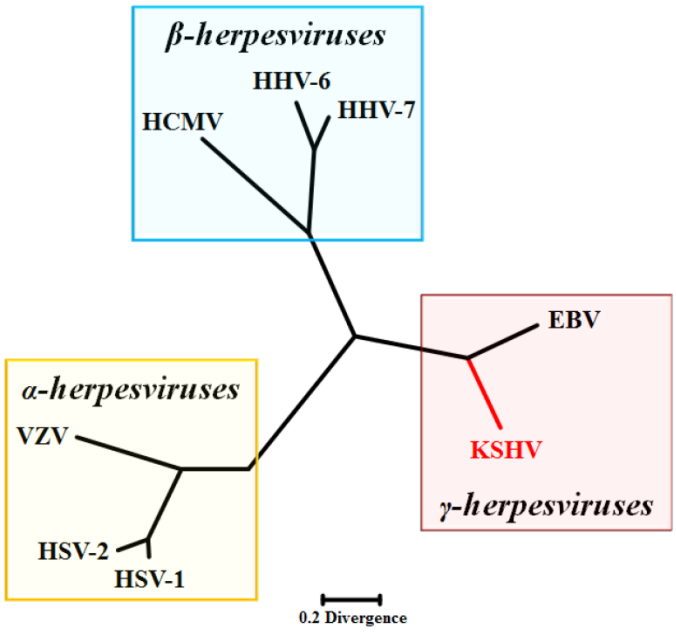

Figure 1.1: Human Herpesvirus Phylogeny. The eight known human herpesviruses are shown based upon amino acid similarity in respective major capsid proteins. The α-herpesviruses; varicella-zoster virus (VZV) and herpes simplex viruses 1 and 2 (HSV-1/2), are shown in orange. The β-herpesviruses; human cytomegalovirus (HCMV) and human herpesviruses 6 and 7 (HHV-6/7), are shown in blue. The gamma (γ) herpesviruses; Epstein-Barr virus (EBV) and Kaposi's sarcoma-associated herpesvirus (KSHV) are shown in red. The gammaherpesviruses are associated with malignancy in infected humans. (Figure adapted from Moore et al., 1996b).

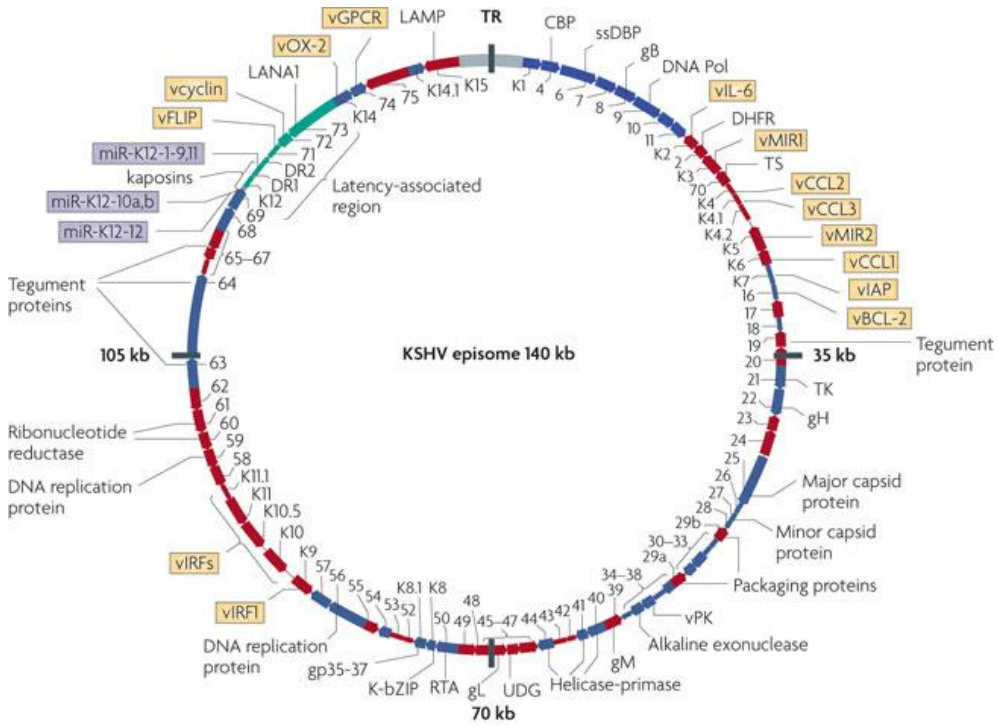

Figure 1.2: The KSHV Episome. The ~140 kilobase (kb) double-stranded DNA coding region of the KSHV genome is circularized in an episomal configuration after infection by fusing of viral terminal repeats (TR). Known KSHV open reading frames (ORF's) are numbered and those unique to the KSHV genome are denoted with a "K" prefix. Viral homologues of cellular genes are designated by yellow boxes and are lettered with a "v" prefix. Constitutively expressed latently-encoded genes, such as LANA, are shown in green. Noncoding RNA's such as the miRNA's are designated with purple boxes. Upon reactivation lytic genes are expressed in an ordered temporal cascade, with early lytic genes encoding transcriptional and viral replication proteins, and later lytic genes involved in the assembly of mature viral particles called virions. (Figure adapted with permission from Mesri et al., 2010).

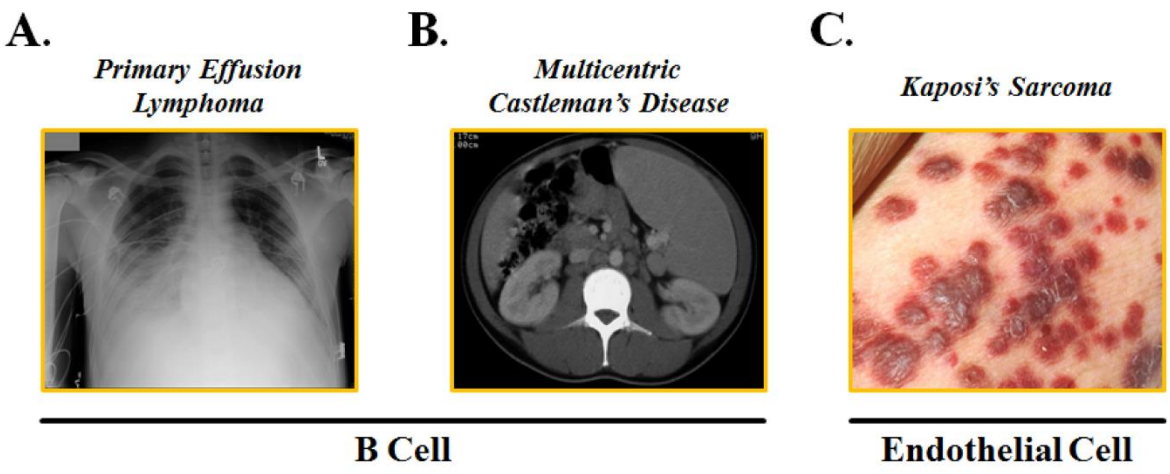

Figure 1.3: KSHV-Associated Malignancies. A. KSHV-induced oncogenesis manifests as Primary Effusion Lymphoma (PEL) in B cells (adapted with permission from Grubb et al., 2006) **B.** B cell infection can also give rise to Multicentric Castleman's Disease (MCD) (adapted with permission from Hillier et al., 2004). **C.** KSHV oncogenesis also occurs in endothelial cells in the form of Kaposi's Sarcoma (image courtesy of the National Cancer Institute).

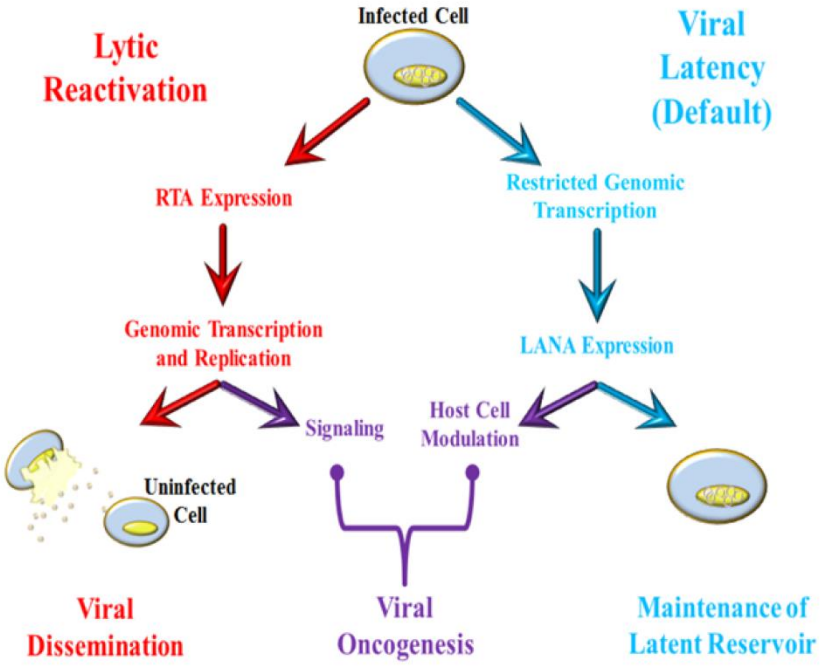

Figure 1.4: The KSHV Life Cycle. After KSHV infection the default viral replication program is latency, during which the viral genome exhibits very restricted gene expression. A handful of genes escape repression during latency including the KSHV Latency Associated Nuclear Antigen (LANA). LANA maintains the viral reservoir by assisting in viral genome replication and maintenance and also modulates the host cell transcriptionally and via protein interactions. Latency can be disrupted by various stimuli which ultimately induce expression of the KSHV Replication and Transcription Activator (RTA). RTA coordinates a temporal cascade of genome-wide viral gene expression and replication which leads to the production of mature virions and viral dissemination by lysis of the infected host cell. Both replication phases of KSHV are involved in mediating oncogenesis by encoding molecules which manipulate host cell signaling, proliferation, and growth.

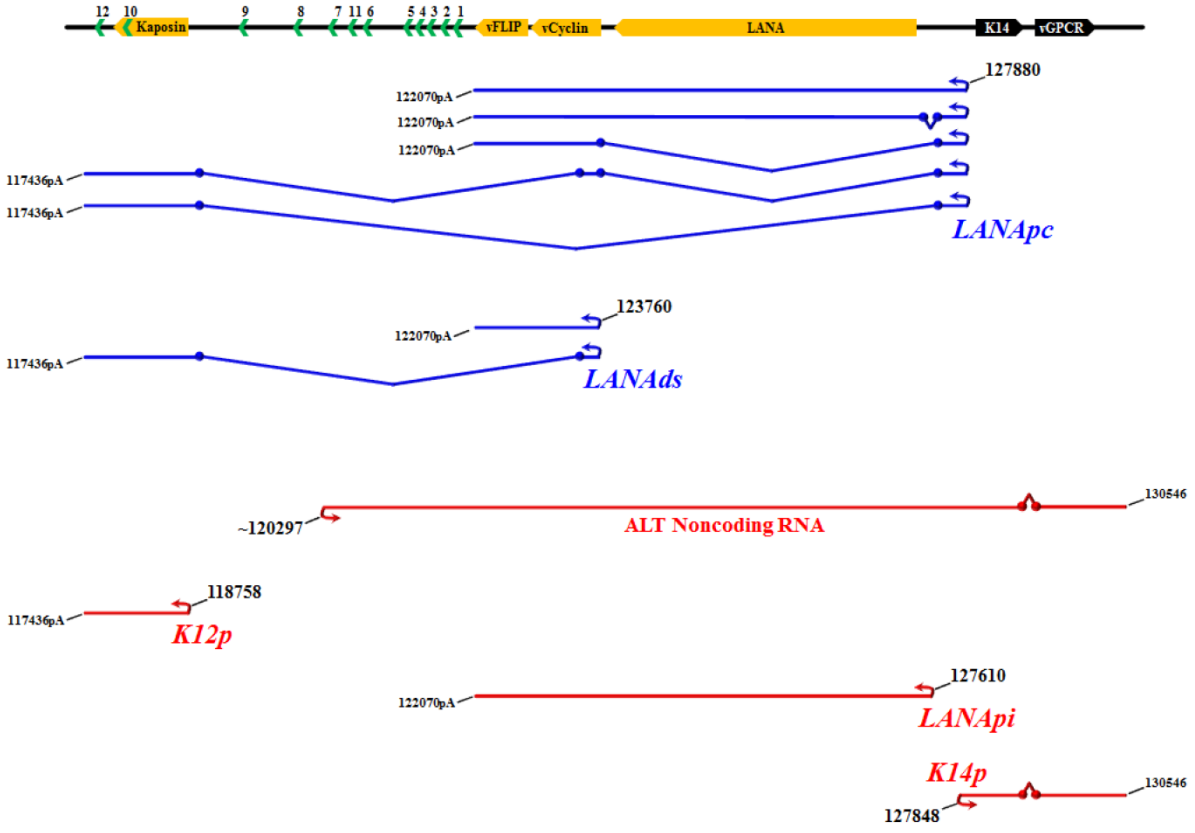

Figure 1.5: Transcripts from the KSHV Latency Locus. Constitutively expressed transcripts (shown in blue) originate from two promoters within the KSHV latency locus; the major latent promoter – the LANApc, and a downstream promoter – the LANAds. Through alternative splicing the LANApc can direct transcription of the viral genes LANA, vCyclin, vFLIP, Kaposin, and all identified viral pre-miRNA's (green chevrons numbered 1-12). During lytic phase induction other transcripts are generated in response to KSHV RTA (shown in red). This includes the Kaposin promoter (K12p) and the Antisense to Latency Transcripts noncoding RNA (ALT) of unknown function, the transcription start site (TSS) of which is incompletely mapped. The LANApi and K14p are members of a bidirectional promoter which responds to RTA. LANApi encodes LANA, vCyclin, and vFLIP but cannot generate the KSHV miRNA's or Kaposin due to lack of an appropriate splice donor. K14p drives expression of a bicistronic message encoding K14 (vOX2) and vGPCR. TSS's (shown as arrows) and polyadenylation sites (pA) are noted with and corresponding nucleotide positions in NC_009333. Splice sites are indicated but lack nucleotide labeling for simplicity.

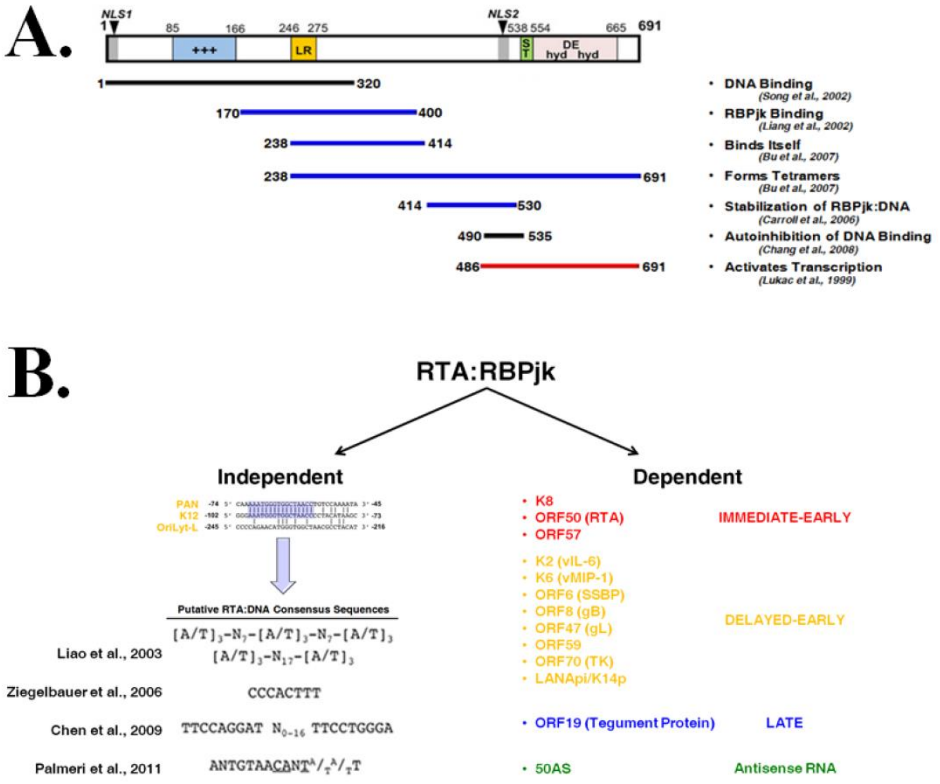

Figure 1.6: The KSHV Lytic Switch Protein: RTA **A.** The RTA protein is 691 amino acids (aa) in length and contains two putative nuclear-localization signals (NLS1/2). The protein is shown along with the corresponding aa numbers for; a basic amino acid rich region (+++), a leucine repeat region (LR), a serine/threonine rich region (ST), and a region containing repeats of hydrophobic/acidic aa. Numbered fragments below indicate mapped interacting domains of RTA and associated citations. The amino terminus of RTA binds DNA and the carboxy terminus contains the transactivation domain. In between are domains involved in self-association and binding to RBPjκ. **B.** RTA transactivates some promoters independently of RBPjκ by directly binding DNA and attempts at derived consensus motifs for RTA DNA binding elements are shown with citations. RTA transactivation is dependent upon the RTA:RBPjκ interaction at several viral promoters. Immediate-early (IE) viral genes (red), delayed-early (DE) viral genes (orange), and late (L) viral genes (blue) are indicated. RTA also relies on RBPjκ to initiate an antisense RNA from the bidirectional 50AS promoter. (Parts of this figure are adapted from Guito and Lukac, 2012).

CHAPTER II

QUANTITATIVE ANALYSIS OF THE BIDIRECTIONAL VIRAL G-PROTEIN-COUPLED RECEPTOR AND LYTIC LATENCY-ASSOCIATED NUCLEAR ANTIGEN PROMOTER OF KAPOSI'S SARCOMA-ASSOCIATED HERPESVIRUS[1]

2.1 Overview

Kaposi's sarcoma-associated herpesvirus (KSHV) establishes sustained latent persistence in susceptible cells. This is dependent on the latency-associated nuclear antigen (LANA). Understanding how LANA transcription is regulated thus aids our fundamental understanding of KSHV biology. Two hundred ninety-four base pairs are sufficient to regulate LANA transcription in response to the viral RTA protein and RBPjκ. The same region controls K14/viral G-protein-coupled receptor (vGPCR) transcription in the opposite direction. We used a quantitative analysis in conjunction with specific nucleotide substitutions and defined gain-of-function and loss-of-function RTA mutants to dissect this region. We used a bidirectional reporter driving red and green luciferase to study the LANApi and K14p promoters simultaneously. This established that LANApi/K14p functions as a canonical bidirectional promoter. Both were TATA dependent. K14p was favored by 50-fold in this context. Eliminating the distal LANApi TATA box increased maximal output and lowered the induction threshold (T) of K14p even further. Two RBPjκ binding sites were independently required; however, at high concentrations of RTA, direct interactions with an RTA-responsive element (RRE) could complement the loss of one RBPjκ binding site. Intracellular Notch (ICN) was no longer able to activate RBPjκ in the viral context.

[1]This chapter has been adapted from: Hilton, I.B., and Dittmer, D.P. (2012). Quantitative analysis of the bidirectional viral G-protein-coupled receptor and lytic latency-associated nuclear antigen promoter of Kaposi's sarcoma-associated herpesvirus. J Virol 86, 9683-9695.

This suggests a model whereby KSHV alters ICN-RBPjκ gene regulation. When the architecture of this pair of head-to-head RBPjκ binding sites is changed, the sites now respond exclusively to the viral transactivator RTA and no longer to the host mediator ICN.

2.2 Introduction

Kaposi's sarcoma-associated herpesvirus (KSHV) is a human oncogenic gammaherpesvirus. The KSHV genome is 137,000 bp long and encodes more than 70 open reading frames (ORFs). KSHV is associated with Kaposi's sarcoma (KS), primary effusion lymphoma (PEL), and multicentric Castleman's disease (MCD). Viral transcription is tightly regulated and can be divided into two well-defined states (Dittmer, 2003; Jenner et al., 2001). (i) During the lytic phase, the genome replicates and every viral promoter is active. (ii) During latency, the viral genome persists within the nucleus as a circular plasmid (episome) and is subject to the same regulation as human chromosomes (Gunther and Grundhoff, 2010; Pantry and Medveczky, 2009; Toth et al., 2010). As a result, this minichromosome is transcriptionally silent, with the exception of some key genes: the KSHV latency locus and a few genes that respond to cell type-specific and environmental stimuli. The KSHV latency locus encodes vital viral genes, which drive latent episome persistence: for instance, the latency-associated nuclear antigen (LANA) gene, as well as all viral microRNAs (Cai and Cullen, 2006; Dittmer et al., 1998; Ganem, 2010; Kang and Lieberman, 2009; Pearce et al., 2005; Talbot et al., 1999; Wen and Damania, 2010). Latent genes are central to KSHV tumorigenesis, since abrogation of LANA protein expression by small interfering RNA (siRNA) results in a loss of the KSHV plasmid and induction of apoptosis (Godfrey et al., 2005). Conversely, LANA expression can drive B cell hyperplasia in vivo (Fakhari et al., 2006; Sin et al., 2010).

LANA, vCyc, vFLIP, the viral microRNAs (miRNAs), and kaposin are transcribed via alternative splicing from a single promoter. Other promoters can regulate kaposin, vCyc/vFLIP, and the microRNAs separately from LANA (Bieleski et al., 2004; Bieleski and Talbot, 2001; Cai and

Cullen, 2006; Dittmer et al., 1998; Li et al., 2002; Pearce et al., 2005; Sarid et al., 1998; Talbot et al., 1999). The LANA promoter ensures the coordinated expression of this KSHV latent gene cluster, including all viral microRNA. Elucidating the molecular details of this regulation can be expected to contribute significantly to our understanding of KSHV persistence and the AIDS-defining malignancies, KS and PEL. A contiguous ~1,200-bp fragment contains all *cis* regulatory elements to ensure constitutive LANA promoter (LANApc) activity (Dittmer et al., 1998; Jeong et al., 2001; Jeong et al., 2002; Jeong et al., 2004). The LANA promoter is never methylated and is free of repressive histone marks (Chen et al., 2001; Gunther and Grundhoff, 2010; Toth et al., 2010). Thus, this locus provides the opportunity to investigate general principles of promoter structure and function in a defined genomic context; however, the situation is more complicated.

During latency, LANApc, a largely constitutive promoter, drives transcription of the LANA mRNA (Fig. 2.1A). It initiates transcription at position 127880. It is B cell-specific in transgenic mice (Jeong et al., 2002) and constitutively active in a large number of tissue culture cell lines. During reactivation, additional promoters are used. These are termed the LANApi, which is a promoter that can drive LANA transcription in response to the viral immediate-early transactivator RTA, and K14p, which is a promoter that drives a large K14/viral G-protein-coupled receptor (vGPCR) mRNA. Transcripts initiating from these two promoters have thus far been detected only in lytically reactivating cells. Nested within the LANApc untranslated region (UTR) is the bidirectional LANApi/K14p promoter (Fig. 2.1A), which is the subject of this study. The LANApi/K14 promoter is small (297 bp), and both transcription start sites (TSSs) are inactive during latency despite being located within an open chromatin environment. The LANApi/K14p region is part of a large class of bidirectional regulatory regions. Approximately 10% of human open reading frames (ORFs) are regulated via bidirectional promoters (Li et al., 2006; Trinklein et al., 2004; Wei et al., 2011). Bidirectional promoters regulate two ORFs positioned 5′ to 5′ (“head to head”) on opposite DNA strands. The TSSs for the majority of these bidirectional promoters are separated by less than 400 bp. Members of bidirectional gene pairs tend to utilize shared *cis* regulatory elements. Another human

gammaherpesvirus, Epstein-Barr virus (EBV), also exploits this mode of regulation (Jimenez-Ramirez et al., 2006).

A number of studies have looked at either K14p or LANApi by itself (Lan et al., 2005b; Liang and Ganem, 2004; Matsumura et al., 2005; Staudt and Dittmer, 2006) but thus far not at both in the bidirectional context. The LANApi TSS is positioned 313 bp upstream of the LANA protein translation initiation site (Matsumura et al., 2005; Staudt and Dittmer, 2006), and the K14p TSS initiates transcription 35 bp upstream of the K14 translation initiation site on the opposite strand (Chiou et al., 2002; Kirshner et al., 1999; Nador et al., 2001). The LANApi TSS utilizes a canonical TATA element (Matsumura et al., 2005; Staudt and Dittmer, 2006). A K14p TATA element has been predicted but not yet confirmed by functional studies. In sum, features of the LANApi/K14p pair resemble the architectural (spacing and strand identity) and functional (coexpression and coregulation) features of bidirectional promoters.

The LANApi and K14p TSSs are induced by the KSHV RTA transactivator. In fact, K14p is the most highly RTA-induced TSS in the entire KSHV genome (Damania et al., 2004). The RTA-mediated transactivation of LANApi and K14p displays a strict reliance upon two binding sites (Fig. 2.1B) for the human transcriptional adaptor RBPjκ (Liang and Ganem, 2004; Matsumura et al., 2005). The RTA-RBPjκ complex binds to these sites and activates the TSS. RTA functions as a multimer (Bu et al., 2007; Palmeri et al., 2011). The situation is more complex, however, since RTA can also bind DNA directly through a loosely defined RTA-responsive element (RRE) (Chen et al., 2009; Song et al., 2003; Song et al., 2002) and thus can activate other viral promoters independent of RBPjκ. Further, RBPjκ can be activated by its host partner intracellular Notch (ICN) independent of any viral proteins; reviewed in -(Miele, 2011). The LANApi/K14p region contains two RBPjκ elements, as well as a centrally located RRE, which could function to regulate K14p, LANApi, or both.

To further understand this regulation, we applied a quantitative model combined with single nucleotide and single amino acid mutant alleles of the *cis* recognition sequence elements and the RTA

DNA binding domain. Transactivators (*trans* inputs) and their cognate sequence elements (*cis* inputs) coalesce to regulate mRNA production in the form of a transcriptional regulatory circuit (Kim et al., 2009). These regulatory circuits can be described in quantitative terms using the Hill function (see equation (1)) (Kim and O'Shea, 2008; Kim et al., 2009; Kuhlman et al., 2007; Rosenfeld et al., 2005). This equation relates promoter output to transactivator concentration. Traditional, enzymatic studies use purified proteins and enzyme activity relates to the enzyme protein concentration. In our transfection studies, we did not know the intracellular RTA concentration, but we established that within the boundaries of our transfection series, doubling the input of a transfected expression plasmid resulted in a linear increase in the RTA protein. Hence, we can use this equation to characterize promoter behavior.

Three parameters describe the Hill function: the maximal output, measured herein as RLU s^{-1}_{max}; T, the induction threshold; and n, the Hill coefficient, which is a measure of cooperativity. By determining these parameters, we can make inferences about regulation and the biochemical mechanism of action.

$$\mathrm{RLU\ s^{-1}_{obs}} = \frac{(\mathrm{RLU\ s^{-1}_{max}}) \cdot [\mathrm{RTA}]^n}{[\mathrm{RTA}]^n + (T)^n} \qquad (1)$$

This mathematical framework is well known and has also been applied to study promoter activity in transfected cells (Kim and O'Shea, 2008; Kim et al., 2009; Kuhlman et al., 2007; Rosenfeld et al., 2005). For instance, the induction threshold T determines at which activator concentration the promoter is 50% active. A promoter with a lower T will be more active at lower transactivator concentrations. The Hill coefficient, n, indicates the cooperativity of the response. A Hill coefficient of >1 indicates a high degree of cooperativity and a step-like, "all-or-nothing" response curve; a Hill coefficient of ≤1 indicates a more gradual response. The maximal output provides a measure of promoter strength. A weak promoter will produce fewer transcripts (specifically, initiation events per unit time) than a strong promoter. One way to understand maximal

output is as follows: at the limit, the promoter initiates as many new transcripts per time unit as possible. Adding more specific transactivator no longer increases this rate, which is determined by how fast the general transcription factor complex can assemble and "reset" at the TATA element.

Using this framework, we investigated the LANApi/K14p response to RTA and report two new findings. (i) Our studies revealed a competitive relationship between the two TSSs, i.e., we found that one function of the LANApi TSS is to dampen the K14p response to RTA. (ii) Since LANApi/K14p contains two RBPjκ sites, we expected RTA-dependent transactivation to be highly cooperative. This was not the case. We found an unconventional utilization of the head-to-head RBPjκ element pair reminiscent of sequence-paired site (SPS) Notch signaling (Arnett et al., 2010; Cave et al., 2005; Ong et al., 2006) but evolved to respond solely to the viral transactivator and no longer to ICN.

2.3 Materials and Methods

Plasmids

All plasmids were sequence verified and match nucleotide positions 127583 to 128879 of the BC-1 KSHV genome (Russo et al., 1996). Site-directed mutations are shown in Fig. 2.1B. LANApi and K14p single reporter constructs (pDD2002 and pDD2005, respectively) were generated by cloning the genomic portion indicated above from pDD919 (nucleotides [nt] 127583 to 127879 in pBluescript II(KS+) [Stratagene]) into pCBG68 Basic and pCBR Basic (Promega Corp.) via SmaI/HindIII and KpnI/SmaI restriction sites, respectively. The bidirectional reporter construct (pDD2000) was generated by cloning the green luciferase isoform (pCBG68 Basic) into pDD919 via HindIII/SalI restriction sites, with a secondary subcloning step to incorporate the red luciferase isoform (pCBR Basic) via ligation of blunt-ended (End-It DNA repair kit; Epicentre), SmaI/BamHI-digested pCBR Basic, with the SmaI-digested, green-only vector intermediate. The LANApi single reporter, K14p single reporter, and bidirectional reporter variants, LANApiTBP (pDD2026, -2027,

and -2029_3-1), RBP A (pDD2024, -2028, and -2031), RBP B (pDD2022, -2023, and -2030), and K14pTBP mutants (pDD2013, -2015, and -2016), respectively, were generated using the GeneTailor site-directed mutagenesis system (Invitrogen) and the GeneAmp high-fidelity PCR system (Applied Biosystems). The bidirectional mutant variants, RRE (pDD2038) and 611-843 REV (pDD2034), were designed as synthetic oligonucleotides (Blue Heron Biotechnology Inc.) with flanking HindIII sites for subcloning into the HindIII self-ligated bidirectional empty vector (pDD2045). Regulatory elements were identified using the software program Alibaba 2.1 and a literature review. The wild-type (WT) ORF50 expression vector was a kind gift from J. Choe (Gwack et al., 2001). 4X-RBPjκ Luc (4X-CBF Luc) was generously provided by S. D. Hayward (Hsieh et al., 1996). The ORF50 mutant expression vectors (ORF50 KK/EE and ORF50 R161A) were generous gifts from G. Miller (Chang and Miller, 2004; Chang et al., 2005b). The Flag-tagged human intracellular Notch- and Myc-tagged RTA (Nakamura et al., 2003)-encoding constructs were kindly provided by J. Jung. Myc-tagged ORF50 KK/EE (pDD2032) and ORF50 R161A (pDD2033) were generated using the same methods as in reference -(Nakamura et al., 2003).

Tissue Culture and Transfection

SLK cells (Herndier et al., 1994) were cultured in Dulbecco's modified Eagle's medium (DMEM) supplemented with 5% fetal bovine serum, penicillin (0.05 μg/ml), and streptomycin (5 U/ml) (Invitrogen Inc.) at 37°C under 5% CO2. SLK cells were seeded at a density of 1.0×10^4 cells per well in 96-well plates (Sarstedt). The next day, transfection mixes were prepared using the RoboGo liquid handling system (Aviso) (or by hand in the case of Fig. 8 only) and then mixed with incomplete medium (DMEM without serum or antibiotic) and Superfect (Qiagen) as per the manufacturer's instructions. Total DNA was normalized with pBluescript II(KS+) (pDD223) such that a total 0.5 μg of total input DNA was transfected per well in all experiments. Similar to previous observations (Staudt and Dittmer, 2006), coincident expression of ORF50 consistently led to deviations in the expression of β-galactosidase, rendering this value unreliable for normalization

purposes. We therefore relied on extensive biological replicates. Transfections utilized the MWG RoboGo liquid handling system and were performed in triplicate, at least three different times. Those transfections that were performed by hand were performed in duplicate, at least two different times.

Luciferase Data Acquisition

Cells were lysed with 100 µl 1X cell Culture lysis reagent (Promega), undergoing gentle orbital rotation for 10 min at room temperature. Lysate was then mixed with the Chromaglo luciferase assay system (Promega) substrate or with luciferase assay system (Promega) substrate as per the manufacturer's instructions. Luciferase activity was measured using a FLUOstar Optima 96-well luminometer (BMG Labtech). Red and green signal outputs were separated as per the manufacturer's instructions using a 590-nm long-pass and 510/60-nm filter (Chroma Corp.), respectively. Luciferase activity was measured from each well for 10 s at 1-s intervals, with the final values derived by the luminometer software as the average of all interval readings (n = 10), such that the output therein was expressed as relative light units observed per second (RLU s^{-1}_{obs}). Filter correction was achieved using the Chroma-Luc technology calculator (Promega).

Data Fitting and Analysis

Raw luciferase data in the form of RLU s^{-1}_{obs} was generated via titration of WT RTA, KKEE RTA, or R161A RTA, with input values of RTA-encoding expression vector ranging from 0 to 86.5, 0 to 76.9, and 0 to 76.9 nM, respectively. Because equal molecular weights were input to maintain the optimal 0.5-µg/well transfection conditions outlined above in all experiments, the different molecular amounts between the input RTA expression vectors are reflective of the differences in double-stranded molecular weights. The raw output curves were fit to the Hill function (see equation (1)) via nonlinear least-squares regression (Kemmer and Keller, 2010), with three freely varying parameters: RLU s^{-1}_{max}, T (expressed in nM), and n (the Hill coefficient). Independent regression analyses were performed on each individual titration curve to generate independent values of RLU s^{-1}_{max}, T, and n

for each individual trial (i.e., $n \geq 9$ data points per titration curve). Global values were subsequently calculated by fitting the averaged outputs across all runs from each condition to generate a global fit, with standard error derived from the variance among individual runs. Initial analyses revealed adherence to first-order Hill kinetics (see Fig. 2.2); as such, we fixed the Hill coefficient to $n = 1$ for subsequent calculations (see equation (2)) (Chow et al., 2011; Kim and O'Shea, 2008; Ong et al., 2010). The apparent k_{cat} and efficiency T were calculated as described above (see equations (3) and (4)). The initial concentration (E_t) used to calculate the apparent k_{cat} was defined as the concentration (in nM) of measurable input reporter construct (held constant throughout each titration curve). This definition expresses the observed output as a function of total detectable molecular quantities, and other definitions (such as potential binding sites, etc.) arbitrarily dilute this relationship. Due to the differences in molecular weight, the single reporter alone, bidirectional reporter, and single reporter in *trans* (1:1) thus had corresponding values of E_t of 138 nM, 99 nM, and 69 nM, respectively.

Immunoblotting

SLK cells were transfected with Myc-tagged WT RTA, Myc-tagged KKEE RTA, Myc-tagged R161A RTA, or Flag-tagged ICN expression vectors as described above. After 4°C 1X phosphate-buffered saline (PBS) rinsing, two of three wells were harvested, rinsed again, and pooled, with subsequent lysis via RIPA buffer (50 mM Tris-HCl [pH 8.0], 150 mM NaCl, 1% NP-40, 0.5% deoxycholate [DOC], 0.1% SDS, 1 mM NaVO3, 1 mM dithiothreitol [DTT], 1X protease inhibitor cocktail [Sigma], and 1 mM phenylmethylsulfonyl fluoride [PMSF]). Total protein from lysates was normalized via a bovine serum albumin (BSA) assay (Pierce) and separated on 10% SDS-PAGE followed by transfer to PVDF membrane (GE Healthcare). Membranes were blocked in 5% nonfat milk in PBST (0.1% Tween 20). Antibodies were diluted in blocking buffer at 1:1,000 for anti-Myc (Cell Signaling), 1:5,000 for anti-Flag (Sigma), 1:5,000 for anti-β-actin (Sigma), and 1:5,000 for anti-mouse horseradish peroxidase (HRP) (Vector Labs). Luciferase analysis was carried out on the

remaining wells to ensure that epitope-tagged RTA variants responded similarly to responses of untagged variants (data not shown).

2.4 Results

LANApi and K14p Form a Bidirectional Promoter

To understand LANApi and K14p, we cloned the KSHV genomic region encompassing both TSSs (nt 127583 to 127879 (Russo et al., 1996)) into a dual reporter context (Fig. 2.3A). The LANApi TSS drove a green-emitting luciferase isoform and the K14p TSS drove a red-emitting luciferase isoform on the same plasmid. Previous experiments by us and others (Lan et al., 2005b; Liang and Ganem, 2004; Matsumura et al., 2005; Staudt and Dittmer, 2006) always used either one or the other promoter but never investigated both TSSs within the same construct.

We transfected the bidirectional-reporter vector and single-reporter controls with increasing amounts of an RTA transactivator expression construct into SLK cells. SLK cells are derived from a KS lesion but do not carry KSHV (Herndier et al., 1994). As a control, we switched the isoforms in some experiments and obtained the same response curves (Fig. 2.4). We used 12 different amounts of RTA expression plasmid to obtain high-resolution response curves. Western blotting confirmed expression of RTA upon transfection (Fig. 2.3D).

$$\mathrm{RLU\ s^{-1}_{obs}} = \frac{(\mathrm{RLU\ s^{-1}_{max}}) \cdot [\mathrm{RTA}]}{[\mathrm{RTA}] + (T)} \qquad (2)$$

To test the hypothesis that RTA cooperatively transactivates either TSS, the response RLU s^{-1}_{obs}) to increasing amounts of input RTA-encoding expression vector was fit to the Hill function. We found no evidence of cooperativity (i.e., Hill coefficient ≤ 1; see Fig. 2.2). This was surprising for a transactivator like RTA, which functions as a dimer or tetramer. The RTA response curves exhibited first-order kinetics. These can be modeled by the simpler equation (2) (Chow et al., 2011; Ong et al., 2010). It suggests that the RTA transactivation complex does not assemble from individual

monomers cooperatively at the DNA interface but that the slowest and thus rate-determining step is RTA dimerization/tetramerization. Our data suggest that in intact cells, RTA dimerization/tetramerization happens prior to DNA binding.

Bidirectional Promoter is Dominated by K14p

Both TSSs were responsive to RTA when transfected as single reporters (Fig. 2.3B and C, triangles) or when positioned in the bidirectional orientation (Fig. 2.3B and C, circles). Regardless of context, however, the K14p TSS had 10- to 100-fold-higher maximal output than the LANApi TSS. K14p was a much stronger promoter.

Since these experiments were conducted in transfected cells rather than with purified components in vitro, they take into account all molecular interactions that lead to luciferase output. Thus, rather than absolute numbers, the relative comparison of LANApi and K14p is important. We assume that the only variable in our experiments is the amount of RTA, and we conducted a series of validation experiments to support our data (see Fig. 2.4). Each data point is the result of three technical replicates. Each titration experiment was conducted in at least three biological replicates on different days. We switched the colored luciferase isoforms to verify that the response curves were defined by the *cis* elements rather than the reporter. We conducted real-time quantitative PCR (qPCR) for each luciferase reporter mRNA to show that the level of luciferase activity was linearly correlated with the level of mRNA and that the amount of transfected reporter DNA was the same among all replicates (see Fig. 2.4). These experiments validated that the luciferase readings are an accurate reflection of TSS activity.

Because the RTA response could be described by a first-order kinetic fit, we were able to calculate the parameters which characterize such a response. The first is k_{cat}, as shown in equation (3) (Garrett and Grisham, 2010):

$$k_{cat} = \frac{(V_{max})}{[E_t]} \rightarrow k_{cat} = \frac{(\mathrm{RLUs}^{-1}{}_{max})}{[\text{Input reporter}]} \qquad (3)$$

k_{cat} describes the promoter behavior at saturating levels of a specific transactivator. A higher k_{cat} value indicates more transcription initiation events per unit time. In kinetic studies, it relates the maximal output to the enzyme concentration (E_t). Here, calculating an apparent k_{cat} allowed us to directly compare experiments that used the bidirectional promoter and experiments that used the single reporter (as well as mutants) and also to normalize across biological replicates that transfect different amounts of luciferase reporter constructs.

K14p had a k_{cat} value of 713 ± 64 RLU s^{-1}, and LANApi had a k_{cat} value of 175 ± 32 RLU s^{-1} (Fig. 2.5A), verifying the differential promoter strength we observed when analyzing the raw data in each individual experiment.

LANApi TATA Element Limits K14p Activity.

We observed a consistent increase in the induction threshold T (Fig. 2.3E) for both TSSs when assayed in the bidirectional context compared to results in the single-reporter context. For K14p, the induction threshold T shifted from 4.2 nM input vector DNA for the single reporter to 13.1 nM in the bidirectional-reporter context. For LANApi, the induction threshold T shifted from 7.4 nM for the single-reporter to 33.7 nM in the bidirectional-reporter context.

A second, very informative and perhaps more relevant parameter (Bauer et al., 2001; Garrett and Grisham, 2010) is the ratio of k_{cat} to T (see equation (4)). This ratio is the promoter efficiency. It can be thought of as promoter activity at physiological levels, i.e., at and around the induction threshold T (the analog to T in enzyme biochemistry is the Km, though that strictly applies only to purified proteins). It is the most biologically relevant comparator among promoters. A promoter can be very strong (high k_{cat}), but if the induction threshold T is high, it will yield little output at low concentrations of transactivator. Conversely, a promoter can be very sensitive, i.e., become active at very low concentrations of transactivator, and still not yield much output if k_{cat} is low.

$$\text{Efficiency} = \frac{k_{cat}}{K_m} \rightarrow \text{Efficiency} = \frac{k_{cat}}{T} \qquad (4)$$

For each LANApi and K14p, the efficiency was much lower in the bidirectional context than in the single-reporter context (Fig. 2.5B, compare filled bars to empty bars). This reduction in efficiency when assayed in the bidirectional promoter construct compared to the single-reporter context was statistically significant, with a P value of ≤ 0.005 for LANApi and a P value of ≤ 0.05 for K14p using Student's t test. Similar differences were observed regardless of the luciferase isoform assayed (Fig. 2.4). These results provided the first indication that in the bidirectional context, more RTA is required for induction than in the single-reporter context. One model to explain this difference proposes that both TSSs compete for a central common RTA binding site. In the single-reporter context, the distal TSS is not functional. Even though a preinitiation complex may assemble, there is no ORF to transcribe and no poly(A) site to support efficient transcription. In the bidirectional reporter, preinitiation complexes assemble around both TATA elements and now can compete for the arriving RTA complex. This model predicts that the distal TATA element negatively regulates promoter activity, i.e., the LANApi TATA would inhibit K14p and vice versa (Fig. 2.6A).

To test this hypothesis, we inactivated the predicted TATA elements through site-directed mutagenesis. LANApi activity was dependent on a proximal TATA element. If we mutated the proximal LANApi TATA element, activity was abolished (Fig. 2.6B, arrow and red triangles). K14p activity also was dependent upon the proximal TATA element (Fig. 2.6C, gray diamonds). Note that panels B and C have different scales to account for the different overall activities. These experiments confirm the LANApi TATA element and define the K14p TATA element, which had been predicted but was not previously experimentally verified.

Deletion of the distal, (LANApi) TATA element dramatically increased the activity of K14p (Fig. 2.6C, red triangles and arrow). This observation is consistent with the aforementioned model in which the distal LANApi element inhibits K14p in the context of the bidirectional promoter. By comparison, deletion of the distal (K14p) TATA element only marginally affected LANApi activity (Fig. 2.6B, gray diamonds). This observation introduces asymmetry into the model. The LANApi TATA element inhibits the K14p TSS, but the K14p TATA element has no impact on the LANApi

TSS. In the absence of the LANApi TATA element, the K14p promoter became hyperresponsive to RTA. This prompted us to hypothesize that a second purpose of LANApi was the inhibition of K14p, more than driving the expression of the LANA protein.

Direct DNA Binding by RTA Augments Promoter Efficiency

Binding of RTA to the bidirectional LANApi/K14p region is mediated by RBPjκ, which is the essential downstream mediator of Notch signaling; reviewed in (Kovall and Blacklow, 2010). Two RBPjκ elements, RBP A and RBP B, mediate the response to RTA (Fig. 2.7A) (Liang and Ganem, 2004; Matsumura et al., 2005). To verify these observations, we mutated each in the context of the bidirectional reporter construct. As predicted, mutation of either RBPjκ element abolished promoter activity (Fig. 2.7B and C; please note the 10-fold difference in scale between the two panels). This demonstrates that both RBP elements were necessary.

In addition to RBPjκ-mediated DNA recognition, RTA can also bind DNA directly (Carroll et al., 2006; Chang et al., 2005b; Liang et al., 2002; Palmeri et al., 2011; Persson and Wilson, 2010). To test the hypothesis that direct RTA-DNA interactions were important, we used an RTA mutant with enhanced DNA binding capacity, called KKEE (Chang and Miller, 2004; Chang et al., 2005b). KKEE RTA increased the activity for both LANApi and K14p TSSs in the context of the bidirectional reporter. The maximal output increased from the WT level of ~17,000 to ~130,000 RLU s^{-1} for the LANApi promoter and from the WT RTA level of ~70,000 to ~880,000 RLU s^{-1} for the K14p. This translated into an increase in k_{cat} of 7.3-fold for LANApi and 12.4-fold for K14p. In contrast, another mutant, RTA R161A, which is capable of interaction with RBPjκ (Chang et al., 2010) but no longer binds DNA directly, decreased the efficiency for each TSS compared to results with wild-type RTA (Fig. 2.8A and D). This demonstrated that in addition to binding via RBPjκ, RTA binds directly to a binding site within K14p/LANApi and that this RTA-DNA interaction modulates the activation efficiency of either TSS.

To test the hypothesis that the KKEE mutant phenotype was dependent on an intact promoter,

we analyzed TSS efficiency for the TATA box mutants. Enhanced DNA binding by RTA could not compensate for a mutated proximal TATA box, presumably because there was no RNA polymerase II (Pol II) complex to activate in the first place. We recorded only a minimal signal (Fig. 2.8B and F). The DNA binding mutant RTA R161A was worse than the wild type under all conditions tested. As before, we observed an increase in K14p efficiency if the distal TATA box was compromised (Fig. 2.8D and E). This was not the case for LANApi (Fig. 2.8A and C). More subtle differences were also evident. In the wild-type situation, the KKEE mutant enhanced efficiency (Fig. 2.8A and D); however, in the context of a mutated distal TATA element (Fig. 2.8E and C), this was no longer the case. In sum, the hypermorphic phenotype of the KKEE mutant can be attributed solely to increased DNA binding. The dependency on the general transcription complex remains.

To test the hypothesis that at saturating concentrations RTA no longer depends on its own DNA binding activity, we used the R161A mutant, which is deficient in binding to the RTA-responsive element (RRE) but still binds to RBPjκ. First, we analyzed RTA R161A in the context of the wild-type promoter. There was no significant difference between the WT and the R161A mutant (Fig. 2.9A, and D, yellow bars). As expected, the KKEE mutant had increased activity (Fig. 2.9A and D, blue bars). The maximal output was 26,458 ± 3,993 RLU s^{-1} for the R161 mutant, compared to 17,275 ± 3,181 RLU s^{-1} for the WT RTA for LANApi and 80,527 ± 9,735 RLU s^{-1} for the R161 mutant for K14p, compared to 70,439 ± 6,347 RLU s^{-1} for the WT RTA for K14p. Thus, direct RTA-DNA interactions are not required at saturating concentrations of RTA. All contacts are established through RBPjκ.

What would happen in the absence of an RBPjκ binding element? Inactivation of either RBP A or RBP B severely reduces the activation by RTA. This was the main message of the results shown in Fig. 2.7. However, the power of our quantitative analysis and the large number of replicates and dose steps allows us to compare accurate parameters, such as maximal output, shown in Fig. 2.9, among promoters of vastly different activities. At saturating concentrations, the DNA binding mutant R161 was no worse than the wild type on the LANApi promoter. (Fig. 2.9B and C, yellow). The

situation was different for K14p (Fig. 2.9E and F, yellow). In the absence of a functional RBP A site, R161A RTA had a lower maximal output than the WT on K14p (Fig. 2.9E, red star). In the absence of a functional RBP B site, which is proximal to K14p, the R161A DNA binding mutant was identical to the wild type. This suggests that the RRE contributes to the activity of K14p. Note that loss of any one RBP site severely cripples the promoter. Hence, this difference should not be overinterpreted.

In each case the KKEE mutant could substitute for the loss of an RBP site (Fig. 2.9, blue bars). In the context of a wild-type promoter, KKEE RTA was better than WT RTA, as previously observed. In the context of an RBP-deficient promoter, KKEE RTA was able to complement the *cis* defect and restore k_{cat} to wild-type levels. These data demonstrate that improved interactions between RTA and an RRE DNA element in the case of KKEE RTA can complement for a loss of interaction between RTA-RBPjκ and a single RBP site.

The absence of functional DNA binding by RTA increased the activation threshold for both TSSs. The induction threshold was 126.4 ± 2.7 nM for the R161 expression plasmid, compared to 33.7 ± 8.3 nM for the WT for the LANApi TSS, and 80 ± 14.2 nM for the R161 mutant, compared to 13.1 ± 5.5 nM for the WT for the K14p TSS. Of note, R161 also makes normal RBPjκ interactions. This verifies two aspects of our model: (i) direct RTA-DNA contacts increase the responsiveness of these TSSs at low concentrations of RTA, and (ii) at saturating concentrations, the direct RTA-DNA contacts can complement RBPjκ element defects.

The direct RTA-DNA contact is mediated by a regulatory element, termed the RTA Response Element (RRE), which is present between the two RBP elements (Fig. 2.10A). Previously this RRE element was shown to have less of an impact upon transactivation than the RBPjκ elements (Liang and Ganem, 2004; Matsumura et al., 2005). We confirmed these observations. Loss of the RRE site led to equivalent reductions in output for both TSSs when assayed with any RTA variant (data not shown). This suggests that three *cis* elements, RBP A, RBP B, and RRE, together define the response behavior of the K14/LANApi bidirectional promoter.

Sequence Architecture between TBP Elements Provided Directionality for RBPjκ Transactivation

Since RTA binding sites function in tandem, transactivation could in principle act toward either side. In isolation, RTA-RBPjκ can bind to and activate promoters independent of orientation (Liang et al., 2002). In contrast, we hypothesized that spacing of the RBPjκ elements imparted directionality to the bidirectional KSHV promoter. To test this hypothesis, we switched the orientation of the intervening sequence between the two TATA elements (Fig. 2.10A). We then cotransfected either the WT or KEEE RTA at a 1:1 molar ratio. Reversing the sequence of binding sites relative to LANApi increased the output of LANApi (Fig. 2.10B). This was true for either mutant. KKEE RTA in this experiment served as a better RTA. The reverse was not true. Reversing the sequence of binding sites relative to K14p did not increase the output of K14p (Fig. 2.10C). This demonstrates that the specific orientation and distance of the two RBPjκ binding sites and the RRE element confer preferential activation of the K14p TSS.

RBPjκ binding sites are RTA specific and insensitive to Notch

Given the stringent reliance of this viral promoter upon the effector of Notch signaling, RBPjκ, we hypothesized that overexpression of the host ligand might also activate these TSSs. The host ligand for RBPjκ is the transcriptionally active, cleaved form of the human Notch protein: intracellular Notch (ICN). Unlike RTA, ICN does not have RBPjκ-independent DNA binding activity and thus cannot engage the RRE. We transfected cells with LANApi, K14p, or a positive control consisting of 4 RBPjκ sites. The positive control containing four RBPjκ sites -(Hsieh et al., 1996) responded as expected (Fig. 2.11A); however, neither K14p nor LANApi responded to activation by ICN. Western blotting confirmed ICN expression (Fig. 2.11B). Thus, even though the RBPjκ elements are essential with regard to RTA-mediated induction of either TSS, their orientation within the viral promoter can no longer use ICN.

We had observed a similar phenotype when we profiled KSHV gene expression in response

to ICN and RTA (Chang et al., 2005a). One possibility to explain this phenotype comes from recent observations that revealed a requirement for ICN target loci to have a head-to-head, paired RBP element orientation as well as strict spacing requirements -(Arnett et al., 2010; Cave et al., 2005; Ong et al., 2006) . In human promoters the canonical architecture is spatially restricted to a maximum distance of ~15 to 19 bp between adjacent RBPjκ sites. In contrast, 79 base pairs bridge the two head-to-head RBPjκ sites in the KSHV promoter (Fig. 2.11C). By extending the sequence spacing, the RBPjκ pair can no longer be bridged by ICN but requires multimers of a different transactivator: RTA.

2.5 Discussion

The KSHV latency control region plays multiple roles during the viral life cycle. During *de novo* infection, the immediate-early transactivator RTA is brought in with the virion (Bechtel et al., 2005; Lan et al., 2005b). This results in an initial burst of lytic and latent transcription (Krishnan et al., 2004). During this phase, RTA drives LANA and K14/vGPCR protein expression from the lytic LANApi and K14/vGPCR promoters (Lu et al., 2011). Eventually the constitutive LANA promoter takes over. It is active independent of RTA or other viral proteins (Jeong et al., 2002; Jeong et al., 2004). As LANA protein accumulates, it also inhibits RTA (Jin et al., 2012; Lan et al., 2004). This leads to a stable autoregulatory loop during which LANA activates its own promoter (Jeong et al., 2001; Jeong et al., 2004). Reexpression of RTA is necessary and sufficient for KSHV reactivation (Lukac et al., 1999; Lukac et al., 1998; Stedman et al., 2008; Xu et al., 2005). Yet LANA is dispensable for KSHV reactivation and replication in KSHV and related gammaherpesviruses (Budt et al., 2011; Li et al., 2008; Lu et al., 2006; Moorman et al., 2003; Wen et al., 2009). Perhaps LANApi evolved not to regulate LANA protein expression during lytic replication. Perhaps the unique architecture of two divergent RTA-dependent TSSs in such close proximity reveals a novel molecular mechanism of RTA/RBPjκ/ICN regulation. To investigate these conjectures, we studied

the regulation of LANApi and of K14p in quantitative terms.

This report demonstrates that the LANApi/K14p locus constitutes a *bona fide* KSHV bidirectional promoter. This is the first functional verification of a bidirectional promoter within the KSHV genome; others are predicted (I. B. Hilton, D. Wang, and D. P. Dittmer, unpublished). Bidirectional transcription has been identified in Epstein-Barr-Virus (EBV) (Jimenez-Ramirez et al., 2006; Laux et al., 1989). It was studied in yeast and other eukaryotic model systems (Neil et al., 2009). By applying the same quantitative framework to KSHV, we have generated a detailed understanding of the functional roles that *cis* (regulatory elements) and *trans* (DNA binding) factors play in the transactivation of this genetic circuit. Each TSS (LANApi, K14p) is responsive to RTA when positioned on the same reporter. At least three shared RTA-responsive elements (RBP A, RBP B, and RRE) modulate this response. There exists a selective advantage for the K14p TSS. K14p is 10X to 100X more active than LANApi.

This report demonstrates a competitive relationship between the two TATA elements. This is reflected in a decreased efficiency for each TSS in the bidirectional reporter relative to the single-reporter-only input condition. The distal LANApi TATA element negatively regulates and limits K14p. A similar phenotype has been seen for some bidirectional promoters in yeast (Neil et al., 2009). Here too, mutation of one TATA element resulted in upregulation of the other. In the majority of those cases, however, the second distal TATA box initiates a noncoding or "cryptic" transcript. In the case of KSHV LANApi, the resulting transcript has the potential to encode the entire LANA ORF. We speculate that perhaps the LANApi TATA box evolved for two purposes: first, to drive transcription of the LANA protein during lytic replication, but more importantly to fine-tune the expression of K14 and vGPCR.

The interaction between RTA and RBPjκ is well established (Chang et al., 2010; Lan et al., 2005b; Liang et al., 2002; Liang and Ganem, 2004; Lu et al., 2011; Matsumura et al., 2005; Palmeri et al., 2011; Persson and Wilson, 2010; Staudt and Dittmer, 2006). Biochemical evidence suggests that RTA functions as a tetramer. This higher-order RTA complex then stabilizes RBPjκ on the DNA

and changes conformation such that the transactivation event takes place (Bu et al., 2007; Carroll et al., 2006; Chang et al., 2008; Palmeri et al., 2011). Here we have shown that while both RBP elements are critical, their importance is differential. The RBP B element is located 71 bp from the K14p TATA element (Fig. 2.12). The RBP A element is located only 7 bp from the LANApi TATA element. This introduces asymmetry. The asymmetry is also reflected in the spacing between the RRE and the RBPjκ elements. The RRE is spaced 17 bp away from the K14p-proximal RBP B element. This is the same spacing as for ICN-dependent RBPjκ pairs. In contrast, the RRE is spaced 50 bp away from the LANApi-proximal RBP A element. The net result is that K14p is 10 to 15 times more active at physiological, low concentrations of RTA. Last, we show that ICN no longer activates these paired RBP sites, because of extended spacing, and that now RTA is required as the bridging factor.

Taken together, we suggest the following model (Fig. 2.12). Based on prior work on RBPjκ - (Miele, 2011), we assume that in the ground state RBPjκ exists as a transcriptional repressor of both the LANApi and K14p TSSs (Fig. 2.12A). RBPjκ bound to RBP A effectively occludes other molecules from binding the LANApi TATA element due to extreme proximity (7 bp). In contrast, 71 base pairs separate the RBP B element from the K14p TATA element. Thus, the repression mediated by RBP B is less potent, resulting in a preassembly of the basal machinery at the K14p TSS. The RTA complex (likely tetrameric) then interfaces with the RBPjκ-bound DNA using the RRE to position the higher-order complex in favor of RBP B (Fig. 2.12B). Only 17 bp separates RRE from RBP B, compared to 50 bp which separates RRE from RBP A. This asymmetric assembly leads to an approximately 10-fold advantage for the K14p TSS over LANApi (Fig. 2.12C).

Since both LANA and vGPCR mediate important phenotypes in KSHV persistence, transmission, and tumorigenesis, the detailed dissection of this regulatory unit may contribute to our overall understanding of KSHV biology and gene regulation.

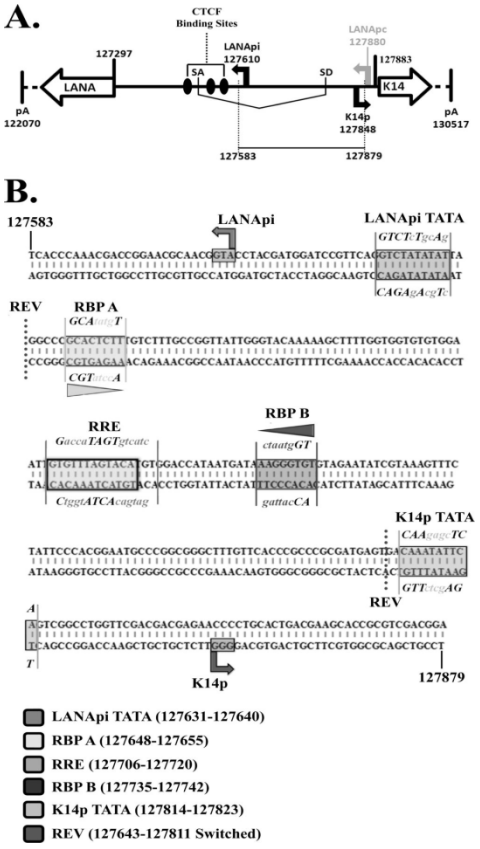

Figure 2.1: KSHV Genomic Organization of the LANApi and K14p TSS's. A. Schematic depiction of the nucleotide positions (according to Russo et al., 1996) spanning the LANA and K14 coding regions within the KSHV latency locus (vCyclin, vFLIP, and vGPCR are omitted for simplicity); SD, splice donor site; SA, splice acceptor site. LANApi, LANApc, and K14p TSSs as previously identified are shown. Also shown are CTCF binding sites as previously identified (Stedman et al., 2008). **B.** Sequence of the cloned genomic fragment used in analyses. Regulatory elements are indicated by text and boxed. Mutated nucleotides described in this report are shown in lowercase text, and nucleotide positions are indicated in the key below. Horizontal triangles indicate relative RBPjκ directionality; REV, location of the internal reversion mutant.

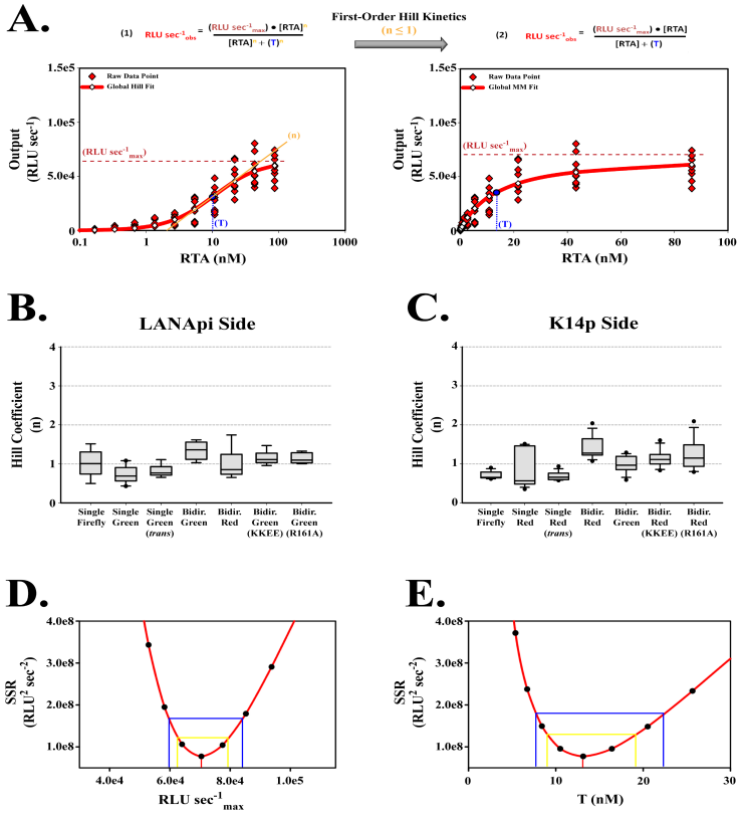

Figure 2.2: WT LANApi and K14p Adhere to First-Order Hill Kinetics. A. The global mean of raw data points (shown as diamonds, here for the WT K14p bidirectional configuration) corresponding to individually fitted response curves ($n \geq 9$ for all quantitative analyses) fit to the Hill equation without (left panel) or with (right panel) fixation of the Hill coefficient (1-3) to n=1 (i.e. MM kinetics). **B.** LANApi Hill coefficient in the absence of fixation reveals adherence to MM kinetics among various WT input configurations (Bidir. Red; bidirectional promoter reversed in which LANApi directs expression of red luciferase isoform). **C.** K14p Hill coefficient in the absence of fixation similarly reveals adherence to MM kinetics among various WT input configurations (Bidir. Green; bidirectional promoter reversed in which K14p directs expression from green luciferase isoform). **D/E.** Plot of the sum of squared residuals (SSR) against extracted parameters $RLUsec^{-1}_{max}$ (1D) and induction threshold (T; 1E) fitted via MM kinetics (shown for the WT K14p bidirectional configuration). Blue and yellow lines indicate 95% and 99% confidence intervals respectively, and vertical red lines indicate fitted values. **(**Figure adapted from Hilton and Dittmer, 2012 supplement).

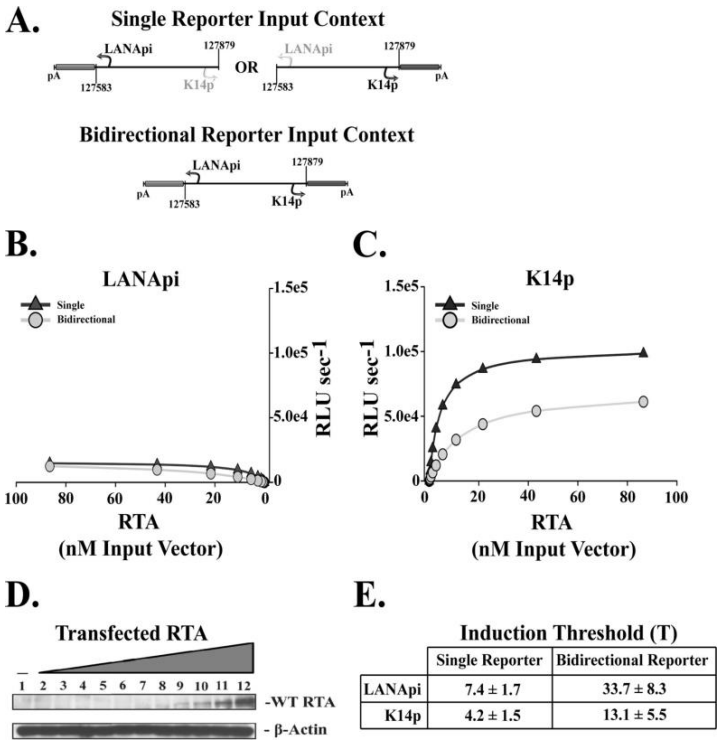

	Single Reporter	Bidirectional Reporter
LANApi	7.4 ± 1.7	33.7 ± 8.3
K14p	4.2 ± 1.5	13.1 ± 5.5

Figure 2.3: LANApi and K14p are a Bidirectional Promoter Activated by RTA. A. Single and bidirectional reporter constructs. LANApi directs expression of a green luciferase isoform, and K14p directs expression of an isogenic red luciferase isoform. **B.** The response to RTA for LANApi in single (triangles) and bidirectional (circles) reporter input contexts. **C.** The K14p response to RTA in single (triangles) and bidirectional (circles) reporter input contexts. **D.** RTA expression over the range of input expression vector as assayed by Western blotting. **E.** Induction threshold ± SE for each TSS. (Figure title adapted by first author from Hilton and Dittmer, 2012).

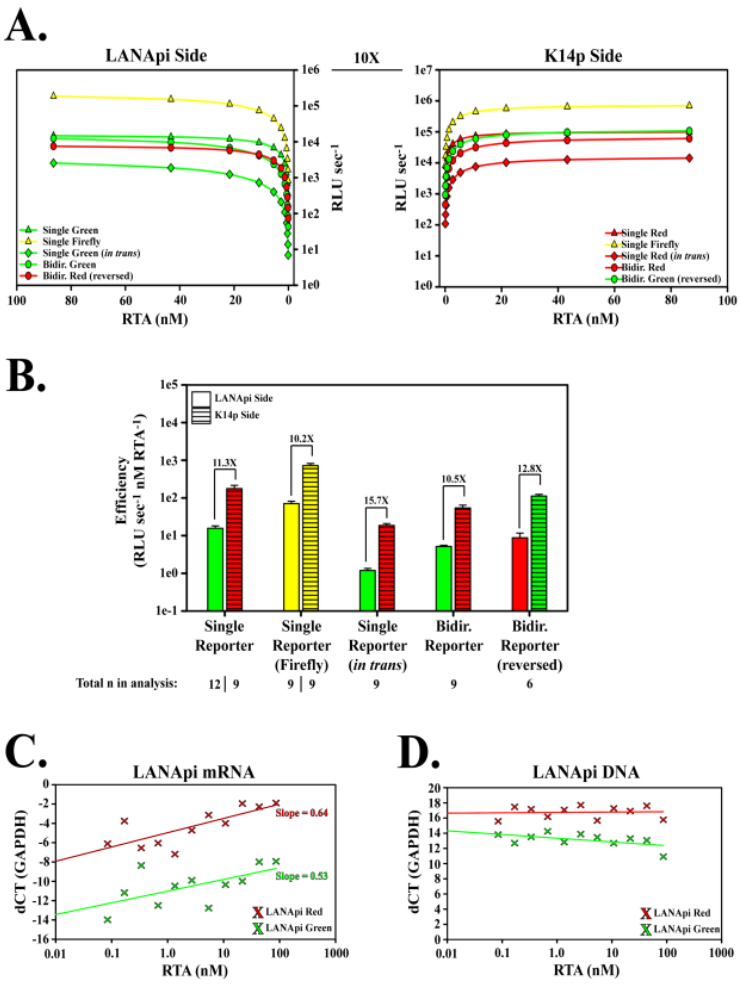

Figure 2.4: The Relative Advantage in Efficiency of WT K14p over WT LANApi is Static. A. Fitted output curves derived from assay with the LANApi (left panel) or the K14p TSS (right panel, note change in scale) in various indicated WT cloning configurations. **B.** The relative differential in the efficiency between K14p and LANApi in response to WT RTA is not significantly different among all WT input configurations independent of luciferase isoform. **C.** mRNA production from the WT LANApi cloned into a red-encoding single reporter construct (red X's and red fitted line) or into a green-encoding single reporter construct (green X's and green fitted line); indicating a similar response to RTA irrespective of luciferase isoform as assayed by QPCR using primer sets specific for each isoform. **D.** Input DNA from the same experiment as in 2C assayed contemporaneously indicating results are not reflective of increased input DNA. (Figure adapted from Hilton and Dittmer, 2012 supplement).

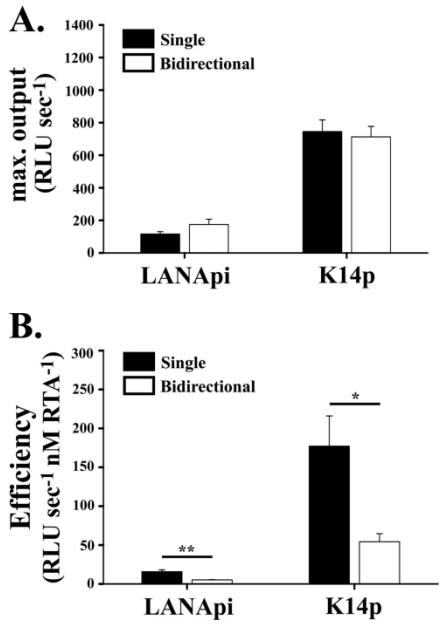

Figure 2.5: RTA Transactivation Based on Fit to Noncooperative Response Model (n = 1). A. The maximal output is shown for each TSS when assayed as single reporters alone (black bars) or in the bidirectional reporter (white bars). **B.** The efficiency of RTA-mediated induction is shown for each TSS as single reporters (black bars) or in the bidirectional reporter (white bars). "*" indicates $P \leq 0.05$; "**" indicates $P \leq 0.01$. P values were determined by Student's t test.

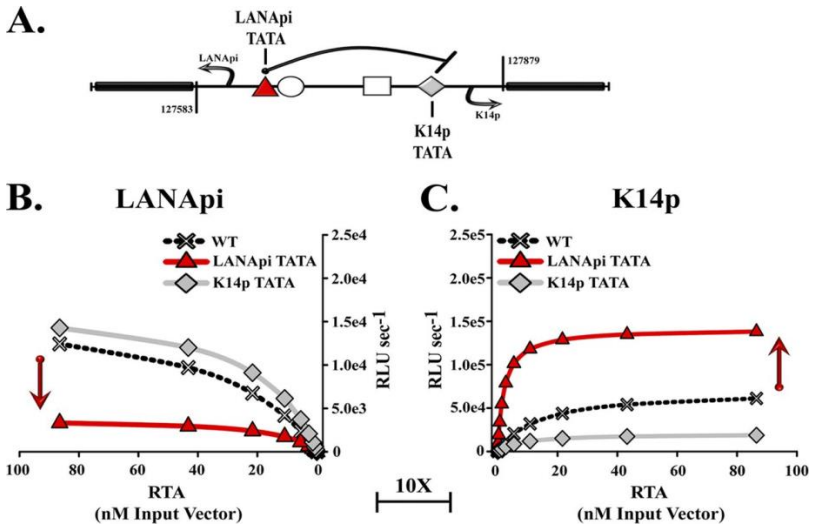

Figure 2.6: The LANApi-Proximal TATA Box Binding Protein (LANApi TATA) Element Limits K14p Output. A. Schematic illustrating the positions of the LANApi and K14p-proximal TATA elements (LANApi TATA [triangle] and K14pTATA [diamond], respectively) that were mutated in the bidirectional reporter construct. **B.** LANApi response to RTA in the presence (WT; cross) or absence of TSS-proximal (LANApi TATA; triangles) or TSS-distal (K14p TATA; diamonds) elements. **C.** K14p response to WT RTA in the presence (WT, X's) or absence of TSS-proximal (K14p TATA; diamonds) or TSS-distal (LANApi TATA; triangles) elements. Note the 10-fold change in scale between panel B and panel C.

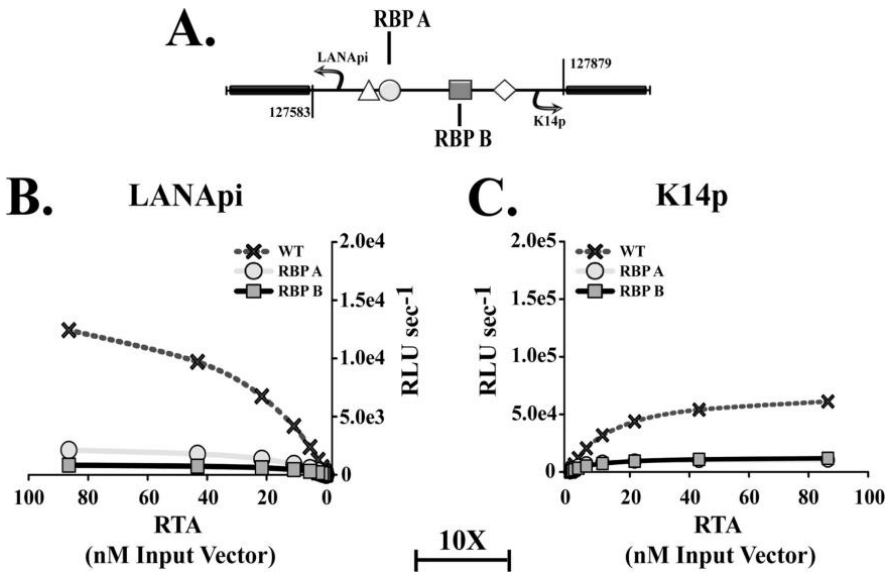

Figure 2.7: Both RBPjκ Elements are Essential. A. Schematic depicting the position of the LANApi- and K14p-proximal RBPjκ elements (RBP A [circle] and RBP B [square], respectively) mutated for analysis in the bidirectional reporter construct. **B.** LANApi response to RTA in the presence (WT; crosses) or absence of TSS-proximal (RBP A; circles) or TSS-distal (RBP B; squares) RBPjκ elements. **C.** K14p response to WT RTA in the presence (WT; Xs) or absence of TSS-proximal (RBP B; squares) or TSS-distal (RBP A; circles) elements. Note the change in scale between panels B and C.

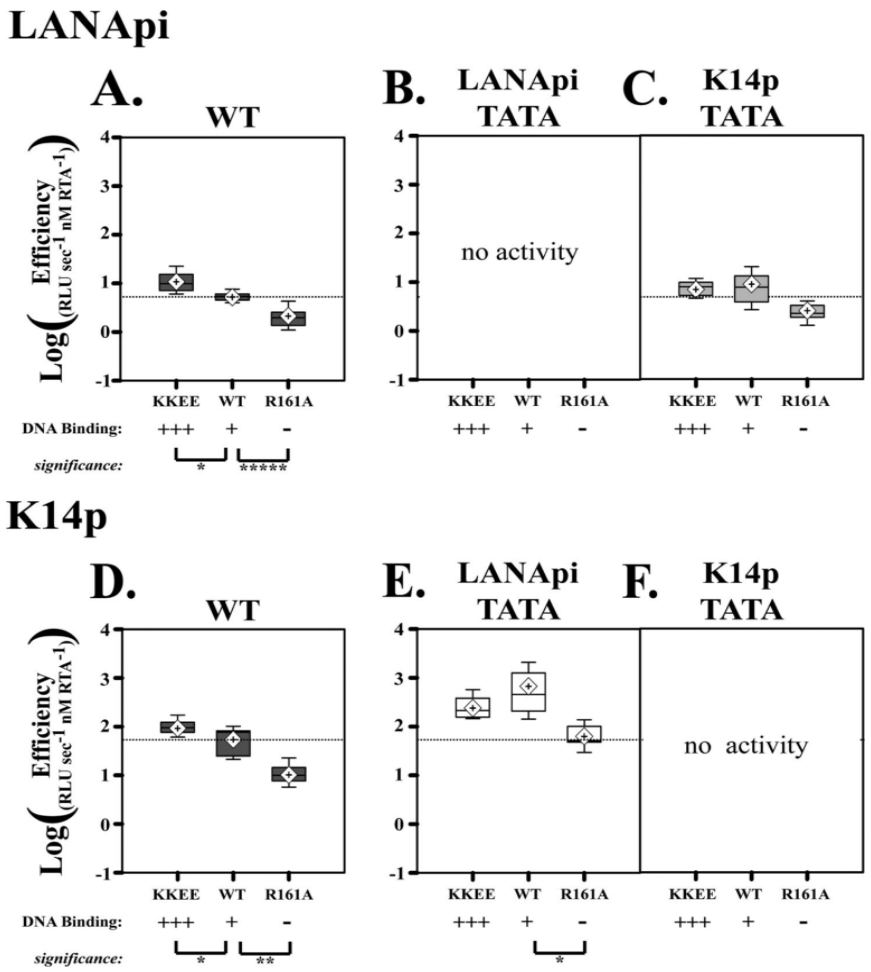

Figure 2.8: Enhanced DNA Binding by RTA Augments Promoter Activity. A. Log LANApi efficiency in response to increased RTA DNA binding (KKEE RTA) or loss of RTA DNA binding (R161A RTA). **B** and **C.** Efficiency of the LANApi response to KKEE, WT, or R161A RTA in the absence of proximal LANApi TATA (B) or distal K14p TATA (C). Note that in the absence of the proximal TATA element (B), we did not see significant reporter activity. **D.** K14p efficiency in response to increased RTA DNA binding (KKEE RTA) or loss of RTA DNA binding (R161A RTA). **E** and **F.** Efficiency of the K14p response to KKEE, WT, or R161A RTA in the absence of distal LANApi TATA (E) or proximal K14p TATA (F). Note that in the absence of the proximal TATA element (F), we did not see significant reporter activity. *, $P \leq 0.05$; ** $P \leq 0.01$; ****, $P \leq 0.001$; P values were determined by Student's t test, and dotted lines indicate mean WT efficiency.

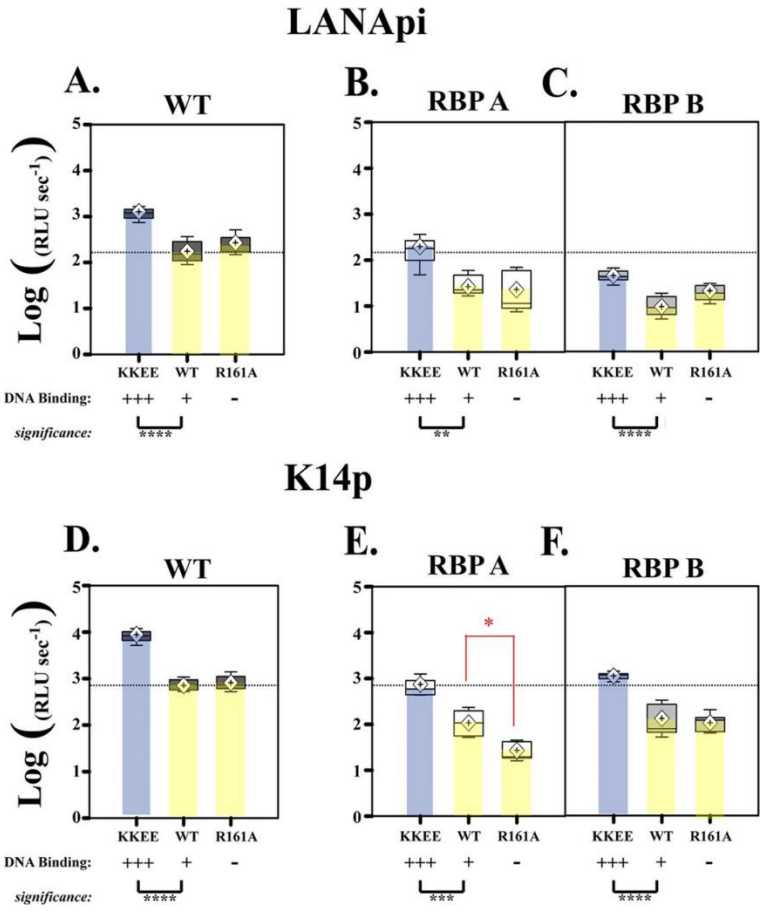

Figure 2.9: At Saturating Levels, RTA DNA Binding Becomes Dispensable. A. Normalized LANApi maximal output (analogous to k_{cat} for enzymes) in response to increased RTA DNA binding (KKEE RTA) or loss of RTA DNA binding (R161A RTA) mutant. **B** and **C.** LANApi response in the absence of proximal RBP A (B) or distal RBP B (C). **D.** Normalized K14p maximal output in response to increased RTA DNA binding (KKEE RTA) or loss of RTA DNA binding (R161A RTA). **E** and **F.** K14p response to KKEE, WT, or R161A RTA in the absence of distal RBP A (E) or proximal RBP B (F). The red star indicates a significant ($P \leq 0.05$) difference between WT and R161A RTA only in K14p with a mutated RBP A element (E). *, $P \leq 0.05$; **, $P \leq 0.01$; ***, $P \leq 0.005$; ****, $P \leq 0.001$. P values were determined by Student's t test; dotted lines indicate the mean WT promoter response to WT RTA.

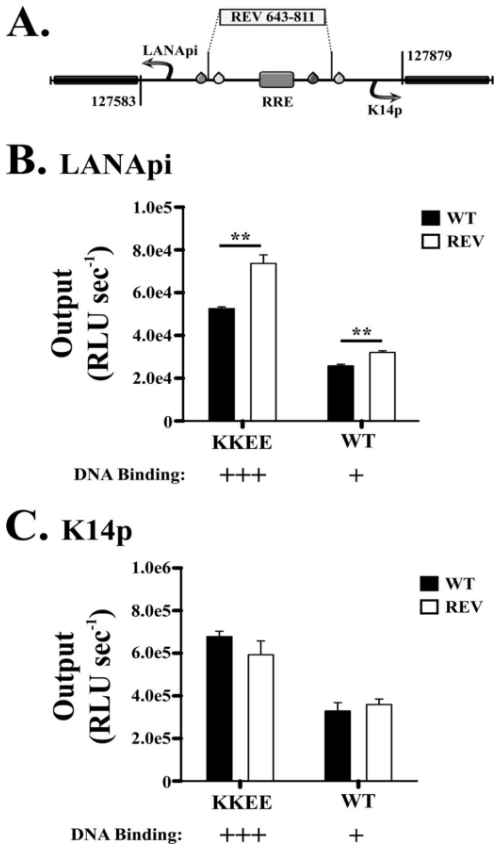

Figure 2.10: Directionality of RTA-RBPjκ Transactivation. A. Depiction of the REV mutant (sequence reversal of −2 bp relative to TATA elements) in the bidirectional reporter. RRE refers to the predicted RTA direct DNA binding element. **B.** LANApi output in the WT (black bars) and REV (white bars) bidirectional promoter variants in response to KKEE or WT RTA. **C.** K14p output in the WT (black bars) and REV (white bars) bidirectional promoter variants in response to KKEE or WT RTA.). **, $P \leq 0.01$; P values were determined by Student's t test.

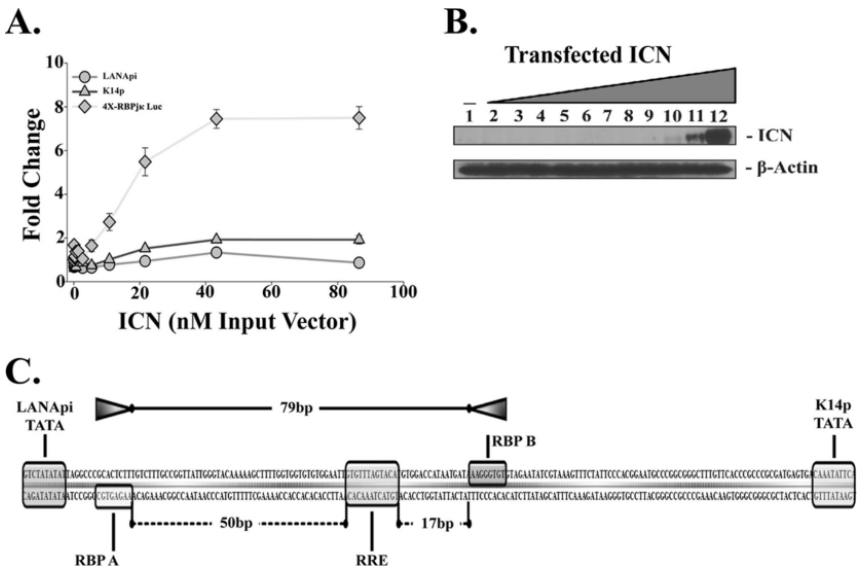

Figure 2.11: LANApi/K14p Response to Intracellular Notch (ICN). A. Fold change in relative luciferase activity in response to ICN for each TSS in the bidirectional reporter (LANApi, circles; K14p, triangles) or the TSS of positive control 4X-RBPjκ Luc (diamonds). **B.** Expression of ICN, detected by Western blotting. **C.** Illustration of the unequal RBPjκ head-to-head spacing within the LANApi/K14p bidirectional promoter. Shown are the distances in bp between the two RBP elements (top) and between each RBP element and the central RRE. Also shown are the two essential TATA elements for each promoter.

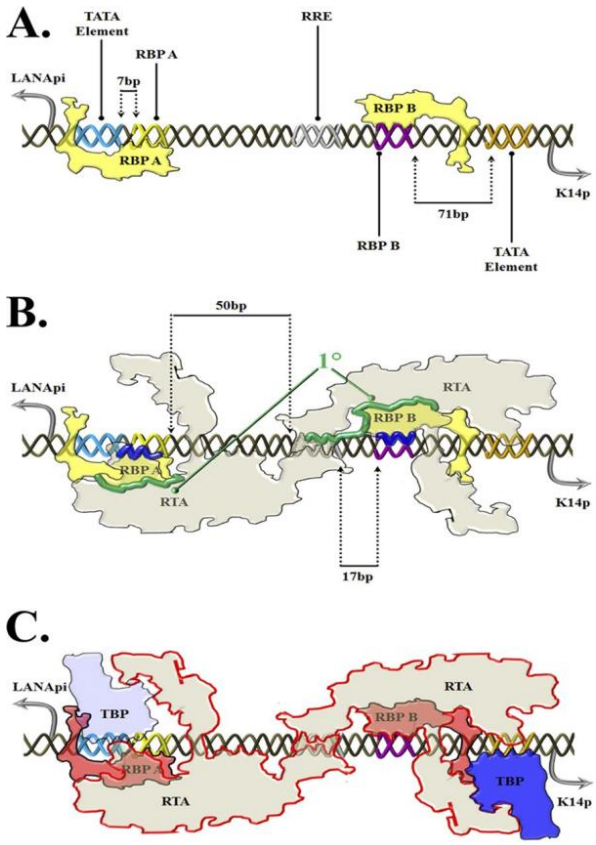

Figure 2.12: Summary and Putative Model of LANApi/K14p Activation by RTA. Shown is an artist's rendition of a general model of RTA/RBPjκ binding to bidirectional LANApi/K14p. **A.** "Ground state" RBPjκ elements are dynamically bound. RBPjκ complex bound to the RBP A *cis* site represses LANApi via shielding of the LANApi TATA *cis* element due to immediate (7 bp) proximity. RBPjκ complex bound to the RBP B *cis* site does not repress K14p because of distance (71 bp). **B.** "Recognition event" The interaction between the DNA surface and RTA is guided by interaction with both RBPjκ elements (1°; green) and the RTA protein complexes (presumably tetramer or higher (Palmeri et al., 2011)). Note that the RRE *cis* element also is recognized by the RTA protein complex. The distance between the RRE *cis* element and the RBP A *cis* element is 50 bp; that between the RRE and RBP B is only 17 bp. **C.** "Activation state" We envision a third state accompanied by overall conformational changes upon recruitment of the TBP complex. This is mediated by RTA DNA binding-dependent selective stabilization of proximal RBPjκ elements and is conveyed via low (LANApi)- or high (K14p)-activity TATA elements. Structural and *cis* regulatory discrepancies result in a suboptimal (LANApi) and optimal (K14p) asymmetric transactivation exclusively via RTA. The abbreviations are as follows: TATA, DNA consensus sequence element; TBP, TATA binding complex consisting of TATA binding protein and TAFs; RRE, DNA sequence element, RBPA/B RBPjκ complex consisting of one or more RBPjκ proteins and associated, undetermined cellular factors.

CHAPTER III

THE OPEN CHROMATIN LANDSCAPE OF KAPOSI'S-SARCOMA ASSOCIATED HERPESVIRUS[2]

3.1 Overview

Kaposi sarcoma-associated herpesvirus (KSHV) is an oncogenic gammaherpesvirus which establishes latent infection in endothelial and B cells, as well as in primary effusion lymphoma (PEL). During latency the viral genome exists as a circular DNA minichromosome (episome) and is packaged into chromatin analogous to human chromosomes. Only a small subset of promoters, those which drive latent RNAs, are active in latent episomes. In general nucleosome depletion, or "open chromatin", is a hallmark of eukaryotic regulatory elements such as promoters and transcriptional enhancers or insulators. We applied formaldehyde-assisted isolation of regulatory elements (FAIRE) followed by Illumina –based next generation sequencing to identify regulatory elements in the KSHV genome on the basis of nucleosome depletion and integrated this data with previously derived histone occupancy and CTCF Chip-Seq data. We find that (i) regions of open chromatin were not restricted to the transcriptionally defined latent loci, (ii) open chromatin was adjacent to regions enriched with activating histone marks, even at transcriptionally inactive loci; (iii) open chromatin overlapped with CTCF binding sites, with few exceptions including the constitutive LANA promoter and the vIL6 promoter. Nucleosome depletion was similar among B or endothelial cell lineage, suggesting a common viral genome architecture in all forms of latency.

[2]This chapter has been adapted from a manuscript in preparation by Hilton I.B., Simon J.M., Lieb J.D., Davis I.D., Damania B., and Dittmer D.P. The open chromatin landscape of Kaposi's sarcoma-associated herpesvirus.

3.2 Introduction

Kaposi sarcoma-associated herpesvirus (KSHV), or human herpesvirus 8 is the most recently discovered human herpesvirus and is a member of the gammaherpesvirus subfamily (Chang et al., 1994). It is linked with three human malignancies of either endothelial or B cell origin: Kaposi sarcoma (KS, of endothelial cell origin), Primary Effusion Lymphoma (PEL, of B cell origin), and a variant of Multicentric Castleman's Disease (MCD, of B cell origin) (Cesarman et al., 1995a; Chang et al., 1994; Soulier et al., 1995).

All herpesviruses display two alternating forms of infection: latency and productive lytic infection. During KSHV latency the ~140 kb viral genome exists as a non-integrated circular nucleosome-associated episome (reviewed in (Knipe et al., 2013; Mesri et al., 2010; Speck and Ganem, 2010)). The KSHV genome encodes over 80 predicted open reading frames (ORFs), 22 known viral microRNAs, and several long noncoding RNAs ((Chandriani et al., 2010; Dresang et al., 2011; Sun et al., 1996); reviewed in (Cullen, 2006; Zheng, 2010)). During latent infection only a few viral genes are transcribed including those within the KSHV latency locus (Dittmer et al., 1998; Sarid et al., 1999; Talbot et al., 1999). This locus employs a complex transcriptional circuitry to generate key viral messages including the mRNAs coding for the KSHV Latency Associated Nuclear Antigen (LANA; ORF73) (Cai and Cullen, 2006; Dittmer et al., 1998; Hilton and Dittmer, 2012; Kedes et al., 1997; Rainbow et al., 1997; Talbot et al., 1999), the viral cyclin homolog vCyclin (ORF72), vFLIP (ORF71), Kaposin, as well as all 12 viral microRNAs genes. Each micro RNA gene encodes one pre-miRNA, which can give rise to two mature miRNAs, albeit at widely differing ratios. LANA is necessary and sufficient to tether the KSHV genome to the human chromosome, thereby ensuring coordinated genome duplication and segregation during host cell division (reviewed in (Ballestas and Kaye, 2011)).

Prior studies established histone occupancy on the latent KSHV episome (Gunther and Grundhoff, 2010; Stedman et al., 2004; Toth et al., 2010), mapping specific activating and repressive

histones signatures, as well as DNA methylation status, PolII occupancy, LANA occupancy, and also CTCF/Cohesin interactions (Chen et al., 2012a; Kang et al., 2013; Kang and Lieberman, 2009; Kang et al., 2011; Stedman et al., 2008; Toth et al., 2012). Most of these prior studies were conducted solely in the prototypical BCBL1 cell line. Many, but not all, achieved single nucleotide resolution using ChIP-Seq technology. By comparison to mapping individual histone modifications little is known about chromatin organization, and how regions of open chromatin in KSHV are integrated with the so-called "histone code". Thanks to the authors of all prior studies making their raw data publicly available, we were able to expand on their work and to add our detailed map of KSHV nucleosome depletion in multiple KSHV infected cell lines at single nucleotide resolution.

The detection of nucleosome depletion has classically been accomplished by techniques such as DNase I hypersensitivity, which rely upon the differential in sensitivity to nuclease digestion of open chromatin relative to regions enriched in nucleosomes (Boyle et al., 2008; Gross and Garrard, 1988; Song and Crawford, 2010). An alternative method, called *F*ormaldehyde-*A*ssisted *I*solation of *R*egulatory *E*lements (FAIRE), has been developed to identify regions of open chromatin (Giresi and Lieb, 2009; Hogan et al., 2006; Nagy et al., 2003; Simon et al., 2012). FAIRE has been used to identify nucleosome depletion in several different eukaryotic organisms, cell lines, and tissues (Calabrese et al., 2012; Dunham et al., 2012; Gaulton et al., 2010; Giresi et al., 2007; Nagy et al., 2003; Ponts et al., 2010; Song et al., 2011). FAIRE is based on differences in cross-linking efficiency between DNA bound to nucleosomes and DNA in nucleosome depleted regions (Giresi and Lieb, 2009). Regions detected by FAIRE are concordant with DNase I hypersensitivity, however the efficacy of FAIRE is not dependent upon antibodies or enzymes making it a more robust approach (Dunham et al., 2012; Giresi et al., 2007; Simon et al., 2012; Song et al., 2011).

We find that histone modifications associated with transcriptional activity (H3K9/K14-ac and H3K4-me3) are enriched near FAIRE peaks, i.e. regions of open chromatin. Nucleosome depletion also overlapped with CTCF binding sites at many, but not all, KSHV loci. In fact, we could for the first time discern two types of open chromatin loci on the KSHV episome: those associated with

CTCF binding, which mapped to regions of immediate early and early genes, known to be transcriptionally silent during latency; and those free of CTCF, which mapped to transcriptionally active regions, such as the major latent promoter (LANA promoter; LANApc) and vIL6 promoter. Patterns of nucleosome depletion were largely conserved across different latently infected cell types, among multiple KSHV isolates, and independent of the episomal copy number in a latently infected cell.

3.2 Materials and Methods

Cell Culture

Latent KSHV infected lymphoma cell lines (BC1, BCBL1, and KSHV-BJAB) were cultured in RPMI supplemented with 10% FBS as previously described (Roy et al., 2011), with the exception that KSHV BJAB cells were maintained under 0.2mg/mL hygromycin selection (Nun et al., 2007). Latent KSHV-infected endothelial L1-TIVE cells (An et al., 2006) were grown in DMEM supplemented with 100 ug/mL streptomycin sulfate and 100 U/mL penicillin G and 5% FBS. Latently infected KSHV-HUVEC cells were cultured in endothelial growth medium (EGM-2, Clonetics) supplemented with 0.5ug/ml puromycin as previously described (Wang and Damania, 2008).

FAIRE-Seq

Chromatin was isolated from ~$1.0x10^7$ cells and subjected to FAIRE as detailed previously (Simon et al., 2012). Briefly, cells were cross-linked with formaldehyde, lysed, and then sonicated to shear DNA to an average fragment length of 200-400bp. Sheared chromatin was then collected by phenol/chloroform extraction. Two biological replicates of cell lines (BC1, KSHV BJAB, KSHV HUVEC, and L1 TIVE) were harvested and processed on different days to account for variation. FAIRE-enriched DNA was then subjected to library preparation using the Illumina Truseq DNA

Sample Preparation Kit V2 (Illumina) as per manufacturers instruction, or was prepared by the UNC High-Throughput Sequencing Facility (BCBL1). Indexed samples were sequenced using the Illumina HiSeq 2000 or GAII (for BCBL1 samples) (UNC High-Throughput Sequencing Facility) with 50bp single-end reads.

Sequence Analysis

Reads were filtered using TagDust (Lassmann et al., 2009) and individual sequencing runs were aligned to the reference KSHV genome NC_009333 using Bowtie (Langmead et al., 2009). Reads were permitted to align to up to four locations in the genome, but the single best possible alignment was chosen. Regions with significantly enriched FAIRE signal were differentiated from background using MACS2 (Feng et al., 2012) assuming the average fragment size was 250bp. Results from biological replicates were merged and resulting .BAM and .BED files were imported into CLC Bio (version 5.5.1) software for graphical display and further analysis. Previously published KSHV histone modification data (Gunther and Grundhoff, 2010) was analyzed, and regions with signal 3 standard deviations above baseline (from "Dataset S1") were considered significant enrichment and imported into CLC Bio. CTCF and KSHV LANA ChIP-Seq data (Chen et al., 2012a) were aligned to NC_009333 in CLC Bio using Gene Expression Omnibus (GEO) datasets GSM941710 and GSM941712 respectively. Further statistical analysis was conducted in R version 2.15.2.

3.4 Results

Open Chromatin Map of the KSHV Episome

To determine the regions of latent open chromatin in KSHV, we performed FAIRE-Seq on representative, latently infected cell lines. Table 3.1 summarizes the sequencing data. Because each latently infected PEL cell contains 20 – 50 viral genomes (Renne et al., 1996b), we achieved deep coverage and thus are confident in the detailed position of each FAIRE peak. Because KSHV-

HUVEC and L1-TIVE contain lower copies of the viral genome (Darst et al., 2013), a fewer percentage of reads from those samples aligned to KSHV. Nevertheless, even in these cases our mean coverage was comparable to the mean coverage used for FAIRE-based analysis of the human genome (Dunham et al., 2012). Confirming earlier data most of the viral episome was covered in nucleosomes and not enriched for open chromatin.

First, we performed FAIRE-Seq on the KSHV infected PEL cell line BCBL1 and aligned the resulting sequence reads to the KSHV reference genome NC_009333. We used the NCBI designated reference genome as the basis for comparison, rather than individual viral strain genomes, to attain common map positions across multiple samples. We showed earlier (Tamburro et al., 2012) that with the exception of the repeat regions, few large InDels exist among KSHV strains. The existing variation of small InDels and SNPs was accommodated by the analysis software. Of the ~2.6 x 10^7 total reads, 0.10% mapped to the KSHV genome in BCBL1 cells (Table 3.1). We used MACS2 to derive statistically significant nucleosome depletion (FAIRE peaks) at single nucleotide resolution. Figure 3.1A shows a linear representation of the KSHV genome and Figure 3.1B the FAIRE-Seq coverage (raw read counts) in BCBL1. FAIRE peaks were not detected in samples processed without crosslinking (Figure 3.1C). Note the difference in scale, with the highest FAIRE signal at 289 fold coverage, whereas the highest non-crosslinked signal was at 18 fold coverage. The coverage was unrelated to viral GC content (Figure 3.1D). Except for the two lytic origins of replication and the terminal repeat latent replication origin, GC content was largely uniform across the genome.

As expected, FAIRE enrichment, i.e. nucleosome depletion, was identified upstream of the constitutively expressed LANA ORF, i.e. at the constitutively active LANA promoter (Figure 3.1B). This held true for a second PEL cell line. To independently confirm the result from BCBL1 cells we profiled the BC1 cell line (Figure 3.2). The same regions gave rise to prominent coverage peaks. Importantly for FAIRE-Seq, as for ChIP-Seq data, the peak height is deceiving and cannot be used to infer a linear relationship of abundance (Lee et al., 2013). We therefore chose to show FAIRE peak region boundaries as boxes beneath the raw data. Open chromatin was observed near the promoter

regions of 14 ORF's in BC1, many of which are strongly induced during lytic reactivation, as well as within lytic origins of replication (OriLyt-L or R) (Figure 3.2, Table 3.2). We could not map any FAIRE signal to the latent origin of replication, which is located within the terminal repeats (reviewed in (Ballestas and Kaye, 2011)), because of the repeat nature of the target sequence. Every FAIRE site corresponded to a previously recognized or predicted regulatory element in the KSHV genome (Table 3.2).

KSHV exhibits tropism for endothelial and B cell lineages. To expand our observations and to determine if differences in chromatin organization existed among different cell lines, and/or among distinct viral isolates, we performed FAIRE-Seq on multiple latently infected KSHV cell lines (Figure 3.3). The majority of FAIRE-enriched regions were identified across most of the cell lines (Table 3.3). In addition the FAIRE-enriched regions spanning 60180-60488nt (the presumed bidirectional ORF39/ORF40 promoter), 68656-69159nt (the presumed ORF45 promoter), and 121605-121917nt (within the KSHV miRNA locus in NC_009333) were only present in the B-cell lineage cell lines, i.e. the PEL lines and the artificially KSHV-infected Burkitt lymphoma cell line KSHV-BJAB, and not in the endothelial cell lines.

Overall, this result supports the notion that during latency in PEL the majority of viral promoters and viral genes are populated by closed chromatin and hence inaccessible to transcription factors/PolII. These regions are likely only accessible during lytic reactivation. 24 viral regulatory regions and genes were not occupied by nucleosomes in latent BC1 cells. These included the KSHV latency region and the OriLyt's as expected; but also other regions that are not associated with high levels of latent transcription but which direct viral early and immediate early lytic transcripts. Open chromatin is necessary, but not sufficient for transcription initiation and this result suggests that other modulators/marks add transcriptional specificity.

Latent Episomal Open Chromatin is Adjacent to Activating Histone Markings

Histones incorporated into the latent KSHV episome display modifications associated with either transcriptionally active or repressed chromatin, except for within the viral latency locus (Gunther and Grundhoff, 2010; Toth et al., 2010). To further characterize the regions of FAIRE enrichment, we integrated our FAIRE data with published ChIP-chip data (Gunther and Grundhoff, 2010) for specific histone modifications (Figure 3.4); specifically H3K9/K14-ac and/or H3K4-me3, which are interpreted to represent activating histone marks associated with transcription. Regions of nucleosome depletion were flanked by these activating histone markings across all FAIRE peak regions (data not shown). 18 of 24 (~75%) regulatory elements identified by FAIRE-Seq in BC1 were within 250bp (i.e. one tiling window length from (Gunther and Grundhoff, 2010)) of regions enriched with H3K9/K14-ac and/or H3K4-me3 histone enrichment. Note that FAIRE regions and regions demarcated by an activating histone modification can never overlap, since by definition FAIRE identifies regions of histone depletion. We used a very stringent cut-off requiring enrichment to be ≥ 3 standard deviations above baseline in Dataset S1 (Gunther and Grundhoff, 2010). For instance, in the OriLyt-L region open chromatin was found adjacent to H3K4-me3 and H3K9/K14-ac enrichment (Figure 3.4A).

In addition, within the Lytic Control Region FAIRE peaks and H3K4-me3 and H3K9/K14-ac were in close proximity (Figure 3.4B). Importantly, neither open chromatin nor activating histone marks were found near the RTA/ORF50 promoter. Repressive H3K27-me3 marks were observed within ORF48 and ORF52. Open chromatin was detected within the RTA/ORF50 intron, consistent with prior experience that splice donor/acceptor/branch sites are often free of nucleosomes and can be detected by FAIRE. A combined FAIRE/activating histone signal was also found at the K8 promoter. Lastly the KSHV latency locus which, as a whole is actively transcribed and subjected to alternative splicing, showed an expected pattern of open chromatin. We observed increased chromatin accessibility at the LANA promoter, at the OriLyt-R, and across the KSHV miRNA locus (Figure 3.4C) which overlapped with previously reported H3K4-me3 and/or H3K9/K14-ac enrichment. This

suggests that these regions are accessible for association with active transcriptional regulators and/or poised to initiate transcription in response to specific regulators, while the virus is in a latent state.

Six FAIRE peaks were not adjacent to activating modifications in BC1 (Table 3.2). Three mapped to introns within ORF29, ORF40/41, and ORF50 (RTA), and three were observed at viral tegument and replication genes; i.e. within the gene body of ORF8, and the near promoter regions of ORF9 and ORF39/40. No FAIRE peaks were observed near regions of H3K9-me3 enrichment. This is expected since H3K9-me3 enrichment typically denotes closed, transcriptionally inactive constitutive heterochromatin. Thus our experiments using a novel, independent technique, verify prior work (Gunther and Grundhoff, 2010; Toth et al., 2010), and the classification of H3K9-me3 as a valuable marker for transcriptionally inactive regions of the latent KSHV genome.

Open Chromatin Regions Overlap with CTCF Binding Sites at Lytic, but not Latent Promoters

Work by Lieberman and colleagues has shown that interactions between gammaherpesvirus genomes and cellular CTCF/associated Cohesins, are key regulators of viral gene expression and genome conformation (Chau et al., 2006; Chen et al., 2012a; Kang and Lieberman, 2009; Tempera et al., 2011). We therefore compared the overlap between regions of nucleosome depletion and CTCF binding sites during KSHV latency using published CTCF ChIP-Seq data (dataset GSM941710 from (Chen et al., 2012a)). 18 of the 24 (75%) regions identified by FAIRE-Seq overlapped with CTCF binding sites in latently infected BC1 cells (Table 3.2).

Six regions identified by FAIRE-Seq did not demonstrate coincident CTCF binding. If CTCF serves in its canonical role as an insulator and repressor, we would predict that these regions represent active regulatory scaffolds during latent infection, which function independently of CTCF. Two of these regions (one intragenic to the noncoding PAN RNA (Sun et al., 1996) and one in the 3'UTR of the K15 gene (Glenn et al., 1999)) contained sites which are bound by LANA based on ChIP-Seq data (GSM941712 from (Chen et al., 2012a)) (Table 3.2). At this point the functional relevance of LANA binding to these regions is unknown. Given LANA's ability to function as a transactivator if bound

to single binding sites outside the TR region (which contain multimeric LANA binding sites) (Jeong et al., 2004), one could speculate that these regions may contain yet to be discovered latent promoters.

"CTCF-free" FAIRE peaks occurred within the promoter regions of vIL6 (vIL6p; (Deng et al., 2002), the constitutive LANA promoter (LANApc; (Dittmer et al., 1998)), and upstream from the lytically induced Kaposin promoter (K12p; (Sadler et al., 1999)) (Figure 3.5). The vIL6 gene is transcribed in otherwise latently infected MCD cells, and K12p expression has been observed during latency (Cai and Cullen, 2006; Chandriani and Ganem, 2010; Chen et al., 2009; Deng et al., 2002; Nicholas et al., 1997; Sadler et al., 1999). The vIL6p is strongly activated by RTA, but also independently of RTA by the IFN signaling pathway and by intracellular Notch (Chang et al., 2005a; Chatterjee et al., 2002). These phenotypes are consistent with the identified open chromatin region in Figure 3.5A, which may be regulated by cellular factors independently of the complete replication cycle, and in certain instances independently of RTA.

Another "CTCF-free" FAIRE peak overlapped with OriLyt-R, K12p, and with the predicted transcription start site (~120544nt in NC_009333) of a novel antisense to latent transcripts (ALT) noncoding RNA (Chandriani et al., 2010) (Figure 3.5B). Hence, it is possible that this region is involved in regulation of three elements: the proximal Kaposin promoter; which is a RTA-responsive early promoter, OriLyt-R accessibility, and the novel ALT promoter. We observed CTCF marks within open chromatin in the miRK3/K4 locus, a region of abundant latent transcription, but no known *cis*-regulatory elements (Figure 3.5B). "CTCF-free" FAIRE peaks also covered the intergenic region between the LANA ORF and K14 ORF. This region contains known CTCF binding sites downstream of the inducible LANApi, however, the constitutive LANApc transcription initiation site was accessible (as expected) and was not bound by CTCF (Figure 3.5C).

Overall this data suggests that nucleosome depleted regions of the latent KSHV genome can be divided into two subsets: first, nucleosome depleted regions that are transcriptionally inaccessible because they are bound by CTCF; and second, nucleosome depleted regions that are not bound by CTCF. These represent constitutively active or poised promoters, such as LANApc and the

Kaposin/OriLyt/ALTp region, or promoters which may be regulated by host factors independent of RTA and KSHV lytic reactivation; such as the vIL6 promoter.

Open Chromatin Regions Overlap with RNA PolII Deposition at Active and Poised Promoters

One way to think about the extensive epigenetic information that has been generated for KSHV is as a tiered arrangement of safety locks; each lock has to be opened before a transcript is produced. The first layer of access is at the nucleosome level. Only sites that are nucleosome depleted can engage transcription factors. These are identifiable by FAIRE. The next layer of access is at the histone-code level. Only regions enriched in activating histone marks are likely to engage transcription factors. A safeguard here is CTCF, which marks open chromatin regions as closed for transcription. The final layer is recruitment of RNA PolII and its activation via CTD serine 5 and 2 hyper-phosphorylation. Toth et al. (Toth et al., 2012) recently determined these activated RNA PolII sites on the KSHV genome. Chen et al. (Chen et al., 2012a) determined the LANA binding sites, which in latent KSHV infection represent another layer of regulation. We were able to integrate these studies with our data set. RNA PolII was enriched at the vIL6, vIRF3, LANApc, K4/5/7, K15 and the OriLyt regions (Figure 3.6A). The same regions were depleted for nucleosomes (Figure 3.6B). As mentioned above FAIRE identified many more regions of open chromatin and the majority of these were bound by CTCF (Figure 3.6C), which excluded PolII enrichment to a large degree. LANA bound in the vicinity of CTCF at the OriLyt's, at the presumed vIRF promoter, and at the inducible LANA promoter (LANApi); but not the constitutively active LANA promoter (LANApc) (Figure 3.6D and Table 3.2).

It is important to recognize the limitations of this type of comparative analysis, which tries to match data from separate experiments, obtained with reagents of differing performance and on different experimental platforms. Array data are normally distributed and have a rather narrow signal to noise ratio. Chip-Seq data follow a Poisson distribution. This type of distribution is highly non-linear and tends to over emphasize peaks (Lee et al., 2013). To compare these data we applied

successive transformation steps to facilitate the comparison between both data types (Figure 3.6E). Each of these transformations incurs some loss of resolution and of course represents averages of many cells in one or more cell lines. These data support the general conclusion of a layered model, in which each of the layers (nucleosome position, histone marks, methylation, CTCF, and LANA) contribute to the final signal, which is RNA PolII recruitment and active transcription.

3.5 Discussion

The goal of this study was to investigate the organization of chromatin in KSHV during latency. It follows our prior work mapping KSHV mRNA and miRNA transcription (Fakhari and Dittmer, 2002; O'Hara et al., 2009). Initially, only two regions of the genome were known to be consistently transcribed in latently infected cells: the KSHV latency locus encoding LANA, vCYC, vFLIP, Kaposin/K12 and all viral miRNAs, and vIRF3/LANA-2 (Dittmer et al., 1998; Rivas et al., 2001). More recently, evidence for more widespread viral transcription has emerged. The vIL6 gene is expressed at high levels in MCD and can respond to IFN-alpha independent of other viral genes (Aoki et al., 2001; Chatterjee et al., 2002). For vIRF1, both a latent and lytic transcription start site has been described (Cunningham et al., 2003), and we previously detected vIRF1 mRNA in KS lesions (Dittmer, 2003). Similarly, K1 was widely expressed in at least a subset of KS tumors (Wang et al., 2006a). Lastly, genomic surveys found extensive transcription, including the expression of non-coding RNAs, across the entire genome (Chandriani et al., 2010; Dresang et al., 2011; Xu and Ganem, 2010). We hypothesized that mapping open chromatin, which is a prerequisite for transcription may yield further insights and may allow us to classify KSHV *cis*-elements into different groups, based on their epigenetic status during latency.

We are not the first to investigate the viral epigenome (reviewed in (Knipe et al., 2013)). Extensive studies by many groups determined the KSHV CpG methylation status and modified histone deposition across the genome (Gunther and Grundhoff, 2010; Toth et al., 2010). We were able

to integrate this information into our approach using FAIRE (Giresi and Lieb, 2009; Simon et al., 2012) as a novel method to map chromatin status in KSHV. The open chromatin regions identified by FAIRE can be thought as a minimal requirement for epigenetic and/or transcriptional regulation (reviewed in (Jiang and Pugh, 2009)). Modified histone marks and transcription factor occupancy represent the next layer, and PolII recruitment and successful elongation the final level of regulation.

We found that regions of open chromatin decorated 7.76% of the latent BC1 genome and hence that most of the KSHV genome was occupied by nucleosomes during latency. This is consistent with prior work by Günther and Grundhoff (Gunther and Grundhoff, 2010), who also reported genome-wide CpG methylation. Repressed chromatin, as ascertained by lack of a significant FAIRE peak, correlated (within the limit of ChIP-chip) well with repressive histone marks H3K9-me3 and H3K27-me3, as well as EZH2 binding as reported by Toth et al. (Toth et al., 2010), and also by Günther and Grundhoff, and others (Chen et al., 2012a; Gunther and Grundhoff, 2010; Stedman et al., 2004) . A few open chromatin regions, devoid of nearby H3K9/K14-ac or H3K4-me3, mapped outside of proximal promoter regions and instead to known splice donor or acceptor sites, which is expected based on other studies that employed FAIRE (Gaulton et al., 2010; Song et al., 2011).

We found 24 highly significant FAIRE peaks, which corresponded to regions of latent open chromatin in the KSHV genome in BC1 (Table 3.2). These were depleted for repressive histone marks, and were in close proximity to previously reported (Gunther and Grundhoff, 2010) histone marks associated with transcriptional activity (H3K4-me3 and H3K9/K14-ac). These 24 regions of open chromatin could be further sub-divided on the basis of CTCF co-occupancy as determined by Chen et al. and others (Chen et al., 2012a; Kang et al., 2013; Kang and Lieberman, 2009; Kang et al., 2011; Stedman et al., 2004; Stedman et al., 2008).

The constitutive LANA promoter (LANApc), the vIL6 promoter, and the proximal Kaposin/presumed promoter for the ALT transcript, represent open chromatin regions not co-occupied by CTCF. Nearly all other regions of nucleosome depletion contained previously reported CTCF occupancy; which we presume prevents transcriptional utility of these regions (Chen et al.,

2012a). CTCF has a predominantly insulating, albeit dynamic and variable, role at cellular loci (reviewed in (Merkenschlager, 2010; Ohlsson et al., 2010a; Phillips and Corces, 2009)). CTCF modulates latent gene regulation and episomal configuration in both human gammaherpesviruses, (Chau and Lieberman, 2004; Chen et al., 2012a; Holdorf et al., 2011; Hughes et al., 2012; Kang and Lieberman, 2009; Kang et al., 2011; Tempera and Lieberman, 2010; Tempera et al., 2010), thus CTCF-mediated silencing represents a mechanism which may prevent the usage of KSHV episomal regulatory scaffolds during latent infection. 11 of 24 (46%) latent regions of open chromatin revealed by FAIRE also localized to known binding sites for the KSHV lytic switch protein; RTA ((Chen et al., 2009; Deng et al., 2002); Table 2), suggesting that latent regions of nucleosome depletion may also require RTA expression for regulatory function.

By and large the nucleosome occupancy pattern was conserved among multiple cells with stably and latently maintained KSHV episomes. PEL cell lines and artificially KSHV-infected BJAB cells yielded largely super-imposable FAIRE profiles. Two endothelial lineage models of latent KSHV infection; L1-TIVE (An et al., 2006) and KSHV-HUVEC (Wang and Damania, 2008), also shared many of the same regions of open chromatin with B cells. However, we also identified B cell-specific regions of open chromatin, which are the subject of further study.

Lastly, we integrated FAIRE data with LANA binding data from Chen et al. ((Chen et al., 2012a); GSM941712), and activated (as determined by PolII CTD serine 5 and 2 hyper-phosphorylation) PolII data from Toth et al. (Toth et al., 2012). This indicated that the most highly PolII associated regions were indeed the extended KSHV latency locus, the vIRF3 locus, and regions on either side of each OriLyt, and that these were bordered by FAIRE peaks. There were fewer PolI peaks than FAIRE peaks, as expected. Additional suppressive mechanisms during latency may arise from negative elongation factor (NELF) mediated PolII stalling, which has been characterized in KSHV, such as within the region spanning OriLyt-L to K7 (Toth et al., 2012) .

In sum FAIRE–Seq represents a robust method, perhaps more so than antibody-dependent ChIP-Seq, to identify regions of open chromatin with single nucleotide resolution. We applied this

method for the first time to the KSHV genome and identified several regions of open chromatin in latent viral episomes. Regions of open chromatin identified by FAIRE are not sufficient to identify regions of active latent transcription, but by integrating prior histone-modification, LANA, PolII, and CTCF mapping data, we were able to generate a consensus epigenetic map of the latent KSHV genome. This effort is in concordance with transcriptional profiling and suggests the presence of additional latent regulatory regions in the viral genome.

SAMPLE	RAW READS	ALIGNED TO KSHV [a]	FRACTION	MEAN COVERAGE	NUMBER OF FAIRE PEAKS [b]
BC1	9,023,981	31,987	0.35 %	11.59 x	24
BCBL1	26,983,911	26,786	0.10 %	9.71 x	27
KSHV BJAB	9,961,339	25,470	0.26 %	9.22 x	28
KSHV HUVEC	72,447,917	17,288	0.02 %	6.26 x	23
L1 TIVE	79,435,320	5,653	0.01 %	2.05 x	15

Table 3.1: Summary of KSHV FAIRE-Sequencing Data. Read information is displayed for each FAIRE-Sequenced KSHV-infected cell line

a. KSHV reference genome NC_009333
b. Using MACS2 software assuming an average fragment size of 250bp

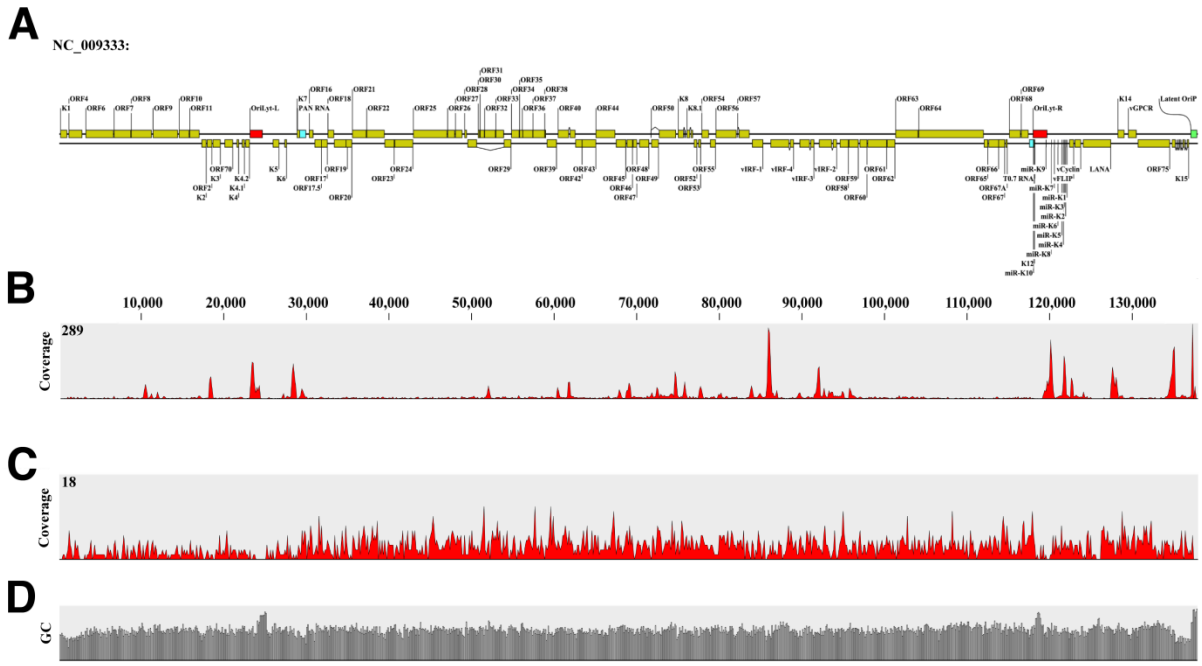

Figure 3.1: FAIRE-Seq Analysis of PEL (BCBL1). A. Schematic of the KSHV genome (depicted linearly). Boxes indicate open reading frames (ORF's). ORF's on the upper strand are transcribed in right-ward directions (with corresponding, predicted or known regulatory regions on the left) and the lower strand corresponds to ORF's transcribed in the leftward direction (with corresponding, predicted or known regulator regions on the right). **B.** Read coverage data for FAIRE across the KSHV genome (BCBL1). Genome position is indicated on top. The maximal peak height was 289 reads covering a single nucleotide. **C.** Read coverage of DNA not subjected to FAIRE cross-linking and enrichment. **D.** Predicted GC content across the KSHV genome.

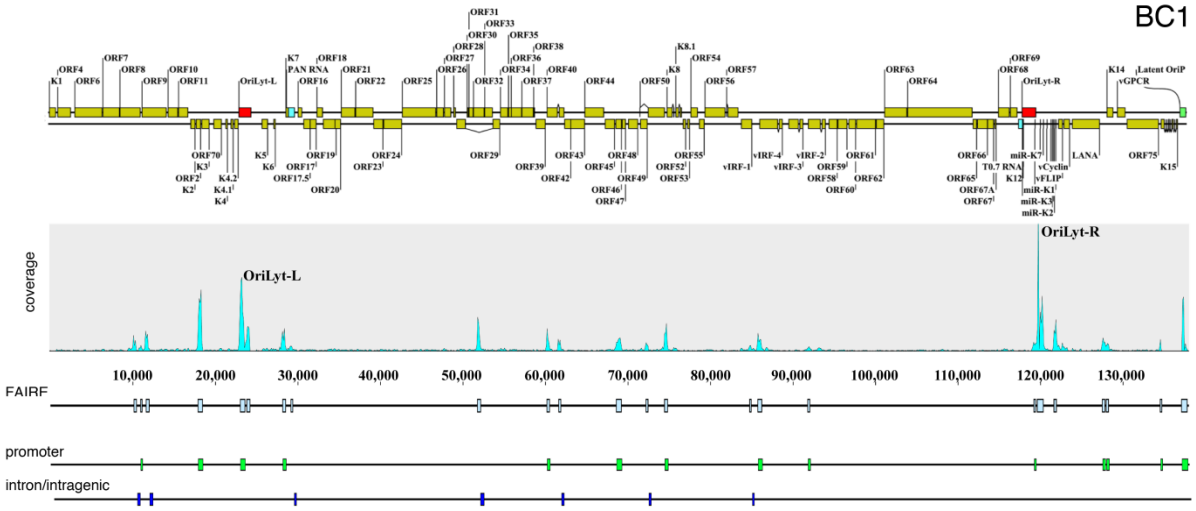

Figure 3.2: Regions of Latent Open Chromatin across the KSHV Genome (BC1). A. FAIRE-Seq reads from latent BC1 cells mapped to the KSHV reference genome NC_009333 are shown as in Figure 3.1. Regions of increased coverage density correspond to regions depleted of nucleosomes. B. FAIRE peaks in BC1 (light blue) are identified as blocks and correspond to nucleotide level resolution latent open chromatin as determined by MACS2. Regions of open chromatin occur in KSHV lytic replication origins (OriLyt-L/R), promoter regions (green), and at intronic/intragenic sites (blue) during latency.

Peak	Region[a]	Size	"Active"[b]	CTCF[c]	LANA[d]	RTA[e]	Promoter	Description	Reference(s)
1	10083-10467	384	X	X	.	.	.	intragenic	-[h]
2	10885-11147	262	.	X	.	.	X	ORF8/ORF9	Lin et al., 1998
3	11567-12002	435	.	X	.	.	.	intragenic	-[h]
4[i]	*17847-18466*	*619*	*X*	.	.	*X[f]*	*X*	*vIL6*	*Deng et al., 2002*
5	22965-23605	640	X	O	.	X	X	K4.2 OriLyt-L	Lin et al., 2003; Wang et al., 2004;
6[i]	*23758-24220*	*462*	*X*	.	.	*X*	.	*OriLyt-L*	*Lin et al., 2003; Wang et al., 2004*
7	28103-28550	447	X	O	.	X	X	K6/K7/PAN	Song et al., 2001; Toth et al., 2012;
8[i]	*29112-29408*	*296*	*X*	.	*X*	.	.	*intragenic*	*Sun et al., 1996*
9	51707-52185	478	.	X	.	X	.	ORF32/ORF29 intron	-[h]
10	60130-60531	401	.	X	.	.	X	ORF39/ORF40-41	-[h]
11	61554-61892	338	.	X	.	.		ORF40-41 intron	-[h]
12	68538-69231	693	X	X	.	X	X	ORF45	Zhu et al., 1999
13	72133-72463	330	.	X	.	.		ORF50 intron	Lukac et al., 1999
14	74384-74835	451	X	X	.	X	X	K8	Lukac et al., 1999
15	84695-84973	278	X	X	.	.	.	intragenic	-[h]
16	85687-86245	558	X	X	.	.	X	vIRF1	Chen et al., 2000
17	91732-92071	339	X	X	.	.	X	vIRF3	Cunningham et al., 2003
18[i]	*119144-119418*	*274*	*X*	.	.	*X*	*X*	*Kaposin/OriLyt-R*	*Li et al., 2002; Cai et al., 2005; Lin et al., 2003*
19	119546-120371	825	X	O	.	X	X	OriLyt-R/ALTp	Lin et al., 2003, Chandriani et al., 2010
20	121573-121961	388	X	X	.	.	.	miR-K12-5…miR-K12-2	Cai et al., 2005; Samols et al., 2005
21	127436-127830	394	X	X	X	X	X	LANApi/K14	Hilton et al., 2012; Matsumura et al., 2005; Kirshner et al., 1999
22[i]	*127900-128276*	*376*	*X*	.	.	.	*X*	*LANApc*	*Dittmer et al., 1998*
23[i]	*134456-134736*	*280*	*X*	.	*X*	.	.	*5' ORF75/ K15 3'*	*Poole et al., 1999; Glenn et al., 1999*
24	137041-137806	765	X	X[g]	X[g]	X	X	K15/TR	Wong and Damania, 2006; Lagunoff and Ganem 1997

Table 3.2: Correlation between FAIRE Peaks in BC1 and Other Notable Chromatin Marks.

a. KSHV reference genome NC_009333

b. Distance to histone mark H3K9-ac/H3K4-me3 ≥250bp, "Dataset S1"; Gunther and Grundhoff, 2010 (PMID: 20532208)

c. GEO dataset GSM941710 (PMID: 22740398), X indicates enrichment of CTCF and Cohesin, O indicates CTCF without Cohesin

d. GEO dataset GSM941712 (PMID: 22740398)

e. Chen et al., 2009 (PMID: 19233445)

f. Deng et al., 2002 (PMID: 12134031)

g. 35 TR added to KSHV reference genome "HQ404500.1" in PMID: 22740398; approximated in NC_009333

h. From Russo et al., 1996 (PMID: 8962146)

i. Regions of accessible latent chromatin based on FAIRE (in red)

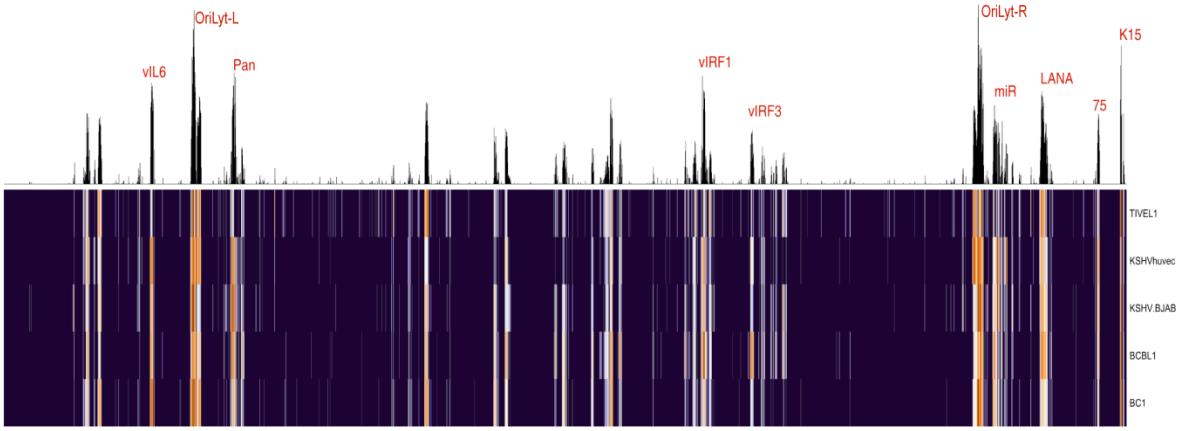

Figure 3.3: Regions of Open Chromatin are Conserved in Latent KSHV Infected Endothelial and B cells. A heatmap of normalized coverage counts across five cell lines (BC1, BCBL1, BJAB carrying latent KSHV, KSHV-HUVEC carrying latent KSHV and TIVE L1 cells) is shown. Orange hues indicate nucleosome depletion, i.e. higher FAIRE coverage (averaged over a 40bp sliding window). On top the average coverage across all cell lines is shown.

Line	BC1		BCBL1		KSHV BJAB		KSHV HUVEC		L1 TIVE	
1					7634	8007				
2					8412	8859				
3	10083	10467	10106	10480	10103	10438	10058	10507	9898	10270
4	10885	11147					10931	11277		
5	11567	12002			11601	11937	11567	11886	11590	11949
6					16365	16620				
7							16695	17101		
8	17847	18466	17970	18428	17966	18420	17933	18418		
9	22965	23605	22964	24198	22963	23560	23001	23554	23114	23539
10	23758	24220					23672	24206	23790	24105
11	28103	28550	27978	28548	27803	28541	27989	28556		
12	29112	29408	29088	29474						
13									33037	33397
14									40507	40782
15	51707	52185	51729	52101	51728	52109	51749	52065	51762	52156
16	60130	60531	60137	60497	60180	60488				
17	61554	61892	61500	61873	61957	62459	61529	61892		
18			67611	67947	67659	67914				
19	68538	69231	68574	69188	68656	69159				
20	72133	72463	72221	72500						
21	74384	74835	74424	74831	74487	74774	74452	74789	74420	74706
22			75540	75901						
23			77464	77820						
24					80008	80348				
25			83657	83995	83688	83938				
26	84695	84973			84714	84986	84654	84966		
27	85687	86245	85669	86376	85692	86160	85696	86185		
28					86688	86939				
29					87271	87575				
30	91732	92071	91502	92168			91716	92089		
31			92475	92741						
32							93132	93408		
33			93468	93759						
34			94688	94968						
35			95651	96078	95598	96132			95657	95907
36									107772	108035
37	119144	119418					118977	119467	119026	119385
38	119546	120371	119611	120385	119655	120362	119643	120363	119667	120036
39	121573	121961	121555	121966	121605	121923*				
40					121998	122313	121918*	122314		
41			122555	122865						
42							123020	123468		
43					123904	124167				
44	127436	127830	127376	128264	127392	128269	127341	127763	127385	127885
45	127900	128276					127956	128233		
46	134456	134736	134396	135248	134164	135188	134243	135178	134300	134625
47	137041	137806	137060	137433	137070	137434	136952	137425	137062	137420

n	24	27	28	22	15
Conserved	14	12	13	14	10
Shared	10	9	8	5	2
Unique	0	6	7	3	3

Conserved Open Chromatin (≥80%) nt boundaries (NC_009333).		
10106	10270	1
11601	11886	2
17970	18418	3
23114	23539	4
23790	24105	5
28103	28541	6
51762	52065	7
74487	74706	8
85696	86160	9
119667	120036	10
127436	127763	11
127956	128233	12
134456	134625	13
137070	137420	14

Conserved Open Chromatin (B Cells Only) nt boundaries (NC_009333).		
60180	60488	1
68656	69159	2
121605	121917	3

Shared Open Chromatin nt boundaries (NC_009333).		
10931	11147	1
29112	29408	2
67611	67914	3
72221	72463	4
83688	83938	5
84714	84966	6
91732	92071	7
95657	95907	8
119144	119385	9
121918	122313	10
127956	128233	11

Unique Open Chromatin nt boundaries (NC_009333).		
7634	8007	1
8412	8859	2
16365	16620	3
16695	17101	4
33037	33397	5
40507	40782	6
75540	75901	7
77464	77820	8
80008	80348	9
86688	86939	10
87271	87575	11
92475	92741	12
93132	93408	13
93468	93759	14
94688	94968	15
107772	108035	16
122555	122865	17
123020	123468	18
123904	124167	19

Table 3.3: Nucleotide Resolution of FAIRE Regions in Latently Infected Cells. Nucleotide (nt) coordinates (in NC_009333) of FAIRE peak regions correspond to regions of open chromatin identified in BC1, BCBL1, KSHV-BJAB, KSHV-HUVEC, and L1 TIVE. The total number of peaks identified (n) is shown, and the numbers of peaks which are conserved (present in ≥80% of isolates), shared (occurring in at least 2 isolates) or unique are shown below. The asterisk "*" indicates a region of overlap (6nt) omitted from conserved B cell nt boundaries. Conserved peaks among all isolates are shown and highlighted in gray. Peaks conserved in B cells, shared, or unique to a viral isolate, are highlighted in orange, green, and in blue, respectively. (Adapted from Supplemental Material of manuscript in preparation).

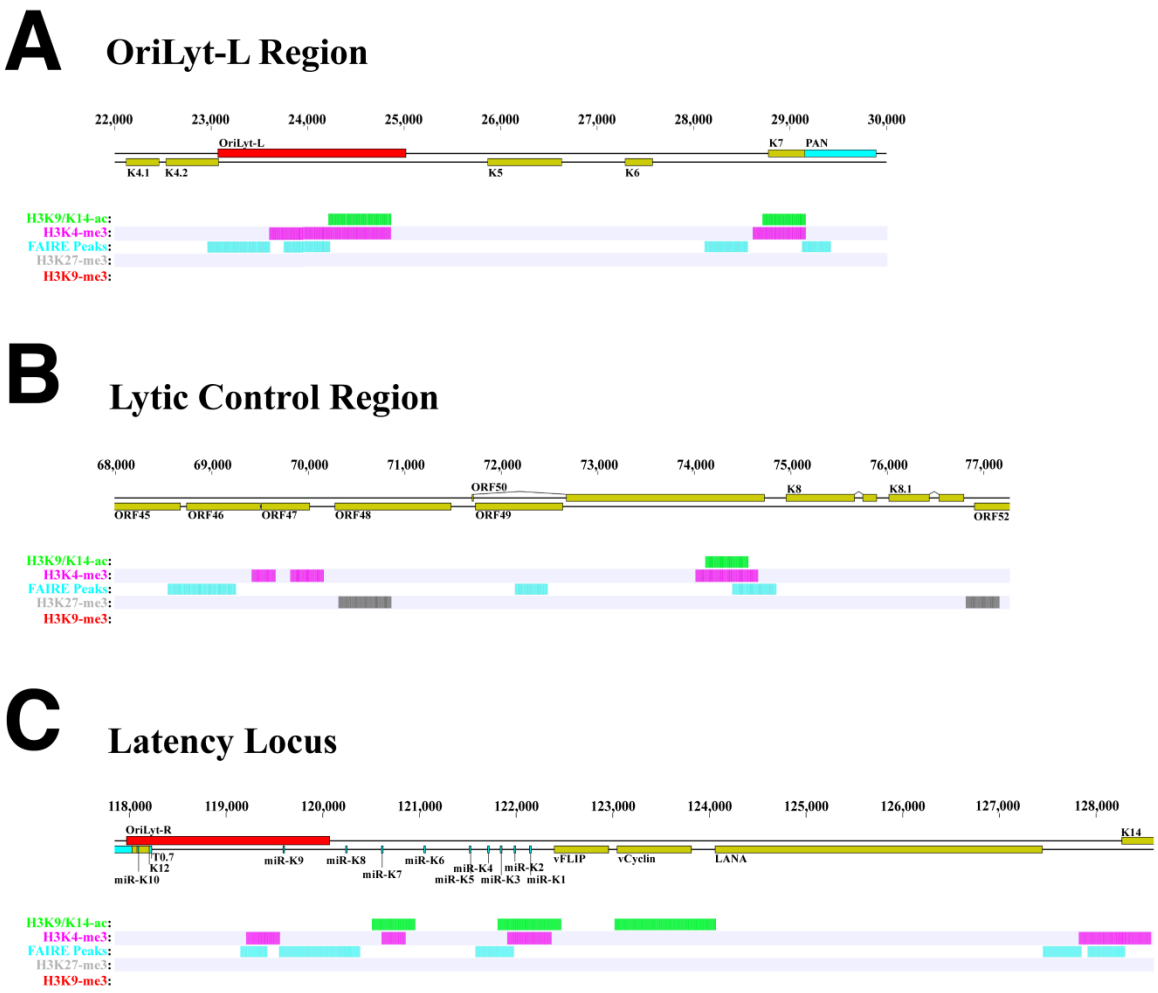

Figure 3.4: Regions of Latent KSHV Open Chromatin Occur Near Activated Histone Modifications. Significant regions of probe enrichment for histone modifications on the latent KSHV genome were annotated from previous work (Gunther and Grundhoff, 2010). Regions of H3K9/K14-ac and H3K4-me3 activating marks are shown in green and pink respectively. FAIRE peaks are shown in light blue. H3K27-me3 and H3K9-me3 modifications are shown in grey and red respectively. The KSHV OriLyt-L region (**A**), Lytic Control Region (RTA promoter; **B**), and the KSHV Latency locus (**C**) are shown.

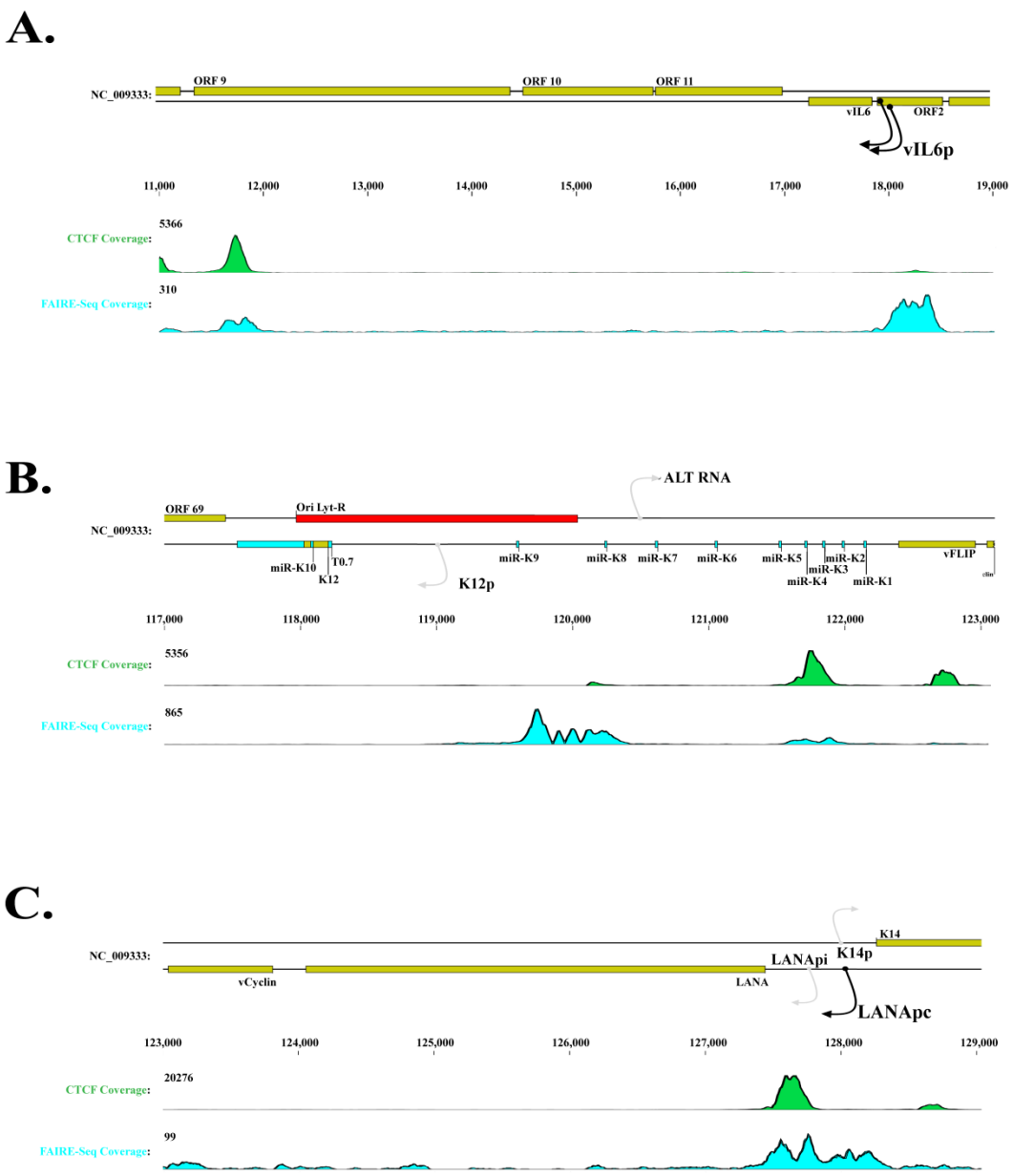

Figure 3.5: Regions of KSHV Open Chromatin Coincide with CTCF Binding Sites. Published CTCF ChIP-Seq enrichment (GSM941710; (Chen et al., 2012a)) is shown in relation to FAIRE-Seq coverage (green and light blue, respectively). **A.** The KSHV genomic region spanning the vIL6p region is shown (11,000-19,000nt) along with two mapped transcription start sites for the vIL6p depicted by black arrows. **B.** The approximately mapped transcription start sites for the K12p and the Antisense to Latent Transcripts (ALT) RNA (Chandriani et al., 2010) are indicated with gray arrows, and the OriLyt-R is shown in red (spanning 117,000-123,000nt). C. The bidirectional transcription start sites for the lytic LANApi and K14p promoters are indicated by gray arrows and the constitutive LANApc is denoted with a black arrow (spanning 123,000-128,000nt). Note changes in scale between panels. All nucleotide coordinates based on NC_009333.

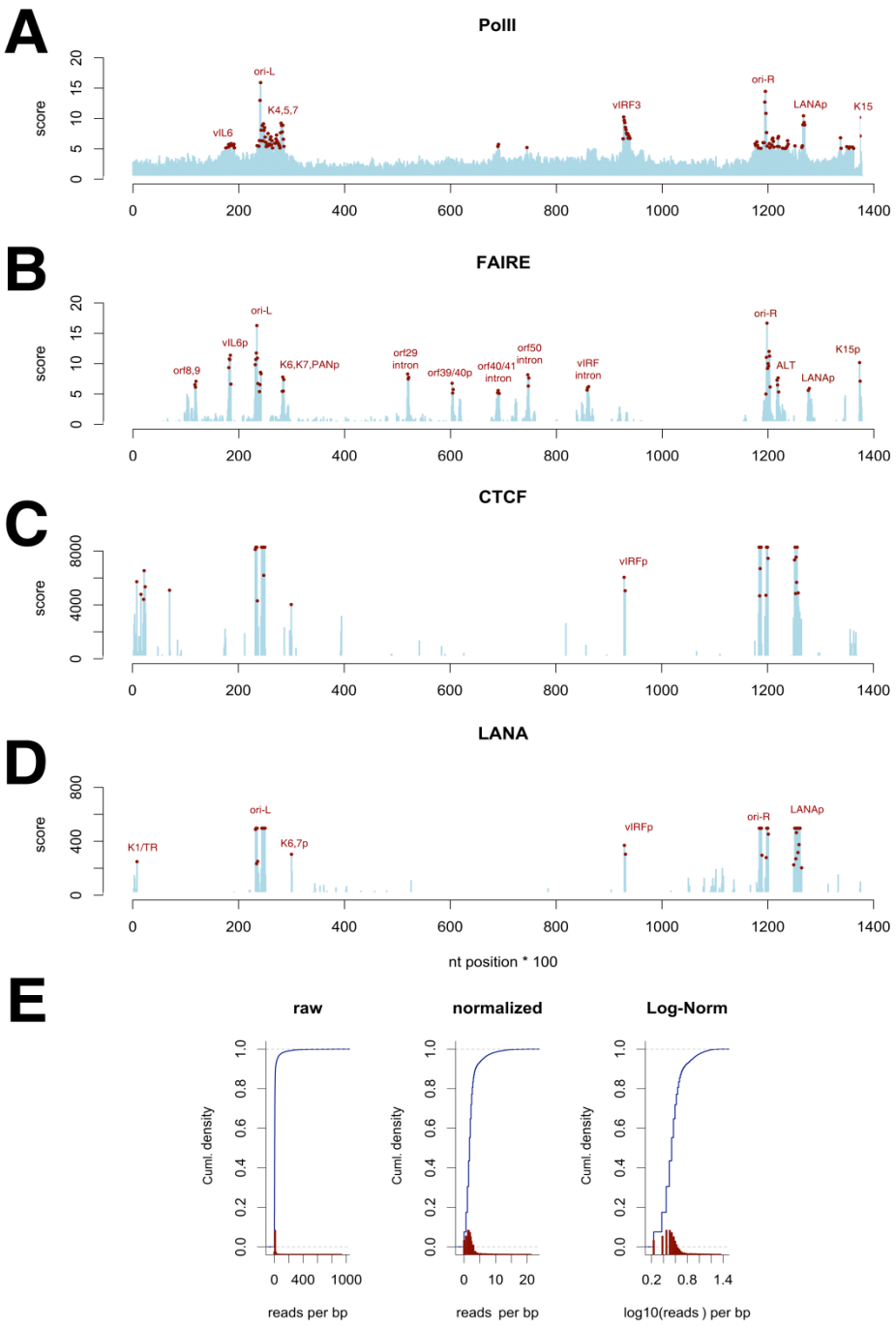

Figure 3.6: RNA PolII Designates KSHV Latent Promoters. Comparison of (**A**) RNA PolII, (**B**) FAIRE, (**C**) CTCF and (**D**) LANA enrichment across the KSHV genome. The horizontal axis represents the genome location, the vertical axis the relative enrichment score over a 100bp sliding window. Dots indicate significant peaks. (**E**) Normalization process: shown on the horizontal axis is the unit and on the vertical axis the cumulative density. Deep sequence-derived coverage counts (raw), normalized counts: $[n^{1/3} - \text{median}(n^{1/3})] / (\text{IQR } n^{1/3}/1.349)$, and log10 of normalized counts, which are approximately normally distributed.

CHAPTER IV

CONCLUSIONS AND PERSPECTIVES

The KSHV genome must navigate between existence within an inert extracellular virion and a dynamic cellular milieu. After engaging a host cell, virion-associated components (proteins and miRNA's) immediately begin to modulate the host and the KSHV genome is trafficked into the nucleus. Within the nucleus host and viral gene expression is rapidly programmed. These activities establish and maintain a life cycle of KSHV infection in humans conventionally divided into latency and lytic phase. The orchestrated regulatory and epigenetic programming of the KSHV genome within host cells is a collaborative process. The simple LANApi/K14p bidirectional transcriptional circuit is a piece of this coordinated effort, and collectively with other viral and host components facilitates a sensitive and adaptable system of KSHV genome propagation.

In this final chapter I have attempted to frame my graduate work in relation to the KSHV field. I have also discussed potential extensions of my work as well as intrinsic connections, and connections to unknown aspects of KSHV biology. Of course nothing exists in a vacuum and bonds among KSHV biology, biomedical research, and human awareness should not be ignored. The human pathology observed coincident with KSHV infection fuels academic intrigue and collective notions of self-preservation. Systems with adequate resources attempt to address these issues by funding research and training. The current length of one lifetime is not enough to adequately understand complex biological problems and systems. Hence like KSHV, researchers should work collaboratively to complete pieces of a large collective puzzle. In my time as a doctoral student I have done my best to characterize RTA activation at the LANApi/K14p and to profile the dispersal of open chromatin in the viral genome. It has always been my hope that my doctoral efforts might contribute to the collective understanding of KSHV.

4.1 The Nature of Bidirectional Transactivation via RTA:Paired RPBjκ

Transcription from the KSHV latency locus has a long history of analysis by Dr. Dirk Dittmer's group and others (Dittmer et al., 1998; Sarid et al., 1999; Talbot et al., 1999). Previous students in Dr. Dittmer's lab characterized the LANApc region in detail, and with others, were instrumental in initial characterization of the overlapping regions of the LANApi and K14p (Jeong et al., 2001; Jeong et al., 2002; Jeong et al., 2004; Lan et al., 2005b; Liang and Ganem, 2004; Matsumura et al., 2005; Staudt and Dittmer, 2006). I extended these observations by taking a uniquely quantitative approach to model transcription from the LANApi/K14p region. My personal goals with these studies were to generate a comprehensive analysis that was robust enough to (i): reveal if the locus was bidirectional and if so, (ii): to allow a detailed mechanistic understanding of LANApi/K14p transactivation by RTA. In this subsection I have considered the nature of this RTA-mediated bidirectional transactivation outside the context of Chapter II; including extended regulatory and functional analysis.

Potential Functions of the LANApi/K14p Bidirectional Promoter

The RTA transactivator can be detected within KSHV virions (Lan et al., 2005b). Early in KSHV infection an initial burst of RTA expression precedes the onset of latency and subsides with latent establishment (Krishnan et al., 2004). The duration of initial RTA expression is cell line dependent. In non-permissive cells, such as fibroblasts, RTA expression is quickly shut down. In permissive and semi-permissive cells (or conditions), RTA expression is maintained, eventually wins out and the virus enters the lytic phase of the replicative cycle. Speculation has arisen that this initial burst of RTA might act on the LANApi/K14p region to induce synthesis of the LANA protein as in Figure 4.1D (Lan et al., 2005b; Matsumura et al., 2005). The LANA protein auto-activates the LANApc and increases in LANA gene expression correlate with the establishment of latency during *de novo* infection, supporting this inference (Jeong et al., 2004; Krishnan et al., 2004). Moreover,

mutation of the RBP B element (K14p proximal) in a KSHV recombinant BAC system (BACLANAp; (Lu et al., 2011)) led to a virus with modest defects in the establishment of latency and higher levels of spontaneous early reactivation and virion production compared to WT.

It remains unclear how RTA could be directed to the LANApi but not to other RTA-responsive promoters early during infection. I suspect that at least two mechanisms could be responsible. (i): The accumulation of LANA protein from the LANApi directly inhibits RTA function early in infection through protein-protein interactions (Lan et al., 2005a; Lan et al., 2004), and/or (ii): the early, naïve KSHV genome is regulated differently than the epigenetically established genome (Gunther and Grundhoff, 2010), which could generate locus specificity at early time points. Complete genetic ablation of KSHV LANA in the BAC36 system generated a virus with an enhanced lytic phenotype in both uninduced and induced *in vitro* cultures (Li et al., 2008). Similarly in the closely related Rhesus monkey rhadinovirus (RRV), genetic disruption of LANA led to increased lytic expression/replication and defects in the establishment of viral latency after *de novo* infection (Wen et al., 2009). Another recombinant KSHV virus, engineered with constitutive RTA expression, entered lytic phase by default after *de novo* infection, which was unaffected by the presence or absence of KSHV LANA (Budt et al., 2011). However, in the related murine gammaherpesvirus 68 (MHV68) a mutant virus engineered with stop codons to prevent mLANA expression led to defects in lytic induction but not viral genome maintenance (Paden et al., 2010). Thus collectively the data suggesting specific utility for LANA expression (and hence the LANApi) during early infection are convincing, but the situation is likely muddled and complex and may depend upon many factors.

The response of K14p to WT RTA was ~10-15 fold more efficient than that of LANApi in all WT input promoter configurations (Figure 2.4). At the lowest levels of RTA tested, the K14p generated over 10 fold more output than the LANApi, whereas near saturation (i.e. k_{cat}) this margin had narrowed to ~4 fold (Figure 4.1E). This suggests that the inhibitory effects of the LANApi upon the K14p increase in direct proportion to RTA concentration. Thus, LANApi acts as an attenuator of transcription, which limits K14p in proportion to RTA amount.

The LANApi inhibits the K14p response to RTA through TATA competition as shown in Figure 2.6. In addition, although in the absence of RBP A K14p output was diminished (Figure 2.7); there was no significant difference in K14p efficiency (Figure 4.1A). This was due to a reduction in K14p induction threshold in the absence of RBP A (Figure 4B). ***Thus both LANApi-proximal cis regulatory elements limit the K14p; the LANApiTATA limits K14p responsiveness and output, whereas the RBP A element limits responsiveness but is critical for K14p output.*** In my opinion the LANApi likely serves to inhibit lytic infection regardless of timing (*de novo*/latency/reactivation). Expression from LANApi/K14p is selective; hence any message produced from the LANApi is a message "lost" to K14p. In this way the LANApi directly inhibits K14p from producing the vOX (also called vOX2/vCD200) and vGPCR proteins. This is important, as each of these viral proteins have potent immuno-modulatory and signaling capabilities outside of the infected cell.

The function(s) of vOX remain relatively unclear, but the protein has been found to have both proinflammatory and immune-suppressive effects on the host cell (Chung et al., 2002; Foster-Cuevas et al., 2004) which may be related to stage of infection (Salata et al., 2009) (i.e. early lytic vs. later). vGPCR is capable of potent signaling both within infected cells and in a paracrine fashion (reviewed in (Lee et al., 2012); see also Section 1.4). vGPCR expression occurs in a subset of KS tumor cells, and this signaling may be involved in sustained lesion progression (Bais et al., 2003; Martin et al., 2011). Limitations upon vOX/vGPCR expression may serve to keep protein levels of these viral signaling molecules appropriately balanced in infected cells. Alternatively, there have also been reports of a cooperative oncogenic phenotype between latent genes (i.e. LANA) and vGPCR (Montaner et al., 2003).

While we found that LANApi directly inhibits K14p (dose-dependently) via proximal TATA/RBPjκ elements, the LANApi likely also has other effects on lytic infection. As mentioned above, LANA may also interact with RBPjκ to repress the RTA promoter and directly inhibit the RTA protein (Lan et al., 2005a; Lan et al., 2004; Lan et al., 2005b). Thus during *de novo* infection and during reactivation the LANApi likely inhibits lytic induction directly and indirectly. These

mechanisms may not be mutually exclusive. The LANApi cannot direct any of the spliced isoforms that originate from the LANApc (Figure 1.5), and it is also possible that transcripts from LANApi are unique in ways that are beyond current levels of scientific characterization.

A Conserved Transcriptional Brake in KSHV

In an effort to find analogous mechanisms I looked for bidirectional promoters in other viruses. DNA viruses like Vaccinia and the KSHV homolog EBV have similar bidirectional loci (Jimenez-Ramirez et al., 2006; Knutson et al., 2009). In Vaccinia 5 out of 6 of these bidirectional loci served to "attenuate" opposing promoter strength through initiator/TATA elements, similarly to the LANApi/K14p. Intriguingly, in EBV paired RBPjκ elements were found within the LMP1/2B bidirectional promoter region. It is unclear if a similar mechanism of attenuation occurs at host eukaryotic bidirectional promoters, but this regulatory device could have been hijacked by these viruses (or *vice versa*).

At the KSHV Lytic Control Region, a second locus responds bidirectionally to RTA (Xu and Ganem, 2010). This bidirectional promoter element is also reliant upon paired RBPjκ elements (Wang et al., 2004c; Wang and Yuan, 2007; Xu and Ganem, 2010) and drives expression of an antisense RNA to ORF50 (ORF50 encodes RTA) and the K8 (also called k-bZIP) protein on the opposite strand. Bioinformatic analysis of this locus revealed that the 50AS/K8DE bidirectional region showed remarkable homology to the LANApi/K14p in terms of regulatory elements (RBP A/B, RRE, K8 TATA element) and their spacing (Figure 4.2).

This homology was especially apparent between the K8DE and K14p "sides" of each respective locus. The 50AS drives expression of an antisense RNA to RTA that may also encode small peptides (Xu and Ganem, 2010). Although the function of the lytic 50AS promoter and resulting transcript(s) remain unknown one group has recently suggested that this RNA encodes a peptide which regulates RTA stability (Jaber and Yuan, 2013). Unlike LANApi, which drives canonical viral ORF's the 50AS promoter does not contain a characterized TATA element to express

the 50AS RNA. The K8DE opposes the 50AS promoter and directs synthesis of the K8 protein, a multifunctional lytic phase gene involved in viral genome replication and transcription. K8 binds the Ori-Lyt regions for viral replication, but also causes cell cycle arrest and inhibition of RTA transactivation at some loci (Izumiya et al., 2003; Lin et al., 2003; Wu et al., 2002). Moreover, K8 gene expression is differential between immediate and delayed-early lytic phase and utilizes two different TSS's; thus fine tuning of K8 expression is likely important, similarly to vOX/vGPCR. Collectively these indicate to me that the homologous bidirectional mechanisms at the latency locus (LANApi/K14p) and lytic locus (50AS/K8DE) act primarily to direct vOX/vGPCR and K8 expression, but have evolved shared *cis* bidirectional architectures to fine tune and balance lytic gene expression by the addition of an opposing TSS (Figure 4.2).

Mechanistic Nuances of the LANApi/K14p Bidirectional Locus

We noted that RTA DNA binding became dispensable at saturation levels (i.e. k_{cat}) of RTA, as there was no difference in output between WT or R161A RTA (Figure 2.9). This was true in the WT promoter configuration, but also in the absence of TSS-proximal RBPjκ elements. Thus given enough RTA, the output from LANApi or K14p is not dependent upon RTA DNA binding, and in the absence of proximal RBPjκ, output is drastically reduced but not due to changes in DNA binding. KKEE RTA could rescue the output in the absence of proximal RBPjκ elements (Figure 2.9), and in every *cis* context examined (mutant or WT) KKEE led to increased output. One could speculate that the increased abundance and altered on/off kinetics (Chang et al., 2008); as well as the enhanced DNA binding of KKEE, contribute to this global increase in promoter output.

Promoter efficiency is related to, but different from, promoter behavior at saturation (see Section 2.4, equations 3 and 4). The efficiency of both WT LANApi and WT K14p was proportional to RTA DNA binding capacity (Figure 2.8A and D). This increase in efficiency in response to KKEE was dependent upon TSS-proximal TATA/RBPjκ elements for both LANApi/K14p (Figure 4.3). Moreover, in the absence of the most critical regulators of efficiency; RPBjκ elements, loss of DNA

binding still compromised efficiency. Collectively the data imply that RTA DNA binding acts through proximal RBPjκ and that this is relayed to respective TSS's via proximal TATA elements.

However RTA DNA binding also activates the locus through other *cis* features, which we showed included a directional component that skews activation towards K14p (i.e. RBP B), a phenomenon likely due to *cis* asymmetry of the RRE (Figure 2.10). I found that mutation of the RRE led to ~30% reduction in all RTA variants (i.e. the RRE was required even without RTA DNA binding). Moreover, a cellular protein(s) binds to the LANApi/K14p RRE *in vitro*, though this protein(s) remains unidentified (Liang and Ganem, 2004) . This led Liang and Ganem to infer that a co-activator occupies the RRE. My data corroborate this finding but also indicate that the RRE asymmetrically directs RTA DNA binding resulting in selective stabilization of RBP B (and hence K14p).

Although the LANApi TATA element competed against K14p, the reverse was not obvious (Figure 2.6). Moreover, even in the REV mutant, LANApi was incapable of K14p levels of output (Figure 2.10). In addition I noticed that in our *in vitro* system K14p displayed basal activity, whereas the LANApi did not (Figure 4.4A and B). This basal K14p activity was dependent upon intact regulatory elements (including the K14p TATA element). Together these data imply that the LANApi TATA is much weaker than the K14p TATA. Evidence suggests that the distance between RBPjκ and TATA elements can regulate RBPjκ -mediated repression via TFIID (Olave et al., 1998). Interestingly in the REV mutant basal activity is reduced in K14p, suggesting that the RBP A element might also have a repressive effect due to its close proximity (7bp) to the LANApi TATA element in WT. In fact in the absence of RTA DNA binding the LANApi TATA element is dispensable for efficiency (Figure 4.3B); and in my opinion the LANApi TATA can only be operational *after* RBP A is activated and stabilized by RTA DNA binding (i.e. TATA repression is relieved by RTA stabilizing RBP A).

The fact that regulatory elements were required for K14p *in vitro* basal activity suggested that the locus must be "programmed" with regulatory elements for a transcriptional event to occur.

Throughout my analysis of this region I was perplexed as to why the single promoter constructs had an approximate 2-fold reduction in k_{cat} when assayed *in trans* (Figure 4.4C). These two concepts are related. Since k_{cat} is a measure of output when saturated with RTA (i.e. RTA is not rate limiting), this indicated that the reduction *in trans* was not related to RTA. I realized that the most logical and simplest explanation was that a refractory period was occurring at saturation. This phenomenon was only observable *in trans*, since at saturation *in trans* the ratio of RTA recognition of a newly "reprogrammed" promoter (Figure 4.4D) would be 1:2 (either single K14p or single LANApi), whereas in the bidirectional or single only input contexts, the newly reprogrammed promoter region would *always* be the bidirectional reporter (1:1) or the single K14p or LANApi (1:1) respectively.

4.2 Applications and Extensions of the LANApi/K14p Bidirectional Promoter

in vivo Mechanistic Consequences

The analysis of the LANApi/K14p bidirectional promoter was performed *in vitro*; hence within the context of the epigenetically programmed viral genome, mechanistic subtleties may exist which we were unable to characterize *in vitro*. To understand this question, and to more fully understand the potential function(s) of the LANApi/K14p (see Section 4.1) we created a bacterial artificial chromosome (BAC) system with the help of a talented research associate in Dr. Blossom Damania's lab named Zhigang Zhang. The KSHV BAC system (reviewed in (Warden et al., 2011)) allowed us to introduce *in vivo* mutations of the LANApiTATA element alone (Lp3BAC) or of the LANApiTATA element and the LANApi TSS (Lp7BAC).

The preliminary data using the BAC system indicates that there may be some differences in growth profiles (Figure 4.5A). Loss of the LANApi TATA element may induce slightly faster cellular growth kinetics (in stable BAC293 cells). However, loss of both the LANApiTATA and LANApi TSS (Lp3BAC) substantially reduces both growth kinetics and maximal confluence. I hesitate to over-speculate and these phenotypes need to be refined, but this could indicate that loss of

LANApi-mediated repression of K14p leads to aberrant viral signaling/replication. Experimental characterization of signaling pathways, defects in the establishment of latent infection, and reactivation potential (to name a few) are required for a more thorough understanding.

Manipulation of the Bidirectional RTA:RBPjκ Mechanism: Implications for Therapy

The bidirectional LANApi/K14p is unique as it synthesizes *either* latent *or* lytic viral gene products in response to the KSHV lytic switch RTA. We found that this occurs selectively and non-simultaneously, and that expression from the LANApi attenuates the strength of the K14p. This attenuation is proportional to RTA concentration. The K14p is extremely sensitive to RTA (Damania et al., 2004) and as outlined above, vGPCR and vOX have potent signaling abilities. In the context of LANApi TATA deletion, the K14p is even more responsive (Hilton and Dittmer, 2012) and thus represents an ideal target for RTA inhibition (Figure 4.5B). The high levels of signal output and the specificity of the response to RTA (and insensitivity to intracellular Notch) are useful properties. Given the homology at the lytic locus with the 50AS/K8DE region, the understanding of this mechanism could shed insight into therapeutic targets aimed at forcing lytic induction by inhibiting transcriptional attenuation at these loci. Additionally, the identification of drugs or compounds which inhibit RTA transactivation could prevent KSHV propagation to naïve host cells.

(Re) Engineering the LANApi/K14p Transcriptional Circuit: Implications for Industry

As synthetic biology and the design of synthetic gene circuitry "evolves", science is capable of engineering transcriptional systems (reviewed in (Slusarczyk et al., 2012)). Although I am biased, the LANApi/K14p bidirectional mechanism represents an exceptional bioengineering substrate in the long-term. First, the promoter is functional in mammalian cells, whereas most synthetic biology underway occurs in prokaryotic systems. Second the response is specific to a non-host transactivator which can be supplied *in vitro* and in the absence of KSHV infection; moreover the region is largely inactive without induction. Third the bidirectional nature allows for one TSS to generate a gene (or

regulatory RNA) of interest (GOI) while the opposing TSS generates a positive or negative regulator (Figure 4.5C).

Advances in synthetic gene circuits allow directed artificial synthesis of biofuels, pharmaceuticals, and other compounds, within engineered cells (Peralta-Yahya and Keasling, 2010; Ro et al., 2006; Wang et al., 2009; Weber et al., 2008). Moreover mammalian biosensors and actuators can be fabricated for numerous applications (Carr and Church, 2009). The LANApi/K14p bidirectional locus has built in transcriptional control and encodes two divergent transcripts within a short (>300bp) stretch of DNA. Implementation of this circuit alone or arrayed in a synthetic networks could allow for a transcriptional system with intricate, layered, and precise regulation.

4.3 Toward a Functional KSHV Epigenetic Atlas

KSHV Genome-Wide Epigenetic Regulation

At present, once infected, the human host will maintain the KSHV DNA genome for the duration of his/her lifetime. This genome will persist as a multicopy circular minichromosome (non-integrated) called an episome. During latent infection the KSHV genome is nucleosome-associated. Latently-expressed genes, such as those encoded within the latency locus, are enriched with nucleosomes bearing histones modifications associated with transcriptional activity (i.e. H3K9/14-ac and H3K4-me3) (Gunther and Grundhoff, 2010; Toth et al., 2010). Similarly, viral genes expressed during immediate-early (IE) or delayed-early (DE) phases of lytic reactivation are enriched in these markings (Figure 4.6A). However IE/DE loci may or may not also bear coincident H3K27-me3 enrichment; interpreted by the KSHV field as being epigenetically "bivalent" or "poised" (Gunther and Grundhoff, 2010; Knipe et al., 2013; Toth et al., 2010). Whereas, viral genes expressed late during reactivation are generally exclusively enriched in heterochromatic H3K9/K27-me3.

Given the wide-scale deposition of nucleosomes in the latent KSHV genome, it is not surprising that cellular proteins involved in histone modification are also associated with the episome.

For instance the histone methyltransferase EZH2, a component of the Polycomb repressive complex 2 (PRC2), co-localizes with H3K27-me3 across the KSHV genome. EZH2 catalyzes the trimethylation of histone H3 lysine 27 which ultimately results in transcriptional repression (reviewed in (Simon and Kingston, 2009)), and in the viral genome EZH2 is similarly involved in the repression of lytic genes and lytic phase induction. In fact, EZH2 is found to be highly expressed in KS tumors and inhibition of PRC2 by the small molecule 3-Deazaneplanocin A leads to reactivation of latent KSHV from PEL cells (He et al., 2012; Toth et al., 2010). Moreover, EZH2 dissociation from certain regions of the KSHV genome (e.g. early lytic genes) occurs in a temporal fashion during reactivation.

JMJD2A, a member of the jmjC domain-containing histone demethylase family, also interacts with the KSHV genome during latency (Chang et al., 2011; Toth et al., 2010). JmjC domain-containing histone demethylases catalyze demethylation of lysines on histones by an oxidative reaction that can remove all three histone methylation states (Hsia et al., 2010; Klose et al., 2006). The primary target of JMJD2A is the repressive H3K9-me3 histone mark, and hence JMJD2A is considered to be a transcriptional coactivator (Shin and Janknecht, 2007; Whetstine et al., 2006). JMJD2A binds across the KSHV genome, and is anti-correlated with H3K9-me3 enrichment during latency (Chang et al., 2011).

Interestingly, JMJD2A demethylase activity was found to be inhibited by the viral k-bZIP protein (encoded by the K8 ORF), the overexpression of which led to increased global and viral H3K9 trimethylation. Interestingly k-bZIP is encoded by K8, the same region exhibiting bidirectional homology to LANApi/K14p (Figure 4.2, (Xu and Ganem, 2010)). JMJD2A knock-down also led to increased lytic replication, however this was only *after* RTA expression was induced and no difference was observed in the basal latent state. Collectively these data have led the field to suggest that JMJD2A binds at H3-ac or H3K4-me3 to prevent methylation of H3K27 and maintain a readied state for reactivation (Chang et al., 2011; Knipe et al., 2013; Toth et al., 2010). However, while JMJD2A binding was observed in regions of the viral genome bearing such marks, to my knowledge no evidence of JMJD2A binding directly to H3-ac or H3K4-me3 has ever been shown.

Another cellular protein called CTCF interacts with gammaherpesvirus (i.e. KSHV) genomes (reviewed in (Deng et al., 2012; Knipe et al., 2013)). CTCF has been called the master weaver of the genome, and over 30,000 binding sites exist in the human genome (Kim et al., 2007; Phillips and Corces, 2009). CTCF is ubiquitous, essential, and known binding sites are highly conserved among different cell types (Heath et al., 2008). CTCF has well-established roles in chromatin folding and gene expression at several human loci including the MHC class II, the H19/Igf2, and the β-globin locus among others (reviewed in (Holwerda and de Laat, 2012)). In addition to higher-order nuclear organization of genomes, CTCF regulation of transcription is versatile and can act locally at promoter regions or over large distances through chromosomal looping (Bell et al., 1999; Filippova et al., 1996; Lobanenkov et al., 1990).

ChIP combined with chromatin conformation capture (ChIA-PET) suggests that a subset of CTCF forms loops in the human genome, while another subset is involved in local gene regulation (Handoko et al., 2011). In the human genome CTCF-mediated loops range from 10-200kb in size and can bring together enhancers and promoters and/or insulate active chromatin from inactive regions or *vice versa*. In KSHV CTCF binding is widespread, and some CTCF-bound molecules are thought to participate in looping of the viral genome, regulating gene expression during cell cycling and latency, and/or programming RNA polymerase for transcription (Figure 4.6B; Figure 3.5; Table 3.2; (Chen et al., 2012a; Kang et al., 2013; Kang et al., 2011)). In many cases in both the human and KSHV genomes CTCF binding is coincident with other factors, namely the Cohesin complex (Chen et al., 2012a; Parelho et al., 2008; Rubio et al., 2008; Wendt et al., 2008).

The Cohesin complex has four subunits (SMC1, SMC3, SCC3, and RAD21) which form a ring like structure linking sister chromatids to ensure appropriate segregation during cellular division, with peak activity in S phase (reviewed in (Lee and Iyer, 2012; Nasmyth and Haering, 2009)). However, other roles for Cohesin are emerging including potential functions at centrosomes, in DNA double-strand break repair, and in transcriptional control at non-sister chromatids. In KSHV shRNA knockdown of Cohesin subunits (but not CTCF) led to viral reactivation in BCBL1 PEL cells, and

moreover knockdown of the RAD21 subunit led to lytic gene induction and enrichment of activated PolII at lytic genes (Chen et al., 2012a). Interestingly, nearly all CTCF-bound sites were also bound by Cohesin in KSHV; with the exception of three regions; (i) near the OriLyt-L, (ii) the K6/K7/PAN promoter regions, and (iii) within the miRNA locus.

CTCF is often found at DNase hypersensitive loci and at regions of nucleosome depletion (Parelho et al., 2008; Song et al., 2011), suggesting that CTCF binding prevents nucleosome deposition or alternatively that CTCF binding sites are refractory to nucleosome incorporation. We found that a similar correlation existed between CTCF and nucleosome depletion across the KSHV genome (Figure 3.5; Table 3.2; Chapter III). The work of the Lieberman group has shown that CTCF and Cohesin can modulate viral transcription, genome maintenance, and latent conformation (Chen et al., 2012a; Kang et al., 2013; Kang et al., 2011; Stedman et al., 2004; Stedman et al., 2008). Our data refine the understanding of latent KSHV epigenetic regulation and suggest that CTCF may reside at regions of open chromatin to insulate genomic regulatory elements from transcriptional utility, prevent the spread of histone modifications, and/or regulate long range episomal interactions (Figure 4.6B).

Most latent open chromatin is bound by CTCF, however we found that a large fraction (~25% in latent BC1) of nucleosome depleted regions in KSHV lacked CTCF binding during latency, indicating that at some viral loci, open chromatin is accessible to other transcription factors/PolII (see Table 3.2). Many of these regions of accessible open chromatin mapped to annotated regions of the viral genome associated with latent transcription, such as the vIL-6 and constitutive LANA promoters (Chandriani and Ganem, 2010; Deng et al., 2002; Dittmer et al., 1998). Some of the CTCF-free regions of latent open chromatin identified by FAIRE-Seq also contained binding sites for KSHV LANA or RTA, and hence may only be active in the presence/absence of these specific viral transactivators. Interestingly LANA has both activating and suppressive effects on transcription as well as coupled binding between host and viral genomes (Ballestas and Kaye, 2011; Han et al., 2010; Renne et al., 2001), thus the nature of LANA binding at CTCF-free regions of open chromatin likely

has importance for our understanding of KSHV biology and pathology.

RNA production from the KSHV genome is complicated and incompletely characterized. Surprisingly; at least to me, analyses of viral mRNA production at the time of this writing have been limited to specific loci or performed using QPCR Arrays/Microarrays (Chandriani and Ganem, 2010; Chandriani et al., 2010; Dittmer, 2003; Dresang et al., 2011; Fakhari and Dittmer, 2002; Jenner et al., 2001; Paulose-Murphy et al., 2001). As of yet no unbiased RNA-Seq experiments have been performed on KSHV during latency nor during reactivation. The KSHV genome generates several RNA species lacking polyadenylation, which have been detected by deep sequencing of small viral RNA's; including mature miRNA's (reviewed in (Gottwein, 2012)), antisense miRNA's (miRNA-AS), and miRNA-offset-RNA's (moRNA's) (Lin et al., 2010).

Classically, KSHV transcript production is divided into latent and lytic programs. However, both infection patterns are disproportionately observed among populations of cells, and I expect that the viral life cycle is more of a balanced continuum; with latency and lytic infection being obvious pathological nodes and with intermediate phases being either too transient or too subtle to currently detect. An inference which is supported by recent evidence of viral heterogeneity within single cells (Darst et al., 2013) and of novel viral transcript/peptide production (Chandriani and Ganem, 2010; Chandriani et al., 2010; Dresang et al., 2011; Jaber and Yuan, 2013). That said data clearly shows that latent infection is associated with a restricted viral expression pattern relative to the lytic phase, and that the reversal of latency (i.e. lytic progression) proceeds in a coordinated temporal manner (see Chapter I).

Genome-wide studies of KSHV gene expression using limited dilution QPCR (Chandriani and Ganem, 2010) or high-resolution mass spectrometry (Dresang et al., 2011) coupled with tiling arrays indicate that latent viral transcription and protein production is likely more widespread than previously appreciated. Further, during reactivation nearly the entire KSHV genome is transcribed on both sense and antisense strands, to generate a multitude of viral RNA and protein species (Chandriani et al., 2010; Dresang et al., 2011). ChIP-chip analysis of RNA polymerase II association

with the KSHV genome supports these notions, with substantial PolII enrichment not only at the latency locus and vIRF-3, but also at the OriLyt's and near the ORF's of K5,K6, and K7 during latency (Toth et al., 2012). PolII enrichment was increased at these loci 8 hours post lytic reactivation, (using Doxycycline in TREx-BCBL1 RTA cells) as well as at most other regions of the viral genome. The carboxy–terminal domain (CTD) tail of PolII at the OriLyt-L, K5, K6, and K7 (OriLyt-K7) was found to be enriched in serine 5 phosphorylation and depleted in serine 2 phosphorylation during latency; which was interpreted by the authors to be "stalled" polymerase (Figure 4.6C; (Toth et al., 2012)). Exogenous inhibition of cellular NELF released the stalled PolII and induced productive transcription at the OriLyt-K7 region suggesting that KSHV may have alternative transcription patterns outside of conventional latency and reactivation, which can occur independently of RTA/LANA transactivation.

Local Epigenetic Modifications and DNA Methylation in the KSHV Genome

Although many of the epigenetic regulatory mechanisms outlined below may very well be in play across the viral genome, they have (at the time of this writing) been characterized only at single, or a few viral loci. While this is not technically the case for DNA methylation, there is some ambiguity surrounding the role of DNA methylation in KSHV gene expression. Further only one genome-wide analysis of KSHV DNA methylation has been performed (Gunther and Grundhoff, 2010); which suggested that DNA methylation plays a minor role in epigenetic regulation of KSHV, long after the onset of stable latency. Thus I have included an overview of these local epigenetic modifications and of viral DNA methylation in this separate subsection.

One such protein that has been shown to interact with a handful of viral loci is a human methyltransferase called Set1. The conserved Set1 complex (Set1A; Set1 hereafter) is composed of several subunits which deposit methylation marks to H3K4 residues (reviewed in (Shilatifard, 2012)). Set1 recruitment was found to occur as several KSHV promoters including RTA, PAN, ORF 57, LANA, and also at the OriLyt's following viral reactivation in a Doxycycline-inducible RTA cell line

called TREx-BCBL1 RTA (Jong et al., 2013). This enrichment was coincident with increases in H3K4-me3 enrichment and was taken to indicate that Set1 catalyzes enhanced H3K4 trimethylation, and hence aids in transcriptional activation of lytic viral loci during reactivation.

One report also indicates that the KRAB domain-associated protein-1 (KAP-1) associates with several KSHV promoters during latency (Chang et al., 2009). This protein interacts with SETDB1 and HP1, as well as other proteins (Ryan et al., 1999; Schultz et al., 2002) to generate heterochromatic signatures in genomic DNA. Knockdown of KAP-1 was shown to enhance KSHV lytic replication and moreover the association between this protein and select viral loci was abolished with the onset of lytic phase (Chang et al., 2009). Chang et al., also found that the viral protein kinase, encoded by KSHV ORF 36, targeted KAP-1 to relieve its repressive effect on lytic genes.

The RTA promoter is also subject to epigenetic modifications, alterations in which can lead to viral reactivation (Figure 4.6D). KSHV can be reactivated by HDAC inhibitors such as sodium butyrate and trichostatin A, chemicals which cause dissociation of HDAC's from the RTA promoter (Lu et al., 2003; Sun et al., 1996), as well as valproic acid and vorinostat ((Lechowicz et al., 2009); Chugh, Dittmer, personal communication). The RTA promoter is also decorated with EZH2, and repressive H3K27-me3, both of which also dissociate during reactivation (Toth et al., 2010). Once RTA expression occurs the protein physically interacts with chromatin remodelers such as the Swi/Snf and TRAP-mediator complexes, to chaperone these elements to lytic viral promoters, including the RTA promoter (Gwack et al., 2003a; Lu et al., 2003). Subsequently RTA can positively autoregulate its own promoter through interaction with RBPjκ, and Oct1 (Deng et al., 2000; Lu et al., 2012b; Sakakibara et al., 2001). In addition, siRNA knockdown of a cellular kinase called Tousled-like kinase 2 (TLK2) leads to a reduction in phospho-histone H3 at the RTA promoter and reactivation of KSHV from latency (Dillon et al., 2013).

RTA expression also induces synthesis of the viral noncoding PAN RNA. PAN is capable of physical interaction with the H3K27 demethylases JMJD3 and UTX, and this interaction directs JMJD3 and UTX to the RTA promoter to augment RTA synthesis during reactivation (Rossetto and

Pari, 2012). Rossetto and Pari also showed that the KSHV PAN RNA physically associates with the H3K4 methylase, MLL2; however a direct interaction between MLL2 and the RTA promoter/KSHV genome was not demonstrated. In addition to the PAN RNA, viral proteins, including RTA and LANA, interact with chromatin remodelers.

RTA interacts with CREB-binding protein (CBP) and HDAC1 and these proteins, as well as the histone acetyltransferase p300, were found to modulate RTA expression levels (Gwack et al., 2001). KSHV LANA interacts with chromatin at the viral TR's and within the host genome to faithfully maintain the viral episome during latency (reviewed in (Ballestas and Kaye, 2011; Ohsaki and Ueda, 2012; Tempera and Lieberman, 2010)). Specifically LANA interacts with chromatin regulatory proteins including CBP, RING3, HBO1, mSin3, SUV39H1, and HP1, as well as cellular replication proteins ORC1 and MCM2 (Krithivas et al., 2002; Krithivas et al., 2000; Lim et al., 2001; Platt et al., 1999; Sakakibara et al., 2004; Stedman et al., 2004; Tempera and Lieberman, 2010). However, these interactions have largely only been characterized at the viral TR's, leading to ambiguity regarding the effects at other viral and human loci.

LANA also associates with cellular proteins involved in DNA methylation including the methyl-cytosine binding protein MeCP2 (Krithivas et al., 2002; Matsumura et al., 2010) and the DNA methyltransferase DNMT3A (Shamay et al., 2006). The role of DNA methylation (which is generally considered a hallmark of transcriptional repression) in KSHV is unclear. Relative to alpha and betaherpesviruses the KSHV genome exhibits CpG suppression indicating that methylation of CpG residues occurs. Further, treatment of latent PEL cells with inhibitors of DNA methylation leads to demethylation of the RTA promoter region and subsequent viral reactivation (Chen et al., 2001).

That said, the establishment of KSHV latency does not seem to be dependent upon DNA methylation of the viral genome (Gunther and Grundhoff, 2010). Instead DNA methylation appears to occur gradually, long after *de novo* infection, after KSHV episomes are stably latent and transcriptionally restricted relative to lytic infection. It has been suggested that this gradual deposition of DNA methylation may help to prevent reactivation of "older" episomes within infected

cells, however this speculation has not been addressed experimentally and the precise function of DNA methylation across the KSHV genome is not entirely clear.

Addressing the Missing Links in a Functional KSHV Epigenetic Atlas

While work by us and others has revealed important information about KSHV transcriptional, oncogenic, and epigenetic regulatory mechanisms, there is still a great deal that remains unknown. For instance how KSHV is programmed for latency after *de novo* infection is not understood. We know that a short burst of lytic gene induction occurs but that this is rapidly silenced coincident with the expression of genes from the latency cluster (i.e. LANA) within 5 days post-infection (Krishnan et al., 2004). The mechanisms which underlie this silencing are not known, but we do know that nucleosome incorporation into the viral genome (in endothelial cells) also occurs within 5 days post-infection whereas DNA methylation takes much longer (Gunther and Grundhoff, 2010). I suspect CTCF is likely also involved in early viral/host gene modulation. I predict that this probably silences local regulatory elements, causes conformational changes in the viral genome, zips the episome to host chromatin, and also localizes the episome to specific compartments within the nucleus. Given the ubiquity and known roles of CTCF this notion seems plausible, but remains untested (reviewed in (Holwerda and de Laat, 2012)).

There is also limited understanding of how the virus manipulates the host cell during infection, and moreover if this manipulation is differential dependent upon infected cell lineage (i.e. B cell vs. Endothelial cell). *In vivo* and *in vitro* studies demonstrate important phenotypic differences in the virus dependent upon infected host cell type (reviewed in (Ganem, 2010); see Section 4.4). Experimental evidence also indicates that viral genes and RNA's from both lytic and latent infection patterns modulate the host cell (Ballestas and Kaye, 2011; Gottwein, 2012; Guito and Lukac, 2012; Haecker et al., 2012; Lee et al., 2012; Lu et al., 2012a; Yada et al., 2006); however a clear atlas of cellular (and viral) modulation is lacking. Hence our understanding of KSHV, and of infected host

cell regulation, requires refinement in order to comprehensively and therapeutically addresses KSHV pathology.

I have considered a few ways in which some of these missing links might be addressed experimentally here and also in Section 4.4 (shown schematically in Figure 4.7). The profile of open chromatin undertaken in Chapter III represents a small component of this potential atlas, and begins to address the tip of the KSHV epigenetic programming iceberg. The way I initially designed the project was to use both KSHV-infected and non-infected syngenic control cells (Figure 4.7A). FAIRE-Seq would be used to generate a map of potential regulatory elements in the viral and cellular genomes and would be performed in parallel with non-polyA selected RNA-Seq and with ChIP-Seq for cellular and viral proteins. In this way alterations in viral and cellular transcripts and in transcript abundance could be mapped back to differential FAIRE signal intensities (i.e. differences in nucleosomal positioning).

To potentially integrate the functional relevance of transcription factor occupancy the analysis would benefit from the tandem ChIP-Seq for proteins with likely roles in cellular/viral programming, such as CTCF or LANA (or other pre-determined candidates). Importantly, while preparing the cells used for FAIRE-Seq analysis of open chromatin profiling (Chapter III), I also collected cell pellets for experiment-matched RNA-Seq and ChIP-Seq analyses. A long term experimental vision could extend these analyses beyond latent infection to encompass all phases of the viral life cycle. This could generate a functional atlas with temporal meaning; from *de novo* KSHV infection through complete viral reactivation. ChIP-Seq reactions could also be coupled with ChIA-PET to generate a contextual understanding of viral genome conformation.

The use of KSHV-infected and non-infected syngenic control cells would allow one to correlate the *cellular* changes associated with KSHV latency. In addition, by using infected/non-infected syngenic cell types of B and Endothelial lineage (BJAB/HUVEC +/- Latent KSHV) one would ideally be able to discern cell type-specific differences that were due solely to viral infection. This approach would be complemented and controlled by the use of *ex-vivo* PEL B cell lines (i.e.

BCBL1) and a model for latent KSHV endothelial infection (L1 TIVE; (An et al., 2006)). By comparing the overlap between cellular loci altered by latent viral infection with those shared among latently infected *ex-vivo* or model cells, one could identify *bona fide* cellular loci modified by KSHV infection for a given assay (FAIRE/ChIP/RNA-Seq) as shown in Figure 4.7B. The resulting overlaps could then be compared in order to generate a functional atlas of cell type-specific and global regulation in infected host cells (Figure 4.7C), and through simpler application and analysis a similar atlas could be derived for the KSHV genome with the same dataset.

4.4 Connecting the Dots; Open Chromatin:CTCF:Cohesin:RTA:LANA

Programmed Nucleosome Depletion and an Open Chromatin Code in the KSHV Genome

Our results characterizing open chromatin across the latent KSHV genome indicated that CTCF binding (Chen et al., 2012a) occupied the majority of nucleosome depleted regions (Figure 3.5, Table 3.2). This is not unexpected given the concordance between CTCF binding and nucleosome depletion in the human genome (Parelho et al., 2008; Song et al., 2011). Moreover, recent evidence suggests that CTCF can displace and alternatively phase nucleosomes within the latency locus of the KSHV genome (Kang et al., 2013). In this final section of my dissertation I have attempted to integrate the literature and our results to further reflect on potential extensions to our studies and on important gaps in our understanding of KSHV transcriptional and conformation control.

In the human genome a so-called "CTCF code" (Ohlsson et al., 2010b) is predicted to exist which could explain how the various functions (insulation vs. activation vs. looping) of CTCF are coordinated at specific sites. I expect that a similar code exists for long-lived coexistent DNA viruses like KSHV. Although CTCF enrichment was found at most regions of latent viral nucleosome depletion, a large fraction of open chromatin was CTCF-free and was observed at important viral loci. This has led me to speculate that regions of viral open chromatin may be programmed for latency and that the resulting "open chromatin code" could direct viral transcription and genome conformation.

The CTCF protein is capable of directly repressing and activating transcription at promoters (Filippova et al., 1996; Yang et al., 1999). CTCF interactions also generate long-range effects on gene regulation and epigenetic topology through looping of DNA and positioning of the genome within the nucleus (Dixon et al., 2012; Guelen et al., 2008; Handoko et al., 2011). It is thought that in mammalian genomes CTCF looping and conformational effects can bridge promoters with enhancers/insulators and create boundaries between conflicting histone marks delineating transcriptionally active loci from those which are transcriptionally repressed (reviewed in (Holwerda and de Laat, 2012; Ohlsson et al., 2010a; Ohlsson et al., 2010b)). CTCF associates with several proteins, including itself, to coordinate these effects. Notably CTCF associates with the large subunit of PolII in the human genome and this relationship is thought to serve several roles in programming local transcription (Chernukhin et al., 2007). This mechanism is complicated by interactions between CTCF and other transcription factors; as well as between inhibitors of transcriptional elongation, such as NELF (Egloff et al., 2009; Ohlsson et al., 2010b).

One of the most well characterized interacting partners of CTCF is the Cohesin complex. CTCF binds to a specific region of the Cohesin subunit SCC3 (SA2; (Xiao et al., 2011)) and this interaction is required for CTCF/Cohesin insulator function. In the presence of CTCF, Cohesin binding across human chromosomes occurs at specific locations whereas without CTCF, Cohesin binding occurs non-specifically; indicating that CTCF positions Cohesin on human chromatin (Parelho et al., 2008; Rubio et al., 2008; Wendt et al., 2008). Tens of thousands of CTCF binding sites occur in the human genome, yet only a fraction of CTCF-bound genomic DNA is looped (Handoko et al., 2011) suggesting that the functional outcome of CTCF binding might be determined by associated cofactors and/or *cis* binding site architecture.

As work by Lieberman and colleagues showed the binding profile of CTCF in KSHV B Cells is widespread (see Figure 3.5; Table 3.2; (Chen et al., 2012a)). Chen et al. showed in 2012 that knockdown of CTCF by shRNA disrupted Cohesin binding but did not significantly alter histones, PolII, or transcription at lytic genes (ORF50; RTA). However, shRNA-mediated loss of Cohesin

(specifically the Rad21 subunit) led to alterations in enrichment of transcriptionally permissive histones and PolII at the Lytic Control Region which did result in RTA expression and viral reactivation (Chen et al., 2012a). Furthermore, reductions in global CTCF levels, or mutation of CTCF binding sites within the viral latency locus have been repeatedly found to disrupt episomal maintenance (Kang et al., 2013; Kang and Lieberman, 2009; Kang et al., 2011; Stedman et al., 2008) potentially suggesting separate roles for CTCF and Cohesin in genome maintenance and viral transcriptional repression respectively. Although roles for Cohesin independent of CTCF have been identified (Kagey et al., 2010; Schmidt et al., 2010) this result is a little difficult to understand given the necessity of CTCF for appropriate Cohesin positioning in the human and viral genomes (Chen et al., 2012a; Kang and Lieberman, 2009; Kang et al., 2011; Parelho et al., 2008; Rubio et al., 2008; Wendt et al., 2008). Furthermore a direct interaction has been established between CTCF and PolII (Chernukhin et al., 2007), whereas Cohesin is not known to directly inhibit PolII, but has been found to interact with NELF to prevent PolII elongation at some loci (Fay et al., 2011).

In latent BC1 PEL cells 75% (18 of 24) of FAIRE-Seq identified regions of open chromatin overlapped published regions of latent CTCF ChIP-Seq enrichment (Chen et al., 2012a). CTCF and Cohesin co-localize at all but 3 regions on the latent KSHV genome, at which CTCF enrichment occurs in the absence of Cohesin (Chen et al., 2012a). We found latent nucleosome depletion at all 3 of these loci; overlapping the K4.2p/OriLyt-L, upstream of the K7 ORF, and overlapping the OriLyt-R/ALTp (Table 3.2). The remaining 25% of regions of latent BC1 open chromatin were not bound by CTCF/Cohesin, but some did contain LANA ChIP-Seq enrichment or RTA Response Elements (RRE'S). Collectively this data suggests that latent viral open chromatin can be CTCF-free or enriched in CTCF/Cohesin or CTCF alone; these states can occur with and without LANA and RTA recognition sites. The potential links between these permutations and control of KSHV transcriptional and conformational are discussed below.

Interpreting the Code: KSHV Transcription

All regions of latent open chromatin identified by FAIRE-Seq in BC1 were shared or conserved in other KSHV episomes examined (Table 3.3). This includes the 18 of 24 (75%) regions adjacent to histones associated with transcriptional activity (H3K9/K14-ac and/or H3K4-me3; Table 3.3; Figure 3.3; (Gunther and Grundhoff, 2010)). This also includes the 6 regions of open chromatin not near these histone marks, which mapped to spliced introns (n=3) or control regions for DE virally encoded DNA replication proteins (e.g. ORF's 9, 39, and 40/41) and all of which were bound by CTCF/Cohesin. A similar trend in proximity was not clear for the facultative heterochromatic H3K27-me3 marks, and no regions of nucleosome depletion were within 250bp of the constitutive heterochromatic mark H3K9-me3 using a stringent enrichment cutoff of 3 Std. deviations above baseline from Gunther and Grundhoff , 2010 "Dataset S1" (Gunther and Grundhoff, 2010). Overall this indicates that the regions of latent open chromatin which are associated with transcription during the viral life cycle (i.e. non-intronic), occur near "active" histones signatures, while regions of intronic and intragenic open chromatin do not (Table 3.2). Most of these H3-ac/H3K4-me3 proximal latent nucleosome depleted regions also contain CTCF, but some remain CTCF-free during latency.

Transcriptional Utility of CTCF-Free Open Chromatin

All CTCF-free regions of nucleosome depletion also lacked Cohesin but were proximal to H3K9/K14-ac and/or H3K4-me3. This includes the vIL-6 region and the constitutive LANApc (Table 3.2), each of which generates latent transcripts (Chandriani and Ganem, 2010; Deng et al., 2002; Dittmer et al., 1998), and hence represent a class of regulatory elements freely available for productive transcription during KSHV latency. Two other CTCF-free regions of open chromatin contained binding sites for KSHV LANA as determined by ChIP-Seq (Chen et al., 2012a); one intergenic to the KSHV noncoding PAN RNA, and one between of KSHV ORF's 75 (a viral tegument protein) and K15 (a viral transmembrane signaling protein). Both OriLyt's also contained CTCF-free open chromatin. At OriLyt-R nucleosome depletion overlapped with the RTA-inducible K12p.

In fact 3 out of 6 CTCF-free regions of latent open chromatin overlapped with annotated RTA Response Elements (RRE's; Table 3.2). This occurred at the vIL-6p (Deng et al., 2002), K12p/OriLyt-R, and OriLyt-L (Chen et al., 2009) regions. While these regions are transcriptionally accessible during latency they likely require RTA for basal and/or inducible gene expression, and this has been observed at each of these loci (AuCoin et al., 2004; Cai and Cullen, 2006; Li et al., 2002; Wang et al., 2006b). The nature of LANA binding to CTCF-free open chromatin during latency is unclear. LANA can positively and negatively regulate transcription and also regulates viral genome maintenance through interaction with host chromatin (reviewed in (Ballestas and Kaye, 2011)). LANA-enriched CTCF-free open chromatin was found intergenic to KSHV PAN RNA, but interestingly only in *ex vivo* cultured PEL BC1 and BCBL1 cell lines (Table 3.3; (Cesarman et al., 1995b; Komanduri et al., 1996)). LANA-enriched CTCF-free open chromatin also occurred between KSHV ORF's 75 and K15, and in all viral isolates examined. ORF 75 and K15 expression have been detected during latency (Chandriani and Ganem, 2010; Wong and Damania, 2006), and moreover transcription of the K15 ORF can read through to give rise to ORF 75 (Glenn et al., 1999). However the function of LANA enrichment at CTCF-free nucleosome depleted regions is unknown.

In sum accessible CTCF-free regions of latent open chromatin occur near H3K9/K14-ac and/or H3K4-me3 and may be constitutively transcriptionally active (vIL-6/LANApc), or may require interaction with viral cofactors such as RTA or LANA, for transcriptional activity (OriLyt's/K12p and PAN/ORF 75/K15 respectively). Constitutively active regions of CTCF-free open chromatin are conserved and those regions interacting with viral cofactors, such as LANA and/or RTA, display a degree of variability in relation to viral isolate (Table 3.3). The functional consequences of LANA binding at open chromatin in the absence of CTCF during latency are unknown but could be related to episomal transcription and/or conformation.

Transcriptional Utility of CTCF-Enriched Open Chromatin

Chen et al., 2012 found that regions of latent open chromatin which contained CTCF were also enriched with Cohesin at all but three loci in BCBL1 cells. These three loci corresponded to the OriLyt-L, K7p, and OriLyt-R/ALTp regions, all of which also contained binding sites for RTA ((Chen et al., 2009; Deng et al., 2002); Table 3.2). Each of these regions is also enriched in RNA PolII during latency, the occupancy of which increases during reactivation (Toth et al., 2012). Toth et al., 2012 showed that at OriLyt-L and the K7p, the cellular NELF complex inhibited stalled PolII elongation and other reports have found evidence of NELF and PolII pausing at the K12p/OriLyt-R region of open chromatin (Kang et al., 2013). Hence all three regions of latent open chromatin which contain CTCF but not Cohesin also contain PolII occupancy during latency. All three also contain RRE's and were conserved among viral isolates (Tables 3.2 and 3.3). This suggests that CTCF-bound open chromatin lacking Cohesin may be poised for RTA during latency (Figure 4.8B).

CTCF and Cohesin co-occupied 15 of 24 (~58%) FAIRE peaks in latent BC1 cells. These 15 regions of open chromatin were proximal (n=9) or distal (n=6) to H3ac and/or H3K4-me3 (Table 3.2; (Gunther and Grundhoff, 2010)) 5 of the 9 (~56%) CTCF/Cohesin-enriched latent FAIRE peaks proximal to H3-ac/H3K4-me3 also contained RRE's (Chen et al., 2009; Deng et al., 2002) and most occurred at annotated lytic promoter regions. The 6 regions of CTCF/Cohesin-enriched open chromatin distal to H3-ac/H3K4-me3 occurred in intragenic/intron regions (5/6) or and near KSHV ORF39/40-41 (viral glycoprotein/helicase-primase, respectively) in B cells (Tables 3.2 and 3.3). This data indicates that regions of open chromatin which contain CTCF and Cohesin during latency can be sub-classified based upon proximity to H3-ac/H3K4-me3. Those near H3-ac/H3K4-me3 largely map to lytic promoter regions, many of which also contain RRE's (Figure 4.8C). Those distal to H3-ac/H3K4-me3 occur within introns and at intragenic regions, and at a promoter region identified as open chromatin only in infected B cells (Figure 4.8D)

Together the data indicates that CTCF-free, accessible latent open chromatin occurs at transcriptionally active latent loci (vIL-6p; LANApc) and at other loci which may or may not require viral cofactors for utility (i.e. RTA and LANA). CTCF-enriched open chromatin occurs in the

absence of Cohesin at loci poised with stalled PolII (such at the OriLyt's, K7p, and ALTp). CTCF-enriched open chromatin which also contains Cohesin during latency can be sub-classified based on proximity to H3-ac/H3K4-me3. CTCF/Cohesin-enriched latent open chromatin near H3-ac/H3K4-me3 occurs at lytic promoter regions, many of which contain RRE's. CTCF/Cohesin-enriched latent open chromatin distal to H3-ac/H3K4-me3 largely occurs at intronic/intragenic regions as summarized in Figure 4.8.

Interpreting the Code: KSHV Genome Conformation and Replication

Loss of CTCF has less dramatic transcriptional effects than loss of Cohesin (Chen et al., 2012a; Kang et al., 2011). However, loss of CTCF (or binding sites within the latency locus) in KSHV leads to instability in viral genome maintenance and similar effects are observed in the related herpesvirus Samiri (HVS) (Chen et al., 2012a; Kang et al., 2013; Kang and Lieberman, 2009; Kang et al., 2011; Stedman et al., 2008; Zielke et al., 2012)). The CTCF binding sites in the KSHV latency locus are thought to generate CTCF/Cohesin mediated intra-episomal looping in the viral genome (Kang et al., 2011). One loop was found between this region and a downstream region near the K12 ORF (Figure 4.9A). This loop potentially directs the programming of latent PolII at the latency locus (Kang et al., 2013). A second inter-episomal loop originating from this major CTCF/Cohesin peak in the latency locus is thought to physically link the latency locus with the Lytic Control Region (i.e. near ORF50/RTA). Thus two CTCF/Cohesin-mediated loops are thought to connect the first LANA intron to either (i) the K12p region or (ii) the RTA promoter region (Figure 4.9B and C). Although CTCF and Cohesin may have functionally distinct roles in the human and KSHV genomes they work together to modulate transcription and also long-range conformation. How specificity between long-range vs. short-range CTCF/Cohesin effects is determined is unclear. How this is coupled to viral proteins expression (i.e. LANA/RTA), viral genome replication, and the nuclear geography are all unknown questions that I have considered in the following section.

The KSHV LANA protein is involved in viral genome maintenance and conformation (Chapter I; reviewed in (Ballestas and Kaye, 2011; Deng et al., 2012)). The LANA C-terminus is responsible for LANA multimerization and DNA binding, both of which are necessary for binding at the KSHV TR's (Ballestas et al., 1999; Ballestas and Kaye, 2001; Garber et al., 2002; Kelley-Clarke et al., 2009; Komatsu et al., 2004; Schwam et al., 2000). The LANA N-terminus represents the dominant chromosome attachment region and binds to host chromosomes through interacting with an acidic patch at the interface of histone H2A and H2B (Barbera et al., 2006). The simultaneous contacts between viral TR's and host chromosomes, allow the LANA protein to tether the viral genome and ensure efficient persistence of the latent extra-chromosomal KSHV genome (Figure 4.10A).

We found latent open chromatin at the regions involved in CTCF/Cohesin long-range episomal interactions between the latency locus and either the K12 region or the Lytic Control Region (Table 3.2; (Kang et al., 2011)). All of these loci contain RRE's, and the first LANA intron (near the inducible LANApi) also contains LANA enrichment during latency (Figure 4.10B; Table 3.2). Regions of CTCF enrichment that lack Cohesin (Figure 4.9B) do not appear to be involved in looping interactions (Chen et al., 2012a; Kang et al., 2011). LANA bound at two regions of CTCF-free latent open chromatin. One occurred only in *ex vivo* PEL lines intragenic to KSHV PAN, and the other occurred in all cell lines between KSHV ORF75/K15. CTCF-free LANA-enriched latent open chromatin exhibited some evidence of long range interaction in chromatin conformation analysis (Figure 4.9C; (Kang et al., 2011)); however the use of very specific primer sets and restriction fragments for 3C analysis limits interpretation to small sections of viral genome only. Since these regions are nucleosome depleted (and thus lack H2A/H2B) I believe this LANA enrichment likely reflects C-terminal LANA DNA binding. C-terminal LANA can modulate transcription and also bind TR DNA and binding at these two loci may specify latent transcriptional modulation and/or long-range episomal contacts independent of CTCF/Cohesin (Figure 4.10C).

12 remaining CTCF/Cohesin-enriched FAIRE-Seq identified open chromatin regions were found in BC1 (Table 3.2), and all were shared in other viral isolates (Table 3.3). These regions occur proximal and distal to H3-ac/H3K4-me3, and may or may not contain and RRE or LANA binding. Given the limited 3C analysis and the known functions of CTCF/Cohesin in the human and viral genomes, it is possible that these remaining CTCF/Cohesin-enriched regions of open chromatin form other long range interactions during latency. These could be inter-episomal or between the episome and host chromosomes (Figure 4.10D).

In latently infected cells the viral genome replicates from the TR's, this is dependent upon LANA and occurs in concert with cell division to maintain appropriate ratios of persistent latent episomes (Garber et al., 2002; Grundhoff and Ganem, 2003; Hu et al., 2002; Hu and Renne, 2005; Stedman et al., 2004; Verma et al., 2006; Verma et al., 2007a). Other reports suggest alternative regions of viral replication during latency (Verma et al., 2007b; Verma et al., 2011), however the results of these studies are dubious and intentionally ambiguous in my opinion.

Regions of CTCF-free and CTCF-enriched open chromatin (without Cohesin) were also found at both KSHV lytic replications during latency (Table 3.2). RTA-mediated transcription at the OriLyt's is required for lytic genome amplification (AuCoin et al., 2004; Wang et al., 2006b) and stalled PolII enrichment during latency has been observed at both OriLyt regions (Kang et al., 2013; Toth et al., 2012). RTA activation at these regions, and at other CTCF/Cohesin-enriched latent open chromatin (Figure 4.10D) could serve to "unzip" the viral episome from the host chromosome and/or "unfold" inter-episomal interactions during lytic reactivation (Figure 4.13). This model would link RTA-induced transcription and genome replication and would allow for the replication of linearized and non-chromatin zed viral genomes for subsequent incorporation into virions during reactivation.

CTCF is also capable of coordinating the nuclear geography, and positioning transcriptionally inactive regions near nuclear Lamina-Associated Domains (LAD's; reviewed in (Holwerda and de Laat, 2012)). A long-term vision could include an investigation of the 3D positioning of KSHV episomes the nucleus. I predict nucleosome depleted regions of the viral genome bearing

CTCF/Cohesin will be enriched in long-range contacts (inter-episomally and with host CTCF sites) and localized to LAD's, whereas open chromatin elements without CTCF and Cohesin will be localized to transcriptionally active regions of the nuclear landscape; such as so called "transcription factories".

Together the data demonstrate that CTCF, Cohesin, and LANA assemble at the TR to replicate and tether the viral genome to host chromosomes during latency (Figure 4.10A). CTCF/Cohesin co-localize with LANA at open chromatin near the first LANA intron and are thought physically link this region with the K12p or Lytic Control Region during latency (Figure 4.10B). LANA-enrichment also occurs at two CTCF-free nucleosome depleted regions in the latent episome and may be involved in CTCF-free loops (Figure 4.10C). LANA binds at over 250 cellular loci (Lu et al., 2012a) and hence these loci could potentially couple the viral genome to host chromatin outside of the TR's (Figure 4.10C). Other CTCF/Cohesin-enriched regions of latent open chromatin are shared among viral episomes (Tables 3.2 and 3.3), and could be involved in "zipping" the viral genome to host chromatin (Figure 4.10D).

Many regions of open chromatin enriched in CTCF also contain RTA binding sites; including both OriLyt's. This suggests that RTA-mediated induction could displace CTCF to transcribe and replicate the lytic genome. In support of this hypothesis, CTCF and Cohesin dissociate from the KSHV genome early during reactivation (Chen et al., 2012a; Kang et al., 2011); a phenomenon which also occurs in HSV (Ertel et al., 2012). In HSV this effect is transcription-dependent, and in KSHV lytic reactivation also requires lytic transcription (Lin et al., 2003). Better conformational analyses are needed to distinguish inter/intra-episomal vs. episomal/host chromosomal interactions. CTCF could also topologically position latent viral open chromatin in specific sub-nuclear compartments to prevent aberrant lytic induction; while CTCF-free chromatin could remain transcriptionally accessible. Understanding how LANA and RTA interact with CTCF, and if CTCF mediates long range interactions between latent episomes and host chromatin are important unknown questions in the field.

Ghost(s) in the Machine: Potential Variance Associated with Cell Type, Cell Division, and Heterogeneic KSHV Genomes

Other unknowns in KSHV biology include (i) the observed phenotypic and morphological differences between KSHV infected B cells and endothelial cells; and (ii) the consistently observed low levels lytic gene expression in KSHV cultures and tumors. In this sub-section I have considered how these unknowns could relate to open chromatin, cell division, and viral heterogeneity in single cells.

The primary *in vivo* target of KSHV is the B cell, and in immuno-competent hosts this is where the virus is localized (Ambroziak et al., 1995). The virus can also infect endothelial cells *in vivo,* such as KS lesion-associated spindle cells and others (Dupin et al., 1999; Parravicini et al., 1997). *In vitro* KSHV infection is counter-intuitive; KSHV cannot infect most established B cell lines, but can infect a variety of adherent cells *in vitro* (reviewed in (Ganem, 2010)), which alters their morphology. Moreover, while B cells can be cultured *ex vivo,* primary endothelial cells rapidly lose KSHV in culture.

Infected B cells also exhibit higher rates of spontaneous KSHV reactivation, better lytic induction, and higher episomal copy numbers than endothelial culture models (An et al., 2006; Renne et al., 1996b), as well as different levels of global gene expression during both viral replication phases (Chandriani and Ganem, 2010; Chandriani et al., 2010). In addition some viral genes are latently expressed only in B cells (i.e. vIRF-3; (Rivas et al., 2001)), and other transcripts can exhibit variable promoter usage in BC1 vs. BCBL1 PEL cells (i.e. K12; (Li et al., 2002)). Thus differences in morphology, phenotype, and gene expression patterns are observed among and between infected B cell and endothelial lineages.

As of yet there is no clear explanation for these differences. However some interesting cell type-specific differences in the nucleosome depletion of latent episomes have emerged. Some regions of latent nucleosome depletion were observed only in B cells. Open chromatin at the

promoters of virally encoded genome replication/tegument proteins (ORF's 39/40/41 and ORF 45, respectively) and encompassing viral miRNA's 5-2 (121605-121917nt), was identified in all B cell derived KSHV genomes, but was absent in the endothelial lineage. In addition, latent open chromatin intragenic to KSHV PAN was observed only in *ex vivo* PEL lines (BC1/BCBL1). This region was unique in that KSHV LANA is localized here in the absence of CTCF/Cohesin during latency. Open chromatin at these B cell specific loci could have transcriptional and conformation effects. This could include differential availability of regulatory elements at promoters encoding viral DNA replication and tegument proteins (ORF40-41 and ORF45, respectively) and altered access of KSHV LANA to CTCF-free open chromatin intragenic to KSHV PAN.

While latent episomes from endothelial cells had unique open chromatin regions (Figure 3.5B) nucleosome depletion that was observed in both endothelial cell lines was also present in B cells. That is; no endothelial-specific nucleosome depletion was observed during latent infection. However some FAIRE-Seq regions displayed increased intensity in endothelial-derived episomes. Regions of open chromatin in the latency locus, upstream of the K12p and LANA ORF's, were hyper-intense in latent endothelial cells (data not shown). The nature of this differential in FAIRE-Seq signal is unclear, but may be related to CTCF mediated PolII programming (Kang et al., 2013), and could indicate differential latency locus chromatin structures between B and endothelial cells. Collectively cell type-specific differences in open chromatin were observed but the functionality thereof remains speculative.

While CTCF binding is highly conserved, Cohesin may have cell type-specificity (reviewed and Cohesin activity cycles with cell division (Mehta et al., 2012; Merkenschlager, 2010)). In addition to infecting endothelial and B cells, KSHV exists latently in actively dividing cells. The LANA protein interacts with the viral TR's and other host proteins to replicate the viral genome during latency to ensure proper segregation to daughter cells, and many LANA-associated interactions may be cell cycle dependent (reviewed in (Ballestas and Kaye, 2011; Deng et al., 2012)). Cohesin activity is cell cycle regulated and is functional surrounding and during S phase to maintain

sister-chromatid cohesion, but is released prior to prophase/anaphase (reviewed in (Mehta et al., 2012)). Studies have shown that Cohesin binding to the KSHV latency locus is also highly enriched in S phase, but dissociated thereafter (Kang and Lieberman, 2009). This transient Cohesin-depletion was correlated with uninduced expression from K14p, and was cell cycle-dependent.

Kang and Lieberman, 2009 further showed that the sub-nuclear localization of CTCF and the CTCF interaction with Cohesin oscillated with cell cycle. Later Kang et al., 2011 found that both CTCF and Cohesin together mediated episomal loops during latency (Figure 4.9; (Kang et al., 2011)). These loops were decreased, but still present, in the absence of either CTCF or Cohesin and were enriched in S phase. More recently, Lieberman and associates have shown that knockdown of Cohesin subunits leads to KSHV lytic gene induction and reactivation, whereas knockdown of CTCF leads to viral genome instability (Chen et al., 2012a). Collectively this indicates that CTCF and Cohesin could have separable roles in the viral genome, and that CTCF/Cohesin-mediated effects at regions of latent open chromatin may display variability during cell cycling, leading to bursts of "lytic" transcription.

Low levels of spontaneous KSHV reactivation and transient lytic gene expression are detected in culture and primary tumors (Dittmer, 2003; Pauk et al., 2000; Renne et al., 1996b; Vieira et al., 1997). The KSHV field is still divided as to whether this represents full reactivation leading to host cell lysis and virion maturation, or transient lytic gene expression. Personally, I think there is a likely continuum of lytic gene expression outside of conventional "reactivation". This is probably linked to KSHV pathology during immunosuppression/HIV infection and may not lead to widespread host cell lysis. Dynamic lytic gene expression could arise from cell type-specific factors and/or cell cycling variance among CTCF/Cohesin (and hence open chromatin accessibility); as well as oscillations in other host and viral proteins (i.e. LANA). Moreover the most recent transcriptional analyses of KSHV suggest that the latent viral episome may be more active than previously appreciated (Chandriani and Ganem, 2010; Dresang et al., 2011).

Many of the regions we identified as nucleosome depleted by FAIRE-Seq in BC1 qualitatively correlate to regions of the viral genome displaying latent transcriptional activity and also latent PolII enrichment (Figure 3.6; Figure 4.11; (Dresang et al., 2011; Kang et al., 2013; Toth et al., 2012)). This includes open chromatin at which CTCF binding occurs without Cohesin and at which PolII is "stalled". This could indicate that once each cell division, coincident with Cohesin degradation, opportunities for lytic gene expression from latent open chromatin could be possible. This could be one explanation for the low levels of lytic gene expression observed in latent KSHV cultures/tumors. Additionally, heterogeneous episomal populations could cause variable latent gene expression.

Recent single-molecule analyses of the LANA, RTA, and vIL-6 promoter regions; using accessibility of local nucleic acid to methylation (MAPit), suggests that a wide range of epigenetic heterogeneity at each locus exits among a given population of episomes (Darst et al., 2013). The largest subset of chromatin at all three loci appeared to be inaccessible, and this subset was higher in endothelial cells compared to B cells. This inaccessible subset of chromatin was not changed upon reactivation. This could explain why even with exogenous TPA/sodium butyrate/RTA treatment, only a small fraction of KSHV can ever be reactivated from latency and why this rate is far lower in endothelial cells relative to B cells. This suggests that diversity exists among latent viral episomes within single cells, and that most episomes are inaccessible. This form of epigenetic drift could also explain why only ~ 1% of available herpesvirus genomes give rise to functional progeny during reactivation (Darst et al., 2013; Kobiler et al., 2010).

The gradual DNA methylation of the KSHV genome occurs slowly after *de novo* infection (Gunther and Grundhoff, 2010) and continued lytic replication is thought to be critical for sustained viral persistence (Grundhoff and Ganem, 2004). Progressive epigenetic silencing of these genomes could lead to decreased LANA synthesis and hence and viral genomes (Grundhoff and Ganem, 2004; Skalsky et al., 2007a), and heterogeneity in latent/lytic gene expression may serve to circumvent this dilution of the infectious capacity of KSHV. Some episomes contained epigenetically accessible

chromatin at the RTA promoter in Darst et at., 2013, indicating that heterogeneous episomal distributions might also generate varied levels of transcription, including low levels of lytic transcripts within a single cell.

The phenotypic and morphological differences observed between infected B and endothelial cells could be related to access to latent open chromatin, but currently this association is unclear. CTCF expression is ubiquitous, whereas expression levels of Cohesin and other cellular proteins can be cell-specific. Low levels of spontaneous lytic transcription and reactivation are observed in KSHV cultures and tumors; the levels of which are higher in B cells. This could be related to cell cycle-mediated degradation of Cohesin and/or heterogeneity among episomes, even within a single cell. Gradual episomal DNA methylation in the KSHV genome could lead to *bona fide* genetic/epigenetic drift. At the human H19/Igf2 locus, CTCF binding is methylation sensitive (reviewed in (Holwerda and de Laat, 2012)). This progressive epigenetic silencing could lead to viral genome instability and the observed low levels of heterogeneic lytic gene expression could provide sustained viral signaling and new progeny.

In sum, the latent viral genome may not be as transcriptionally silent as was once believed. Low levels of spontaneous lytic activity occur in KSHV infected cell populations which is variable between B and endothelial cells. This could be related to differences in open chromatin between B and endothelial cells and/or differences in associated factors such as Cohesin. Given the variances observed in the KSHV genome across cell cycle and within single cells, it is plausible that FAIRE-Seq identified regions of nucleosome depletion are dynamically accessed (Figure 4.11) within a single cell and among entire populations of infected cells (i.e. viral tumors).

The KSHV Episome Comes Full-Circle

The cell cycle-associated fluctuations in Cohesin discussed in the previous subsection were observed with functional consequences at the KSHV latency locus (Kang and Lieberman, 2009). Later the Lieberman lab found that CTCF/Cohesin mediated a chromatin loop in between the KSHV

latency locus and the Lytic Control Region, and that this loop was dynamic through cell cycling and lost during viral reactivation (Kang et al., 2011). This looping is thought to coordinate a transcriptional balance between the Lytic Control Region and the latency locus; both of which contain RTA-responsive bidirectional promoters (Figure 4.2). In addition these two regions also shared open chromatin/CTCF-enrichment profiles (Figure 4.12). Both loci contain strong CTCF/Cohesin-enrichment and nucleosome depletion downstream of the LANApi/50AS TSS's. However at the latency locus the constitutive LANApc occupied a distinct CTCF-free region of open chromatin. This suggests that the LANApi/K14p and 50AS/K8DE bidirectional promoters share *cis* homology, open chromatin profiles, and physical proximity (Figure 4.12). This results is the physically linkage of these transcriptional attenuation circuits. This could allow dynamic and coordinated control of both bidirectional loci in response to RTA and/or cell cycling.

Validated long range conformational interactions in KSHV include extra-episomal attachment to host chromatin via LANA and the viral TR's (reviewed in (Ballestas and Kaye, 2011)) and CTCF/Cohesin-mediated inter-episomal contacts between the latency locus and the K12 and/or Lytic Control Regions (Kang et al., 2011). Given that there are over 30,000 ubiquitous binding sites for CTCF in the human genome (Kim et al., 2007; Phillips and Corces, 2009), it is hard to imagine how the several latent viral loci enriched with CTCF and/or Cohesin binding avoid interaction with cellular CTCF/Cohesin sites. It remains unknown how CTCF-mediated loops are specified in the human genome (reviewed in (Holwerda and de Laat, 2012; Mehta et al., 2012; Merkenschlager, 2010)).

In the KSHV genome, outside of the viral TR's, long range interactions between regions of nucleosome depletion could potentially be specified by KSHV LANA. This could occur at CTCF/Cohesin-enriched open chromatin (the latency locus) and at CTCF-free open chromatin (intragenic to PAN). LANA is expressed in all infected cells to maintain the viral genome and can also modulate host and viral transcription. LANA also binds host chromatin in the presence or absence of the viral genome (Ballestas et al., 1999; Lu et al., 2012a). Hence the nature of LANA-

enrichment at regions of open chromatin is not fully clear but could serve transcriptional and/or conformational functions.

Many regions of open chromatin identified by FAIRE-Seq which were enriched in CTCF and/or Cohesin during latency also contained RTA binding sites (Table 3.2). This included both of the KSHV OriLyt's, which depend upon RTA transcription for the activation of viral lytic genome replication (Wang et al., 2006b). This could suggest that RTA and CTCF physically interact at some regions of open chromatin during lytic induction. The simplest scenario is one in which RTA could physically displace CTCF to activate transcription and viral genome replication. Studies examining this direct interaction are limited but CTCF/Cohesin dissociate from the viral genome during reactivation, and this dissociation disrupts inter-episomal long range contacts (Chen et al., 2012a; Kang et al., 2011). Thus upon external stimuli which result in RTA expression, these regions of latent open chromatin can "unfold" the latent episome. If long range CTCF/Cohesin interactions between episomal and host chromatin exist these linkages are also likely similarly "unzipped" during RTA expression.

Collectively I believe the model with the most parsimony is one in which the latent KSHV episome adheres to host chromosomes, not only at the TR's, but also at other CTCF/Cohesin bearing sites in an arrangement termed the CTCF "zipper" model (Figure 4.13). This organization would allow the viral genome to be packaged into chromatin and intimately linked with the host genome; avoiding host DNA damage triggers, nuclear/chromosomal malformation, and also allowing topological epigenetic regulation. With over 6 billion bp in the haploid host genome, this would easily accommodate the highest estimates of hundreds of viral genomes per cell (~3,000 viral genomes if interactions with host chromatin are non-specific).

Reactivation stimuli could cause displacement of CTCF/Cohesin thus coupling the lytic transcriptional response to viral lytic genome detachment and subsequent histone-free packaging into virions. The facts that (i) CTCF/Cohesin dissociate from the viral genome during reactivation; that (ii) activated histones surround these RRE-containing open chromatin regions but are insulated by

CTCF/Cohesin; that (iii) lytic DNA replication results in linear, nucleosome free KSHV genomes; and that (iv) in HSV CTCF dissociation during reactivation is dependent upon lytic transcription (Ertel et al., 2012); all support this hypothesis. If this speculation is indeed true, then it begs the question: "Would viral:host genomic interactions occur at specific cellular loci (other than CTCF enrichment)?" The answer cannot be generated at present, which in no way obviates its pursuit.

So what "programs" the non-chromatin associated incoming viral genome for latency following *de novo* infection? Data indicates that DNA methylation of the viral genome accrues slowly (Gunther and Grundhoff, 2010); however CTCF and nucleosomes are abundant and ubiquitous and nucleosome incorporation into the viral genome occurs within 5 days post-infection. Moreover, regions of conserved latent open chromatin not only bind CTCF (Figures 3.4 and 3.5; Table 3.2), but CTCF binding are over-represented at regions of open chromatin as determined by motif elicitation programs (Figure 4.14). This implies that nucleosomes are not deposited and *then* displaced by CTCF, but rather that CTCF occupies recognition elements within open chromatin to prevent and nucleosome deposition and maintain nucleosome depletion. Other regions of latent open chromatin contained over-representation of AT-rich motifs. DNA polymers with AT-rich architectures may be refractory to nucleosome incorporation (reviewed in (Kaplan et al., 2010)); alternatively this could reflect RTA recognition elements (Liao et al., 2003), or recognition elements of other associated transcription factors (TBP or developmental transcription factors; SOX12/21).

Potential Targeting of Latent KSHV Open Chromatin

While targeting latent virus is a recurring challenge in herpesvirus biology, the targeting of reactivated virus is clinically feasible (Dittmer et al., 2012). The FAIRE-Seq identified regions of latent KSHV open chromatin were enriched in CTCF and AT rich motifs (Figure 4.14). CTCF/Cohesin displays episome-wide distribution in latent KSHV (Figure 3.5), and loss of CTCF or Cohesin leads to loss of viral genome integrity and lytic induction respectively (Chen et al., 2012a;

Kang et al., 2011). This suggests that these two host proteins, and the open chromatin which they occupy, represent ideal targets for latent viral infection (Figure 4.15A).

I am not aware of any pharmacological compounds which directly target CTCF or Cohesin; however endogenous factors may play a role in their displacement/degradation. For instance Cohesin is naturally degraded by the protein Separase during cellular division (reviewed in (Mehta et al., 2012)). Overexpression or alterations in Separase function could disrupt viral latency. CTCF can be displaced from endogenous binding sites by noncoding RNA's (Faust et al., 2012; Taft et al., 2011)), and manipulation of this mechanism could have therapeutic impact. However, directly targeting CTCF/Cohesin would likely lead to widespread effects on the host genome and may be of limited clinical utility.

Specific targeting of the viral genome may avert interference with the host cell. For instance delivery of long noncoding RNA's (lncRNA's) with specific homology to regions of viral open chromatin could potentially displace CTCF/Cohesin and/or limit the function of open chromatin scaffolds. This could lead to alterations in viral gene expression and conformation, and ideally lytic reactivation. Possible obstacles include off-target effects of exogenous lncRNA's, failure to illicit any response, failure to reactivate epigenetically refractory viral sub-populations, and the difficulty of *in vivo* delivery of noncoding RNA's. However, if the lncRNA's were specific enough off-target effects could be avoided, even in KSHV negative cells, and would not alter open chromatin nor CTCF/Cohesin binding at cellular loci. *in vitro* systems employing rKSHV.219, which generates RFP during lytic viral gene expression (Vieira and O'Hearn, 2004), would be a useful starting point for robust screening. While clearly a long-term vision, projects such as this could lead to novel therapeutic means to awaken dormant herpesviruses for subsequent elimination.

Potential Engineering of Gammaherpesviral Genomes as Substrates for Programmable Genetic Networks

Understanding gammaherpesviral biology is fascinating and it is necessary for the prevention of associated illnesses. The continued pursuit of this understanding has the potential to facilitate awareness in other scientific arenas. A long term vision could include the use of engineered herpesviral genomes for multiple applications; both clinical and industrial. Gammaherpesviral genomes have many unique properties which make them ideal substrates for guided design. Unlike other viral systems these circular genomes do not integrate, have potential for massive genetic payloads (>200kb), exist as multiple copies per cell, and can be controllably maintained. As synthetic genetic circuit and protein design advances (Khalil and Collins, 2010; Nandagopal and Elowitz, 2011; Ruder et al., 2011; Slusarczyk et al., 2012), coupled use of gammaherpesvirus episomal derivatives could assist delivery and network assimilation.

This possibility currently has many obstacles, but if a complete understanding of transcriptional circuitry, viral entry specification, and synthetic protein design (i.e. synthetic LANA for maintenance), can be generated, the potential applications for artificial herpesviral genomes are diverse (Figure 4.15B). Once delivered to host cells these non-integrated genomes could respond to varying endogenous (immune activation/oncogene levels, nutrients) or exogenous (drugs/toxins) signals. With a comprehensive transcriptional network, both host and episomal behavior could be specifically manipulated for a desired response. Moreover, controlled episomal maintenance through toggled loss (preset synthetic LANA silencing) or robust genome replication and viral spread (i.e. reactivation), could allow for tunable control among tissues or populations of unicellular organisms (bacteria/yeast). This technology could be useful for enzyme replacement, population skewing, cell-specific targeting, and the creation of single-cell level factories.

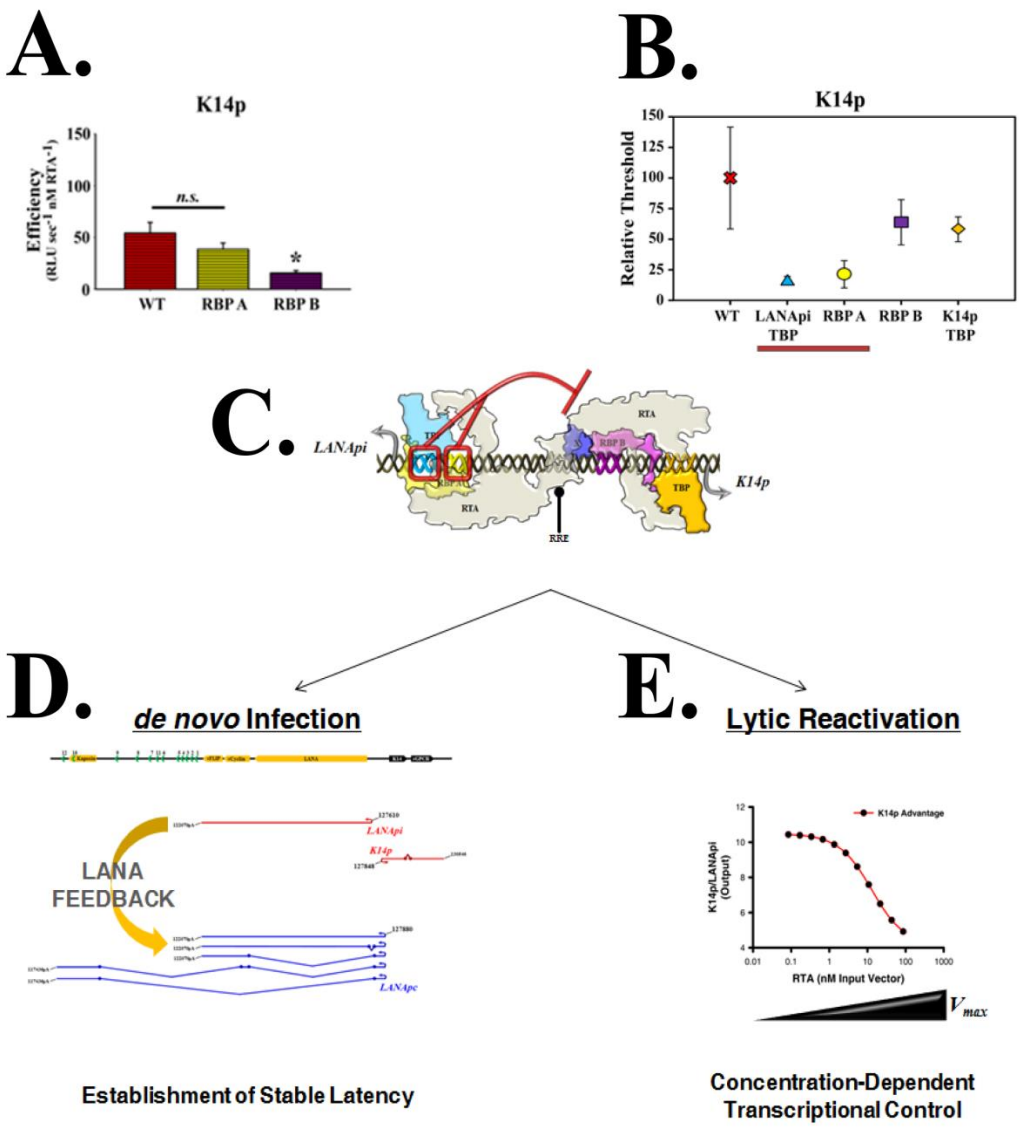

Figure 4.1: Potential Functions of the LANApi/K14p. A. Although K14p output was reduced ~6 fold in the absence of the LANApi-proximal RBP A (see Figure 2.7), this was accompanied by a drop in induction threshold from 13.1 to 2.8 nM (~80% reduction) in response to WT RTA as shown in Panel **B. C.** Both LANApi-proximal TATA and RBPjκ elements (LANApiTATA shown in light blue; and RBP A shown in yellow, respectively) limit K14p. The LANApiTATA limits K14p output and response, and the RBP A limits K14p response but is crucial for output. **D.** During *de novo* infection the LANApi might produce LANA. The LANA protein then induces the constitutive LANApc and also inhibits RTA to establish latency. **E.** The K14p generates ~10 fold more output than the LANApi at low levels of RTA (in our *in vitro* system). However at saturation this margin narrows to ~4 fold, suggesting that the potency of LANApi attenuation occurs in proportion to RTA concentration. See section 4.1.

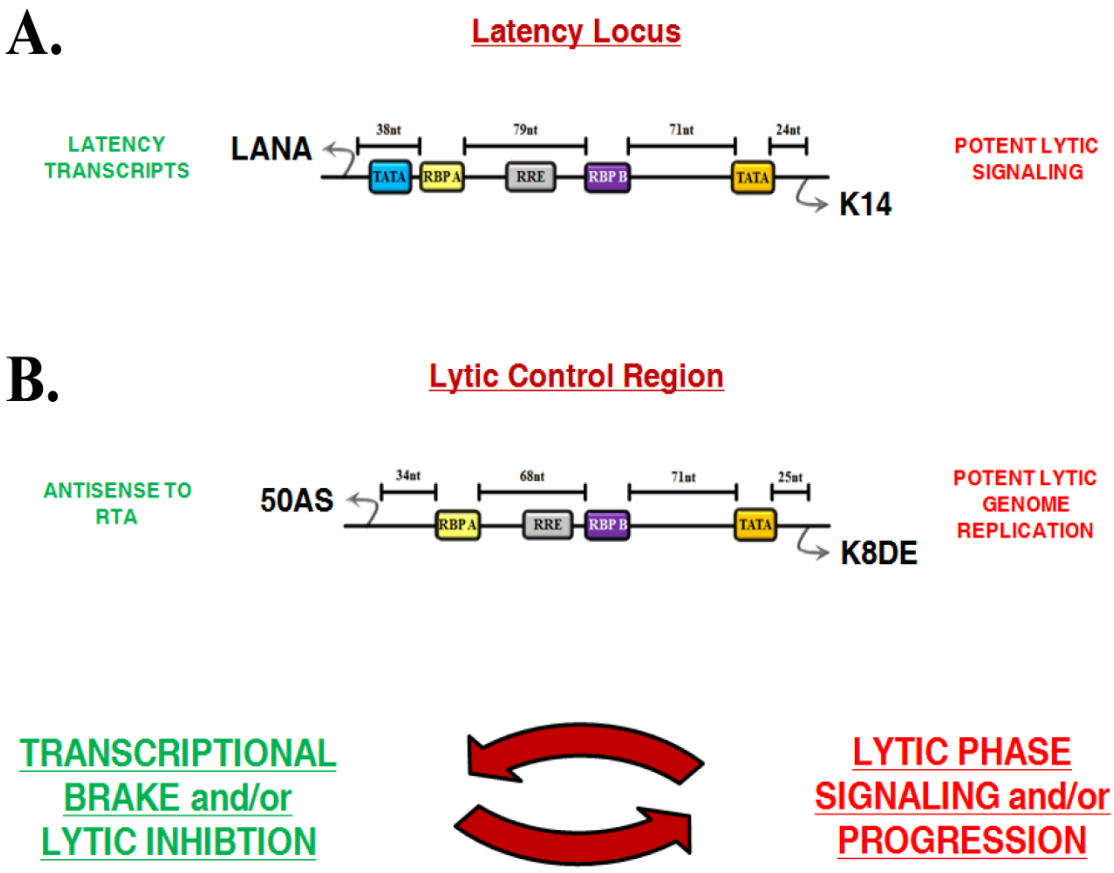

Figure 4.2: A Conserved Transcriptional Brake in KSHV. A. The LANApi/K14p bidirectional promoter at the KSHV latency locus is depicted schematically. LANApiTATA, RBP A, the RRE, RBP B, and the K14p TATA element are shown in light blue, yellow, gray, purple, and orange, respectively. **B.** The bidirectional 50AS/K8DE region (Xu and Ganem, 2010) is depicted schematically as in A. Both K8DE and K14p synthesize potent lytic molecules in response to RTA, whereas LANApi generates latent transcripts and the 50AS encodes an antisense RNA to ORF50 (RTA; see Section 4.1).

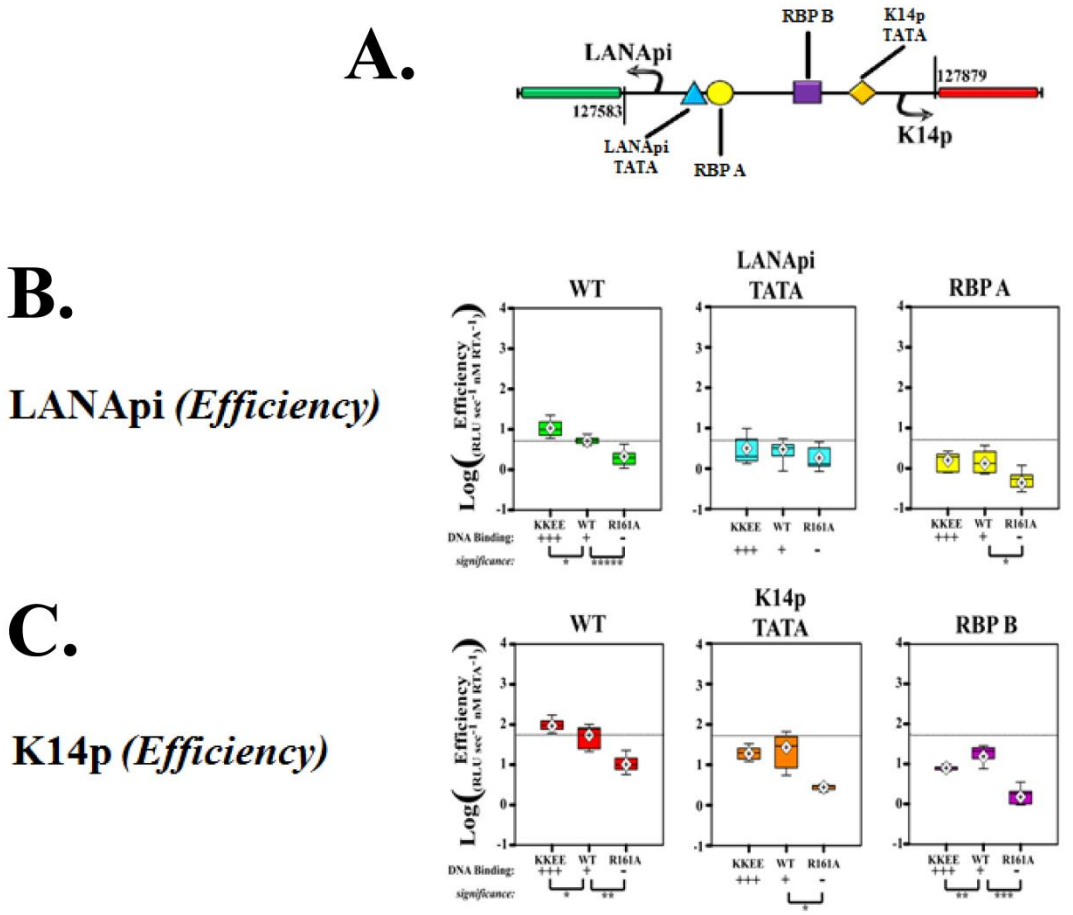

Figure 4.3: RTA DNA Binding Increases Efficiency via TSS-Proximal Regulatory Elements. A. The LANApi/K14p bidirectional promoter at the KSHV latency locus is depicted schematically. LANApiTATA, RBP A, RBP B, and the K14p TATA element are shown in light blue, yellow, purple, and orange, respectively. **B.** The efficiency of LANApi in response to KKEE, WT, or RI61A RTA is shown (on a log scale) for the WT promoter (left panel), LANApiTATA deleted promoter (center panel), and RBP A deleted promoter (right panel) configurations respectively. **C.** The efficiency of K14p in response to KKEE, WT, or RI61A RTA is shown as in B. The dotted line represents the mean efficiency of LANApi (B) or K14p (C) in response to WT RTA. Note that TSS-proximal elements are required for increased efficiency in response to KKEE RTA and that in the absence of TSS-proximal RBPjκ elements, DNA Binding by RTA is still required for interaction at the RRE (see Section 4.1; Figures 2.10 and 2.11).

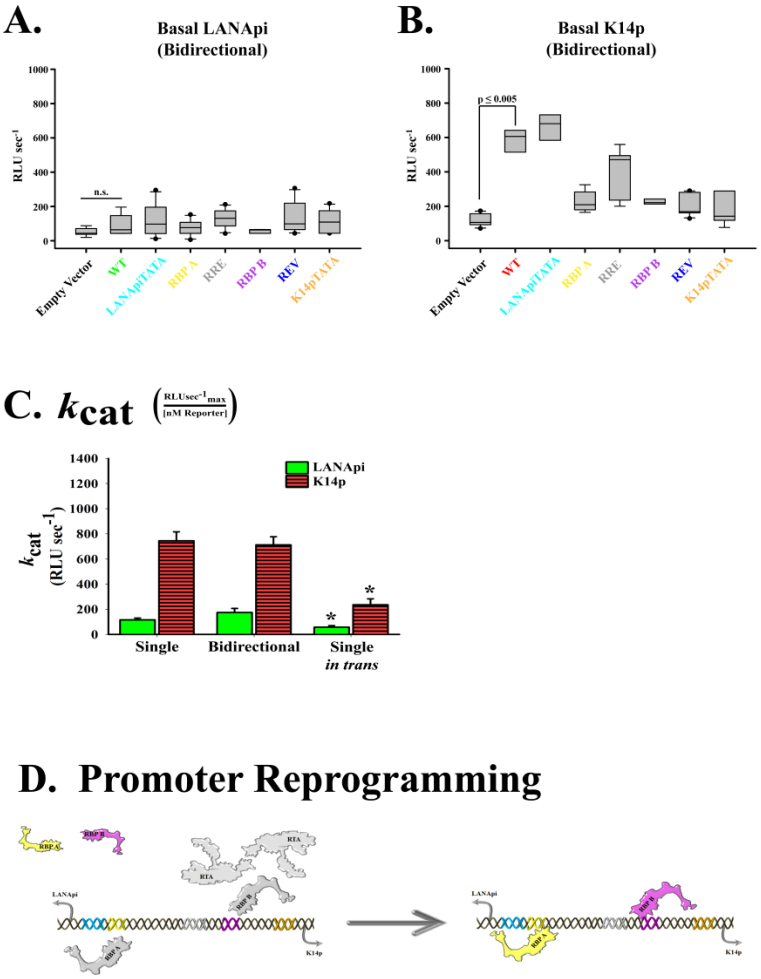

Figure 4.4: Promoter Reprogramming Creates a Refractory Period and Limits k_{cat} *in trans*. A. Basal activity (in our *in vitro* system) in the LANApi TSS from the bidirectional reporter is shown in the WT and indicated mutant configurations. **B.** Similarly to A., K14p basal activity is shown. Note that the K14p basal output is dependent upon intact *cis* regulatory elements *in vitro*. **C.** k_{cat} is shown for LANApi (green bars) and K14p (red, hashed bars) in the single reporter only, bidirectional reporter only, and single reporter together *in trans* inputs. At saturation with RTA (k_{cat}) output is reduced ~2 fold *in trans* due to a refractory period during which the promoter region must likely be "reprogrammed" for activation as shown in **D.** All reprogrammed input molecules are identical in the single only/bidirectional input contexts, and hence newly reprogrammed promoters are activated at a ratio of 1:1 at saturation; *in trans* this ratio is 1:2 (see Section 4.1). n.s., not significant, asterisks (*) indicate a significant difference from single only/bidirectional reporter inputs as determined by Student's T-test.

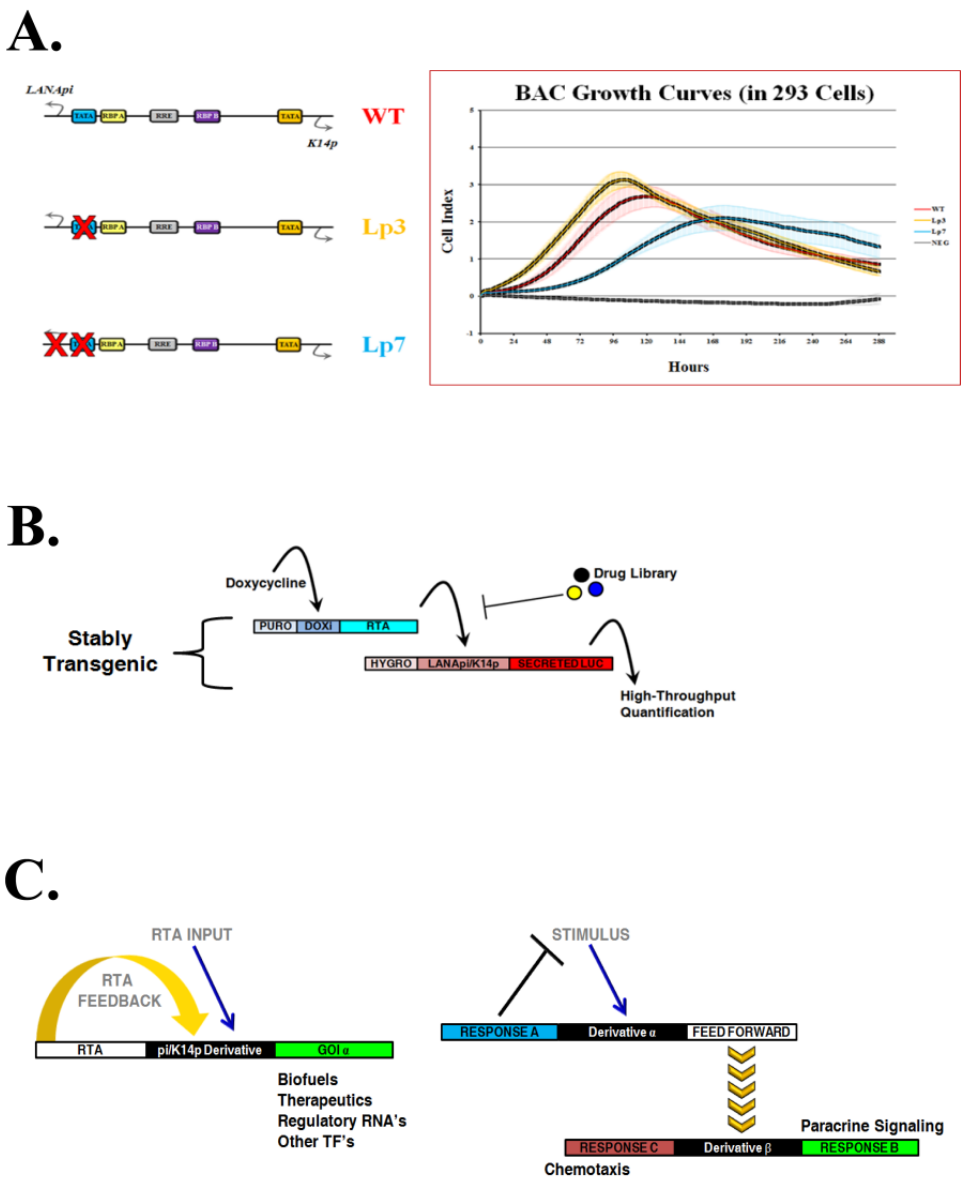

Figure 4.5: Applications and Extensions of the LANApi/K14p Bidirectional Promoter. A. Preliminary analysis of the manipulation of the LANApi/K14p locus *in vivo* using a KSHV Bacterial Artificial Chromosome (BAC) system. Growth curves, in stable BAC-harboring 293 cells are shown. **B.** One potential high-throughput screening scheme to identify reagents that block RTA-mediated induction is shown. **C.** The use of the bidirectional LANApi/K14p promoter as a substrate to engineer positive transcriptional feedback to generate any gene (or transcript) of interest (GOI) in producer cells is shown on the left. Similar circuits could be arrayed in more complex networks to collaboratively respond to any number of stimuli. The example shown here is in relation to immune surveillance by a "sentinel" cell, but other applications could be similarly designed.

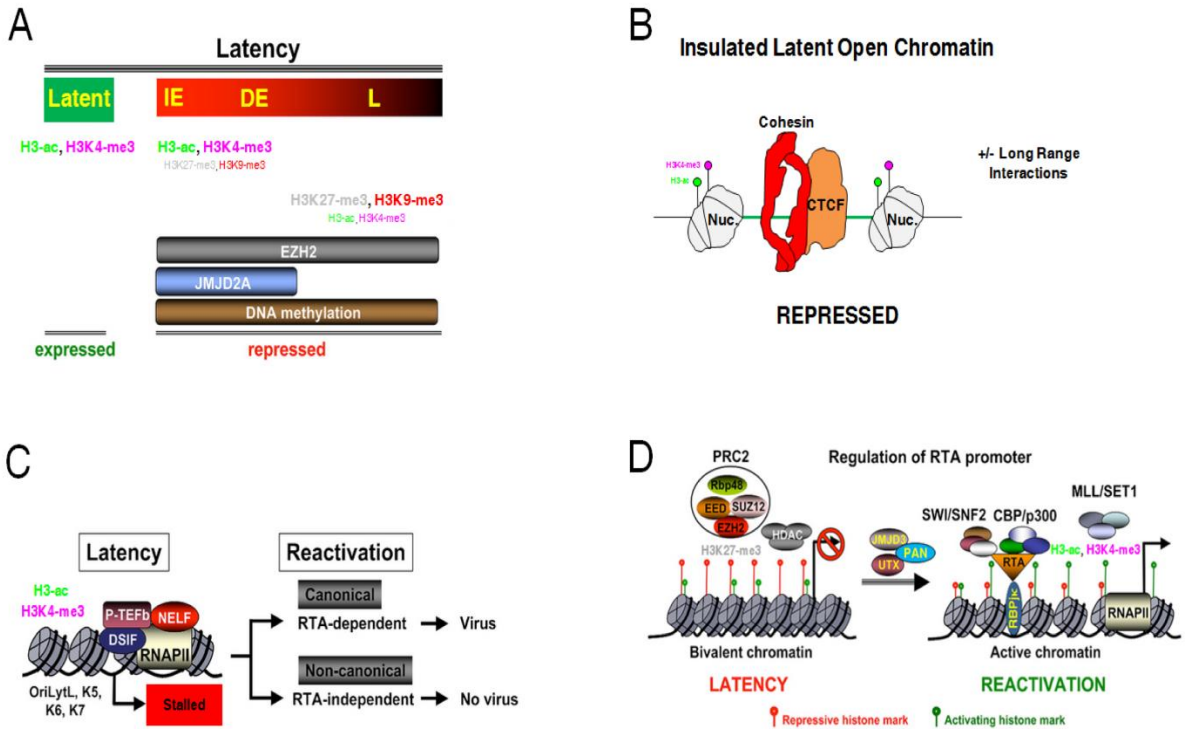

Figure 4.6: Overview of KSHV Epigenetic Regulation. A. During viral latency latent genes are enriched in acetylated histone H3 (H3-ac; green) and trimethylation of histone H3 lysine 4 (H3K4-me3; pink) and are constitutively expressed. Temporally expressed immediate-early (IE), delayed-early (DE) lytic viral genes display similar enrichment with and without coincident trimethylation of histone H3 lysine 27 (H3K27-me3; gray) and/or histone H3 lysine 9 (H3K9-me3; red), whereas viral genes expressed late during lytic induction (L) are generally only enriched with H3K27-me3 and H3K9-me3. The JMJD2A histone demethylase associates with IE/DE viral loci during latency, and the EZH2 histone methyltransferase co-localizes with H3K27-me3 enrichment. Additional methylation of viral DNA leads to repression of lytic loci during latency. **B.** Regions of episomal latent open chromatin occur near H3-ac/H3K4-me3 and may be accessible or repressed by CTCF/Cohesin binding. CTCF/Cohesin may also coordinate long range episomal interactions. **C.** RNA polymerase II (here; RNAPII) many regions of the latent episome. At latent loci active RNAPII generates productive transcription, whereas at certain lytic loci/origins of lytic replication (OriLyt's) RNAPII is stalled by NELF-mediated suppression. This can result in "canonical" and "non-canonical" lytic gene expression; with and without the production of new virus respectively. **D.** At the RTA promoter region Polycomb repressive complex (PRC2) and HDAC's mediate transcriptional suppression. Coincident H3K27-me3 and H3-ac/H3K4-me3 are interpreted by the KSHV field as "bivalent" chromatin. Upon varying stimuli chromatin remodeling can occur at the RTA promoter leading to transcription and regulated viral reactivation. This is coordinated by several proteins including Swi/Snf, CBP/p300, MLL/Set1, recruitment of JMJD3/UTX by KSHV PAN RNA, and interactions between RTA and RBPjκ. See Section 4.3 for more information. Panels A,C, and D were modified with permission from (Knipe et al., 2013).

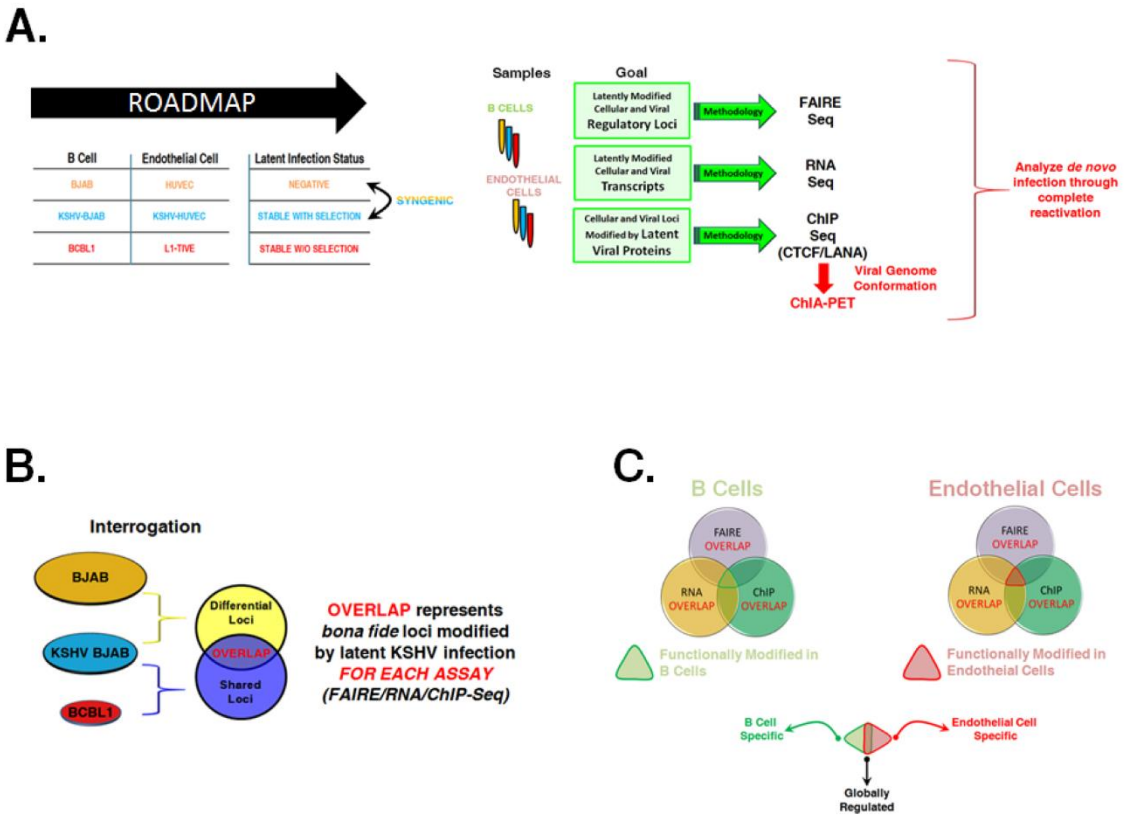

Figure 4.7: Toward a Functional KSHV Epigenetic Atlas. A. Latently KSHV-infected B cells (BCBL1) and endothelial cells (L1-TIVE), as well as infected (KSHV-BJAB, KSHV-HUVEC) and non-infected syngenic control cells (BJAB, HUVEC) could be examined on the basis of regulatory loci (FAIRE-Seq), transcript production (RNA-Seq), and viral/cellular transcription factors (LANA, CTCF, others) enrichment (ChIP-Seq). A long term vision could include temporal context (*de novo* through lytic infection) and viral genome conformation (ChIA-PET) as components of a functional atlas (shown in red). **B.** By appropriately interrogating the resulting data from each assay, overlaps between differentially modified loci (+/- KSHV infection) and shared modified loci (+ KSHV infection) would result in high-confidence targets with functional relevance for each cell type. **C.** By comparing the resulting targets from B, functionally modified loci for each cell lineage could be determined; the overlap of which would indicate a target shared among lineage, whereas B and endothelial cell specific targets would be non-overlapping and distinct. A simpler experimental approach could be employed for the identification of virus specific targets.

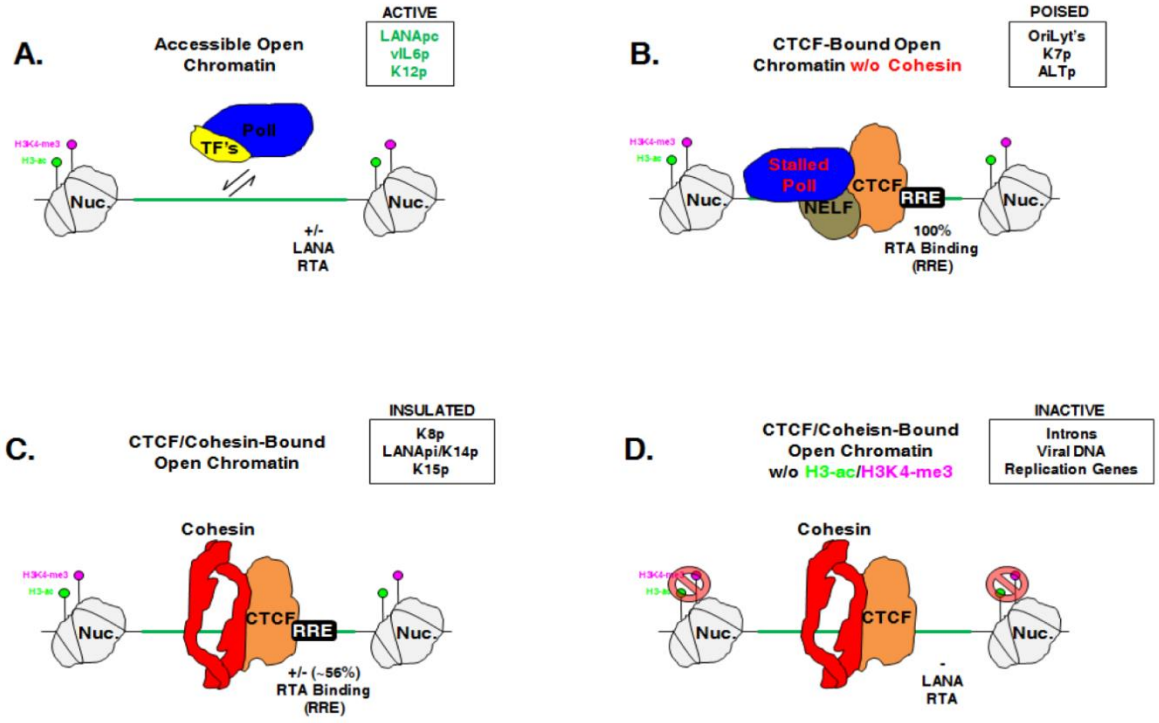

Figure 4.8: An Open Chromatin Code for Latent KSHV Transcription. A. Some regions of latent KSHV open chromatin are accessible to transcription factors and RNA polymerase II (PolII), such as the constitutive LANA and vIL-6 promoters (LANApc and vIL-6p respectively). These regions of open chromatin occur near H3K4-me3/H3-ac, may or may not contain binding sites for viral transcription factors (i.e. LANA and/or RTA), and are not enriched in CTCF or Cohesin binding. **B.** Other regions of FAIRE-Seq identified latent viral open chromatin contain CTCF binding, but lack Cohesin (Chen et al., 2012a); such as the lytic replication origins (OriLyt's), and promoter regions of K7 (K7p) and the Antisense to Latent Transcripts (ALT) noncoding RNA (ALTp). These loci are also near H3K4-me3/H3-ac and contain stalled PolII (Kang et al., 2013; Toth et al., 2012) likely in a poised configuration in addition to response elements for the KSHV lytic switch RTA (RRE's). **C.** The majority of latent viral open chromatin contains coincident CTCF and Cohesin enrichment. These insulated regions may or may not contain an RRE and are near H3K4-me3/H3-ac signatures, but are not generally transcriptionally active during latency. **D.** A subset of latent episomal open chromatin is distal to H3K4-me3/H3-ac, bears CTCF/Cohesin occupancy, and is not enriched in LANA/RTA binding. These inactive regions correspond to spliced intronic regions and near the promoters of ORF's encoding viral DNA replication proteins, such as ORF 9 (KSHV DNA polymerase) and ORF 40/41 (KSHV helicase/primase).

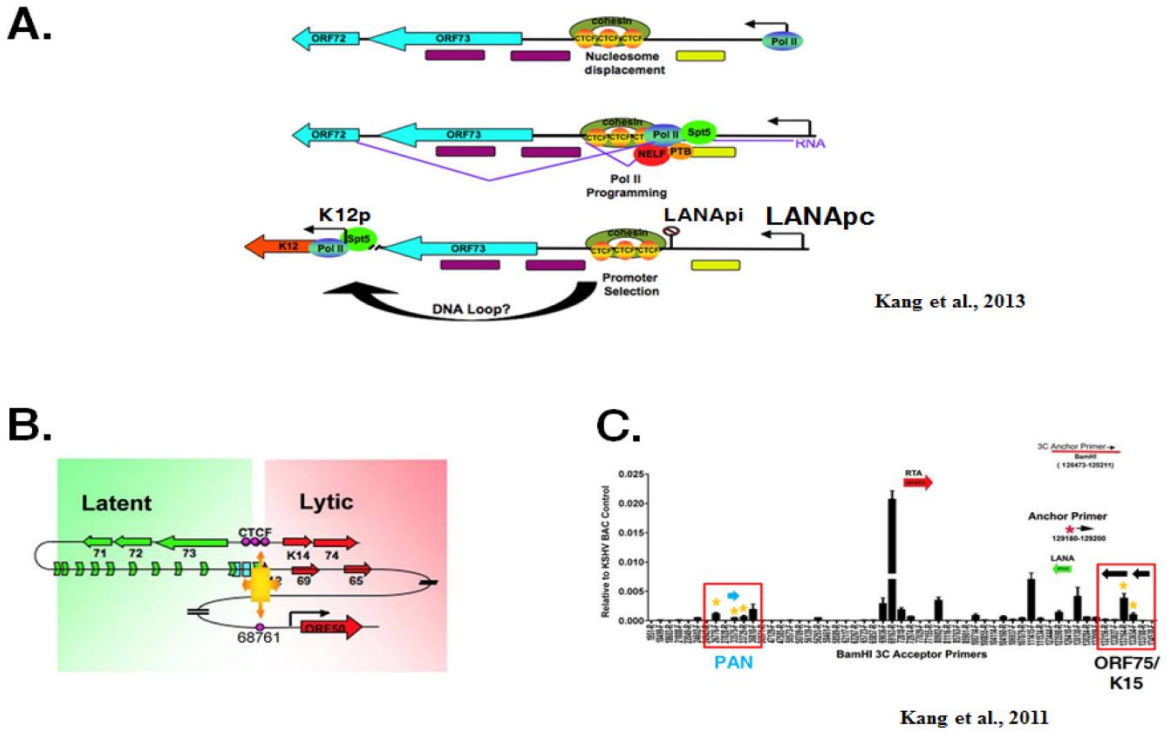

Figure 4.9: Overview of CTCF and Cohesin-Mediated Looping in the KSHV Episome. A. During viral latency a site of major CTCF/Cohesin enrichment is thought to program nucleosome displacement and RNA polymerase II (PolII) activity at the KSHV latency locus. This site has previously been shown to modulate looping within the viral genome between both the K12 region and the Lytic Control Region (upstream of the RTA ORF). B. Model of CTCF/Cohesin-mediated linkage between the viral latency locus and the K12 and Lytic Control Regions determined by chromatin conformation capture (3C). **C.** 3C analysis using BamHI fragments from the latent KSHV episome and specified primer sets. Fragments which contain FAIRE-Seq identified open chromatin enriched in LANA binding, but lacking CTCF/Cohesin (Chen et al., 2012a) are indicated by orange asterisks. Regions in red boxes were not discussed in the main text of (Kang et al., 2011), but could potentially be involved in transcriptional and/or conformational regulation via LANA. The genomic region of open chromatin encompassing the KSHV noncoding RNA; PAN, is depicted in light blue lettering to indicate B cell specificity. Panel A modified with permission from (Kang et al., 2013), and panels B/C modified with permission from (Kang et al., 2011).

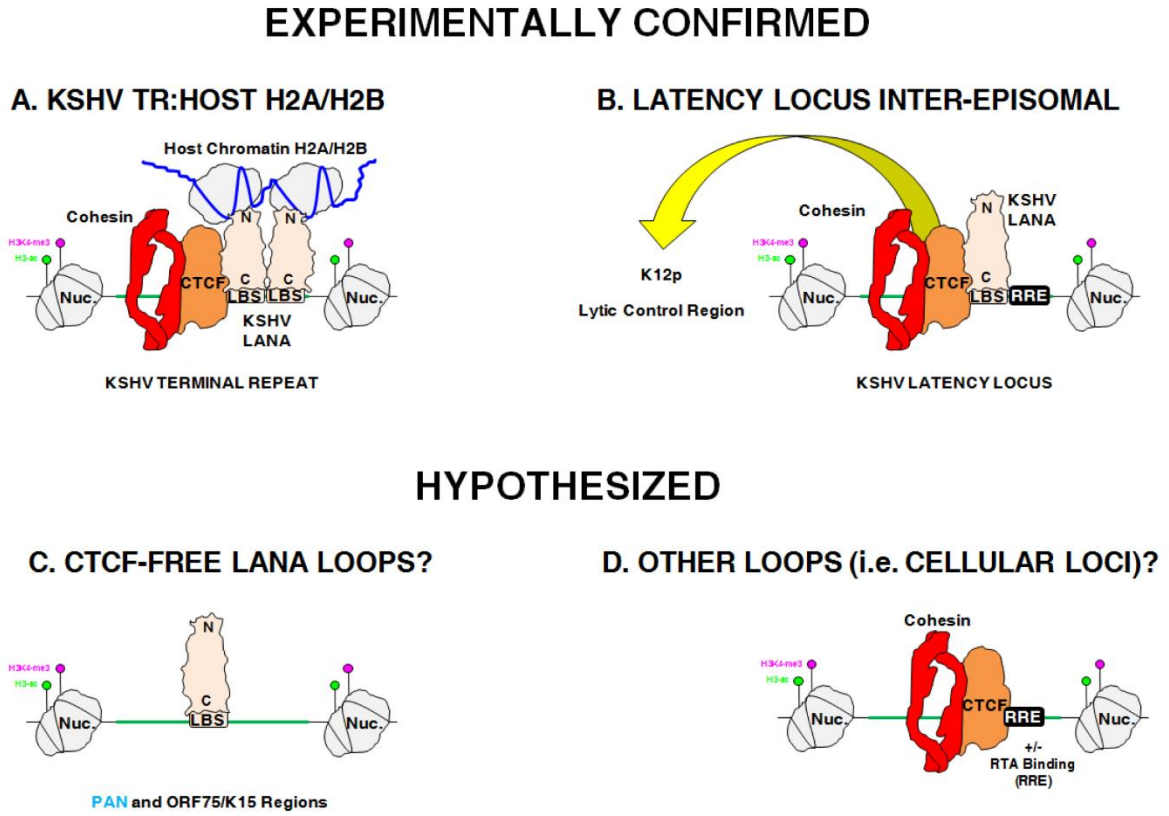

Figure 4.10: An Open Chromatin Code for Latent KSHV Conformation. A. KSHV LANA, CTCF, Cohesin, H3-ac, H3K4-me3, and cellular replication machinery (not shown) localize to the viral TR's during latency. The interaction between the N-terminus of KSHV LANA with an acidic patch of the histone H2A/H2B dimer and the C-terminus of LANA with the terminal repeats of the KSHV genome tethers the episome to host chromatin. This maintains the episome through cellular divisions and also serves as the latent viral origin of replication (reviewed in (Ballestas and Kaye, 2011)). **B.** A major CTCF/Cohesin site at the KSHV latency locus is thought to coordinate long range inter-episomal looping (see Figure 4.9). This likely occurs between the latency locus and the K12p and/or Lytic Control Region (Kang et al., 2013; Kang et al., 2011). **C.** LANA occupancy occurs independently of CTCF/Cohesin intergenic to KSHV PAN (in B cells; light blue lettering) and between KSHV ORF75 and K15. These regions overlap latent nucleosome depletion and were enhanced in 3C analysis (see Figure 4.9C). I predict transcriptional or conformational latent functionality at these loci. **D.** Other CTCF-mediated loops may exist among KSHV episomes and between episomes and host chromatin. Some regions of latent episomal open chromatin contained coincident occupancy of CTCF/Cohesin. These regions lack KSHV LANA binding, may or may not contain an RTA Response Element (RRE), and may or may not occur near H3-ac/H3K4-me3. How the various transcriptional functions of CTCF are delineated and how long range CTCF looping is specified in the human genome is incompletely understood. It is difficult to imagine a scenario in which these regions of episomal open chromatin are prevented from interaction with host open chromatin enriched in CTCF.

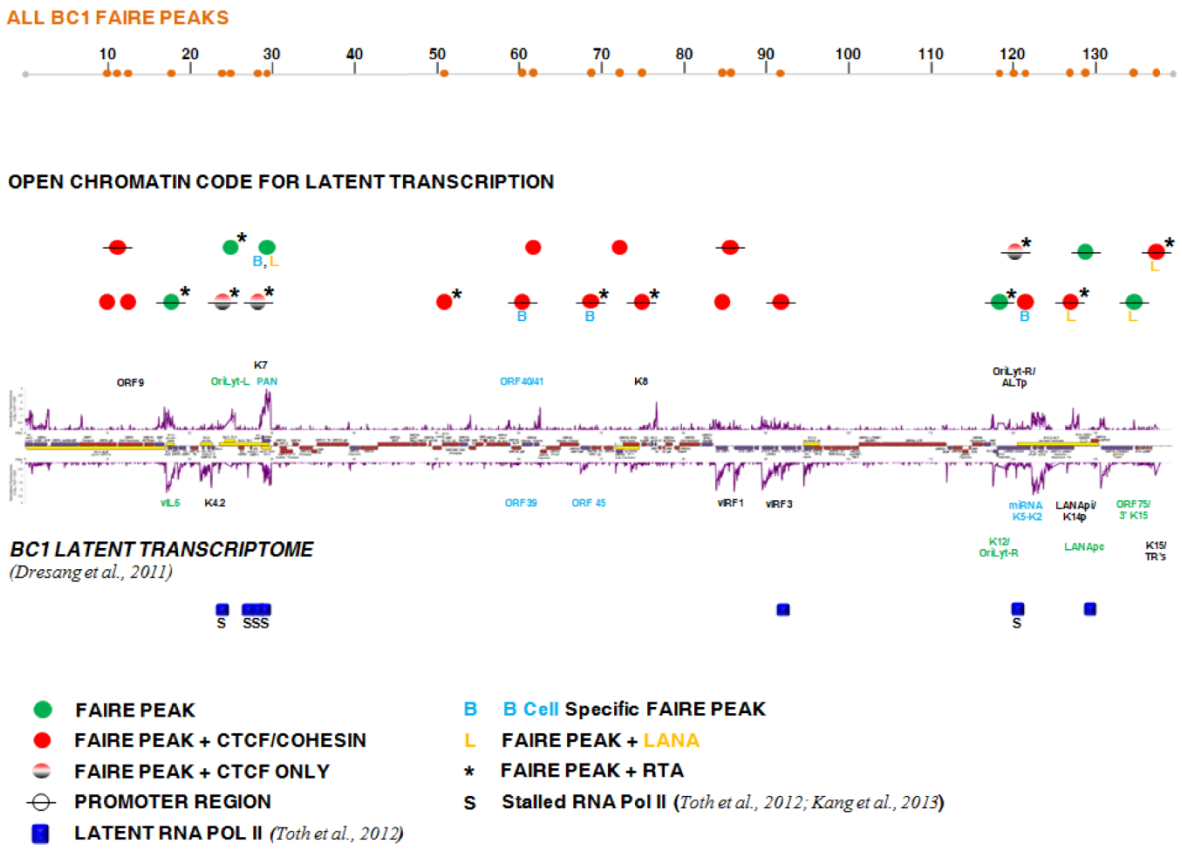

Figure 4.11: Transcriptional Profile of "Latent" KSHV in BC1 PEL Cells. The approximate locations of all identified FAIRE peak regions in the latent KSHV episome in BC1 cells are shown as orange dots across a linearized depiction of the KSHV genome (genomic coordinates are in units of kbp). The predicted "open chromatin code" for KSHV transcription is indicated by closed circles annotated as per the legend at the bottom of the figure. The BC1 latent transcriptome as determined by tiling array (in purple (Dresang et al., 2011)) is shown beneath the coded regions of latent nucleosome depletion and annotated with nearby viral ORF's. RNA PolII occupancy on the latent KSHV genome as determined by ChIP-chip is shown beneath the latent BC1 transcriptome. "S" indicates "stalled" polymerase as determined by Ser5 hyperphosphorylation and Ser2 hypophosphorylation of carboxy tail of the large RNA pol II subunit (Kang et al., 2013; Toth et al., 2012). Many latent regions of open chromatin qualitatively occur near loci not conventionally associated with "latent" transcription. This could be related to cell cycle, cell lineage, and/or episomal diversity (see Section 4.4).

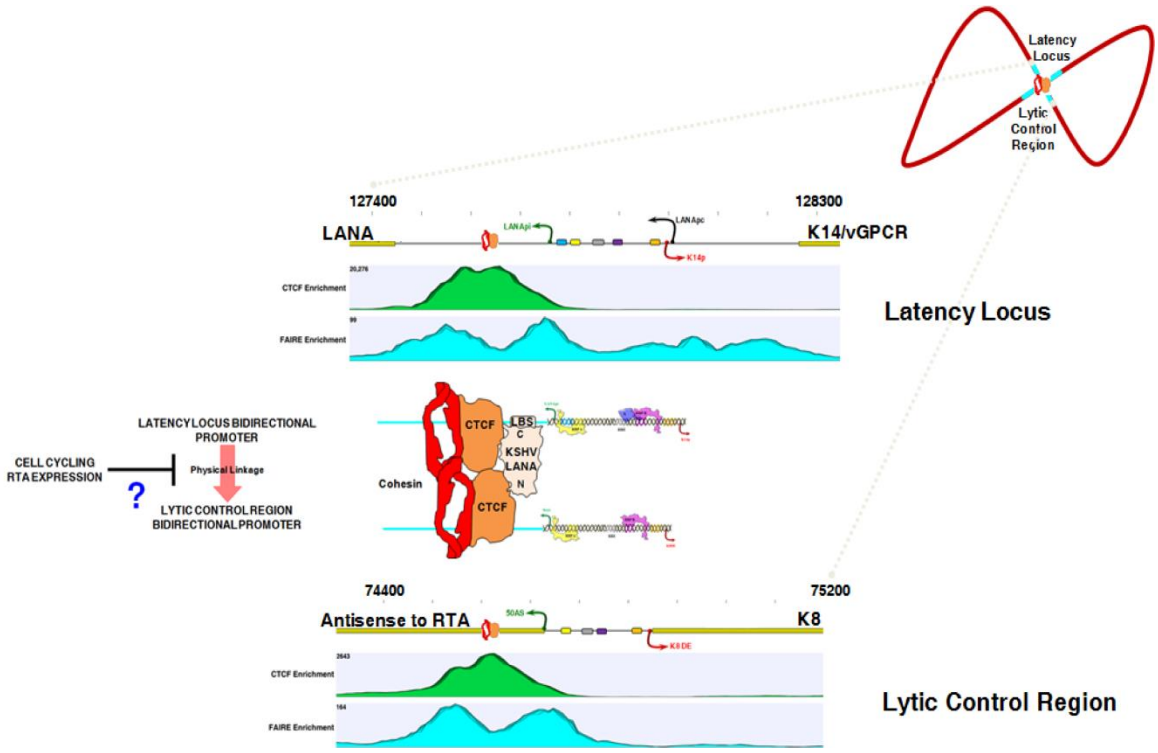

Figure 4.12: The KSHV Episome Comes Full-Circle. The LANApi/K14p and 50AS/K8DE bidirectional promoters share *cis* homology, open chromatin profiles, and physical proximity. A major CTCF/Cohesin peak occurs immediately downstream of the LANApi/K14p within the first intron of the LANA ORF. The LANApi start site generates latent transcripts and the K14p start site synthesizes a bicistronic message encoding two lytic signaling molecules; vOX and vGPCR. CTCF/Cohesin occupancy at this region prevents nucleosome deposition and is thought to link the locus to the K12 and Lytic Control Region (see Figures 4.9 and 4.10). The Lytic Control Region also contains latent CTCF/Cohesin enrichment downstream of the homologous 50AS/K8DE bidirectional promoter. The 50AS start site generates a transcript antisense to the RTA ORF and the K8 delayed-early (DE) start site drives expression of a transcript encoding k-bZIP; a multifunctional lytic protein involved in viral DNA replication and transcription (see Section 4.4).

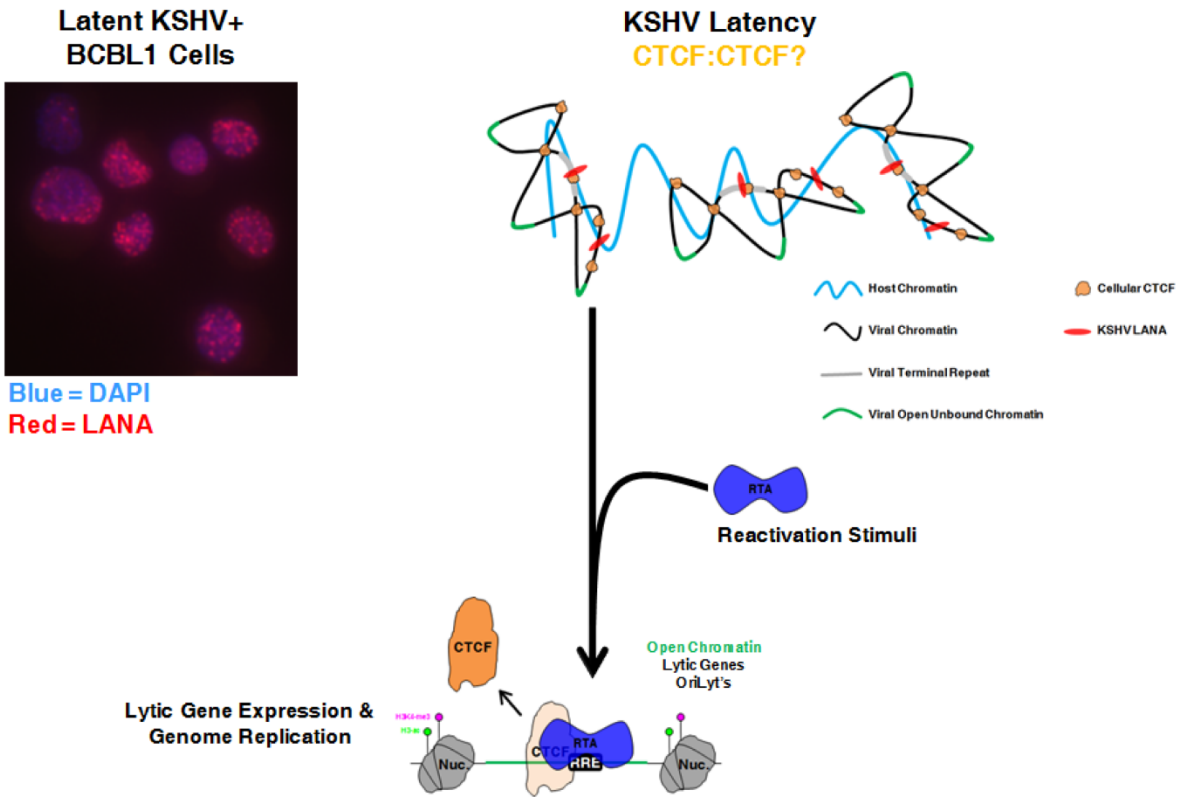

Figure 4.13: The Zipper Model of Latent Infection. Immunofluorescence of DAPI-stained nuclei and Texas-red stained KSHV LANA in latently infected BCBL1 cells. LANA appears punctate in host nuclei due to multicopy localization at viral TR's while tethered to host chromatin. Interactions with CTCF/Cohesin can form inter-episomal loops, but could hypothetically also topologically position the viral genome within the host nucleus through interaction with host CTCF binding sites. This would allow accessible open chromatin to be localized and utilized differently than insulated or inactive (CTCF/Cohesin enriched) open chromatin. This would also prevent aberrant viral immunological signaling/recognition. Many regions of open chromatin which bind CTCF/Cohesin also contain transcriptionally responsive RRE's, including open chromatin near the OriLyt's. This raises the possibility that RTA expression could, in response to appropriate stimuli, transcriptionally activate the latent episome while simultaneously physically decoupling the host and viral genomes. This would facilitate the observed robust viral transcription and viral genome replication which occurs prior to nucleosome-free packaging into infectious virions.

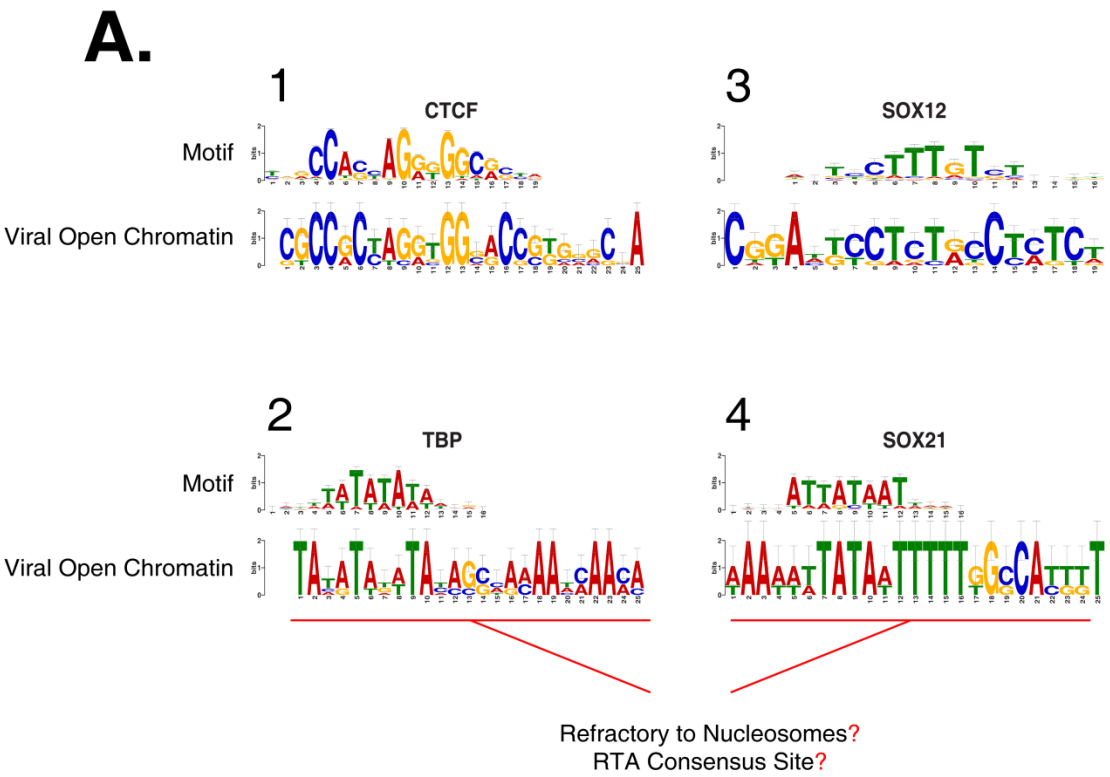

B.

	Putative RTA:DNA Consensus Sequences
Liao et al., 2003	$[A/T]_3$-N_7-$[A/T]_3$-N_7-$[A/T]_3$ $[A/T]_3$-N_{17}-$[A/T]_3$
Palmeri et al., 2011	ANTGTAACANT$^{A}/_{T}{}^{A}/_{T}$T

Figure 4.14: Regions of Conserved Latent Viral Open Chromatin Contain CTCF binding sites and AT-rich Regions. A. Motif elucidation software (MEME Suite) analysis of the conserved regions of latent open chromatin display over-representation of CTCF recognition elements and AT-rich regions. The top 4 recurrent motifs in viral open chromatin are shown along with associated transcription factor recognition sites (TOMTOM). TBP (TATA binding protein) is involved in basal transcription and the SOX family encodes developmental transcription factors. Poly dA:dT tracts have been shown to be anti-correlated with nucleosome occupancy, but could also serve as recognition sites for the viral RTA transcription factor as shown in panel **B.**, or recognition sites for other host factors. Collectively I believe that these regions of open chromatin are *cis*-programmed for nucleosome depletion. CTCF is likely recruited to most of these regions early in infection to maintain this depletion and to coordinate viral transcription and conformation. Cell cycling and RTA expression could cause dynamic access to these regions thereafter.

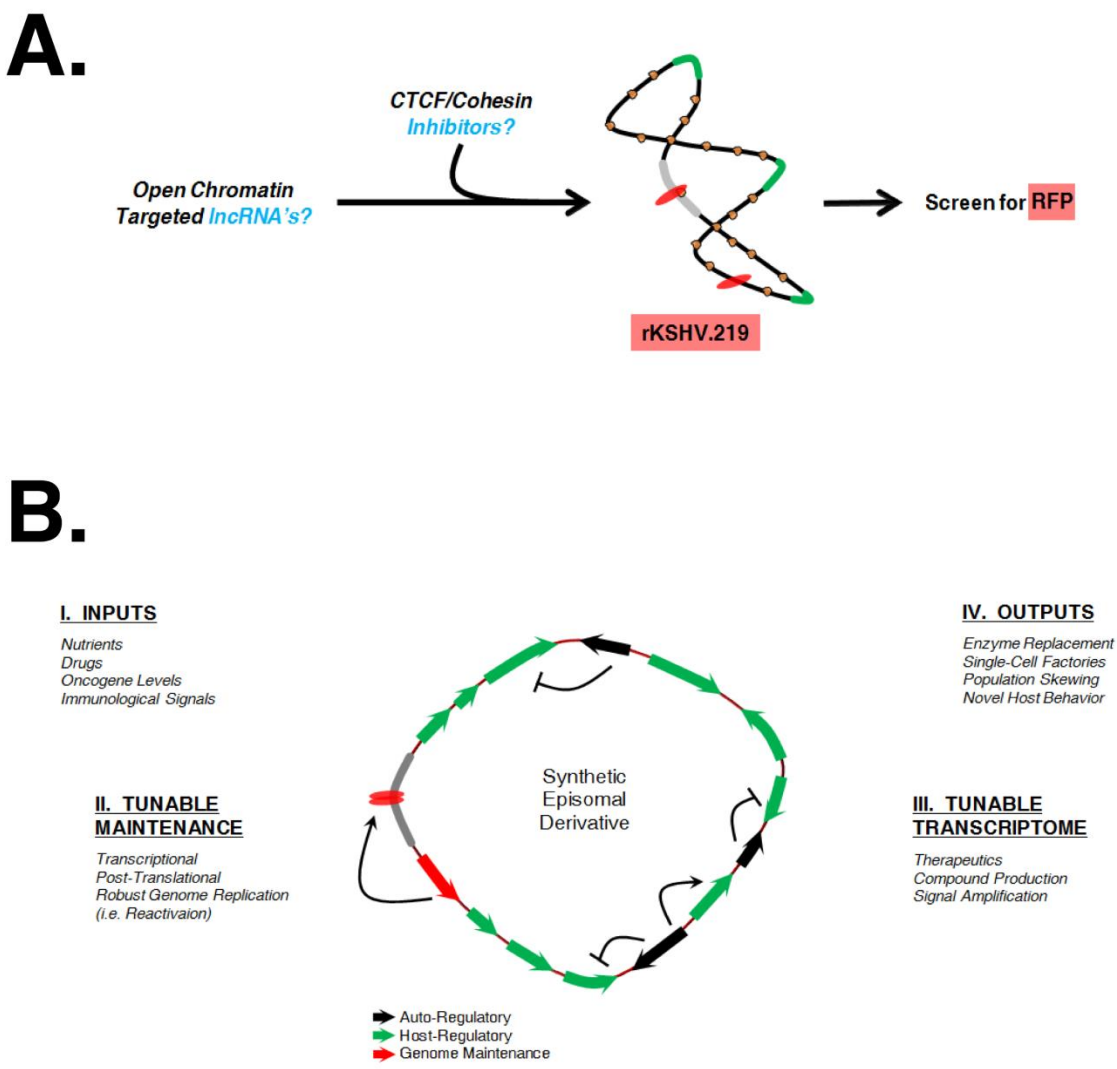

Figure 4.15: Extensions to Profiling Latent Episomal Open Chromatin. A. CTCF/Cohesin inhibitors, or manipulation of endogenous regulators such as Separase, could prove effective in unzipping the viral genome from the host and in inducing lytic viral transactivation. However disruption of CTCF/Cohesin would likely be deleterious to host cells and would thus be difficult to administer therapeutically. CTCF binding has been shown to be modulated by noncoding RNA's (Taft et al., 2011; Yao et al., 2010), further noncoding RNA's can be designed for specificity (i.e. homology). This methodology could afford targeted disruption of CTCF/Cohesin at viral open chromatin only, minimizing side effects. **B.** One long term vision of herpesviral episomal derivatives as non-integrating, self-propagating, on/off tunable genetic systems, which could be "zipped" onto and off of host genomes.

REFERENCES

(2012). Biological agents. Volume 100 B. A review of human carcinogens. IARC Monogr Eval Carcinog Risks Hum *100*, 1-441.

Ambroziak, J.A., Blackbourn, D.J., Herndier, B.G., Glogau, R.G., Gullett, J.H., McDonald, A.R., Lennette, E.T., and Levy, J.A. (1995). Herpes-like sequences in HIV-infected and uninfected Kaposi's sarcoma patients. Science *268*, 582-583.

An, F.Q., Compitello, N., Horwitz, E., Sramkoski, M., Knudsen, E.S., and Renne, R. (2005). The latency-associated nuclear antigen of Kaposi's sarcoma-associated herpesvirus modulates cellular gene expression and protects lymphoid cells from p16 INK4A-induced cell cycle arrest. J Biol Chem *280*, 3862-3874.

An, F.Q., Folarin, H.M., Compitello, N., Roth, J., Gerson, S.L., McCrae, K.R., Fakhari, F.D., Dittmer, D.P., and Renne, R. (2006). Long-term-infected telomerase-immortalized endothelial cells: a model for Kaposi's sarcoma-associated herpesvirus latency in vitro and in vivo. J Virol *80*, 4833-4846.

An, J., Sun, Y., and Rettig, M.B. (2004). Transcriptional coactivation of c-Jun by the KSHV-encoded LANA. Blood *103*, 222-228.

Aoki, Y., Jaffe, E.S., Chang, Y., Jones, K., Teruya-Feldstein, J., Moore, P.S., and Tosato, G. (1999). Angiogenesis and hematopoiesis induced by Kaposi's sarcoma-associated herpesvirus-encoded interleukin-6. Blood *93*, 4034-4043.

Aoki, Y., Tosato, G., Fonville, T.W., and Pittaluga, S. (2001). Serum viral interleukin-6 in AIDS-related multicentric Castleman disease. Blood *97*, 2526-2527.

Arnett, K.L., Hass, M., McArthur, D.G., Ilagan, M.X., Aster, J.C., Kopan, R., and Blacklow, S.C. (2010). Structural and mechanistic insights into cooperative assembly of dimeric Notch transcription complexes. Nat Struct Mol Biol *17*, 1312-1317.

Arvanitakis, L., Geras-Raaka, E., Varma, A., Gershengorn, M.C., and Cesarman, E. (1997). Human herpesvirus KSHV encodes a constitutively active G-protein-coupled receptor linked to cell proliferation. Nature *385*, 347-350.

AuCoin, D.P., Colletti, K.S., Cei, S.A., Papouskova, I., Tarrant, M., and Pari, G.S. (2004). Amplification of the Kaposi's sarcoma-associated herpesvirus/human herpesvirus 8 lytic origin of DNA replication is dependent upon a cis-acting AT-rich region and an ORF50 response element and the trans-acting factors ORF50 (K-Rta) and K8 (K-bZIP). Virology *318*, 542-555.

Bais, C., Santomasso, B., Coso, O., Arvanitakis, L., Raaka, E.G., Gutkind, J.S., Asch, A.S., Cesarman, E., Gershengorn, M.C., and Mesri, E.A. (1998). G-protein-coupled receptor of Kaposi's sarcoma-associated herpesvirus is a viral oncogene and angiogenesis activator. Nature *391*, 86-89.

Bais, C., Van Geelen, A., Eroles, P., Mutlu, A., Chiozzini, C., Dias, S., Silverstein, R.L., Rafii, S., and Mesri, E.A. (2003). Kaposi's sarcoma associated herpesvirus G protein-coupled receptor immortalizes human endothelial cells by activation of the VEGF receptor-2/ KDR. Cancer Cell *3*, 131-143.

Bala, K., Bosco, R., Gramolelli, S., Haas, D.A., Kati, S., Pietrek, M., Havemeier, A., Yakushko, Y., Singh, V.V., Dittrich-Breiholz, O., *et al.* (2012). Kaposi's sarcoma herpesvirus K15 protein contributes to virus-induced angiogenesis by recruiting PLCgamma1 and activating NFAT1-dependent RCAN1 expression. PLoS Pathog *8*, e1002927.

Ballestas, M.E., Chatis, P.A., and Kaye, K.M. (1999). Efficient persistence of extrachromosomal KSHV DNA mediated by latency-associated nuclear antigen. Science *284*, 641-644.

Ballestas, M.E., and Kaye, K.M. (2001). Kaposi's sarcoma-associated herpesvirus latency-associated nuclear antigen 1 mediates episome persistence through cis-acting terminal repeat (TR) sequence and specifically binds TR DNA. J Virol *75*, 3250-3258.

Ballestas, M.E., and Kaye, K.M. (2011). The latency-associated nuclear antigen, a multifunctional protein central to Kaposi's sarcoma-associated herpesvirus latency. Future Microbiol *6*, 1399-1413.

Ballon, G., Chen, K., Perez, R., Tam, W., and Cesarman, E. (2011). Kaposi sarcoma herpesvirus (KSHV) vFLIP oncoprotein induces B cell transdifferentiation and tumorigenesis in mice. J Clin Invest *121*, 1141-1153.

Barbera, A.J., Ballestas, M.E., and Kaye, K.M. (2004). The Kaposi's sarcoma-associated herpesvirus latency-associated nuclear antigen 1 N terminus is essential for chromosome association, DNA replication, and episome persistence. J Virol *78*, 294-301.

Barbera, A.J., Chodaparambil, J.V., Kelley-Clarke, B., Joukov, V., Walter, J.C., Luger, K., and Kaye, K.M. (2006). The nucleosomal surface as a docking station for Kaposi's sarcoma herpesvirus LANA. Science *311*, 856-861.

Baresova, P., Pitha, P.M., and Lubyova, B. (2012). Kaposi sarcoma-associated herpesvirus vIRF-3 protein binds to F-box of Skp2 protein and acts as a regulator of c-Myc protein function and stability. J Biol Chem *287*, 16199-16208.

Barozzi, P., Luppi, M., Facchetti, F., Mecucci, C., Alu, M., Sarid, R., Rasini, V., Ravazzini, L., Rossi, E., Festa, S., *et al.* (2003). Post-transplant Kaposi sarcoma originates from the seeding of donor-derived progenitors. Nat Med *9*, 554-561.

Barski, A., Cuddapah, S., Cui, K., Roh, T.Y., Schones, D.E., Wang, Z., Wei, G., Chepelev, I., and Zhao, K. (2007). High-resolution profiling of histone methylations in the human genome. Cell *129*, 823-837.

Bauer, C., Osman, A.M., Cercignani, G., Gialluca, N., and Paolini, M. (2001). A unified theory of enzyme kinetics based upon the systematic analysis of the variations of k(cat), K(M), and k(cat)/K(M) and the relevant DeltaG(0 not equal) values-possible implications in chemotherapy and biotechnology. Biochem Pharmacol *61*, 1049-1055.

Bechtel, J.T., Winant, R.C., and Ganem, D. (2005). Host and viral proteins in the virion of Kaposi's sarcoma-associated herpesvirus. J Virol *79*, 4952-4964.

Bell, A.C., West, A.G., and Felsenfeld, G. (1999). The protein CTCF is required for the enhancer blocking activity of vertebrate insulators. Cell *98*, 387-396.

Bieleski, L., Hindley, C., and Talbot, S.J. (2004). A polypyrimidine tract facilitates the expression of Kaposi's sarcoma-associated herpesvirus vFLIP through an internal ribosome entry site. J Gen Virol *85*, 615-620.

Bieleski, L., and Talbot, S.J. (2001). Kaposi's sarcoma-associated herpesvirus vCyclin open reading frame contains an internal ribosome entry site. J Virol *75*, 1864-1869.

Boss, I.W., Nadeau, P.E., Abbott, J.R., Yang, Y., Mergia, A., and Renne, R. (2011). A Kaposi's sarcoma-associated herpesvirus-encoded ortholog of microRNA miR-155 induces human splenic B-cell expansion in NOD/LtSz-scid IL2Rgammanull mice. J Virol *85*, 9877-9886.

Bouvard, V., Baan, R., Straif, K., Grosse, Y., Secretan, B., El Ghissassi, F., Benbrahim-Tallaa, L., Guha, N., Freeman, C., Galichet, L., *et al.* (2009). A review of human carcinogens--Part B: biological agents. Lancet Oncol *10*, 321-322.

Bowser, B.S., DeWire, S.M., and Damania, B. (2002). Transcriptional regulation of the K1 gene product of Kaposi's sarcoma-associated herpesvirus. J Virol *76*, 12574-12583.

Boyle, A.P., Davis, S., Shulha, H.P., Meltzer, P., Margulies, E.H., Weng, Z., Furey, T.S., and Crawford, G.E. (2008). High-resolution mapping and characterization of open chromatin across the genome. Cell *132*, 311-322.

Brinkmann, M.M., Glenn, M., Rainbow, L., Kieser, A., Henke-Gendo, C., and Schulz, T.F. (2003). Activation of mitogen-activated protein kinase and NF-kappaB pathways by a Kaposi's sarcoma-associated herpesvirus K15 membrane protein. J Virol *77*, 9346-9358.

Bu, W., Carroll, K.D., Palmeri, D., and Lukac, D.M. (2007). Kaposi's sarcoma-associated herpesvirus/human herpesvirus 8 ORF50/Rta lytic switch protein functions as a tetramer. J Virol *81*, 5788-5806.

Bubman, D., Guasparri, I., and Cesarman, E. (2007). Deregulation of c-Myc in primary effusion lymphoma by Kaposi's sarcoma herpesvirus latency-associated nuclear antigen. Oncogene *26*, 4979-4986.

Budt, M., Hristozova, T., Hille, G., Berger, K., and Brune, W. (2011). Construction of a lytically replicating Kaposi's sarcoma-associated herpesvirus. J Virol *85*, 10415-10420.

Burger, O., Baudisch, A., and Vaupel, J.W. (2012). Human mortality improvement in evolutionary context. Proc Natl Acad Sci U S A *109*, 18210-18214.

Butt, A.Q., and Miggin, S.M. (2012). Cancer and viruses: a double-edged sword. Proteomics *12*, 2127-2138.

Cai, Q., Lan, K., Verma, S.C., Si, H., Lin, D., and Robertson, E.S. (2006). Kaposi's sarcoma-associated herpesvirus latent protein LANA interacts with HIF-1 alpha to upregulate RTA expression during hypoxia: Latency control under low oxygen conditions. J Virol *80*, 7965-7975.

Cai, X., and Cullen, B.R. (2006). Transcriptional origin of Kaposi's sarcoma-associated herpesvirus microRNAs. J Virol *80*, 2234-2242.

Cai, X., Lu, S., Zhang, Z., Gonzalez, C.M., Damania, B., and Cullen, B.R. (2005). Kaposi's sarcoma-associated herpesvirus expresses an array of viral microRNAs in latently infected cells. Proc Natl Acad Sci U S A *102*, 5570-5575.

Calabrese, J.M., Sun, W., Song, L., Mugford, J.W., Williams, L., Yee, D., Starmer, J., Mieczkowski, P., Crawford, G.E., and Magnuson, T. (2012). Site-specific silencing of regulatory elements as a mechanism of X inactivation. Cell *151*, 951-963.

Cannon, M., Philpott, N.J., and Cesarman, E. (2003). The Kaposi's sarcoma-associated herpesvirus G protein-coupled receptor has broad signaling effects in primary effusion lymphoma cells. J Virol *77*, 57-67.

Cannon, M.L., and Cesarman, E. (2004). The KSHV G protein-coupled receptor signals via multiple pathways to induce transcription factor activation in primary effusion lymphoma cells. Oncogene *23*, 514-523.

Carr, P.A., and Church, G.M. (2009). Genome engineering. Nat Biotechnol *27*, 1151-1162.

Carroll, K.D., Bu, W., Palmeri, D., Spadavecchia, S., Lynch, S.J., Marras, S.A., Tyagi, S., and Lukac, D.M. (2006). Kaposi's Sarcoma-associated herpesvirus lytic switch protein stimulates DNA binding of RBP-Jk/CSL to activate the Notch pathway. J Virol *80*, 9697-9709.

Carroll, K.D., Khadim, F., Spadavecchia, S., Palmeri, D., and Lukac, D.M. (2007). Direct interactions of Kaposi's sarcoma-associated herpesvirus/human herpesvirus 8 ORF50/Rta protein with the cellular protein octamer-1 and DNA are critical for specifying transactivation of a delayed-early promoter and stimulating viral reactivation. J Virol *81*, 8451-8467.

Cave, J.W., Loh, F., Surpris, J.W., Xia, L., and Caudy, M.A. (2005). A DNA transcription code for cell-specific gene activation by notch signaling. Curr Biol *15*, 94-104.

Cesarman, E. (2011). Gammaherpesvirus and lymphoproliferative disorders in immunocompromised patients. Cancer Lett *305*, 163-174.

Cesarman, E., Chang, Y., Moore, P.S., Said, J.W., and Knowles, D.M. (1995a). Kaposi's sarcoma-associated herpesvirus-like DNA sequences in AIDS-related body-cavity-based lymphomas. N Engl J Med *332*, 1186-1191.

Cesarman, E., Moore, P.S., Rao, P.H., Inghirami, G., Knowles, D.M., and Chang, Y. (1995b). In vitro establishment and characterization of two acquired immunodeficiency syndrome-related lymphoma cell lines (BC-1 and BC-2) containing Kaposi's sarcoma-associated herpesvirus-like (KSHV) DNA sequences. Blood *86*, 2708-2714.

Cesarman, E., Nador, R.G., Bai, F., Bohenzky, R.A., Russo, J.J., Moore, P.S., Chang, Y., and Knowles, D.M. (1996). Kaposi's sarcoma-associated herpesvirus contains G protein-coupled receptor and cyclin D homologs which are expressed in Kaposi's sarcoma and malignant lymphoma. J Virol *70*, 8218-8223.

Chadburn, A., Hyjek, E., Mathew, S., Cesarman, E., Said, J., and Knowles, D.M. (2004). KSHV-positive solid lymphomas represent an extra-cavitary variant of primary effusion lymphoma. Am J Surg Pathol *28*, 1401-1416.

Chakraborty, S., Veettil, M.V., and Chandran, B. (2012). Kaposi's Sarcoma Associated Herpesvirus Entry into Target Cells. Front Microbiol *3*, 6.

Chandriani, S., and Ganem, D. (2010). Array-based transcript profiling and limiting-dilution reverse transcription-PCR analysis identify additional latent genes in Kaposi's sarcoma-associated herpesvirus. J Virol *84*, 5565-5573.

Chandriani, S., Xu, Y., and Ganem, D. (2010). The lytic transcriptome of Kaposi's sarcoma-associated herpesvirus reveals extensive transcription of noncoding regions, including regions antisense to important genes. J Virol *84*, 7934-7942.

Chang, H., Dittmer, D.P., Shin, Y.C., Hong, Y., and Jung, J.U. (2005a). Role of Notch signal transduction in Kaposi's sarcoma-associated herpesvirus gene expression. J Virol *79*, 14371-14382.

Chang, J., Renne, R., Dittmer, D., and Ganem, D. (2000). Inflammatory cytokines and the reactivation of Kaposi's sarcoma-associated herpesvirus lytic replication. Virology *266*, 17-25.

Chang, P.C., Fitzgerald, L.D., Hsia, D.A., Izumiya, Y., Wu, C.Y., Hsieh, W.P., Lin, S.F., Campbell, M., Lam, K.S., Luciw, P.A., *et al.* (2011). Histone demethylase JMJD2A regulates Kaposi's sarcoma-associated herpesvirus replication and is targeted by a viral transcriptional factor. J Virol *85*, 3283-3293.

Chang, P.C., Fitzgerald, L.D., Van Geelen, A., Izumiya, Y., Ellison, T.J., Wang, D.H., Ann, D.K., Luciw, P.A., and Kung, H.J. (2009). Kruppel-associated box domain-associated protein-1 as a latency regulator for Kaposi's sarcoma-associated herpesvirus and its modulation by the viral protein kinase. Cancer Res *69*, 5681-5689.

Chang, P.J., Boonsiri, J., Wang, S.S., Chen, L.Y., and Miller, G. (2010). Binding of RBP-Jkappa (CSL) protein to the promoter of the Kaposi's sarcoma-associated herpesvirus ORF47 (gL) gene is a critical but not sufficient determinant of transactivation by ORF50 protein. Virology *398*, 38-48.

Chang, P.J., and Miller, G. (2004). Autoregulation of DNA binding and protein stability of Kaposi's sarcoma-associated herpesvirus ORF50 protein. J Virol *78*, 10657-10673.

Chang, P.J., Shedd, D., Gradoville, L., Cho, M.S., Chen, L.W., Chang, J., and Miller, G. (2002). Open reading frame 50 protein of Kaposi's sarcoma-associated herpesvirus directly activates the viral PAN and K12 genes by binding to related response elements. J Virol *76*, 3168-3178.

Chang, P.J., Shedd, D., and Miller, G. (2005b). Two subclasses of Kaposi's sarcoma-associated herpesvirus lytic cycle promoters distinguished by open reading frame 50 mutant proteins that are deficient in binding to DNA. J Virol *79*, 8750-8763.

Chang, P.J., Shedd, D., and Miller, G. (2008). A mobile functional region of Kaposi's sarcoma-associated herpesvirus ORF50 protein independently regulates DNA binding and protein abundance. J Virol *82*, 9700-9716.

Chang, Y., Cesarman, E., Pessin, M.S., Lee, F., Culpepper, J., Knowles, D.M., and Moore, P.S. (1994). Identification of herpesvirus-like DNA sequences in AIDS-associated Kaposi's sarcoma. Science *266*, 1865-1869.

Chatterjee, M., Osborne, J., Bestetti, G., Chang, Y., and Moore, P.S. (2002). Viral IL-6-induced cell proliferation and immune evasion of interferon activity. Science *298*, 1432-1435.

Chau, C.M., and Lieberman, P.M. (2004). Dynamic chromatin boundaries delineate a latency control region of Epstein-Barr virus. J Virol *78*, 12308-12319.

Chau, C.M., Zhang, X.Y., McMahon, S.B., and Lieberman, P.M. (2006). Regulation of Epstein-Barr virus latency type by the chromatin boundary factor CTCF. J Virol *80*, 5723-5732.

Chaudhary, P.M., Jasmin, A., Eby, M.T., and Hood, L. (1999). Modulation of the NF-kappa B pathway by virally encoded death effector domains-containing proteins. Oncogene *18*, 5738-5746.

Chen, H.S., Wikramasinghe, P., Showe, L., and Lieberman, P.M. (2012a). Cohesins repress Kaposi's sarcoma-associated herpesvirus immediate early gene transcription during latency. J Virol *86*, 9454-9464.

Chen, J., Ueda, K., Sakakibara, S., Okuno, T., Parravicini, C., Corbellino, M., and Yamanishi, K. (2001). Activation of latent Kaposi's sarcoma-associated herpesvirus by demethylation of the promoter of the lytic transactivator. Proc Natl Acad Sci U S A *98*, 4119-4124.

Chen, J., Ueda, K., Sakakibara, S., Okuno, T., and Yamanishi, K. (2000). Transcriptional regulation of the Kaposi's sarcoma-associated herpesvirus viral interferon regulatory factor gene. J Virol *74*, 8623-8634.

Chen, J., Ye, F., Xie, J., Kuhne, K., and Gao, S.J. (2009). Genome-wide identification of binding sites for Kaposi's sarcoma-associated herpesvirus lytic switch protein, RTA. Virology *386*, 290-302.

Chen, W., Hilton, I.B., Staudt, M.R., Burd, C.E., and Dittmer, D.P. (2010). Distinct p53, p53:LANA, and LANA complexes in Kaposi's Sarcoma--associated Herpesvirus Lymphomas. J Virol *84*, 3898-3908.

Chen, W., Sin, S.H., Wen, K.W., Damania, B., and Dittmer, D.P. (2012b). Hsp90 Inhibitors Are Efficacious against Kaposi Sarcoma by Enhancing the Degradation of the Essential Viral Gene LANA, of the Viral Co-Receptor EphA2 as well as Other Client Proteins. PLoS Pathog *8*, e1003048.

Chernukhin, I., Shamsuddin, S., Kang, S.Y., Bergstrom, R., Kwon, Y.W., Yu, W., Whitehead, J., Mukhopadhyay, R., Docquier, F., Farrar, D., *et al.* (2007). CTCF interacts with and recruits the

largest subunit of RNA polymerase II to CTCF target sites genome-wide. Mol Cell Biol *27*, 1631-1648.

Chiou, C.J., Poole, L.J., Kim, P.S., Ciufo, D.M., Cannon, J.S., ap Rhys, C.M., Alcendor, D.J., Zong, J.C., Ambinder, R.F., and Hayward, G.S. (2002). Patterns of gene expression and a transactivation function exhibited by the vGCR (ORF74) chemokine receptor protein of Kaposi's sarcoma-associated herpesvirus. J Virol *76*, 3421-3439.

Chodaparambil, J.V., Barbera, A.J., Lu, X., Kaye, K.M., Hansen, J.C., and Luger, K. (2007). A charged and contoured surface on the nucleosome regulates chromatin compaction. Nat Struct Mol Biol *14*, 1105-1107.

Choi, J.K., Lee, B.S., Shim, S.N., Li, M., and Jung, J.U. (2000). Identification of the novel K15 gene at the rightmost end of the Kaposi's sarcoma-associated herpesvirus genome. J Virol *74*, 436-446.

Chow, C.C., Ong, K.M., Dougherty, E.J., and Simons, S.S., Jr. (2011). Inferring mechanisms from dose-response curves. Methods Enzymol *487*, 465-483.

Chugh, P., Matta, H., Schamus, S., Zachariah, S., Kumar, A., Richardson, J.A., Smith, A.L., and Chaudhary, P.M. (2005). Constitutive NF-kappaB activation, normal Fas-induced apoptosis, and increased incidence of lymphoma in human herpes virus 8 K13 transgenic mice. Proc Natl Acad Sci U S A *102*, 12885-12890.

Chung, Y.H., Means, R.E., Choi, J.K., Lee, B.S., and Jung, J.U. (2002). Kaposi's sarcoma-associated herpesvirus OX2 glycoprotein activates myeloid-lineage cells to induce inflammatory cytokine production. J Virol *76*, 4688-4698.

Coscoy, L., and Ganem, D. (2000). Kaposi's sarcoma-associated herpesvirus encodes two proteins that block cell surface display of MHC class I chains by enhancing their endocytosis. Proc Natl Acad Sci U S A *97*, 8051-8056.

Coscoy, L., and Ganem, D. (2001). A viral protein that selectively downregulates ICAM-1 and B7-2 and modulates T cell costimulation. J Clin Invest *107*, 1599-1606.

Cotter, M.A., 2nd, and Robertson, E.S. (1999). The latency-associated nuclear antigen tethers the Kaposi's sarcoma-associated herpesvirus genome to host chromosomes in body cavity-based lymphoma cells. Virology *264*, 254-264.

Cullen, B.R. (2006). Viruses and microRNAs. Nat Genet *38 Suppl*, S25-30.

Cunningham, C., Barnard, S., Blackbourn, D.J., and Davison, A.J. (2003). Transcription mapping of human herpesvirus 8 genes encoding viral interferon regulatory factors. J Gen Virol *84*, 1471-1483.

Damania, B., Jeong, J.H., Bowser, B.S., DeWire, S.M., Staudt, M.R., and Dittmer, D.P. (2004). Comparison of the Rta/Orf50 transactivator proteins of gamma-2-herpesviruses. J Virol *78*, 5491-5499.

Darst, R.P., Haecker, I., Pardo, C.E., Renne, R., and Kladde, M.P. (2013). Epigenetic diversity of Kaposi's sarcoma-associated herpesvirus. Nucleic Acids Res.

Davison, A.J. (2007). Overview of classification. In Human Herpesviruses: Biology, Therapy, and Immunoprophylaxis, A. Arvin, G. Campadelli-Fiume, E. Mocarski, P.S. Moore, B. Roizman, R. Whitley, and K. Yamanishi, eds. (Cambridge).

Deng, H., Song, M.J., Chu, J.T., and Sun, R. (2002). Transcriptional regulation of the interleukin-6 gene of human herpesvirus 8 (Kaposi's sarcoma-associated herpesvirus). J Virol *76*, 8252-8264.

Deng, H., Young, A., and Sun, R. (2000). Auto-activation of the rta gene of human herpesvirus-8/Kaposi's sarcoma-associated herpesvirus. J Gen Virol *81*, 3043-3048.

Deng, Z., Wang, Z., and Lieberman, P.M. (2012). Telomeres and viruses: common themes of genome maintenance. Front Oncol *2*, 201.

Dezube, B.J. (1996). Clinical presentation and natural history of AIDS--related Kaposi's sarcoma. Hematol Oncol Clin North Am *10*, 1023-1029.

Dezube, B.J., Zambela, M., Sage, D.R., Wang, J.F., and Fingeroth, J.D. (2002). Characterization of Kaposi sarcoma-associated herpesvirus/human herpesvirus-8 infection of human vascular endothelial cells: early events. Blood *100*, 888-896.

Dillon, P.J., Gregory, S.M., Tamburro, K., Sanders, M.K., Johnson, G.L., Raab-Traub, N., Dittmer, D.P., and Damania, B. (2013). Tousled-like Kinases Modulate Reactivation of Gammaherpesviruses from Latency. Cell Host Microbe *13*, 204-214.

Dittmer, D., Lagunoff, M., Renne, R., Staskus, K., Haase, A., and Ganem, D. (1998). A cluster of latently expressed genes in Kaposi's sarcoma-associated herpesvirus. J Virol *72*, 8309-8315.

Dittmer, D.P. (2003). Transcription profile of Kaposi's sarcoma-associated herpesvirus in primary Kaposi's sarcoma lesions as determined by real-time PCR arrays. Cancer Res *63*, 2010-2015.

Dittmer, D.P., Richards, K.L., and Damania, B. (2012). Treatment of Kaposi sarcoma-associated herpesvirus-associated cancers. Front Microbiol *3*, 141.

Dixon, J.R., Selvaraj, S., Yue, F., Kim, A., Li, Y., Shen, Y., Hu, M., Liu, J.S., and Ren, B. (2012). Topological domains in mammalian genomes identified by analysis of chromatin interactions. Nature *485*, 376-380.

Djerbi, M., Screpanti, V., Catrina, A.I., Bogen, B., Biberfeld, P., and Grandien, A. (1999). The inhibitor of death receptor signaling, FLICE-inhibitory protein defines a new class of tumor progression factors. J Exp Med *190*, 1025-1032.

Donohoe, M.E., Silva, S.S., Pinter, S.F., Xu, N., and Lee, J.T. (2009). The pluripotency factor Oct4 interacts with Ctcf and also controls X-chromosome pairing and counting. Nature *460*, 128-132.

Dresang, L.R., Teuton, J.R., Feng, H., Jacobs, J.M., Camp, D.G., 2nd, Purvine, S.O., Gritsenko, M.A., Li, Z., Smith, R.D., Sugden, B., *et al.* (2011). Coupled transcriptome and proteome analysis of human lymphotropic tumor viruses: insights on the detection and discovery of viral genes. BMC Genomics *12*, 625.

Du, M.Q., Liu, H., Diss, T.C., Ye, H., Hamoudi, R.A., Dupin, N., Meignin, V., Oksenhendler, E., Boshoff, C., and Isaacson, P.G. (2001). Kaposi sarcoma-associated herpesvirus infects monotypic (IgM lambda) but polyclonal naive B cells in Castleman disease and associated lymphoproliferative disorders. Blood *97*, 2130-2136.

Dunham, I., Kundaje, A., Aldred, S.F., Collins, P.J., Davis, C.A., Doyle, F., Epstein, C.B., Frietze, S., Harrow, J., Kaul, R., *et al.* (2012). An integrated encyclopedia of DNA elements in the human genome. Nature *489*, 57-74.

Dupin, N., Diss, T.L., Kellam, P., Tulliez, M., Du, M.Q., Sicard, D., Weiss, R.A., Isaacson, P.G., and Boshoff, C. (2000). HHV-8 is associated with a plasmablastic variant of Castleman disease that is linked to HHV-8-positive plasmablastic lymphoma. Blood *95*, 1406-1412.

Dupin, N., Fisher, C., Kellam, P., Ariad, S., Tulliez, M., Franck, N., van Marck, E., Salmon, D., Gorin, I., Escande, J.P., *et al.* (1999). Distribution of human herpesvirus-8 latently infected cells in Kaposi's sarcoma, multicentric Castleman's disease, and primary effusion lymphoma. Proc Natl Acad Sci U S A *96*, 4546-4551.

Duprez, R., Lacoste, V., Briere, J., Couppie, P., Frances, C., Sainte-Marie, D., Kassa-Kelembho, E., Lando, M.J., Essame Oyono, J.L., Nkegoum, B., *et al.* (2007). Evidence for a multiclonal origin of multicentric advanced lesions of Kaposi sarcoma. J Natl Cancer Inst *99*, 1086-1094.

Egloff, S., Al-Rawaf, H., O'Reilly, D., and Murphy, S. (2009). Chromatin structure is implicated in "late" elongation checkpoints on the U2 snRNA and beta-actin genes. Mol Cell Biol *29*, 4002-4013.

Ellis, M., Chew, Y.P., Fallis, L., Freddersdorf, S., Boshoff, C., Weiss, R.A., Lu, X., and Mittnacht, S. (1999). Degradation of p27(Kip) cdk inhibitor triggered by Kaposi's sarcoma virus cyclin-cdk6 complex. EMBO J *18*, 644-653.

Ellison, T.J., Izumiya, Y., Izumiya, C., Luciw, P.A., and Kung, H.J. (2009). A comprehensive analysis of recruitment and transactivation potential of K-Rta and K-bZIP during reactivation of Kaposi's sarcoma-associated herpesvirus. Virology *387*, 76-88.

Ertel, M.K., Cammarata, A.L., Hron, R.J., and Neumann, D.M. (2012). CTCF occupation of the herpes simplex virus 1 genome is disrupted at early times postreactivation in a transcription-dependent manner. J Virol *86*, 12741-12759.

Esteban, M., Garcia, M.A., Domingo-Gil, E., Arroyo, J., Nombela, C., and Rivas, C. (2003). The latency protein LANA2 from Kaposi's sarcoma-associated herpesvirus inhibits apoptosis induced by dsRNA-activated protein kinase but not RNase L activation. J Gen Virol *84*, 1463-1470.

Fakhari, F.D., and Dittmer, D.P. (2002). Charting latency transcripts in Kaposi's sarcoma-associated herpesvirus by whole-genome real-time quantitative PCR. J Virol *76*, 6213-6223.

Fakhari, F.D., Jeong, J.H., Kanan, Y., and Dittmer, D.P. (2006). The latency-associated nuclear antigen of Kaposi sarcoma-associated herpesvirus induces B cell hyperplasia and lymphoma. J Clin Invest *116*, 735-742.

Faust, T., Frankel, A., and D'Orso, I. (2012). Transcription control by long non-coding RNAs. Transcription *3*, 78-86.

Fay, A., Misulovin, Z., Li, J., Schaaf, C.A., Gause, M., Gilmour, D.S., and Dorsett, D. (2011). Cohesin selectively binds and regulates genes with paused RNA polymerase. Curr Biol *21*, 1624-1634.

Feng, J., Liu, T., Qin, B., Zhang, Y., and Liu, X.S. (2012). Identifying ChIP-seq enrichment using MACS. Nat Protoc *7*, 1728-1740.

Field, N., Low, W., Daniels, M., Howell, S., Daviet, L., Boshoff, C., and Collins, M. (2003). KSHV vFLIP binds to IKK-gamma to activate IKK. J Cell Sci *116*, 3721-3728.

Filippova, G.N., Fagerlie, S., Klenova, E.M., Myers, C., Dehner, Y., Goodwin, G., Neiman, P.E., Collins, S.J., and Lobanenkov, V.V. (1996). An exceptionally conserved transcriptional repressor,

CTCF, employs different combinations of zinc fingers to bind diverged promoter sequences of avian and mammalian c-myc oncogenes. Mol Cell Biol *16*, 2802-2813.

Foster-Cuevas, M., Wright, G.J., Puklavec, M.J., Brown, M.H., and Barclay, A.N. (2004). Human herpesvirus 8 K14 protein mimics CD200 in down-regulating macrophage activation through CD200 receptor. J Virol *78*, 7667-7676.

Friborg, J., Jr., Kong, W., Hottiger, M.O., and Nabel, G.J. (1999). p53 inhibition by the LANA protein of KSHV protects against cell death. Nature *402*, 889-894.

Fu, Y., Sinha, M., Peterson, C.L., and Weng, Z. (2008). The insulator binding protein CTCF positions 20 nucleosomes around its binding sites across the human genome. PLoS Genet *4*, e1000138.

Fujimuro, M., and Hayward, S.D. (2003). The latency-associated nuclear antigen of Kaposi's sarcoma-associated herpesvirus manipulates the activity of glycogen synthase kinase-3beta. J Virol *77*, 8019-8030.

Fujimuro, M., Wu, F.Y., ApRhys, C., Kajumbula, H., Young, D.B., Hayward, G.S., and Hayward, S.D. (2003). A novel viral mechanism for dysregulation of beta-catenin in Kaposi's sarcoma-associated herpesvirus latency. Nat Med *9*, 300-306.

Ganem, D. (2006). KSHV infection and the pathogenesis of Kaposi's sarcoma. Annu Rev Pathol *1*, 273-296.

Ganem, D. (2010). KSHV and the pathogenesis of Kaposi sarcoma: listening to human biology and medicine. J Clin Invest *120*, 939-949.

Gao, S.J., Boshoff, C., Jayachandra, S., Weiss, R.A., Chang, Y., and Moore, P.S. (1997). KSHV ORF K9 (vIRF) is an oncogene which inhibits the interferon signaling pathway. Oncogene *15*, 1979-1985.

Gao, S.J., Kingsley, L., Hoover, D.R., Spira, T.J., Rinaldo, C.R., Saah, A., Phair, J., Detels, R., Parry, P., Chang, Y., *et al.* (1996). Seroconversion to antibodies against Kaposi's sarcoma-associated herpesvirus-related latent nuclear antigens before the development of Kaposi's sarcoma. N Engl J Med *335*, 233-241.

Garber, A.C., Hu, J., and Renne, R. (2002). Latency-associated nuclear antigen (LANA) cooperatively binds to two sites within the terminal repeat, and both sites contribute to the ability of LANA to suppress transcription and to facilitate DNA replication. J Biol Chem *277*, 27401-27411.

Garrett, R., and Grisham, C.M. (2010). Biochemistry, 4th edn (Belmont, CA: Brooks/Cole, Cengage Learning).

Gaulton, K.J., Nammo, T., Pasquali, L., Simon, J.M., Giresi, P.G., Fogarty, M.P., Panhuis, T.M., Mieczkowski, P., Secchi, A., Bosco, D., *et al.* (2010). A map of open chromatin in human pancreatic islets. Nat Genet *42*, 255-259.

Giresi, P.G., Kim, J., McDaniell, R.M., Iyer, V.R., and Lieb, J.D. (2007). FAIRE (Formaldehyde-Assisted Isolation of Regulatory Elements) isolates active regulatory elements from human chromatin. Genome Res *17*, 877-885.

Giresi, P.G., and Lieb, J.D. (2009). Isolation of active regulatory elements from eukaryotic chromatin using FAIRE (Formaldehyde Assisted Isolation of Regulatory Elements). Methods *48*, 233-239.

Glenn, M., Rainbow, L., Aurade, F., Davison, A., and Schulz, T.F. (1999). Identification of a spliced gene from Kaposi's sarcoma-associated herpesvirus encoding a protein with similarities to latent membrane proteins 1 and 2A of Epstein-Barr virus. J Virol *73*, 6953-6963.

Godden-Kent, D., Talbot, S.J., Boshoff, C., Chang, Y., Moore, P., Weiss, R.A., and Mittnacht, S. (1997). The cyclin encoded by Kaposi's sarcoma-associated herpesvirus stimulates cdk6 to phosphorylate the retinoblastoma protein and histone H1. J Virol *71*, 4193-4198.

Godfrey, A., Anderson, J., Papanastasiou, A., Takeuchi, Y., and Boshoff, C. (2005). Inhibiting primary effusion lymphoma by lentiviral vectors encoding short hairpin RNA. Blood *105*, 2510-2518.

Gottwein, E. (2012). Kaposi's Sarcoma-Associated Herpesvirus microRNAs. Front Microbiol *3*, 165.

Gottwein, E., Corcoran, D.L., Mukherjee, N., Skalsky, R.L., Hafner, M., Nusbaum, J.D., Shamulailatpam, P., Love, C.L., Dave, S.S., Tuschl, T., *et al.* (2011). Viral microRNA targetome of KSHV-infected primary effusion lymphoma cell lines. Cell Host Microbe *10*, 515-526.

Gottwein, E., Mukherjee, N., Sachse, C., Frenzel, C., Majoros, W.H., Chi, J.T., Braich, R., Manoharan, M., Soutschek, J., Ohler, U., *et al.* (2007). A viral microRNA functions as an orthologue of cellular miR-155. Nature *450*, 1096-1099.

Gould, F., Harrison, S.M., Hewitt, E.W., and Whitehouse, A. (2009). Kaposi's sarcoma-associated herpesvirus RTA promotes degradation of the Hey1 repressor protein through the ubiquitin proteasome pathway. J Virol *83*, 6727-6738.

Gregory, S.M., West, J.A., Dillon, P.J., Hilscher, C., Dittmer, D.P., and Damania, B. (2009). Toll-like receptor signaling controls reactivation of KSHV from latency. Proc Natl Acad Sci U S A *106*, 11725-11730.

Gross, D.S., and Garrard, W.T. (1988). Nuclease hypersensitive sites in chromatin. Annu Rev Biochem *57*, 159-197.

Grubb, J.R., Moorman, A.C., Baker, R.K., and Masur, H. (2006). The changing spectrum of pulmonary disease in patients with HIV infection on antiretroviral therapy. AIDS *20*, 1095-1107.

Grundhoff, A., and Ganem, D. (2001). Mechanisms governing expression of the v-FLIP gene of Kaposi's sarcoma-associated herpesvirus. J Virol *75*, 1857-1863.

Grundhoff, A., and Ganem, D. (2003). The latency-associated nuclear antigen of Kaposi's sarcoma-associated herpesvirus permits replication of terminal repeat-containing plasmids. J Virol *77*, 2779-2783.

Grundhoff, A., and Ganem, D. (2004). Inefficient establishment of KSHV latency suggests an additional role for continued lytic replication in Kaposi sarcoma pathogenesis. J Clin Invest *113*, 124-136.

Guasparri, I., Keller, S.A., and Cesarman, E. (2004). KSHV vFLIP is essential for the survival of infected lymphoma cells. J Exp Med *199*, 993-1003.

Guasparri, I., Wu, H., and Cesarman, E. (2006). The KSHV oncoprotein vFLIP contains a TRAF-interacting motif and requires TRAF2 and TRAF3 for signalling. EMBO Rep *7*, 114-119.

Guelen, L., Pagie, L., Brasset, E., Meuleman, W., Faza, M.B., Talhout, W., Eussen, B.H., de Klein, A., Wessels, L., de Laat, W., *et al.* (2008). Domain organization of human chromosomes revealed by mapping of nuclear lamina interactions. Nature *453*, 948-951.

Guito, J., and Lukac, D.M. (2012). KSHV Rta Promoter Specification and Viral Reactivation. Front Microbiol *3*, 30.

Gunther, T., and Grundhoff, A. (2010). The epigenetic landscape of latent Kaposi sarcoma-associated herpesvirus genomes. PLoS Pathog *6*, e1000935.

Guo, H.G., Browning, P., Nicholas, J., Hayward, G.S., Tschachler, E., Jiang, Y.W., Sadowska, M., Raffeld, M., Colombini, S., Gallo, R.C., *et al.* (1997). Characterization of a chemokine receptor-related gene in human herpesvirus 8 and its expression in Kaposi's sarcoma. Virology *228*, 371-378.

Gwack, Y., Baek, H.J., Nakamura, H., Lee, S.H., Meisterernst, M., Roeder, R.G., and Jung, J.U. (2003a). Principal role of TRAP/mediator and SWI/SNF complexes in Kaposi's sarcoma-associated herpesvirus RTA-mediated lytic reactivation. Mol Cell Biol *23*, 2055-2067.

Gwack, Y., Byun, H., Hwang, S., Lim, C., and Choe, J. (2001). CREB-binding protein and histone deacetylase regulate the transcriptional activity of Kaposi's sarcoma-associated herpesvirus open reading frame 50. J Virol *75*, 1909-1917.

Gwack, Y., Hwang, S., Lim, C., Won, Y.S., Lee, C.H., and Choe, J. (2002). Kaposi's Sarcoma-associated herpesvirus open reading frame 50 stimulates the transcriptional activity of STAT3. J Biol Chem *277*, 6438-6442.

Gwack, Y., Nakamura, H., Lee, S.H., Souvlis, J., Yustein, J.T., Gygi, S., Kung, H.J., and Jung, J.U. (2003b). Poly(ADP-ribose) polymerase 1 and Ste20-like kinase hKFC act as transcriptional repressors for gamma-2 herpesvirus lytic replication. Mol Cell Biol *23*, 8282-8294.

Haecker, I., Gay, L.A., Yang, Y., Hu, J., Morse, A.M., McIntyre, L.M., and Renne, R. (2012). Ago HITS-CLIP expands understanding of Kaposi's sarcoma-associated herpesvirus miRNA function in primary effusion lymphomas. PLoS Pathog *8*, e1002884.

Han, S.J., Hu, J., Pierce, B., Weng, Z., and Renne, R. (2010). Mutational analysis of the latency-associated nuclear antigen DNA-binding domain of Kaposi's sarcoma-associated herpesvirus reveals structural conservation among gammaherpesvirus origin-binding proteins. J Gen Virol *91*, 2203-2215.

Handoko, L., Xu, H., Li, G., Ngan, C.Y., Chew, E., Schnapp, M., Lee, C.W., Ye, C., Ping, J.L., Mulawadi, F., *et al.* (2011). CTCF-mediated functional chromatin interactome in pluripotent cells. Nat Genet *43*, 630-638.

Hansen, A., Henderson, S., Lagos, D., Nikitenko, L., Coulter, E., Roberts, S., Gratrix, F., Plaisance, K., Renne, R., Bower, M., *et al.* (2010). KSHV-encoded miRNAs target MAF to induce endothelial cell reprogramming. Genes Dev *24*, 195-205.

Harrison, S.M., and Whitehouse, A. (2008). Kaposi's sarcoma-associated herpesvirus (KSHV) Rta and cellular HMGB1 proteins synergistically transactivate the KSHV ORF50 promoter. FEBS Lett *582*, 3080-3084.

Hayward, G.S. (1999). KSHV strains: the origins and global spread of the virus. Semin Cancer Biol *9*, 187-199.

Hayward, S.D. (2004). Viral interactions with the Notch pathway. Semin Cancer Biol *14*, 387-396.

He, M., Zhang, W., Bakken, T., Schutten, M., Toth, Z., Jung, J.U., Gill, P., Cannon, M., and Gao, S.J. (2012). Cancer angiogenesis induced by Kaposi sarcoma-associated herpesvirus is mediated by EZH2. Cancer Res *72*, 3582-3592.

He, Z., Liu, Y., Liang, D., Wang, Z., Robertson, E.S., and Lan, K. (2010). Cellular corepressor TLE2 inhibits replication-and-transcription- activator-mediated transactivation and lytic reactivation of Kaposi's sarcoma-associated herpesvirus. J Virol *84*, 2047-2062.

Heath, H., Ribeiro de Almeida, C., Sleutels, F., Dingjan, G., van de Nobelen, S., Jonkers, I., Ling, K.W., Gribnau, J., Renkawitz, R., Grosveld, F., *et al.* (2008). CTCF regulates cell cycle progression of alphabeta T cells in the thymus. EMBO J *27*, 2839-2850.

Herndier, B.G., Werner, A., Arnstein, P., Abbey, N.W., Demartis, F., Cohen, R.L., Shuman, M.A., and Levy, J.A. (1994). Characterization of a human Kaposi's sarcoma cell line that induces angiogenic tumors in animals. AIDS *8*, 575-581.

Hillier, J.C., Shaw, P., Miller, R.F., Cartledge, J.D., Nelson, M., Bower, M., Francis, N., and Padley, S.P. (2004). Imaging features of multicentric Castleman's disease in HIV infection. Clin Radiol *59*, 596-601.

Hilton, I.B., and Dittmer, D.P. (2012). Quantitative analysis of the bidirectional viral G-protein-coupled receptor and lytic latency-associated nuclear antigen promoter of Kaposi's sarcoma-associated herpesvirus. J Virol *86*, 9683-9695.

Hogan, G.J., Lee, C.K., and Lieb, J.D. (2006). Cell cycle-specified fluctuation of nucleosome occupancy at gene promoters. PLoS Genet *2*, e158.

Holdorf, M.M., Cooper, S.B., Yamamoto, K.R., and Miranda, J.J. (2011). Occupancy of chromatin organizers in the Epstein-Barr virus genome. Virology *415*, 1-5.

Holwerda, S., and de Laat, W. (2012). Chromatin loops, gene positioning, and gene expression. Front Genet *3*, 217.

Hsia, D.A., Tepper, C.G., Pochampalli, M.R., Hsia, E.Y., Izumiya, C., Huerta, S.B., Wright, M.E., Chen, H.W., Kung, H.J., and Izumiya, Y. (2010). KDM8, a H3K36me2 histone demethylase that acts in the cyclin A1 coding region to regulate cancer cell proliferation. Proc Natl Acad Sci U S A *107*, 9671-9676.

Hsieh, J.J., Henkel, T., Salmon, P., Robey, E., Peterson, M.G., and Hayward, S.D. (1996). Truncated mammalian Notch1 activates CBF1/RBPJk-repressed genes by a mechanism resembling that of Epstein-Barr virus EBNA2. Mol Cell Biol *16*, 952-959.

Hu, J., Garber, A.C., and Renne, R. (2002). The latency-associated nuclear antigen of Kaposi's sarcoma-associated herpesvirus supports latent DNA replication in dividing cells. J Virol *76*, 11677-11687.

Hu, J., Liu, E., and Renne, R. (2009). Involvement of SSRP1 in latent replication of Kaposi's sarcoma-associated herpesvirus. J Virol *83*, 11051-11063.

Hu, J., and Renne, R. (2005). Characterization of the minimal replicator of Kaposi's sarcoma-associated herpesvirus latent origin. J Virol *79*, 2637-2642.

Hughes, D.J., Marendy, E.M., Dickerson, C.A., Yetming, K.D., Sample, C.E., and Sample, J.T. (2012). Contributions of CTCF and DNA methyltransferases DNMT1 and DNMT3B to Epstein-Barr virus restricted latency. J Virol *86*, 1034-1045.

Ishido, S., Wang, C., Lee, B.S., Cohen, G.B., and Jung, J.U. (2000). Downregulation of major histocompatibility complex class I molecules by Kaposi's sarcoma-associated herpesvirus K3 and K5 proteins. J Virol *74*, 5300-5309.

Izumiya, Y., Lin, S.F., Ellison, T., Chen, L.Y., Izumiya, C., Luciw, P., and Kung, H.J. (2003). Kaposi's sarcoma-associated herpesvirus K-bZIP is a coregulator of K-Rta: physical association and promoter-dependent transcriptional repression. J Virol *77*, 1441-1451.

Jaber, T., and Yuan, Y. (2013). A Virally Encoded Small Peptide Regulates RTA Stability and Facilitates Kaposi's Sarcoma-associated Herpesvirus Lytic Replication. J Virol.

Jacobs, S.R., and Damania, B. (2011). The viral interferon regulatory factors of KSHV: immunosuppressors or oncogenes? Front Immunol *2*, 19.

Jayachandra, S., Low, K.G., Thlick, A.E., Yu, J., Ling, P.D., Chang, Y., and Moore, P.S. (1999). Three unrelated viral transforming proteins (vIRF, EBNA2, and E1A) induce the MYC oncogene through the interferon-responsive PRF element by using different transcription coadaptors. Proc Natl Acad Sci U S A *96*, 11566-11571.

Jenner, R.G., Alba, M.M., Boshoff, C., and Kellam, P. (2001). Kaposi's sarcoma-associated herpesvirus latent and lytic gene expression as revealed by DNA arrays. J Virol *75*, 891-902.

Jeong, J., Papin, J., and Dittmer, D. (2001). Differential regulation of the overlapping Kaposi's sarcoma-associated herpesvirus vGCR (orf74) and LANA (orf73) promoters. J Virol *75*, 1798-1807.

Jeong, J.H., Hines-Boykin, R., Ash, J.D., and Dittmer, D.P. (2002). Tissue specificity of the Kaposi's sarcoma-associated herpesvirus latent nuclear antigen (LANA/orf73) promoter in transgenic mice. J Virol *76*, 11024-11032.

Jeong, J.H., Orvis, J., Kim, J.W., McMurtrey, C.P., Renne, R., and Dittmer, D.P. (2004). Regulation and autoregulation of the promoter for the latency-associated nuclear antigen of Kaposi's sarcoma-associated herpesvirus. J Biol Chem *279*, 16822-16831.

Jiang, C., and Pugh, B.F. (2009). Nucleosome positioning and gene regulation: advances through genomics. Nat Rev Genet *10*, 161-172.

Jimenez-Ramirez, C., Brooks, A.J., Forshell, L.P., Yakimchuk, K., Zhao, B., Fulgham, T.Z., and Sample, C.E. (2006). Epstein-Barr virus EBNA-3C is targeted to and regulates expression from the bidirectional LMP-1/2B promoter. J Virol *80*, 11200-11208.

Jin, Y., He, Z., Liang, D., Zhang, Q., Zhang, H., Deng, Q., Robertson, E.S., and Lan, K. (2012). Carboxyl-terminal amino acids 1052 to 1082 of the latency-associated nuclear antigen (LANA) interact with RBP-Jkappa and are responsible for LANA-mediated RTA repression. J Virol *86*, 4956-4969.

Jong, J.E., Cha, S., Jang, J.H., and Seo, T. (2013). Alteration of Histone H3 Lysine 4 Trimethylation on Putative Lytic Gene Promoters by Human Set1 Complex during Reactivation of Kaposi's Sarcoma-Associated Herpesvirus. Intervirology *56*, 91-103.

Kagey, M.H., Newman, J.J., Bilodeau, S., Zhan, Y., Orlando, D.A., van Berkum, N.L., Ebmeier, C.C., Goossens, J., Rahl, P.B., Levine, S.S., *et al.* (2010). Mediator and cohesin connect gene expression and chromatin architecture. Nature *467*, 430-435.

Kang, H., Cho, H., Sung, G.H., and Lieberman, P.M. (2013). CTCF regulates Kaposi's sarcoma-associated herpesvirus latency transcription by nucleosome displacement and RNA polymerase programming. J Virol *87*, 1789-1799.

Kang, H., and Lieberman, P.M. (2009). Cell cycle control of Kaposi's sarcoma-associated herpesvirus latency transcription by CTCF-cohesin interactions. J Virol *83*, 6199-6210.

Kang, H., Wiedmer, A., Yuan, Y., Robertson, E., and Lieberman, P.M. (2011). Coordination of KSHV latent and lytic gene control by CTCF-cohesin mediated chromosome conformation. PLoS Pathog *7*, e1002140.

Kaplan, N., Hughes, T.R., Lieb, J.D., Widom, J., and Segal, E. (2010). Contribution of histone sequence preferences to nucleosome organization: proposed definitions and methodology. Genome Biol *11*, 140.

Kaposi, M. (1872). Idiopathisches multiples Pigmentsarkom der Haut. . Arch Dermatol Syph *4*, 265-273.

Karki, R., Lang, S.M., and Means, R.E. (2011). The MARCH family E3 ubiquitin ligase K5 alters monocyte metabolism and proliferation through receptor tyrosine kinase modulation. PLoS Pathog *7*, e1001331.

Katano, H., Sato, Y., and Sata, T. (2001). Expression of p53 and human herpesvirus-8 (HHV-8)-encoded latency-associated nuclear antigen with inhibition of apoptosis in HHV-8-associated malignancies. Cancer *92*, 3076-3084.

Kedes, D.H., Lagunoff, M., Renne, R., and Ganem, D. (1997). Identification of the gene encoding the major latency-associated nuclear antigen of the Kaposi's sarcoma-associated herpesvirus. J Clin Invest *100*, 2606-2610.

Kelley-Clarke, B., Ballestas, M.E., Komatsu, T., and Kaye, K.M. (2007). Kaposi's sarcoma herpesvirus C-terminal LANA concentrates at pericentromeric and peri-telomeric regions of a subset of mitotic chromosomes. Virology *357*, 149-157.

Kelley-Clarke, B., De Leon-Vazquez, E., Slain, K., Barbera, A.J., and Kaye, K.M. (2009). Role of Kaposi's sarcoma-associated herpesvirus C-terminal LANA chromosome binding in episome persistence. J Virol *83*, 4326-4337.

Kemmer, G., and Keller, S. (2010). Nonlinear least-squares data fitting in Excel spreadsheets. Nat Protoc *5*, 267-281.

Khalil, A.S., and Collins, J.J. (2010). Synthetic biology: applications come of age. Nat Rev Genet *11*, 367-379.

Kim, H.D., and O'Shea, E.K. (2008). A quantitative model of transcription factor-activated gene expression. Nat Struct Mol Biol *15*, 1192-1198.

Kim, H.D., Shay, T., O'Shea, E.K., and Regev, A. (2009). Transcriptional regulatory circuits: predicting numbers from alphabets. Science *325*, 429-432.

Kim, T.H., Abdullaev, Z.K., Smith, A.D., Ching, K.A., Loukinov, D.I., Green, R.D., Zhang, M.Q., Lobanenkov, V.V., and Ren, B. (2007). Analysis of the vertebrate insulator protein CTCF-binding sites in the human genome. Cell *128*, 1231-1245.

Kirshner, J.R., Staskus, K., Haase, A., Lagunoff, M., and Ganem, D. (1999). Expression of the open reading frame 74 (G-protein-coupled receptor) gene of Kaposi's sarcoma (KS)-associated herpesvirus: implications for KS pathogenesis. J Virol *73*, 6006-6014.

Kishimoto, T. (2010). IL-6: from its discovery to clinical applications. Int Immunol *22*, 347-352.

Kliche, S., Nagel, W., Kremmer, E., Atzler, C., Ege, A., Knorr, T., Koszinowski, U., Kolanus, W., and Haas, J. (2001). Signaling by human herpesvirus 8 kaposin A through direct membrane recruitment of cytohesin-1. Mol Cell *7*, 833-843.

Klose, R.J., Kallin, E.M., and Zhang, Y. (2006). JmjC-domain-containing proteins and histone demethylation. Nat Rev Genet *7*, 715-727.

Knipe, D.M., Lieberman, P.M., Jung, J.U., McBride, A.A., Morris, K.V., Ott, M., Margolis, D., Nieto, A., Nevels, M., Parks, R.J., *et al.* (2013). Snapshots: Chromatin control of viral infection. Virology *435*, 141-156.

Knutson, B.A., Drennan, M., Liu, X., and Broyles, S.S. (2009). Bidirectional transcriptional promoters in the vaccinia virus genome. Virology *385*, 198-203.

Kobiler, O., Lipman, Y., Therkelsen, K., Daubechies, I., and Enquist, L.W. (2010). Herpesviruses carrying a Brainbow cassette reveal replication and expression of limited numbers of incoming genomes. Nat Commun *1*, 146.

Komanduri, K.V., Luce, J.A., McGrath, M.S., Herndier, B.G., and Ng, V.L. (1996). The natural history and molecular heterogeneity of HIV-associated primary malignant lymphomatous effusions. J Acquir Immune Defic Syndr Hum Retrovirol *13*, 215-226.

Komatsu, T., Ballestas, M.E., Barbera, A.J., Kelley-Clarke, B., and Kaye, K.M. (2004). KSHV LANA1 binds DNA as an oligomer and residues N-terminal to the oligomerization domain are essential for DNA binding, replication, and episome persistence. Virology *319*, 225-236.

Kovall, R.A., and Blacklow, S.C. (2010). Mechanistic insights into Notch receptor signaling from structural and biochemical studies. Curr Top Dev Biol *92*, 31-71.

Krishnan, H.H., Naranatt, P.P., Smith, M.S., Zeng, L., Bloomer, C., and Chandran, B. (2004). Concurrent expression of latent and a limited number of lytic genes with immune modulation and antiapoptotic function by Kaposi's sarcoma-associated herpesvirus early during infection of primary endothelial and fibroblast cells and subsequent decline of lytic gene expression. J Virol *78*, 3601-3620.

Krithivas, A., Fujimuro, M., Weidner, M., Young, D.B., and Hayward, S.D. (2002). Protein interactions targeting the latency-associated nuclear antigen of Kaposi's sarcoma-associated herpesvirus to cell chromosomes. J Virol *76*, 11596-11604.

Krithivas, A., Young, D.B., Liao, G., Greene, D., and Hayward, S.D. (2000). Human herpesvirus 8 LANA interacts with proteins of the mSin3 corepressor complex and negatively regulates Epstein-Barr virus gene expression in dually infected PEL cells. J Virol *74*, 9637-9645.

Kuhlman, T., Zhang, Z., Saier, M.H., Jr., and Hwa, T. (2007). Combinatorial transcriptional control of the lactose operon of Escherichia coli. Proc Natl Acad Sci U S A *104*, 6043-6048.

Kusano, S., and Eizuru, Y. (2010). Human I-mfa domain proteins specifically interact with KSHV LANA and affect its regulation of Wnt signaling-dependent transcription. Biochem Biophys Res Commun *396*, 608-613.

Lagunoff, M., and Ganem, D. (1997). The structure and coding organization of the genomic termini of Kaposi's sarcoma-associated herpesvirus. Virology *236*, 147-154.

Lagunoff, M., Majeti, R., Weiss, A., and Ganem, D. (1999). Deregulated signal transduction by the K1 gene product of Kaposi's sarcoma-associated herpesvirus. Proc Natl Acad Sci U S A *96*, 5704-5709.

Lan, K., Kuppers, D.A., and Robertson, E.S. (2005a). Kaposi's sarcoma-associated herpesvirus reactivation is regulated by interaction of latency-associated nuclear antigen with recombination signal sequence-binding protein Jkappa, the major downstream effector of the Notch signaling pathway. J Virol *79*, 3468-3478.

Lan, K., Kuppers, D.A., Verma, S.C., and Robertson, E.S. (2004). Kaposi's sarcoma-associated herpesvirus-encoded latency-associated nuclear antigen inhibits lytic replication by targeting Rta: a potential mechanism for virus-mediated control of latency. J Virol *78*, 6585-6594.

Lan, K., Kuppers, D.A., Verma, S.C., Sharma, N., Murakami, M., and Robertson, E.S. (2005b). Induction of Kaposi's sarcoma-associated herpesvirus latency-associated nuclear antigen by the lytic transactivator RTA: a novel mechanism for establishment of latency. J Virol *79*, 7453-7465.

Lan, K., Murakami, M., Choudhuri, T., Kuppers, D.A., and Robertson, E.S. (2006). Intracellular-activated Notch1 can reactivate Kaposi's sarcoma-associated herpesvirus from latency. Virology *351*, 393-403.

Langmead, B., Trapnell, C., Pop, M., and Salzberg, S.L. (2009). Ultrafast and memory-efficient alignment of short DNA sequences to the human genome. Genome Biol *10*, R25.

Lassmann, T., Hayashizaki, Y., and Daub, C.O. (2009). TagDust--a program to eliminate artifacts from next generation sequencing data. Bioinformatics *25*, 2839-2840.

Laux, G., Economou, A., and Farrell, P.J. (1989). The terminal protein gene 2 of Epstein-Barr virus is transcribed from a bidirectional latent promoter region. J Gen Virol *70 (Pt 11)*, 3079-3084.

Lechowicz, M., Dittmer, D.P., Lee, J.Y., Krown, S.E., Wachsman, W., Aboulafia, D., Dezube, B.J., Ratner, L., Said, J., and Ambinder, R.F. (2009). Molecular and clinical assessment in the treatment of AIDS Kaposi sarcoma with valproic Acid. Clin Infect Dis *49*, 1946-1949.

Lee, B.K., and Iyer, V.R. (2012). Genome-wide studies of CCCTC-binding factor (CTCF) and cohesin provide insight into chromatin structure and regulation. J Biol Chem *287*, 30906-30913.

Lee, H., Guo, J., Li, M., Choi, J.K., DeMaria, M., Rosenzweig, M., and Jung, J.U. (1998a). Identification of an immunoreceptor tyrosine-based activation motif of K1 transforming protein of Kaposi's sarcoma-associated herpesvirus. Mol Cell Biol *18*, 5219-5228.

Lee, H., Veazey, R., Williams, K., Li, M., Guo, J., Neipel, F., Fleckenstein, B., Lackner, A., Desrosiers, R.C., and Jung, J.U. (1998b). Deregulation of cell growth by the K1 gene of Kaposi's sarcoma-associated herpesvirus. Nat Med *4*, 435-440.

Lee, H.R., Brulois, K., Wong, L., and Jung, J.U. (2012). Modulation of Immune System by Kaposi's Sarcoma-Associated Herpesvirus: Lessons from Viral Evasion Strategies. Front Microbiol *3*, 44.

Lee, H.R., Kim, M.H., Lee, J.S., Liang, C., and Jung, J.U. (2009a). Viral interferon regulatory factors. J Interferon Cytokine Res *29*, 621-627.

Lee, J.S., Li, Q., Lee, J.Y., Lee, S.H., Jeong, J.H., Lee, H.R., Chang, H., Zhou, F.C., Gao, S.J., Liang, C., *et al.* (2009b). FLIP-mediated autophagy regulation in cell death control. Nat Cell Biol *11*, 1355-1362.

Lee, S., Chugh, P.E., Shen, H., Eberle, R.W., and Dittmer, D.P. (2013). Poisson Factor Models with Applications to Non-normalized MicroRNA Profiling. Bioinformatics.

Li, H., Komatsu, T., Dezube, B.J., and Kaye, K.M. (2002). The Kaposi's sarcoma-associated herpesvirus K12 transcript from a primary effusion lymphoma contains complex repeat elements, is spliced, and initiates from a novel promoter. J Virol *76*, 11880-11888.

Li, Q., Zhou, F., Ye, F., and Gao, S.J. (2008). Genetic disruption of KSHV major latent nuclear antigen LANA enhances viral lytic transcriptional program. Virology *379*, 234-244.

Li, Y.Y., Yu, H., Guo, Z.M., Guo, T.Q., Tu, K., and Li, Y.X. (2006). Systematic analysis of head-to-head gene organization: evolutionary conservation and potential biological relevance. PLoS Comput Biol *2*, e74.

Liang, Y., Chang, J., Lynch, S.J., Lukac, D.M., and Ganem, D. (2002). The lytic switch protein of KSHV activates gene expression via functional interaction with RBP-Jkappa (CSL), the target of the Notch signaling pathway. Genes Dev *16*, 1977-1989.

Liang, Y., and Ganem, D. (2003). Lytic but not latent infection by Kaposi's sarcoma-associated herpesvirus requires host CSL protein, the mediator of Notch signaling. Proc Natl Acad Sci U S A *100*, 8490-8495.

Liang, Y., and Ganem, D. (2004). RBP-J (CSL) is essential for activation of the K14/vGPCR promoter of Kaposi's sarcoma-associated herpesvirus by the lytic switch protein RTA. J Virol *78*, 6818-6826.

Liao, W., Tang, Y., Kuo, Y.L., Liu, B.Y., Xu, C.J., and Giam, C.Z. (2003). Kaposi's sarcoma-associated herpesvirus/human herpesvirus 8 transcriptional activator Rta is an oligomeric DNA-binding protein that interacts with tandem arrays of phased A/T-trinucleotide motifs. J Virol *77*, 9399-9411.

Lim, C., Gwack, Y., Hwang, S., Kim, S., and Choe, J. (2001). The transcriptional activity of cAMP response element-binding protein-binding protein is modulated by the latency associated nuclear antigen of Kaposi's sarcoma-associated herpesvirus. J Biol Chem *276*, 31016-31022.

Lim, C., Sohn, H., Gwack, Y., and Choe, J. (2000). Latency-associated nuclear antigen of Kaposi's sarcoma-associated herpesvirus (human herpesvirus-8) binds ATF4/CREB2 and inhibits its transcriptional activation activity. J Gen Virol *81*, 2645-2652.

Lin, C.L., Li, H., Wang, Y., Zhu, F.X., Kudchodkar, S., and Yuan, Y. (2003). Kaposi's sarcoma-associated herpesvirus lytic origin (ori-Lyt)-dependent DNA replication: identification of the ori-Lyt and association of K8 bZip protein with the origin. J Virol *77*, 5578-5588.

Lin, Y.T., Kincaid, R.P., Arasappan, D., Dowd, S.E., Hunicke-Smith, S.P., and Sullivan, C.S. (2010). Small RNA profiling reveals antisense transcription throughout the KSHV genome and novel small RNAs. RNA *16*, 1540-1558.

Liu, C., Okruzhnov, Y., Li, H., and Nicholas, J. (2001). Human herpesvirus 8 (HHV-8)-encoded cytokines induce expression of and autocrine signaling by vascular endothelial growth factor (VEGF) in HHV-8-infected primary-effusion lymphoma cell lines and mediate VEGF-independent antiapoptotic effects. J Virol *75*, 10933-10940.

Liu, J., Martin, H.J., Liao, G., and Hayward, S.D. (2007). The Kaposi's sarcoma-associated herpesvirus LANA protein stabilizes and activates c-Myc. J Virol *81*, 10451-10459.

Liu, Y., Cao, Y., Liang, D., Gao, Y., Xia, T., Robertson, E.S., and Lan, K. (2008). Kaposi's sarcoma-associated herpesvirus RTA activates the processivity factor ORF59 through interaction with RBP-Jkappa and a cis-acting RTA responsive element. Virology *380*, 264-275.

Liu, Y., Sun, R., Lin, X., Liang, D., Deng, Q., and Lan, K. (2012). Kaposi's sarcoma-associated herpesvirus-encoded microRNA miR-K12-11 attenuates transforming growth factor beta signaling through suppression of SMAD5. J Virol *86*, 1372-1381.

Lobanenkov, V.V., Nicolas, R.H., Adler, V.V., Paterson, H., Klenova, E.M., Polotskaja, A.V., and Goodwin, G.H. (1990). A novel sequence-specific DNA binding protein which interacts with three regularly spaced direct repeats of the CCCTC-motif in the 5'-flanking sequence of the chicken c-myc gene. Oncogene *5*, 1743-1753.

Low, W., Harries, M., Ye, H., Du, M.Q., Boshoff, C., and Collins, M. (2001). Internal ribosome entry site regulates translation of Kaposi's sarcoma-associated herpesvirus FLICE inhibitory protein. J Virol *75*, 2938-2945.

Lu, F., Day, L., Gao, S.J., and Lieberman, P.M. (2006). Acetylation of the latency-associated nuclear antigen regulates repression of Kaposi's sarcoma-associated herpesvirus lytic transcription. J Virol *80*, 5273-5282.

Lu, F., Stedman, W., Yousef, M., Renne, R., and Lieberman, P.M. (2010). Epigenetic regulation of Kaposi's sarcoma-associated herpesvirus latency by virus-encoded microRNAs that target Rta and the cellular Rbl2-DNMT pathway. J Virol *84*, 2697-2706.

Lu, F., Tsai, K., Chen, H.S., Wikramasinghe, P., Davuluri, R.V., Showe, L., Domsic, J., Marmorstein, R., and Lieberman, P.M. (2012a). Identification of host-chromosome binding sites and candidate gene targets for Kaposi's sarcoma-associated herpesvirus LANA. J Virol *86*, 5752-5762.

Lu, F., Zhou, J., Wiedmer, A., Madden, K., Yuan, Y., and Lieberman, P.M. (2003). Chromatin remodeling of the Kaposi's sarcoma-associated herpesvirus ORF50 promoter correlates with reactivation from latency. J Virol *77*, 11425-11435.

Lu, J., Verma, S.C., Cai, Q., and Robertson, E.S. (2011). The single RBP-Jkappa site within the LANA promoter is crucial for establishing Kaposi's sarcoma-associated herpesvirus latency during primary infection. J Virol *85*, 6148-6161.

Lu, J., Verma, S.C., Cai, Q., Saha, A., Dzeng, R.K., and Robertson, E.S. (2012b). The RBP-Jkappa binding sites within the RTA promoter regulate KSHV latent infection and cell proliferation. PLoS Pathog *8*, e1002479.

Lu, M., Suen, J., Frias, C., Pfeiffer, R., Tsai, M.H., Chuang, E., and Zeichner, S.L. (2004). Dissection of the Kaposi's sarcoma-associated herpesvirus gene expression program by using the viral DNA replication inhibitor cidofovir. J Virol *78*, 13637-13652.

Lubyova, B., and Pitha, P.M. (2000). Characterization of a novel human herpesvirus 8-encoded protein, vIRF-3, that shows homology to viral and cellular interferon regulatory factors. J Virol *74*, 8194-8201.

Luger, K., Dechassa, M.L., and Tremethick, D.J. (2012). New insights into nucleosome and chromatin structure: an ordered state or a disordered affair? Nat Rev Mol Cell Biol *13*, 436-447.

Lukac, D.M., Garibyan, L., Kirshner, J.R., Palmeri, D., and Ganem, D. (2001). DNA binding by Kaposi's sarcoma-associated herpesvirus lytic switch protein is necessary for transcriptional activation of two viral delayed early promoters. J Virol *75*, 6786-6799.

Lukac, D.M., Kirshner, J.R., and Ganem, D. (1999). Transcriptional activation by the product of open reading frame 50 of Kaposi's sarcoma-associated herpesvirus is required for lytic viral reactivation in B cells. J Virol *73*, 9348-9361.

Lukac, D.M., Renne, R., Kirshner, J.R., and Ganem, D. (1998). Reactivation of Kaposi's sarcoma-associated herpesvirus infection from latency by expression of the ORF 50 transactivator, a homolog of the EBV R protein. Virology *252*, 304-312.

Maclean, C.M. (1963). Kaposi's Sarcoma in Nigeria. Br J Cancer *17*, 195-205.

Marshall, V., Parks, T., Bagni, R., Wang, C.D., Samols, M.A., Hu, J., Wyvil, K.M., Aleman, K., Little, R.F., Yarchoan, R., *et al.* (2007). Conservation of virally encoded microRNAs in Kaposi sarcoma--associated herpesvirus in primary effusion lymphoma cell lines and in patients with Kaposi sarcoma or multicentric Castleman disease. J Infect Dis *195*, 645-659.

Martin, D., Galisteo, R., Molinolo, A.A., Wetzker, R., Hirsch, E., and Gutkind, J.S. (2011). PI3Kgamma mediates kaposi's sarcoma-associated herpesvirus vGPCR-induced sarcomagenesis. Cancer Cell *19*, 805-813.

Martin, D., and Gutkind, J.S. (2008). Human tumor-associated viruses and new insights into the molecular mechanisms of cancer. Oncogene *27 Suppl 2*, S31-42.

Matsumura, S., Fujita, Y., Gomez, E., Tanese, N., and Wilson, A.C. (2005). Activation of the Kaposi's sarcoma-associated herpesvirus major latency locus by the lytic switch protein RTA (ORF50). J Virol *79*, 8493-8505.

Matsumura, S., Persson, L.M., Wong, L., and Wilson, A.C. (2010). The latency-associated nuclear antigen interacts with MeCP2 and nucleosomes through separate domains. J Virol *84*, 2318-2330.

Matta, H., and Chaudhary, P.M. (2004). Activation of alternative NF-kappa B pathway by human herpes virus 8-encoded Fas-associated death domain-like IL-1 beta-converting enzyme inhibitory protein (vFLIP). Proc Natl Acad Sci U S A *101*, 9399-9404.

McCormick, C., and Ganem, D. (2005). The kaposin B protein of KSHV activates the p38/MK2 pathway and stabilizes cytokine mRNAs. Science *307*, 739-741.

Mehta, G.D., Rizvi, S.M., and Ghosh, S.K. (2012). Cohesin: a guardian of genome integrity. Biochim Biophys Acta *1823*, 1324-1342.

Mercader, M., Taddeo, B., Panella, J.R., Chandran, B., Nickoloff, B.J., and Foreman, K.E. (2000). Induction of HHV-8 lytic cycle replication by inflammatory cytokines produced by HIV-1-infected T cells. Am J Pathol *156*, 1961-1971.

Merkenschlager, M. (2010). Cohesin: a global player in chromosome biology with local ties to gene regulation. Curr Opin Genet Dev *20*, 555-561.

Mesri, E.A., Cesarman, E., and Boshoff, C. (2010). Kaposi's sarcoma and its associated herpesvirus. Nat Rev Cancer *10*, 707-719.

Miele, L. (2011). Transcription factor RBPJ/CSL: a genome-wide look at transcriptional regulation. Proc Natl Acad Sci U S A *108*, 14715-14716.

Molden, J., Chang, Y., You, Y., Moore, P.S., and Goldsmith, M.A. (1997). A Kaposi's sarcoma-associated herpesvirus-encoded cytokine homolog (vIL-6) activates signaling through the shared gp130 receptor subunit. J Biol Chem *272*, 19625-19631.

Montaner, S. (2007). Akt/TSC/mTOR activation by the KSHV G protein-coupled receptor: emerging insights into the molecular oncogenesis and treatment of Kaposi's sarcoma. Cell Cycle *6*, 438-443.

Montaner, S., Sodhi, A., Molinolo, A., Bugge, T.H., Sawai, E.T., He, Y., Li, Y., Ray, P.E., and Gutkind, J.S. (2003). Endothelial infection with KSHV genes in vivo reveals that vGPCR initiates Kaposi's sarcomagenesis and can promote the tumorigenic potential of viral latent genes. Cancer Cell *3*, 23-36.

Montaner, S., Sodhi, A., Pece, S., Mesri, E.A., and Gutkind, J.S. (2001). The Kaposi's sarcoma-associated herpesvirus G protein-coupled receptor promotes endothelial cell survival through the activation of Akt/protein kinase B. Cancer Res *61*, 2641-2648.

Montaner, S., Sodhi, A., Servitja, J.M., Ramsdell, A.K., Barac, A., Sawai, E.T., and Gutkind, J.S. (2004). The small GTPase Rac1 links the Kaposi sarcoma-associated herpesvirus vGPCR to cytokine secretion and paracrine neoplasia. Blood *104*, 2903-2911.

Moore, P.S., Boshoff, C., Weiss, R.A., and Chang, Y. (1996a). Molecular mimicry of human cytokine and cytokine response pathway genes by KSHV. Science *274*, 1739-1744.

Moore, P.S., and Chang, Y. (2010). Why do viruses cause cancer? Highlights of the first century of human tumour virology. Nat Rev Cancer *10*, 878-889.

Moore, P.S., Gao, S.J., Dominguez, G., Cesarman, E., Lungu, O., Knowles, D.M., Garber, R., Pellett, P.E., McGeoch, D.J., and Chang, Y. (1996b). Primary characterization of a herpesvirus agent associated with Kaposi's sarcomae. J Virol *70*, 549-558.

Moorman, N.J., Willer, D.O., and Speck, S.H. (2003). The gammaherpesvirus 68 latency-associated nuclear antigen homolog is critical for the establishment of splenic latency. J Virol *77*, 10295-10303.

Muralidhar, S., Pumfery, A.M., Hassani, M., Sadaie, M.R., Kishishita, M., Brady, J.N., Doniger, J., Medveczky, P., and Rosenthal, L.J. (1998). Identification of kaposin (open reading frame K12) as a human herpesvirus 8 (Kaposi's sarcoma-associated herpesvirus) transforming gene. J Virol *72*, 4980-4988.

Nador, R.G., Cesarman, E., Chadburn, A., Dawson, D.B., Ansari, M.Q., Sald, J., and Knowles, D.M. (1996). Primary effusion lymphoma: a distinct clinicopathologic entity associated with the Kaposi's sarcoma-associated herpes virus. Blood *88*, 645-656.

Nador, R.G., Milligan, L.L., Flore, O., Wang, X., Arvanitakis, L., Knowles, D.M., and Cesarman, E. (2001). Expression of Kaposi's sarcoma-associated herpesvirus G protein-coupled receptor monocistronic and bicistronic transcripts in primary effusion lymphomas. Virology *287*, 62-70.

Nagy, P.L., Cleary, M.L., Brown, P.O., and Lieb, J.D. (2003). Genomewide demarcation of RNA polymerase II transcription units revealed by physical fractionation of chromatin. Proc Natl Acad Sci U S A *100*, 6364-6369.

Nakamura, H., Li, M., Zarycki, J., and Jung, J.U. (2001). Inhibition of p53 tumor suppressor by viral interferon regulatory factor. J Virol *75*, 7572-7582.

Nakamura, H., Lu, M., Gwack, Y., Souvlis, J., Zeichner, S.L., and Jung, J.U. (2003). Global changes in Kaposi's sarcoma-associated virus gene expression patterns following expression of a tetracycline-inducible Rta transactivator. J Virol *77*, 4205-4220.

Nakano, K., Isegawa, Y., Zou, P., Tadagaki, K., Inagi, R., and Yamanishi, K. (2003). Kaposi's sarcoma-associated herpesvirus (KSHV)-encoded vMIP-I and vMIP-II induce signal transduction and chemotaxis in monocytic cells. Arch Virol *148*, 871-890.

Nandagopal, N., and Elowitz, M.B. (2011). Synthetic biology: integrated gene circuits. Science *333*, 1244-1248.

Nasmyth, K., and Haering, C.H. (2009). Cohesin: its roles and mechanisms. Annu Rev Genet *43*, 525-558.

Neil, H., Malabat, C., d'Aubenton-Carafa, Y., Xu, Z., Steinmetz, L.M., and Jacquier, A. (2009). Widespread bidirectional promoters are the major source of cryptic transcripts in yeast. Nature *457*, 1038-1042.

Neipel, F., and Fleckenstein, B. (1999). The role of HHV-8 in Kaposi's sarcoma. Semin Cancer Biol *9*, 151-164.

Nicholas, J., Ruvolo, V.R., Burns, W.H., Sandford, G., Wan, X., Ciufo, D., Hendrickson, S.B., Guo, H.G., Hayward, G.S., and Reitz, M.S. (1997). Kaposi's sarcoma-associated human herpesvirus-8 encodes homologues of macrophage inflammatory protein-1 and interleukin-6. Nat Med *3*, 287-292.

Nun, T.K., Kroll, D.J., Oberlies, N.H., Soejarto, D.D., Case, R.J., Piskaut, P., Matainaho, T., Hilscher, C., Wang, L., Dittmer, D.P., *et al.* (2007). Development of a fluorescence-based assay to screen antiviral drugs against Kaposi's sarcoma associated herpesvirus. Mol Cancer Ther *6*, 2360-2370.

O'Hara, A.J., Chugh, P., Wang, L., Netto, E.M., Luz, E., Harrington, W.J., Dezube, B.J., Damania, B., and Dittmer, D.P. (2009). Pre-micro RNA signatures delineate stages of endothelial cell transformation in Kaposi sarcoma. PLoS Pathog *5*, e1000389.

O'Hara, A.J., Vahrson, W., and Dittmer, D.P. (2008). Gene alteration and precursor and mature microRNA transcription changes contribute to the miRNA signature of primary effusion lymphoma. Blood *111*, 2347-2353.

Ohlsson, R., Bartkuhn, M., and Renkawitz, R. (2010a). CTCF shapes chromatin by multiple mechanisms: the impact of 20 years of CTCF research on understanding the workings of chromatin. Chromosoma *119*, 351-360.

Ohlsson, R., Lobanenkov, V., and Klenova, E. (2010b). Does CTCF mediate between nuclear organization and gene expression? Bioessays *32*, 37-50.

Ohsaki, E., and Ueda, K. (2012). Kaposi's Sarcoma-Associated Herpesvirus Genome Replication, Partitioning, and Maintenance in Latency. Front Microbiol *3*, 7.

Olave, I., Reinberg, D., and Vales, L.D. (1998). The mammalian transcriptional repressor RBP (CBF1) targets TFIID and TFIIA to prevent activated transcription. Genes Dev *12*, 1621-1637.

Ong, C.T., Cheng, H.T., Chang, L.W., Ohtsuka, T., Kageyama, R., Stormo, G.D., and Kopan, R. (2006). Target selectivity of vertebrate notch proteins. Collaboration between discrete domains and CSL-binding site architecture determines activation probability. J Biol Chem *281*, 5106-5119.

Ong, K.M., Blackford, J.A., Jr., Kagan, B.L., Simons, S.S., Jr., and Chow, C.C. (2010). A theoretical framework for gene induction and experimental comparisons. Proc Natl Acad Sci U S A *107*, 7107-7112.

Osborne, J., Moore, P.S., and Chang, Y. (1999). KSHV-encoded viral IL-6 activates multiple human IL-6 signaling pathways. Hum Immunol *60*, 921-927.

Ottinger, M., Christalla, T., Nathan, K., Brinkmann, M.M., Viejo-Borbolla, A., and Schulz, T.F. (2006). Kaposi's sarcoma-associated herpesvirus LANA-1 interacts with the short variant of BRD4 and releases cells from a BRD4- and BRD2/RING3-induced G1 cell cycle arrest. J Virol *80*, 10772-10786.

Paden, C.R., Forrest, J.C., Moorman, N.J., and Speck, S.H. (2010). Murine gammaherpesvirus 68 LANA is essential for virus reactivation from splenocytes but not long-term carriage of viral genome. J Virol *84*, 7214-7224.

Palmeri, D., Carroll, K.D., Gonzalez-Lopez, O., and Lukac, D.M. (2011). Kaposi's sarcoma-associated herpesvirus Rta tetramers make high-affinity interactions with repetitive DNA elements in the Mta promoter to stimulate DNA binding of RBP-Jk/CSL. J Virol *85*, 11901-11915.

Palmeri, D., Spadavecchia, S., Carroll, K.D., and Lukac, D.M. (2007). Promoter- and cell-specific transcriptional transactivation by the Kaposi's sarcoma-associated herpesvirus ORF57/Mta protein. J Virol *81*, 13299-13314.

Pantry, S.N., and Medveczky, P.G. (2009). Epigenetic regulation of Kaposi's sarcoma-associated herpesvirus replication. Semin Cancer Biol *19*, 153-157.

Parelho, V., Hadjur, S., Spivakov, M., Leleu, M., Sauer, S., Gregson, H.C., Jarmuz, A., Canzonetta, C., Webster, Z., Nesterova, T., *et al.* (2008). Cohesins functionally associate with CTCF on mammalian chromosome arms. Cell *132*, 422-433.

Parkin, D.M. (2006). The global health burden of infection-associated cancers in the year 2002. Int J Cancer *118*, 3030-3044.

Parravicini, C., Chandran, B., Corbellino, M., Berti, E., Paulli, M., Moore, P.S., and Chang, Y. (2000). Differential viral protein expression in Kaposi's sarcoma-associated herpesvirus-infected diseases: Kaposi's sarcoma, primary effusion lymphoma, and multicentric Castleman's disease. Am J Pathol *156*, 743-749.

Parravicini, C., Corbellino, M., Paulli, M., Magrini, U., Lazzarino, M., Moore, P.S., and Chang, Y. (1997). Expression of a virus-derived cytokine, KSHV vIL-6, in HIV-seronegative Castleman's disease. Am J Pathol *151*, 1517-1522.

Pauk, J., Huang, M.L., Brodie, S.J., Wald, A., Koelle, D.M., Schacker, T., Celum, C., Selke, S., and Corey, L. (2000). Mucosal shedding of human herpesvirus 8 in men. N Engl J Med *343*, 1369-1377.

Paulose-Murphy, M., Ha, N.K., Xiang, C., Chen, Y., Gillim, L., Yarchoan, R., Meltzer, P., Bittner, M., Trent, J., and Zeichner, S. (2001). Transcription program of human herpesvirus 8 (kaposi's sarcoma-associated herpesvirus). J Virol *75*, 4843-4853.

Pearce, M., Matsumura, S., and Wilson, A.C. (2005). Transcripts encoding K12, v-FLIP, v-cyclin, and the microRNA cluster of Kaposi's sarcoma-associated herpesvirus originate from a common promoter. J Virol *79*, 14457-14464.

Peralta-Yahya, P.P., and Keasling, J.D. (2010). Advanced biofuel production in microbes. Biotechnol J *5*, 147-162.

Persson, L.M., and Wilson, A.C. (2010). Wide-scale use of Notch signaling factor CSL/RBP-Jkappa in RTA-mediated activation of Kaposi's sarcoma-associated herpesvirus lytic genes. J Virol *84*, 1334-1347.

Pfeffer, S., Sewer, A., Lagos-Quintana, M., Sheridan, R., Sander, C., Grasser, F.A., van Dyk, L.F., Ho, C.K., Shuman, S., Chien, M., *et al.* (2005). Identification of microRNAs of the herpesvirus family. Nat Methods *2*, 269-276.

Phillips, J.E., and Corces, V.G. (2009). CTCF: master weaver of the genome. Cell *137*, 1194-1211.

Pietrek, M., Brinkmann, M.M., Glowacka, I., Enlund, A., Havemeier, A., Dittrich-Breiholz, O., Kracht, M., Lewitzky, M., Saksela, K., Feller, S.M., *et al.* (2010). Role of the Kaposi's sarcoma-associated herpesvirus K15 SH3 binding site in inflammatory signaling and B-cell activation. J Virol *84*, 8231-8240.

Platt, G.M., Simpson, G.R., Mittnacht, S., and Schulz, T.F. (1999). Latent nuclear antigen of Kaposi's sarcoma-associated herpesvirus interacts with RING3, a homolog of the Drosophila female sterile homeotic (fsh) gene. J Virol *73*, 9789-9795.

Ponts, N., Harris, E.Y., Prudhomme, J., Wick, I., Eckhardt-Ludka, C., Hicks, G.R., Hardiman, G., Lonardi, S., and Le Roch, K.G. (2010). Nucleosome landscape and control of transcription in the human malaria parasite. Genome Res *20*, 228-238.

Poole, L.J., Zong, J.C., Ciufo, D.M., Alcendor, D.J., Cannon, J.S., Ambinder, R., Orenstein, J.M., Reitz, M.S., and Hayward, G.S. (1999). Comparison of genetic variability at multiple loci across the genomes of the major subtypes of Kaposi's sarcoma-associated herpesvirus reveals evidence for recombination and for two distinct types of open reading frame K15 alleles at the right-hand end. J Virol *73*, 6646-6660.

Prakash, O., Tang, Z.Y., Peng, X., Coleman, R., Gill, J., Farr, G., and Samaniego, F. (2002). Tumorigenesis and aberrant signaling in transgenic mice expressing the human herpesvirus-8 K1 gene. J Natl Cancer Inst *94*, 926-935.

Purushothaman, P., McDowell, M.E., McGuinness, J., Salas, R., Rumjahn, S.M., and Verma, S.C. (2012). Kaposi's sarcoma-associated herpesvirus-encoded LANA recruits topoisomerase IIbeta for latent DNA replication of the terminal repeats. J Virol *86*, 9983-9994.

Radkov, S.A., Kellam, P., and Boshoff, C. (2000). The latent nuclear antigen of Kaposi sarcoma-associated herpesvirus targets the retinoblastoma-E2F pathway and with the oncogene Hras transforms primary rat cells. Nat Med *6*, 1121-1127.

Rainbow, L., Platt, G.M., Simpson, G.R., Sarid, R., Gao, S.J., Stoiber, H., Herrington, C.S., Moore, P.S., and Schulz, T.F. (1997). The 222- to 234-kilodalton latent nuclear protein (LNA) of Kaposi's sarcoma-associated herpesvirus (human herpesvirus 8) is encoded by orf73 and is a component of the latency-associated nuclear antigen. J Virol *71*, 5915-5921.

Ramalingam, D., Kieffer-Kwon, P., and Ziegelbauer, J.M. (2012). Emerging Themes from EBV and KSHV microRNA Targets. Viruses *4*, 1687-1710.

Renne, R., Barry, C., Dittmer, D., Compitello, N., Brown, P.O., and Ganem, D. (2001). Modulation of cellular and viral gene expression by the latency-associated nuclear antigen of Kaposi's sarcoma-associated herpesvirus. J Virol *75*, 458-468.

Renne, R., Lagunoff, M., Zhong, W., and Ganem, D. (1996a). The size and conformation of Kaposi's sarcoma-associated herpesvirus (human herpesvirus 8) DNA in infected cells and virions. J Virol *70*, 8151-8154.

Renne, R., Zhong, W., Herndier, B., McGrath, M., Abbey, N., Kedes, D., and Ganem, D. (1996b). Lytic growth of Kaposi's sarcoma-associated herpesvirus (human herpesvirus 8) in culture. Nat Med *2*, 342-346.

Rivas, C., Thlick, A.E., Parravicini, C., Moore, P.S., and Chang, Y. (2001). Kaposi's sarcoma-associated herpesvirus LANA2 is a B-cell-specific latent viral protein that inhibits p53. J Virol *75*, 429-438.

Ro, D.K., Paradise, E.M., Ouellet, M., Fisher, K.J., Newman, K.L., Ndungu, J.M., Ho, K.A., Eachus, R.A., Ham, T.S., Kirby, J., *et al.* (2006). Production of the antimalarial drug precursor artemisinic acid in engineered yeast. Nature *440*, 940-943.

Rosenfeld, N., Young, J.W., Alon, U., Swain, P.S., and Elowitz, M.B. (2005). Gene regulation at the single-cell level. Science *307*, 1962-1965.

Rosenkilde, M.M., Kledal, T.N., Brauner-Osborne, H., and Schwartz, T.W. (1999). Agonists and inverse agonists for the herpesvirus 8-encoded constitutively active seven-transmembrane oncogene product, ORF-74. J Biol Chem *274*, 956-961.

Rossetto, C.C., and Pari, G. (2012). KSHV PAN RNA associates with demethylases UTX and JMJD3 to activate lytic replication through a physical interaction with the virus genome. PLoS Pathog *8*, e1002680.

Roupelieva, M., Griffiths, S.J., Kremmer, E., Meisterernst, M., Viejo-Borbolla, A., Schulz, T., and Haas, J. (2010). Kaposi's sarcoma-associated herpesvirus Lana-1 is a major activator of the serum response element and mitogen-activated protein kinase pathways via interactions with the Mediator complex. J Gen Virol *91*, 1138-1149.

Roy, D., Sin, S.H., Damania, B., and Dittmer, D.P. (2011). Tumor suppressor genes FHIT and WWOX are deleted in primary effusion lymphoma (PEL) cell lines. Blood *118*, e32-39.

Rubio, E.D., Reiss, D.J., Welcsh, P.L., Disteche, C.M., Filippova, G.N., Baliga, N.S., Aebersold, R., Ranish, J.A., and Krumm, A. (2008). CTCF physically links cohesin to chromatin. Proc Natl Acad Sci U S A *105*, 8309-8314.

Ruder, W.C., Lu, T., and Collins, J.J. (2011). Synthetic biology moving into the clinic. Science *333*, 1248-1252.

Russo, J.J., Bohenzky, R.A., Chien, M.C., Chen, J., Yan, M., Maddalena, D., Parry, J.P., Peruzzi, D., Edelman, I.S., Chang, Y., *et al.* (1996). Nucleotide sequence of the Kaposi sarcoma-associated herpesvirus (HHV8). Proc Natl Acad Sci U S A *93*, 14862-14867.

Ryan, R.F., Schultz, D.C., Ayyanathan, K., Singh, P.B., Friedman, J.R., Fredericks, W.J., and Rauscher, F.J., 3rd (1999). KAP-1 corepressor protein interacts and colocalizes with heterochromatic and euchromatic HP1 proteins: a potential role for Kruppel-associated box-zinc finger proteins in heterochromatin-mediated gene silencing. Mol Cell Biol *19*, 4366-4378.

Sadler, R., Wu, L., Forghani, B., Renne, R., Zhong, W., Herndier, B., and Ganem, D. (1999). A complex translational program generates multiple novel proteins from the latently expressed kaposin (K12) locus of Kaposi's sarcoma-associated herpesvirus. J Virol *73*, 5722-5730.

Safai, B. (1984). Kaposi's sarcoma: a review of the classical and epidemic forms. Ann N Y Acad Sci *437*, 373-382.

Sakakibara, S., and Tosato, G. (2011). Viral interleukin-6: role in Kaposi's sarcoma-associated herpesvirus: associated malignancies. J Interferon Cytokine Res *31*, 791-801.

Sakakibara, S., Ueda, K., Chen, J., Okuno, T., and Yamanishi, K. (2001). Octamer-binding sequence is a key element for the autoregulation of Kaposi's sarcoma-associated herpesvirus ORF50/Lyta gene expression. J Virol *75*, 6894-6900.

Sakakibara, S., Ueda, K., Nishimura, K., Do, E., Ohsaki, E., Okuno, T., and Yamanishi, K. (2004). Accumulation of heterochromatin components on the terminal repeat sequence of Kaposi's sarcoma-associated herpesvirus mediated by the latency-associated nuclear antigen. J Virol *78*, 7299-7310.

Salata, C., Curtarello, M., Calistri, A., Sartori, E., Sette, P., de Bernard, M., Parolin, C., and Palu, G. (2009). vOX2 glycoprotein of human herpesvirus 8 modulates human primary macrophages activity. J Cell Physiol *219*, 698-706.

Samols, M.A., Hu, J., Skalsky, R.L., and Renne, R. (2005). Cloning and identification of a microRNA cluster within the latency-associated region of Kaposi's sarcoma-associated herpesvirus. J Virol *79*, 9301-9305.

Samols, M.A., Skalsky, R.L., Maldonado, A.M., Riva, A., Lopez, M.C., Baker, H.V., and Renne, R. (2007). Identification of cellular genes targeted by KSHV-encoded microRNAs. PLoS Pathog *3*, e65.

Sarid, R., Flore, O., Bohenzky, R.A., Chang, Y., and Moore, P.S. (1998). Transcription mapping of the Kaposi's sarcoma-associated herpesvirus (human herpesvirus 8) genome in a body cavity-based lymphoma cell line (BC-1). J Virol *72*, 1005-1012.

Sarid, R., Wiezorek, J.S., Moore, P.S., and Chang, Y. (1999). Characterization and cell cycle regulation of the major Kaposi's sarcoma-associated herpesvirus (human herpesvirus 8) latent genes and their promoter. J Virol *73*, 1438-1446.

Schmidt, D., Schwalie, P.C., Ross-Innes, C.S., Hurtado, A., Brown, G.D., Carroll, J.S., Flicek, P., and Odom, D.T. (2010). A CTCF-independent role for cohesin in tissue-specific transcription. Genome Res *20*, 578-588.

Schultz, D.C., Ayyanathan, K., Negorev, D., Maul, G.G., and Rauscher, F.J., 3rd (2002). SETDB1: a novel KAP-1-associated histone H3, lysine 9-specific methyltransferase that contributes to HP1-mediated silencing of euchromatic genes by KRAB zinc-finger proteins. Genes Dev *16*, 919-932.

Schwam, D.R., Luciano, R.L., Mahajan, S.S., Wong, L., and Wilson, A.C. (2000). Carboxy terminus of human herpesvirus 8 latency-associated nuclear antigen mediates dimerization, transcriptional repression, and targeting to nuclear bodies. J Virol *74*, 8532-8540.

Seo, T., Park, J., Lee, D., Hwang, S.G., and Choe, J. (2001). Viral interferon regulatory factor 1 of Kaposi's sarcoma-associated herpesvirus binds to p53 and represses p53-dependent transcription and apoptosis. J Virol *75*, 6193-6198.

Seo, T., Park, J., Lim, C., and Choe, J. (2004). Inhibition of nuclear factor kappaB activity by viral interferon regulatory factor 3 of Kaposi's sarcoma-associated herpesvirus. Oncogene *23*, 6146-6155.

Shamay, M., Krithivas, A., Zhang, J., and Hayward, S.D. (2006). Recruitment of the de novo DNA methyltransferase Dnmt3a by Kaposi's sarcoma-associated herpesvirus LANA. Proc Natl Acad Sci U S A *103*, 14554-14559.

Sharp, T.V., Wang, H.W., Koumi, A., Hollyman, D., Endo, Y., Ye, H., Du, M.Q., and Boshoff, C. (2002). K15 protein of Kaposi's sarcoma-associated herpesvirus is latently expressed and binds to HAX-1, a protein with antiapoptotic function. J Virol *76*, 802-816.

Shepard, L.W., Yang, M., Xie, P., Browning, D.D., Voyno-Yasenetskaya, T., Kozasa, T., and Ye, R.D. (2001). Constitutive activation of NF-kappa B and secretion of interleukin-8 induced by the G protein-coupled receptor of Kaposi's sarcoma-associated herpesvirus involve G alpha(13) and RhoA. J Biol Chem *276*, 45979-45987.

Shilatifard, A. (2012). The COMPASS family of histone H3K4 methylases: mechanisms of regulation in development and disease pathogenesis. Annu Rev Biochem *81*, 65-95.

Shin, S., and Janknecht, R. (2007). Activation of androgen receptor by histone demethylases JMJD2A and JMJD2D. Biochem Biophys Res Commun *359*, 742-746.

Shin, Y.C., Joo, C.H., Gack, M.U., Lee, H.R., and Jung, J.U. (2008). Kaposi's sarcoma-associated herpesvirus viral IFN regulatory factor 3 stabilizes hypoxia-inducible factor-1 alpha to induce vascular endothelial growth factor expression. Cancer Res *68*, 1751-1759.

Simon, J.A., and Kingston, R.E. (2009). Mechanisms of polycomb gene silencing: knowns and unknowns. Nat Rev Mol Cell Biol *10*, 697-708.

Simon, J.M., Giresi, P.G., Davis, I.J., and Lieb, J.D. (2012). Using formaldehyde-assisted isolation of regulatory elements (FAIRE) to isolate active regulatory DNA. Nat Protoc *7*, 256-267.

Sin, S.H., Fakhari, F.D., and Dittmer, D.P. (2010). The viral latency-associated nuclear antigen augments the B-cell response to antigen in vivo. J Virol *84*, 10653-10660.

Skalsky, R.L., Hu, J., and Renne, R. (2007a). Analysis of viral cis elements conferring Kaposi's sarcoma-associated herpesvirus episome partitioning and maintenance. J Virol *81*, 9825-9837.

Skalsky, R.L., Samols, M.A., Plaisance, K.B., Boss, I.W., Riva, A., Lopez, M.C., Baker, H.V., and Renne, R. (2007b). Kaposi's sarcoma-associated herpesvirus encodes an ortholog of miR-155. J Virol *81*, 12836-12845.

Slavin, G., Cameron, H.M., Forbes, C., and Mitchell, R.M. (1970). Kaposi's sarcoma in East African children: a report of 51 cases. J Pathol *100*, 187-199.

Slusarczyk, A.L., Lin, A., and Weiss, R. (2012). Foundations for the design and implementation of synthetic genetic circuits. Nat Rev Genet *13*, 406-420.

Sodhi, A., Montaner, S., Patel, V., Zohar, M., Bais, C., Mesri, E.A., and Gutkind, J.S. (2000). The Kaposi's sarcoma-associated herpes virus G protein-coupled receptor up-regulates vascular endothelial growth factor expression and secretion through mitogen-activated protein kinase and p38 pathways acting on hypoxia-inducible factor 1alpha. Cancer Res *60*, 4873-4880.

Song, L., and Crawford, G.E. (2010). DNase-seq: a high-resolution technique for mapping active gene regulatory elements across the genome from mammalian cells. Cold Spring Harb Protoc *2010*, pdb prot5384.

Song, L., Zhang, Z., Grasfeder, L.L., Boyle, A.P., Giresi, P.G., Lee, B.K., Sheffield, N.C., Graf, S., Huss, M., Keefe, D., *et al.* (2011). Open chromatin defined by DNaseI and FAIRE identifies regulatory elements that shape cell-type identity. Genome Res *21*, 1757-1767.

Song, M.J., Brown, H.J., Wu, T.T., and Sun, R. (2001). Transcription activation of polyadenylated nuclear rna by rta in human herpesvirus 8/Kaposi's sarcoma-associated herpesvirus. J Virol *75*, 3129-3140.

Song, M.J., Deng, H., and Sun, R. (2003). Comparative study of regulation of RTA-responsive genes in Kaposi's sarcoma-associated herpesvirus/human herpesvirus 8. J Virol *77*, 9451-9462.

Song, M.J., Li, X., Brown, H.J., and Sun, R. (2002). Characterization of interactions between RTA and the promoter of polyadenylated nuclear RNA in Kaposi's sarcoma-associated herpesvirus/human herpesvirus 8. J Virol *76*, 5000-5013.

Soulier, J., Grollet, L., Oksenhendler, E., Cacoub, P., Cazals-Hatem, D., Babinet, P., d'Agay, M.F., Clauvel, J.P., Raphael, M., Degos, L., *et al.* (1995). Kaposi's sarcoma-associated herpesvirus-like DNA sequences in multicentric Castleman's disease. Blood *86*, 1276-1280.

Speck, S.H., and Ganem, D. (2010). Viral latency and its regulation: lessons from the gamma-herpesviruses. Cell Host Microbe *8*, 100-115.

Srinivasan, V., Komatsu, T., Ballestas, M.E., and Kaye, K.M. (2004). Definition of sequence requirements for latency-associated nuclear antigen 1 binding to Kaposi's sarcoma-associated herpesvirus DNA. J Virol *78*, 14033-14038.

Staskus, K.A., Sun, R., Miller, G., Racz, P., Jaslowski, A., Metroka, C., Brett-Smith, H., and Haase, A.T. (1999). Cellular tropism and viral interleukin-6 expression distinguish human herpesvirus 8 involvement in Kaposi's sarcoma, primary effusion lymphoma, and multicentric Castleman's disease. J Virol *73*, 4181-4187.

Staskus, K.A., Zhong, W., Gebhard, K., Herndier, B., Wang, H., Renne, R., Beneke, J., Pudney, J., Anderson, D.J., Ganem, D., *et al.* (1997). Kaposi's sarcoma-associated herpesvirus gene expression in endothelial (spindle) tumor cells. J Virol *71*, 715-719.

Staudt, M.R., and Dittmer, D.P. (2006). Promoter switching allows simultaneous transcription of LANA and K14/vGPCR of Kaposi's sarcoma-associated herpesvirus. Virology *350*, 192-205.

Stedman, W., Deng, Z., Lu, F., and Lieberman, P.M. (2004). ORC, MCM, and histone hyperacetylation at the Kaposi's sarcoma-associated herpesvirus latent replication origin. J Virol *78*, 12566-12575.

Stedman, W., Kang, H., Lin, S., Kissil, J.L., Bartolomei, M.S., and Lieberman, P.M. (2008). Cohesins localize with CTCF at the KSHV latency control region and at cellular c-myc and H19/Igf2 insulators. EMBO J *27*, 654-666.

Stuber, G., Mattsson, K., Flaberg, E., Kati, E., Markasz, L., Sheldon, J.A., Klein, G., Schulz, T.F., and Szekely, L. (2007). HHV-8 encoded LANA-1 alters the higher organization of the cell nucleus. Mol Cancer *6*, 28.

Suffert, G., Malterer, G., Hausser, J., Viiliainen, J., Fender, A., Contrant, M., Ivacevic, T., Benes, V., Gros, F., Voinnet, O., *et al.* (2011). Kaposi's sarcoma herpesvirus microRNAs target caspase 3 and regulate apoptosis. PLoS Pathog *7*, e1002405.

Sun, R., Lin, S.F., Gradoville, L., and Miller, G. (1996). Polyadenylylated nuclear RNA encoded by Kaposi sarcoma-associated herpesvirus. Proceedings of the National Academy of Sciences of the United States of America *93*, 11883-11888.

Sun, R., Lin, S.F., Gradoville, L., Yuan, Y., Zhu, F., and Miller, G. (1998). A viral gene that activates lytic cycle expression of Kaposi's sarcoma-associated herpesvirus. Proc Natl Acad Sci U S A *95*, 10866-10871.

Sun, R., Lin, S.F., Staskus, K., Gradoville, L., Grogan, E., Haase, A., and Miller, G. (1999). Kinetics of Kaposi's sarcoma-associated herpesvirus gene expression. J Virol *73*, 2232-2242.

Taft, R.J., Hawkins, P.G., Mattick, J.S., and Morris, K.V. (2011). The relationship between transcription initiation RNAs and CCCTC-binding factor (CTCF) localization. Epigenetics Chromatin *4*, 13.

Talbot, S.J., Weiss, R.A., Kellam, P., and Boshoff, C. (1999). Transcriptional analysis of human herpesvirus-8 open reading frames 71, 72, 73, K14, and 74 in a primary effusion lymphoma cell line. Virology *257*, 84-94.

Tamburro, K.M., Yang, D., Poisson, J., Fedoriw, Y., Roy, D., Lucas, A., Sin, S.H., Malouf, N., Moylan, V., Damania, B., *et al.* (2012). Vironome of Kaposi sarcoma associated herpesvirus-inflammatory cytokine syndrome in an AIDS patient reveals co-infection of human herpesvirus 8 and human herpesvirus 6A. Virology *433*, 220-225.

Tang, J., Gordon, G.M., Muller, M.G., Dahiya, M., and Foreman, K.E. (2003). Kaposi's sarcoma-associated herpesvirus latency-associated nuclear antigen induces expression of the helix-loop-helix protein Id-1 in human endothelial cells. J Virol *77*, 5975-5984.

Tempera, I., Klichinsky, M., and Lieberman, P.M. (2011). EBV latency types adopt alternative chromatin conformations. PLoS Pathog *7*, e1002180.

Tempera, I., and Lieberman, P.M. (2010). Chromatin organization of gammaherpesvirus latent genomes. Biochim Biophys Acta *1799*, 236-245.

Tempera, I., Wiedmer, A., Dheekollu, J., and Lieberman, P.M. (2010). CTCF prevents the epigenetic drift of EBV latency promoter Qp. PLoS Pathog *6*, e1001048.

Thome, M., Schneider, P., Hofmann, K., Fickenscher, H., Meinl, E., Neipel, F., Mattmann, C., Burns, K., Bodmer, J.L., Schroter, M., *et al.* (1997). Viral FLICE-inhibitory proteins (FLIPs) prevent apoptosis induced by death receptors. Nature *386*, 517-521.

Tomlinson, C.C., and Damania, B. (2004). The K1 protein of Kaposi's sarcoma-associated herpesvirus activates the Akt signaling pathway. J Virol *78*, 1918-1927.

Toth, Z., Brulois, K.F., Wong, L.Y., Lee, H.R., Chung, B., and Jung, J.U. (2012). Negative elongation factor-mediated suppression of RNA polymerase II elongation of Kaposi's sarcoma-associated herpesvirus lytic gene expression. J Virol *86*, 9696-9707.

Toth, Z., Maglinte, D.T., Lee, S.H., Lee, H.R., Wong, L.Y., Brulois, K.F., Lee, S., Buckley, J.D., Laird, P.W., Marquez, V.E., *et al.* (2010). Epigenetic analysis of KSHV latent and lytic genomes. PLoS Pathog *6*, e1001013.

Trinklein, N.D., Aldred, S.F., Hartman, S.J., Schroeder, D.I., Otillar, R.P., and Myers, R.M. (2004). An abundance of bidirectional promoters in the human genome. Genome Res *14*, 62-66.

Trus, B.L., Heymann, J.B., Nealon, K., Cheng, N., Newcomb, W.W., Brown, J.C., Kedes, D.H., and Steven, A.C. (2001). Capsid structure of Kaposi's sarcoma-associated herpesvirus, a gammaherpesvirus, compared to those of an alphaherpesvirus, herpes simplex virus type 1, and a betaherpesvirus, cytomegalovirus. J Virol *75*, 2879-2890.

Tun, T., Hamaguchi, Y., Matsunami, N., Furukawa, T., Honjo, T., and Kawaichi, M. (1994). Recognition sequence of a highly conserved DNA binding protein RBP-J kappa. Nucleic Acids Res *22*, 965-971.

Uldrick, T.S., Polizzotto, M.N., and Yarchoan, R. (2012). Recent advances in Kaposi sarcoma herpesvirus-associated multicentric Castleman disease. Curr Opin Oncol *24*, 495-505.

Verma, S.C., Borah, S., and Robertson, E.S. (2004). Latency-associated nuclear antigen of Kaposi's sarcoma-associated herpesvirus up-regulates transcription of human telomerase reverse transcriptase promoter through interaction with transcription factor Sp1. J Virol *78*, 10348-10359.

Verma, S.C., Choudhuri, T., Kaul, R., and Robertson, E.S. (2006). Latency-associated nuclear antigen (LANA) of Kaposi's sarcoma-associated herpesvirus interacts with origin recognition complexes at the LANA binding sequence within the terminal repeats. J Virol *80*, 2243-2256.

Verma, S.C., Choudhuri, T., and Robertson, E.S. (2007a). The minimal replicator element of the Kaposi's sarcoma-associated herpesvirus terminal repeat supports replication in a semiconservative and cell-cycle-dependent manner. J Virol *81*, 3402-3413.

Verma, S.C., Lan, K., Choudhuri, T., Cotter, M.A., and Robertson, E.S. (2007b). An autonomous replicating element within the KSHV genome. Cell Host Microbe *2*, 106-118.

Verma, S.C., Lu, J., Cai, Q., Kosiyatrakul, S., McDowell, M.E., Schildkraut, C.L., and Robertson, E.S. (2011). Single molecule analysis of replicated DNA reveals the usage of multiple KSHV genome regions for latent replication. PLoS Pathog *7*, e1002365.

Verschuren, E.W., Klefstrom, J., Evan, G.I., and Jones, N. (2002). The oncogenic potential of Kaposi's sarcoma-associated herpesvirus cyclin is exposed by p53 loss in vitro and in vivo. Cancer Cell *2*, 229-241.

Vieira, J., Huang, M.L., Koelle, D.M., and Corey, L. (1997). Transmissible Kaposi's sarcoma-associated herpesvirus (human herpesvirus 8) in saliva of men with a history of Kaposi's sarcoma. J Virol *71*, 7083-7087.

Vieira, J., and O'Hearn, P.M. (2004). Use of the red fluorescent protein as a marker of Kaposi's sarcoma-associated herpesvirus lytic gene expression. Virology *325*, 225-240.

Wang, H.H., Isaacs, F.J., Carr, P.A., Sun, Z.Z., Xu, G., Forest, C.R., and Church, G.M. (2009). Programming cells by multiplex genome engineering and accelerated evolution. Nature *460*, 894-898.

Wang, H.W., Sharp, T.V., Koumi, A., Koentges, G., and Boshoff, C. (2002). Characterization of an anti-apoptotic glycoprotein encoded by Kaposi's sarcoma-associated herpesvirus which resembles a spliced variant of human survivin. EMBO J *21*, 2602-2615.

Wang, L., and Damania, B. (2008). Kaposi's sarcoma-associated herpesvirus confers a survival advantage to endothelial cells. Cancer Res *68*, 4640-4648.

Wang, L., Dittmer, D.P., Tomlinson, C.C., Fakhari, F.D., and Damania, B. (2006a). Immortalization of primary endothelial cells by the K1 protein of Kaposi's sarcoma-associated herpesvirus. Cancer Res *66*, 3658-3666.

Wang, L., Wakisaka, N., Tomlinson, C.C., DeWire, S.M., Krall, S., Pagano, J.S., and Damania, B. (2004a). The Kaposi's sarcoma-associated herpesvirus (KSHV/HHV-8) K1 protein induces expression of angiogenic and invasion factors. Cancer Res *64*, 2774-2781.

Wang, S.E., Wu, F.Y., Chen, H., Shamay, M., Zheng, Q., and Hayward, G.S. (2004b). Early activation of the Kaposi's sarcoma-associated herpesvirus RTA, RAP, and MTA promoters by the tetradecanoyl phorbol acetate-induced AP1 pathway. J Virol *78*, 4248-4267.

Wang, S.E., Wu, F.Y., Fujimuro, M., Zong, J., Hayward, S.D., and Hayward, G.S. (2003). Role of CCAAT/enhancer-binding protein alpha (C/EBPalpha) in activation of the Kaposi's sarcoma-associated herpesvirus (KSHV) lytic-cycle replication-associated protein (RAP) promoter in cooperation with the KSHV replication and transcription activator (RTA) and RAP. J Virol *77*, 600-623.

Wang, Y., Chong, O.T., and Yuan, Y. (2004c). Differential regulation of K8 gene expression in immediate-early and delayed-early stages of Kaposi's sarcoma-associated herpesvirus. Virology *325*, 149-163.

Wang, Y., Li, H., Chan, M.Y., Zhu, F.X., Lukac, D.M., and Yuan, Y. (2004d). Kaposi's sarcoma-associated herpesvirus ori-Lyt-dependent DNA replication: cis-acting requirements for replication and ori-Lyt-associated RNA transcription. J Virol *78*, 8615-8629.

Wang, Y., Tang, Q., Maul, G.G., and Yuan, Y. (2006b). Kaposi's sarcoma-associated herpesvirus ori-Lyt-dependent DNA replication: dual role of replication and transcription activator. J Virol *80*, 12171-12186.

Wang, Y., and Yuan, Y. (2007). Essential role of RBP-Jkappa in activation of the K8 delayed-early promoter of Kaposi's sarcoma-associated herpesvirus by ORF50/RTA. Virology *359*, 19-27.

Warden, C., Tang, Q., and Zhu, H. (2011). Herpesvirus BACs: past, present, and future. J Biomed Biotechnol *2011*, 124595.

Weber, W., Schoenmakers, R., Keller, B., Gitzinger, M., Grau, T., Daoud-El Baba, M., Sander, P., and Fussenegger, M. (2008). A synthetic mammalian gene circuit reveals antituberculosis compounds. Proc Natl Acad Sci U S A *105*, 9994-9998.

Wei, W., Pelechano, V., Jarvelin, A.I., and Steinmetz, L.M. (2011). Functional consequences of bidirectional promoters. Trends Genet *27*, 267-276.

Wen, K.W., and Damania, B. (2010). Kaposi sarcoma-associated herpesvirus (KSHV): molecular biology and oncogenesis. Cancer Lett *289*, 140-150.

Wen, K.W., Dittmer, D.P., and Damania, B. (2009). Disruption of LANA in rhesus rhadinovirus generates a highly lytic recombinant virus. J Virol *83*, 9786-9802.

Wendt, K.S., Yoshida, K., Itoh, T., Bando, M., Koch, B., Schirghuber, E., Tsutsumi, S., Nagae, G., Ishihara, K., Mishiro, T., *et al.* (2008). Cohesin mediates transcriptional insulation by CCCTC-binding factor. Nature *451*, 796-801.

Whetstine, J.R., Nottke, A., Lan, F., Huarte, M., Smolikov, S., Chen, Z., Spooner, E., Li, E., Zhang, G., Colaiacovo, M., *et al.* (2006). Reversal of histone lysine trimethylation by the JMJD2 family of histone demethylases. Cell *125*, 467-481.

Wies, E., Mori, Y., Hahn, A., Kremmer, E., Sturzl, M., Fleckenstein, B., and Neipel, F. (2008). The viral interferon-regulatory factor-3 is required for the survival of KSHV-infected primary effusion lymphoma cells. Blood *111*, 320-327.

Wong, E.L., and Damania, B. (2006). Transcriptional regulation of the Kaposi's sarcoma-associated herpesvirus K15 gene. J Virol *80*, 1385-1392.

Wu, F.Y., Tang, Q.Q., Chen, H., ApRhys, C., Farrell, C., Chen, J., Fujimuro, M., Lane, M.D., and Hayward, G.S. (2002). Lytic replication-associated protein (RAP) encoded by Kaposi sarcoma-associated herpesvirus causes p21CIP-1-mediated G1 cell cycle arrest through CCAAT/enhancer-binding protein-alpha. Proc Natl Acad Sci U S A *99*, 10683-10688.

Xiao, T., Wallace, J., and Felsenfeld, G. (2011). Specific sites in the C terminus of CTCF interact with the SA2 subunit of the cohesin complex and are required for cohesin-dependent insulation activity. Mol Cell Biol *31*, 2174-2183.

Xu, Y., AuCoin, D.P., Huete, A.R., Cei, S.A., Hanson, L.J., and Pari, G.S. (2005). A Kaposi's sarcoma-associated herpesvirus/human herpesvirus 8 ORF50 deletion mutant is defective for reactivation of latent virus and DNA replication. J Virol *79*, 3479-3487.

Xu, Y., and Ganem, D. (2010). Making sense of antisense: seemingly noncoding RNAs antisense to the master regulator of Kaposi's sarcoma-associated herpesvirus lytic replication do not regulate that transcript but serve as mRNAs encoding small peptides. J Virol *84*, 5465-5475.

Yada, K., Do, E., Sakakibara, S., Ohsaki, E., Ito, E., Watanabe, S., and Ueda, K. (2006). KSHV RTA induces a transcriptional repressor, HEY1 that represses rta promoter. Biochem Biophys Res Commun *345*, 410-418.

Yang, T.Y., Chen, S.C., Leach, M.W., Manfra, D., Homey, B., Wiekowski, M., Sullivan, L., Jenh, C.H., Narula, S.K., Chensue, S.W., *et al.* (2000). Transgenic expression of the chemokine receptor encoded by human herpesvirus 8 induces an angioproliferative disease resembling Kaposi's sarcoma. J Exp Med *191*, 445-454.

Yang, Y., Quitschke, W.W., Vostrov, A.A., and Brewer, G.J. (1999). CTCF is essential for up-regulating expression from the amyloid precursor protein promoter during differentiation of primary hippocampal neurons. J Neurochem *73*, 2286-2298.

Yang, Z., Yan, Z., and Wood, C. (2008). Kaposi's sarcoma-associated herpesvirus transactivator RTA promotes degradation of the repressors to regulate viral lytic replication. J Virol *82*, 3590-3603.

Yao, H., Brick, K., Evrard, Y., Xiao, T., Camerini-Otero, R.D., and Felsenfeld, G. (2010). Mediation of CTCF transcriptional insulation by DEAD-box RNA-binding protein p68 and steroid receptor RNA activator SRA. Genes Dev *24*, 2543-2555.

Yu, F., Feng, J., Harada, J.N., Chanda, S.K., Kenney, S.C., and Sun, R. (2007). B cell terminal differentiation factor XBP-1 induces reactivation of Kaposi's sarcoma-associated herpesvirus. FEBS Lett *581*, 3485-3488.

Yu, Y., Black, J.B., Goldsmith, C.S., Browning, P.J., Bhalla, K., and Offermann, M.K. (1999). Induction of human herpesvirus-8 DNA replication and transcription by butyrate and TPA in BCBL-1 cells. J Gen Virol *80 (Pt 1)*, 83-90.

Yu, Y., Wang, S.E., and Hayward, G.S. (2005). The KSHV immediate-early transcription factor RTA encodes ubiquitin E3 ligase activity that targets IRF7 for proteosome-mediated degradation. Immunity *22*, 59-70.

Zamora, M.R. (2011). DNA viruses (CMV, EBV, and the herpesviruses). Semin Respir Crit Care Med *32*, 454-470.

Zheng, Z.M. (2010). Viral oncogenes, noncoding RNAs, and RNA splicing in human tumor viruses. Int J Biol Sci *6*, 730-755.

Zhong, W., Wang, H., Herndier, B., and Ganem, D. (1996). Restricted expression of Kaposi sarcoma-associated herpesvirus (human herpesvirus 8) genes in Kaposi sarcoma. Proc Natl Acad Sci U S A *93*, 6641-6646.

Zhu, F.X., Cusano, T., and Yuan, Y. (1999). Identification of the immediate-early transcripts of Kaposi's sarcoma-associated herpesvirus. J Virol *73*, 5556-5567.

Ziegelbauer, J., Grundhoff, A., and Ganem, D. (2006). Exploring the DNA binding interactions of the Kaposi's sarcoma-associated herpesvirus lytic switch protein by selective amplification of bound sequences in vitro. J Virol *80*, 2958-2967.

Ziegelbauer, J.M., Sullivan, C.S., and Ganem, D. (2009). Tandem array-based expression screens identify host mRNA targets of virus-encoded microRNAs. Nat Genet *41*, 130-134.

Zielke, K., Full, F., Teufert, N., Schmidt, M., Muller-Fleckenstein, I., Alberter, B., and Ensser, A. (2012). The insulator protein CTCF binding sites in the orf73/LANA promoter region of herpesvirus saimiri are involved in conferring episomal stability in latently infected human T cells. J Virol *86*, 1862-1873.